τ decay
and the structure of the a_1

Dissertation

zur Erlangung des Doktorgrades
der naturwissenschaftlichen Fachbereiche
der Justus-Liebig-Universität Gießen

Fachbereich 7 - Mathematik, Physik, Geographie

vorgelegt von

Markus Wagner

aus Linden

Gießen, 2007

Dekan : Prof. Dr. Bernd Baumann
I.Gutachter : Prof. Ulrich Mosel
II.Gutachter : PD Dr. Stefan Leupold
Tag der mündlichen Prüfung : 20.12.2007

Contents

Chapter 1.

Introduction

> *If you have built castles in the air, your work need not be lost; that is where they should be. Now put the foundations under them.*
>
> Henry David Thoreau

In the Fifties and Sixties lots of new particles were discovered in the newly built particle accelerators, and the days of field theory seemed to be over, at least in the theory of the strong interactions [Gro99]. First of all, one did not know which particles to use as the relevant degrees of freedom, since they all seemed to be equally qualified at that time. In addition, the couplings in the strong interactions were too large to admit a perturbative treatment. In the mid-Sixties the quark model restored the order in the particle zoo, and it allowed a group-theoretical classification of the observed hadron spectrum [GMN00]. In the Seventies Quantum Chromo Dynamics (QCD) [GW73b, Wei73] arose as a field theory which could explain asymptotic freedom [GW73b, GW73a, Pol73]. Thus, one had a field theory at hand, which in principle was capable to describe the observations, with the quarks as fundamental fields. At short distances QCD was used to tackle many problems, and no contradiction to experiment has been found. Unfortunately, the low-energy part of QCD can not be treated in perturbation theory due to the increase of the coupling at low momentum transfers. Today, one still lacks an analytic tool for treating that region and calculating, for example, the particle masses from QCD directly.

Besides the SU(3) colour gauge symmetry, the QCD Lagrangian possesses an approximate global symmetry, the so called chiral symmetry. The chiral symmetry leads to conserved charges and currents with opposite parity, and if that symmetry was realised in nature, every hadron would have a chiral partner with degenerate mass but with opposite parity. These parity partners are missing in the observed hadron spectrum, which suggests that the symmetry is spontaneously broken. The pseudoscalar mesons are very good candidates for the Goldstone bosons of the broken symmetry, which are not exactly massless due to the chiral symmetry breaking quark mass terms in the QCD Lagrangian. Chiral Perturbation Theory (CHPT) [Wei79, GL84, GL85] describes the interactions among the lightest mesons in terms of an effective field theory, which is based on these symmetry properties. Although one returns to a field theory in terms of non-elementary particles, one has a systematic way of treating interactions in orders of momenta, opposed to an expansion in the coupling. The possible interaction terms are constrained by the symmetry, which reduces the number of parameters and endows the theory with predictive power. The momentum expansion, however, restricts its applicability to energies well below $1\,\text{GeV}$. It is also possible to include additional particles, as for example baryons and vector mesons, in a systematic way into the Lagrangian [Kra90, CWZ69, Geo84], which leads to a chiral effective field theory with a broader applicability.

In the energy region between the applicability domains of CHPT and of perturbative QCD one still has to rely on models, which leads back to the question of the relevant degrees of freedom. Is a given hadron, for example, a two- or three-quark state (constituent quark model [GI85, CI86, PDG06]) or is it a bound state of two different hadrons ('dynamically generated','molecule' - see below)? In any case, one does not have to start from the beginning, but the experiences and constraints from QCD and CHPT should be incorporated in these models. The constituent quark model has been very successful in describing part of the observed hadron spectrum, especially for the heavy-quark systems, e.g. charmonia and bottomonia [Swa06]. On the other hand, especially in the light-quark sector, there is still a lively debate about the nature of many hadronic states. One sector with a lot of activity is, for example, the light scalar meson sector ($\sigma, a_0(980), f_0(980), \kappa(900)$). These states can not be explained within the naive constituent quark model, and many models have been proposed to explain the phenomenology of these resonances. The suggestions for the nature of these resonances vary between $q\bar{q}$ states, multiquark states, $K\overline{K}$ bound states and superpositions of them (see e.g. [PDG06, AT04, Pen06] and references therein). A different route to explain the low-lying scalars has been taken in [OO97, OO99]. In these works the authors explain the states as being dynamically generated by the interactions of the pseudoscalar mesons. The scattering amplitudes are calculated by iterating the lowest order amplitudes of CHPT, which leads to a unitarisation of the amplitudes and creates poles which can be associated with the scalars. A similar question about the nature of hadronic resonances one encounters in the baryon sector, where the quark model also has trouble to describe the baryon excitations and their properties in a satisfying way (see e.g. [BM00, CR00] and references therein). As in the scalar case, an alternative approach to explain the resonance structure has been to generate resonances by iterating the leading order interactions of a chiral effective theory. The pioneering work in that direction has been done in [KSW95a, KSW95b] and was followed by many other works [OR98, OM01, JOO$^+$03, LK02, GRLN04], which suggest a number of $J^P = \frac{1}{2}^-$ baryon resonances to be generated dynamically by the interactions of Goldstone bosons and baryons, e.g. $\Lambda(1405)$ and $N^*(1535)$. Studying the interaction of the pseudoscalar mesons with the decuplet of baryons [KL04, SOVV05] also led to the generation of many known $J^P = \frac{3}{2}^-$ resonances, as for example the $\Lambda(1520)$.

Recent works applied the approach to the interactions of the octet of Goldstone bosons with the nonet of vector mesons [LK04, ROS05]. The authors calculate the scattering amplitude by solving a Bethe-Salpeter equation with a kernel fixed by the lowest order interaction of a chiral expansion. The leading order expression for the scattering of Goldstone bosons off vector mesons in a chiral framework is given by the Weinberg-Tomozawa (WT) term [Wei66, Tom66] and leads to a parameter free interaction. The only free parameter in the calculation enters through the regularisation of the loop integral in the Bethe-Salpeter equation. Poles have been found, which have been attributed to the axial-vector mesons.

A comparison of the pole position and width is necessarily indirect and depends on the model, which is used to extract these quantities from the actual observables. In addition, the height of the scattering amplitude, or in other words the strength of the interaction, is not tested in this way. We apply the method of dynamical generation directly to a physical process, namely the τ decay. The τ decay offers a clean probe to study the hadronic interactions, since the weak interaction part is well understood and can be cleanly separated from the hadronic part, which we are interested in. The τ decay into three pions is dominated by a resonance structure, which is usually ascribed to the a_1. So far the descriptions of the τ decay into the a_1 are mostly based upon a parametrisation in terms of Breit-Wigner functions and many parameters (see [PDG06] and references therein), which leads to model dependent results. A different approach using the chiral effective field theory including vector mesons and axial-
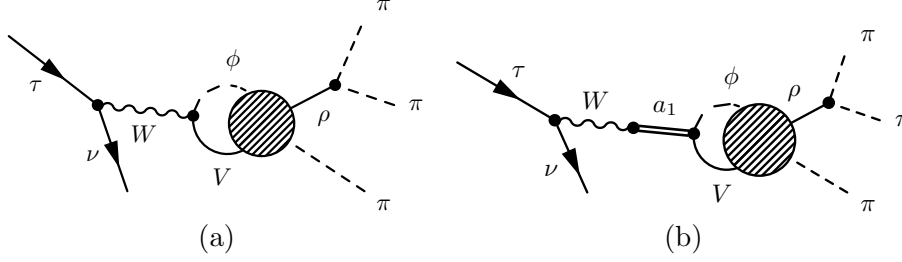
Figure 1.1.: (a) Basic diagram describing the dynamically generated a_1 in the τ decay and (b) additional diagram, when the a_1 is included explicitly. ϕ and V are the intermediate Goldstone boson and vector meson, respectively, which can be either $\pi\rho$ or KK^*.

vector mesons has been performed in [GDPP04]. The method yields a good description of the spectral function for the decay into three pions. However, the width of the a_1 has been parametrised in that work, whereas in the present work we generate the width by the decay into vector meson and Goldstone boson. In [A+00] a big contribution was found from a_1 decay into $\sigma\pi$, $f_0(1370)\pi$ and $f_2(1270)\pi$ and from that point of view the good agreement in [GDPP04] by just including the decay of the a_1 into $\rho\pi$ comes as a surprise and shows the model dependence of the extracted information from the τ decay. In [UBW02] the authors successfully describe the spectral function for the decay $\tau^- \rightarrow 2\pi^0\pi^-\nu_\tau$ in the framework of the linear σ-model. The width of the a_1 in this work is generated from the elementary decays of the a_1, but without considering the WT interaction.

The a_1 is especially interesting, since it is considered to be the chiral partner of the ρ [Wei67, Sch03]. As already mentioned, one expects a chiral partner for every particle from chiral symmetry. Due to the spontaneous symmetry breaking, one does not find degenerate one-particle states with the right quantum numbers. Nevertheless, the chiral partners have to exist, not necessarily as one-particle states, but at least as multi-particle states. Unmasking the a_1 as a bound state of a vector meson with a Goldstone boson would therefore approve its role of the chiral partner and disapprove its existence as a one-particle state. In the meson-meson and meson-baryon scattering examples, mentioned before, one can also see that the dynamically generated resonances would qualify as the chiral partners of the scattered particles, although the question of the chiral partner for these particles is not as clear as for the a_1 and the ρ. Even for the chiral partner of the ρ a different suggestion besides the a_1 exists, namely the $b_1(1235)$ [CP76].

We calculate the τ decay in two different ways. We first calculate it by assuming that the a_1 is generated dynamically and use the method from [LK04, ROS05] to describe the decay. This means that in this framework the τ decay is essentially described as follows: From the weak interactions a pair of mesons emerges (one pseudoscalar meson, one vector meson). Their final state interaction produces the resonant a_1 structure. This process is depicted in Fig. 1.1(a), where the blob stands for the iterated loop diagrams. The required vertices relevant for the process are calculated in a chiral effective field theory and the standard weak interactions. There are at most two free parameters in that calculation (in the simplest case only one), which enter through the regularisation of different loops. In a second calculation, we introduce the a_1 explicitly. Different to [GDPP04], where the width of the a_1 is parametrised, we will generate the width by the a_1 decay into pseudoscalar and vector mesons. In addition, we still include the WT term, since there is no reason to neglect it. We note that including the a_1 and the WT term is not double counting, as will be explained in Chapter 3. The essential additional diagram is shown in Fig. 1.1(b), where the blob again represents the iterated loop diagrams,

but this time the kernel also includes the a_1 interaction, which will be discussed in detail in Chapter 6. Afterwards we compare both calculations to experiment and see which scenario is favoured by the data. Since there exist excellent data for the τ decay [S$^+$05], one can expect that the results will be quite decisive. In case that the first scenario is favoured by experiment, this would be a sign that the a_1 is a dynamically generated resonance (molecule state) and in case the second calculation is favoured, this would be a hint that the a_1 is a quark-antiquark state.

Generally, different effective theories or different formalisms do not necessarily have to exclude each other. However, the more informative and more decisive situation appears, if the different approaches lead to deviating results. The importance of knowing the right formalism to describe particle interactions can be seen, for example, in the discussion about the ω spectral function in a cold baryon rich medium. To leading order in the baryon density, modifications of the spectral distribution are determined by vector meson nucleon scattering amplitudes. In [LWF02] the nucleon resonances in these channels are dynamically generated and the ωN amplitude is calculated in a similar framework as mentioned above, however without constraints from chiral symmetry. In other models the ωN scattering amplitude is calculated in a K-matrix approach [MSL$^+$06] or at tree level [KKW97] including the resonances explicitly. The results on the shape of the in-medium spectral function of all three calculations differ quantitatively as well as qualitatively. One can of course find more differences in these models than the one mentioned, but knowing the right framework to describe the process, would already be a major step forward. Due to the small amount of information and the high complexity, in-medium physics is often based on vague assumptions and crude approximations, and whenever informations can be extracted from the vacuum sector, that should be done.

The work is structured as follows. In Chapter 2 we will give a brief summary of CHPT in order to settle the notation and to remind of the most important facts. In Chapter 3 we introduce the vector mesons in the chiral Lagrangian and construct the interaction terms, which are relevant for this work. We will also discuss the influence of the choice of interpolating fields on the vertices. The most important ingredient in our calculation is the unitarisation of the scattering amplitude, which will be discussed in detail in Chapter 4. We will describe the most important methods to unitarise the scattering amplitude and comment on their differences or equivalence. In order to solve the resulting equations, we will use the so called projector formalism, which will be described in Chapter 5. The formalism is based on the work in [LK04], but takes a deviating route to determine the final form of the projectors, which, however, will not influence the result. We will address the differences and the reasons for them to appear. In Chapter 6 we will outline the calculation and show the formalism at work. (The interested reader may find further details on the calculations in the appendices.) In Chapter 7 we will show results for the spectral functions obtained in the two different scenarios. We will also investigate the Dalitz projection data from [A$^+$00] within the first scenario. Finally we will close with a summary and an outlook in Chapter 8.

Chapter 2.

Chiral Perturbation Theory

Chiral Perturbation Theory (CHPT) is an effective field theory describing the interactions of the pseudoscalar mesons at low energies, where low in that case basically means below the ρ meson mass. We will briefly recall some facts about CHPT, and we will see how the theory emerges from QCD. Due to the extensive literature on that subject, we will be rather short on most issues. For a detailed introduction to CHPT see for example [Sch03].

2.1. Chiral symmetry

We start by writing down the QCD Lagrangian [PS95],

$$\mathcal{L}_{\mathrm{QCD}} = \sum_{f=u,d,s,c,b,t} \bar{q}_f (i\slashed{D} - m_f) q_f - \frac{1}{4} \mathcal{G}_{\mu\nu,a} \mathcal{G}_a^{\mu\nu} \,, \tag{2.1}$$

with the covariant derivative

$$D_\mu = \partial_\mu - ig \frac{\lambda_a}{2} A_{\mu,a} \tag{2.2}$$

and the field strength tensor of the gluons

$$\mathcal{G}_{\mu\nu,a} = \partial_\mu A_{\nu,a} - \partial_\nu A_{\mu,a} + g f_{abc} A_{\mu,b} A_{\nu,c} \,. \tag{2.3}$$

The matrices λ_a are the Gell-Mann matrices, which can be found in Appendix A, and f_{abc} are the SU(3) structure constants, which can also be found in Appendix A.

In the following we will neglect the heavy flavours c, b and t, which means we will ignore effects due to virtual heavy quark pairs. This is a reasonable approximation for the energy regime, we are interested in.

The QCD Lagrangian describes the interactions of quarks and gluons in terms of an SU(3) colour gauge symmetry. Besides the SU(3) gauge symmetry and many more symmetries (e.g. parity, charge conjugation or time reversal), the Lagrangian possesses an additional symmetry in the case of massless quarks. Since the quark masses are very small compared to hadronic scales, one can expect this approximate symmetry to be useful. In order to see the symmetry, we introduce projectors on so called left- and right-handed states

$$P_R = \frac{1}{2}(1 + \gamma_5) \,, \quad P_L = \frac{1}{2}(1 - \gamma_5) \,. \tag{2.4}$$

It is easy to verify that these objects are indeed projectors. Using these operators, we can write the QCD Lagrangian for massless quarks (and only light flavours) as

$$\mathcal{L}_{\mathrm{QCD}}^0 = \sum_{f=u,d,s} i\bar{q}_{f,R} \slashed{D} q_{f,R} + i\bar{q}_{f,L} \slashed{D} q_{f,L} - \frac{1}{4} \mathcal{G}_{\mu\nu,a} \mathcal{G}_a^{\mu\nu} \tag{2.5}$$

with

$$q_{f,L} = P_L q_f, \quad q_{f,R} = P_R q_f.$$ (2.6)

Since the covariant derivative does not depend on flavour, $\mathcal{L}^0_{\text{QCD}}$ is invariant under independent U(3) rotations of the left- and right-handed quarks

$$\begin{pmatrix} u_L \\ d_L \\ s_L \end{pmatrix} \to V_L \begin{pmatrix} u_L \\ d_L \\ s_L \end{pmatrix} = \exp\left(-i\theta_a^L \frac{\lambda_a}{2}\right) e^{-i\theta^L} \begin{pmatrix} u_L \\ d_L \\ s_L \end{pmatrix},$$ (2.7)

$$\begin{pmatrix} u_R \\ d_R \\ s_R \end{pmatrix} \to V_R \begin{pmatrix} u_R \\ d_R \\ s_R \end{pmatrix} = \exp\left(-i\theta_a^R \frac{\lambda_a}{2}\right) e^{-i\theta^R} \begin{pmatrix} u_R \\ d_R \\ s_R \end{pmatrix}.$$ (2.8)

λ_a are again the Gell-Mann matrices, but now acting on flavour instead of colour. We see that the symmetry can also be written as an $\text{SU}(3)_L \times \text{SU}(3)_R \times \text{U}(1)_R \times \text{U}(1)_L$ symmetry. This global symmetry leads according to Noether's theorem to 18 conserved currents

$$L^{\mu,a} = \bar{q}_L \gamma^\mu \frac{\lambda_a}{2} q_L, \quad R^{\mu,a} = \bar{q}_R \gamma^\mu \frac{\lambda_a}{2} q_R$$ (2.9)

and

$$L^\mu = \bar{q}_L \gamma^\mu q_L, \quad R^\mu = \bar{q}_R \gamma^\mu q_R.$$ (2.10)

Instead of these currents it is more convenient to use linear combinations of these expressions, which have a definite transformation behaviour under parity, namely

$$V^{\mu,a} = R^{\mu,a} + L^{\mu,a} = \bar{q}\gamma^\mu \frac{\lambda_a}{2} q,$$ (2.11)

$$A^{\mu,a} = R^{\mu,a} - L^{\mu,a} = \bar{q}\gamma^\mu \gamma_5 \frac{\lambda_a}{2} q,$$ (2.12)

$$V^\mu = R^\mu + L^\mu = \bar{q}\gamma^\mu q,$$ (2.13)

$$A^\mu = R^\mu - L^\mu = \bar{q}\gamma^\mu \gamma_5 q.$$ (2.14)

These currents transform as vector and axial-vector currents under parity. They correspond to transformations of the left- and right-handed quarks with the same phase and with an opposite phase, respectively.

The singlet axial-vector current is not preserved by quantisation. This phenomenon is referred to as anomaly and for further information we refer to [PS95]. The singlet vector current leads to baryon conservation, which yields the classification of hadrons into mesons and baryons. The $\text{SU}(3)_V$ symmetry is reflected in the particle spectrum, since the particles are ordered according to representations of $\text{SU}(3)_V$, e.g. the octet of vector mesons or the decuplet of baryons. Neglecting strangeness and considering only $\text{SU}(2)_V$, the symmetry is almost perfectly realised, which can be seen in for example the triplet of pions or the triplet of ρ mesons. The whole $\text{SU}(3)_L \times \text{SU}(3)_R$ or equivalently $\text{SU}(3)_V \times \text{SU}(3)_A$ symmetry is the chiral symmetry, which we are interested in, and which we will investigate further.

The associated charge operators to the conserved currents of the chiral symmetry are defined as the space integrals of the charge densities

$$Q_{R/L}^a = \int d^3x \, q_{R/L}^\dagger \frac{\lambda^a}{2} q_{R/L}$$ (2.15)

and

$$Q_V^a = Q_R^a + Q_L^a, \quad Q_A^a = Q_R^a - Q_L^a,$$ (2.16)

which commute with the Hamiltonian corresponding to $\mathcal{L}_{QCD}^0$ (cf. Eq.(2.5)).

If the Hamiltonian is invariant under certain symmetry transformations, one usually orders the physical states according to irreducible representations of the symmetry group. In case of the chiral symmetry, we would expect that for every state, there exists a state of opposite parity with the same mass, which can be seen as follows. Let $|i, +>$ be a single-particle eigenstate of the Hamiltonian with energy eigenvalue E_i and positive parity. Defining $|\phi> = Q_A^a|i, +>$, we know

$$H_{QCD}^0|\phi> = H_{QCD}^0 Q_A^a|i, +> = Q_A^a H_{QCD}^0|i, +> = E_i|\phi> \tag{2.17}$$

and

$$P|\phi> = P Q_A^a P^{-1} P|i, +> = -Q_A^a|i, +> = -|\phi>, \tag{2.18}$$

where P is the parity operator. Thus, the states have opposite parity and the same energy eigenvalue. However, the derivation does not tell us, whether the state $|\phi>$ is a single-particle state. For that conclusion one has to assume that the operator annihilates the ground state. Under this assumption one gets

$$Q_A^a|i, +> = Q_A^a a_i^\dagger|0> = ([Q_A^a, a_i^\dagger] + a_i^\dagger Q_A^a)|0> = -\frac{\lambda_{ij}^a}{2} b_j^\dagger|0>, \tag{2.19}$$

where we used

$$[Q_A^a, a_i^\dagger] = -\frac{\lambda_{ij}^a}{2} b_j^\dagger \tag{2.20}$$

and $b_j^\dagger$ generates quanta of opposite parity as $a_j^\dagger$. The relation (2.20) can be verified by explicitly evaluating the commutator. In turn, if Q_A^a does not annihilate the ground state, the state with opposite parity will not be a single-particle state. Since the degenerate multiplets of opposite parity are not observed in the physical particle spectrum, the ground state is not invariant under the symmetry, i.e. the symmetry must be spontaneously broken. As already mentioned, the $\mathrm{SU}(3)_V$ symmetry is realised in the particles spectrum, and thus the chiral symmetry is broken down to $\mathrm{SU}(3)_V \times \mathrm{SU}(3)_A \longrightarrow \mathrm{SU}(3)_V$. In this case Goldstone's theorem tells us that there are eight massless Goldstone bosons with transformation properties closely connected to those of the broken generators. The pseudoscalar mesons have the right quantum numbers, and although they are not massless, there is a definite mass gap to all other states, which makes them a very good candidate for the Goldstone bosons. The small masses are due to the explicit symmetry breaking by the quark mass terms.

2.2. Chiral Lagrangian

Now we want to describe the pseudoscalar mesons as Goldstone bosons of the spontaneously broken symmetry $\mathrm{SU}(3)_V \times \mathrm{SU}(3)_A \longrightarrow \mathrm{SU}(3)_V$. We will see that we need to introduce the concept of a non-linear realisation [CWZ69]. The usual linear representations are not suited to describe the interaction of the Goldstone bosons alone. An example is the linear σ-model [AH03, Mos89], where the price for the linear transformation of the pion is the introduction of the σ meson, whose nature is still controversal. The problem in that case is cured by the non-linear σ-model [AH03, Mos89], which is an example of a non-linear realisation.

In order to describe the pions, we will look at the connection between the pions and the coset space $(\mathrm{SU}(3)_V \times \mathrm{SU}(3)_A)/\mathrm{SU}(3)_V$. We briefly recall the definition of a coset space and the relevant properties. The left coset of g is defined by

$$gH = \{gh | h \in H\}, \tag{2.21}$$

and the set of all left cosets is called the quotient group G/H. Given any representation φ of $G = \mathrm{SU}(3)_V \times \mathrm{SU}(3)_A$

$$\varphi : \quad (G \times M) \longrightarrow M \,, \tag{2.22}$$

where M is some vector space, we can make the following observation. If H is the subgroup, which leaves the ground state invariant, then all elements of a coset map the origin onto the same vector, since

$$\varphi(gh, 0) = \varphi(g, 0) \tag{2.23}$$

by the homomorphism property. It is also easy to show [Sch03] that the mapping

$$gH \longrightarrow \varphi(g, 0) \tag{2.24}$$

is injective, and therefore there exists a one-to-one correspondence between the quotient group and the ground state excitations of the group G. The ground state excitations are caused by the generators of the broken group, i.e. by $Q_A^a |0\rangle \neq |0\rangle$, which are directly connected to the Goldstone bosons. Thus, the next step is to parametrise the coset space, which in our case is isomorph to $\mathrm{SU}(3)$, by the Goldstone boson fields. There are several ways to do that and we will use the most popular exponential parametrisation

$$U = e^{i\phi/F_0} \tag{2.25}$$

with

$$\phi = \begin{pmatrix} \pi^0 + \frac{1}{\sqrt{3}}\eta & \sqrt{2}\pi^+ & \sqrt{2}K^+ \\ \sqrt{2}\pi^- & -\pi^0 + \frac{1}{\sqrt{3}}\eta & \sqrt{2}K^0 \\ \sqrt{2}K^- & \sqrt{2}\,\overline{K}^0 & -\frac{2}{\sqrt{3}}\eta \end{pmatrix} \tag{2.26}$$

and the pion decay constant F_0. The transformation of the Goldstone bosons can be figured out by multiplying the coset space element with the corresponding transformation. In order to do that explicitly, we choose a representative of the coset space element. In the following we will use that a general element $g \in G$ can be denoted with $g = (L, R)$ since $\mathrm{SU}(3)_V \times \mathrm{SU}(3)_A$ is isomorph to $\mathrm{SU}(3)_L \times \mathrm{SU}(3)_R$ and an element of the subgroup $h \in \mathrm{SU}(3)_V$ is then to be identified with $h = (V, V)$. Noting that

$$(L, R)\underbrace{(V, V)}_{\in H} = (LV, RV) = (1, RL^\dagger)\underbrace{(LV, LV)}_{\in H},$$

we see that the coset space elements can be characterised by $RL^\dagger$. Multiplying with a transformation $g' \in G$ yields

$$(L', R')\underbrace{(1, RL^\dagger)H}_{=gH} = (L', R'RL^\dagger)H = (1, R'RL^\dagger L'^\dagger)H \,.$$

Thus, under a transformation $g = (L, R) \in G$ the Goldstone bosons transform as

$$U \to U' = RUL^\dagger \,. \tag{2.27}$$

Using this transformation law, we can construct the lowest order chiral Lagrangian, where lowest order means that one orders the interaction in powers of the external momenta and the Goldstone boson masses. The construction is straightforward and the Lagrangian reads

$$\mathcal{L}_{\mathrm{eff}} = \frac{F_0^2}{4} \mathrm{Tr}[\partial_\mu U (\partial^\mu U)^\dagger] \,, \tag{2.28}$$

where Tr denotes the trace in flavour space. One can easily convince oneself that there are no other terms with two derivatives or less. Eq.(2.28) would be the Lagrangian for a perfect $SU(3)_V \times SU(3)_A$ symmetry. However, we already noted that the quark mass term breaks the chiral symmetry explicitly

$$\mathcal{L}_{quark-mass} = -\bar{q}_R M q_L - \bar{q}_L M^\dagger q_R \,, \quad M = \begin{pmatrix} m_u & 0 & 0 \\ 0 & m_d & 0 \\ 0 & 0 & m_s \end{pmatrix} \,. \tag{2.29}$$

Although M is a constant matrix and does not transform, the Lagrangian $\mathcal{L}_{\text{QCD}}$ would be invariant if M transformed according to

$$M \longrightarrow RML^\dagger. \tag{2.30}$$

One then constructs the most general Lagrangian by including M together with U transforming according to Eq.(2.27) and Eq.(2.30). At lowest order this leads to

$$\mathcal{L}_{\text{s.b.}} = \frac{F_0^2 B_0}{2} \text{Tr}[MU^\dagger + UM^\dagger] \,, \tag{2.31}$$

where B_0 parametrises the connection between the Goldstone boson masses and the quark masses. Identifying the terms of quadratic order in the fields ϕ, one gets for example

$$\mathcal{L}_{\text{s.b.}} = -\frac{B_0}{2} \text{Tr}[\phi^2 M] + \cdots = -B_0(m_u + m_d)\pi^+\pi^- - B_0(m_u + m_s)K^+K^-$$
$$- B_0(m_d + m_s)K^0\overline{K}^0 - \frac{B_0}{2}(m_u + m_d)\pi^0\pi^0 + \dots . \tag{2.32}$$

Using $m_u \approx m_d \approx m$ the masses of the pions and kaons are given by

$$m_\pi^2 = 2B_0 m \,, \tag{2.33}$$
$$m_K^2 = B_0(m + m_s) \,. \tag{2.34}$$

So far we have only considered global symmetries, which we will now promote to local ones, which requires some explanation. The link between the underlying theory and the effective field theory is formulated via the path integral formalism (see [GL84]). In the absence of anomalies the Ward identities can be expressed as a local invariance of the generating functional including external fields (see e.g. [Sch03]). But, there is still a subtlety. In the path integral formalism, one does not need the Lagrangian to be invariant under the symmetry; the action is the quantity, which has to be invariant. That means that the Lagrangian has only to be invariant up to a total derivative. However, in [Leu94] it was shown that the freedom of adding total derivatives and performing field transformations can be used to bring the Lagrangian into a manifestly gauge invariant form.

The QCD Lagrangian including the couplings of the eight vector currents, eight axial-vector currents as well as scalar and pseudoscalar quark densities to external fields reads

$$\mathcal{L} = \mathcal{L}_{\text{QCD}}^0 + \mathcal{L}_{\text{ext}} = \mathcal{L}_{\text{QCD}}^0 + \bar{q}\gamma_\mu(v^\mu + \gamma_5 a^\mu)q - \bar{q}(s - i\gamma_5 p)q \,. \tag{2.35}$$

Instead of external vector and axial-vector fields one can use

$$v_\mu = \frac{1}{2}(r_\mu + l_\mu) \,, \quad a_\mu = \frac{1}{2}(r_\mu - l_\mu). \tag{2.36}$$

The transformation behaviour of the external fields is such that they cancel the terms resulting from the local chiral transformation and the transformations are given by

$$r_\mu \longrightarrow V_R r_\mu V_R^\dagger + i V_R \partial_\mu V_R^\dagger \tag{2.37}$$

$$l_\mu \longrightarrow V_L l_\mu V_L^\dagger + i V_L \partial_\mu V_L^\dagger \tag{2.38}$$

$$s + ip \longrightarrow V_R(s + ip)V_L^\dagger \tag{2.39}$$

$$s - ip \longrightarrow V_L(s - ip)V_R^\dagger . \tag{2.40}$$

Using these fields to guarantee the local invariance of the lowest order chiral Lagrangian, one gets

$$\mathcal{L}_2 = \frac{F_0^2}{4}\text{Tr}[D_\mu U(D^\mu U)^\dagger] + \frac{F_0^2}{4}\text{Tr}[\chi U^\dagger + U\chi^\dagger] \tag{2.41}$$

with

$$\partial_\mu U \to D_\mu U = \partial_\mu U - ir_\mu U + iU l_\mu \tag{2.42}$$

and

$$\chi = 2B_0(s + ip) , \tag{2.43}$$

where s incorporates explicit chiral symmetry breaking through the quark mass matrix $s = M$. Another advantage of using the external fields is the convenient way of connecting the effective theory to the weak interactions [PS95]. One of the couplings, we will need, is the coupling of the weak gauge boson W to the pions, which can be determined by setting

$$r_\mu = 0, \quad l_\mu = -\frac{g}{\sqrt{2}}(W_\mu^+ T_+ + h.c.) , \tag{2.44}$$

where $h.c.$ refers to the hermitian conjugate and

$$T_+ = \begin{pmatrix} 0 & V_{ud} & V_{us} \\ 0 & 0 & 0 \\ 0 & 0 & 0 \end{pmatrix} . \tag{2.45}$$

Here, V_{ij} denote the elements of the Cabibbo-Kobayashi-Maskawa quark mixing matrix. The constant g is related to the W mass and the Fermi constant by

$$G_F = \sqrt{2}\frac{g^2}{8M_W^2} . \tag{2.46}$$

The external fields in Eq.(2.44) are chosen such that with these settings in the quark Lagrangian with external fields one gets exactly the standard charged-current weak interaction in the light-quark sector.

We will use the Langrangian in Eq.(2.41) to describe the decay of the W boson into three pions to lowest order. However, CHPT is only capable to describe the τ decay at energies well below $1\,\text{GeV}$. In particular, the theory can not reproduce the resonance structure seen in the τ decay. Therefore, we will discuss the inclusion of the vector mesons into the Lagrangian in the next chapter.

Chapter 3.

Vector Mesons and Chiral Symmetry

At low energies the dynamics of the pseudoscalar mesons are described by the chiral Lagrangian. That description is doomed to fail in processes dominated by the heavier mesons, most notably the vector mesons. Several models have been proposed to introduce the vector mesons in the chiral Lagrangian and most of them were motivated by the phenomenological successful ideas of vector-meson dominance and universal coupling [Sak69]. A very prominent way of introducing the vector mesons is the so called Hidden Symmetry Approach [BKY88]. In this approach the vector mesons are introduced as gauge bosons of a hidden local symmetry, which in case one just wants to include the ρ meson, would be for example $SU(2)_V$. Choosing one parameter, which is introduced by the model, the KSFR relation ([BKY88] and references therein), universality of the coupling and vector dominance emerges naturally. On the other hand introducing the vector mesons as gauge bosons is quite an assumption and the inclusion of the axial-vector mesons into the Lagrangian is also troublesome. If one tries to include the axial-vector mesons, one has to add higher order terms to the Lagrangian in order to still fit the phenomenological constraints [KM90].

A more general way to treat the vector mesons was already introduced in [Wei68, CWZ69, CCWZ69], along with the non-linear realisation of the Goldstone bosons. The only restriction on the vector mesons, in that approach, is that they transform as an octet under $SU(3)_V$. We will refer to that scheme as the WCCWZ scheme, named after the people who contributed to the development (Weinberg, Callan, Coleman, Wess, Zumino). In that approach the phenomenological constraints are implemented by putting constraints on the couplings.

In addition to the different assumptions on the nature of the vector mesons, there is also a choice on the interpolating fields. Instead of describing the particles in terms of four-vectors, the vector mesons can also be represented by antisymmetric tensor fields [EGPdR89, EGL$^+$89]. The approaches are of course equivalent since the choice of fields can not influence the physics. However, in practice the Lagrangians are truncated in a derivative expansion and the Lagrangian might differ in 'higher' order contact terms (see e.g. [EGL$^+$89, BP96]), which especially influence the behaviour at higher energies. We put 'higher' in quotation marks, since the contact terms are higher order than the lowest order CHPT Lagrangian, but may not be of higher order than the process involving the vector mesons. We will discuss the appearance and form of these contact terms in more detail later. In the calculation in [EGL$^+$89], for example, the calculation employing tensor fields led to a reasonable high-energy behaviour, whereas in the calculation using vector fields, one had to introduce contact terms in order to get the same result as in the tensor field approach. However, one has to be careful to use constraints from high energies in a scheme which is ordered in powers of momenta. In principle both schemes are not suited to be valid in that energy region and an improvement at high energies does not have to lead to an improvement at low energies. In this work, we will use the WCCWZ scheme and describe the vector mesons by vector fields. In addition, we will include the higher order terms to improve the high-energy behaviour.

In contrast to CHPT the power counting for loop diagrams is not straightforward anymore in the presence of vector mesons. The appearance of a heavy mass scale in the loop jeopardises the power counting, which has also been noted in the baryon sector [GSS88]. There are several methods to renormalise the loops such that power counting is restored. We will shortly describe the methods and then comment on the way, in which we will renormalise the loop diagrams in our calculations.

3.1. The WCCWZ scheme

The only requirement, we want the vector mesons to fulfil, is that they transform as an octet under $\mathrm{SU}(3)_V$, i.e. we want them to live in the adjoint representation of $\mathrm{SU}(3)_V$. That leaves some freedom of how the vector mesons transform under the whole group $\mathrm{SU}(3)_V \times \mathrm{SU}(3)_A$, and one needs some kind of connection between the different choices. That connection has been investigated in [CWZ69]. It was shown that any non-linear realisation which becomes linear when restricted to the subgroup can be brought into a standard form. The different descriptions can be connected by field transformations, and therefore they are equivalent. We do not want to repeat the general proof, which can be found in [CWZ69], but we will give a short example. Let V_μ and $\tilde{V}_\mu$ be two different choices for the vector mesons fields with the following transformation behaviour

$$V_\mu \stackrel{\mathrm{SU}(3)_V \times \mathrm{SU}(3)_A}{\longrightarrow} L V_\mu L^\dagger \,, \tag{3.1}$$

$$\tilde{V}_\mu \stackrel{\mathrm{SU}(3)_V \times \mathrm{SU}(3)_A}{\longrightarrow} R \tilde{V}_\mu L^\dagger \,. \tag{3.2}$$

These transformations are obviously different, but when restricted to the subgroup $\mathrm{SU}(3)_V$ $((L, R) = (B, B))$, the fields transform in the same way

$$V_\mu \stackrel{\mathrm{SU}(3)_V}{\longrightarrow} B V_\mu B^\dagger \,, \tag{3.3}$$

$$\tilde{V}_\mu \stackrel{\mathrm{SU}(3)_V}{\longrightarrow} B \tilde{V}_\mu B^\dagger \,. \tag{3.4}$$

Now we want to find a transformation, which transforms V_μ into $\tilde{V}_\mu$. This simple field transformation is given by

$$\tilde{V}_\mu = U V_\mu \,, \tag{3.5}$$

where we recall that U contains the Goldstone boson fields according to Eq.(2.25). Eq.(3.5) is verified by the transformation behaviour

$$\tilde{V}_\mu \stackrel{\mathrm{SU}(3)_V \times \mathrm{SU}(3)_A}{\longrightarrow} R U L^\dagger L V_\mu L^\dagger = R \tilde{V} L^\dagger \,. \tag{3.6}$$

The reason for that freedom is that the $\mathrm{SU}(3)_V \times \mathrm{SU}(3)_A$ symmetry is broken, and it is only the transformation properties of the vector mesons under $\mathrm{SU}(3)_V$ which matter. Using that freedom to choose the fields, we will use a form [Geo84] which is very convenient for the construction of the Lagrangian and which is more or less the standard form, which is used by many other authors. In order to do so, we first define the auxiliary quantity u, which is the square root of U

$$u^2 = U \,. \tag{3.7}$$

The transformation on U induces a transformation on u, which is given by

$$u \longrightarrow u' = \sqrt{R U L^\dagger} \equiv R U K^{-1}(L, R, U) = K U L^\dagger \,. \tag{3.8}$$

We define the transformation of the vector fields in terms of K

$$\begin{pmatrix} U \\ V \end{pmatrix} \rightarrow \begin{pmatrix} U' \\ V' \end{pmatrix} = \begin{pmatrix} RUL^\dagger \\ K(L,R,U)VK^\dagger(L,R,U) \end{pmatrix} . \tag{3.9}$$

The matrix K carries the $\mathrm{SU}(3)_V \times \mathrm{SU}(3)_A$ transformation in a non-linear way. That description is very much in the line of the original paper [CWZ69], where also the transformation of a certain parametrisation of the coset space was used to induce the transformation on the other fields. The important feature is that under the subgroup $\mathrm{SU}(3)_V$ the transformation becomes linear, which can be seen by noting that

$$\sqrt{Bu^2B^\dagger} = \sqrt{BuB^\dagger BuB^\dagger} = BuB^\dagger \tag{3.10}$$

and looking at Eq.(3.8).

At first sight that representation looks somewhat messy, but it is quite handy for the construction of the Lagrangian, since one does not need to know the exact form of K at any time. One just needs building blocks, which transform the same way as V_μ, which will be defined in the following. For an explicit verification of the transformation of these terms, we refer to [Sch03]. The vector meson octet is given by

$$V_\mu = \begin{pmatrix} \rho_\mu^0 + \omega_\mu^8/\sqrt{3} & \sqrt{2}\rho_\mu^+ & \sqrt{2}K_\mu^+ \\ \sqrt{2}\rho_\mu^- & -\rho_\mu^0 + \omega_\mu^8/\sqrt{3} & \sqrt{2}K_\mu^0 \\ \sqrt{2}K_\mu^- & \sqrt{2}\,\overline{K}_\mu^0 & -2\omega_\mu^8/\sqrt{3} \end{pmatrix} . \tag{3.11}$$

ω_μ^8 is an admixture of the physical states ω_μ and ϕ_μ (for details see e.g. [PDG06]). We do not care about the details of this mixing, since these states do not contribute to our calculation. The covariant derivative of the vector mesons is given by

$$\nabla_\mu V_\nu = \partial_\mu V_\nu + [\Gamma_\mu, V_\nu], \quad \Gamma_\mu = \frac{1}{2}(u^\dagger(\partial_\mu - ir_\mu)u + u(\partial_\mu - il_\mu)u^\dagger), \tag{3.12}$$

which also transforms as

$$\nabla_\mu \longrightarrow \nabla_\mu' = K\nabla_\mu K^\dagger . \tag{3.13}$$

Thus, the field strength tensor of the vector mesons, defined by

$$V_{\mu\nu} = \nabla_\mu V_\nu - \nabla_\nu V_\mu , \tag{3.14}$$

also transforms the same as V_μ.

A very important building block is

$$u_\mu = iu^\dagger D_\mu U u^\dagger \tag{3.15}$$

with the covariant derivative D_μ defined in Eq.(2.42). Another expression, containing basically the external fields (in our case we are interested in the W boson, see Eq.(2.44)), is given by

$$f_\pm^{\mu\nu} = uF_L^{\mu\nu}u^\dagger \pm u^\dagger F_R^{\mu\nu}u , \tag{3.16}$$

where $F_{L/R}^{\mu\nu}$ are the field strength tensors of the external left and right handed vector fields

$$F_L^{\mu\nu} = \partial_\mu l_\nu - \partial_\nu l_\mu - i[l_\mu, l_\nu], \quad F_R^{\mu\nu} = \partial_\mu r_\nu - \partial_\nu r_\mu - i[r_\mu, r_\nu]. \tag{3.17}$$

3.1.1. Vector-meson couplings

Since all building blocks (V_μ, Eq.(3.14), Eq.(3.15), Eq.(3.16)) transform the same under chiral symmetry, one simply multiplies the objects and takes the flavour trace in order to get an invariant. Taking also care of parity and charge conjugation (see Tab. C.1), the Lagrangian containing the coupling of the W to a Goldstone boson and a vector meson to lowest order is given by

$$\mathcal{L}_{vec} = -\frac{1}{8}\,\mathrm{Tr}[V_{\mu\nu}V^{\mu\nu}] - \frac{f_V}{4}\,\mathrm{Tr}[V_{\mu\nu}f_+^{\mu\nu}] - \frac{ig_V}{4}\,\mathrm{Tr}[V_{\mu\nu}[u^\mu, u^\nu]]\,, \tag{3.18}$$

which has already been written down in [EGL$^+$89]. We note that the definition of V_μ in [EGL$^+$89] differs from our definition by a factor of $\sqrt{2}$, which yields different prefactors in front of our terms. The external field l_μ is connected to the W boson by Eq.(2.44). The last term on the right hand side of Eq.(3.18), for example, incorporates a contribution to the $W \to \phi V$ vertex, as well as the $\rho \to \pi\pi$ vertex:

$$-\frac{ig_V}{4}\,\mathrm{Tr}[V_{\mu\nu}[u^\mu, u^\nu]] \to -\frac{ig_V}{2F_0^2}\,\mathrm{Tr}[(\partial_\mu V_\nu - \partial_\nu V_\mu)\partial^\mu\phi\partial^\nu\phi] \tag{3.19}$$

and

$$-\frac{ig_V}{4}\,\mathrm{Tr}[V_{\mu\nu}[u^\mu, u^\nu]] \to \frac{ig_V g}{2\sqrt{2}F_0}\,\mathrm{Tr}[\partial^\mu V^\nu([\partial_\mu\phi, W_\nu^- T_+^t] - [\partial_\nu\phi, W_\mu^- T_+^t])] \tag{3.20}$$

with T_+ given in Eq.(2.45). The important point to note in Eq.(3.18) is that chiral symmetry (breaking) connects the desired couplings of W to mesons on the one hand side to the couplings of vector mesons to a virtual photon and to two Goldstone bosons on the other hand side. Therefore, the constants f_V and g_V can be determined from $\Gamma(\rho^0 \to e^+e^-)$ and $\Gamma(\rho \to 2\pi)$, which yields

$$f_V = \frac{0.154\,\mathrm{GeV}}{M_\rho}\,, \quad g_V = \frac{0.069\,\mathrm{GeV}}{M_\rho}\,, \tag{3.21}$$

which are the values given in e.g. [EGL$^+$89]. In the same work the authors also used theoretical considerations and approximations to estimate the constants. Using the KSFR relation in the form

$$f_V = 2g_V \tag{3.22}$$

and

$$f_V g_V = \frac{f_\pi^2}{M_\rho^2}\,, \tag{3.23}$$

which origins in constraints on the high-energy behaviour of the pion form factor [EGL$^+$89], the two coefficients can be pinned down to be

$$f_V = \frac{\sqrt{2}f_\pi}{M_\rho} \approx \frac{0.127\,\mathrm{GeV}}{M_\rho}\,, \quad g_V = \frac{f_\pi}{\sqrt{2}M_\rho} \approx \frac{0.064\,\mathrm{GeV}}{M_\rho}\,, \tag{3.24}$$

which roughly reproduces Eq.(3.21). However, these values are not determined by exact hard constraints. The constraint coming from the high-energy behaviour is questionable. The theory was written down to hold for small momenta, and there will be no inconsistency, if the theory breaks down for high energies. Fixing the constants by high-energy behaviour does not mean that the low-energy behaviour is improved. In the following we will use the values in Eq.(3.21) determined from experiment. We will also explore the impact of variations of these values on our results in Chapter 7.

The Weinberg-Tomozawa (WT) term, which was mentioned already in Chapter 1, is contained in the kinetic term of Eq.(3.18). The explicit expression together with the other vertices, which we will use in our work, resulting from the Lagrangian in Eq.(3.18), can be found in Appendix D.

3.1.2. Power counting

Since the number of vector mesons in a process might change (opposed to for example the number of baryons in a process), the power counting for processes involving vector mesons might work different for different processes. In principle there are two situations, where it works. We keep the following discussion on the tree level and postpone the power counting for loop diagrams to Section 3.3.1, since this an extra topic.

1. For energies much smaller than the vector meson mass, *every* derivative counts as $\mathcal{O}(q)$ (also the ones on the vector mesons) [EGL$^+$89]. In particular, since the energies are much smaller than the vector meson mass, the vector mesons can only appear as intermediate particles, and the chiral order of the diagram can be determined by integrating out the vector mesons. We can study this situation by looking for example at the contribution to pion scattering stemming from the Lagrangian in Eq.(3.18). The coupling of the vector meson to the pseudoscalar mesons starts at $\mathcal{O}(q^3)$. Since the propagator cannot decrease the chiral counting a contribution to pion scattering would be at least

$$\mathcal{O}(q^3)\frac{1}{M_V^2}\mathcal{O}(q^3) = \mathcal{O}(q^6)\,. \tag{3.25}$$

   This power counting changes, if one uses the tensor instead of the vector realisation to describe the vector mesons. We will come back to that point in Section 3.2.

2. In case the number of vector mesons does not change in a process, a systematic power counting is possible as long as all three-momenta are small compared to the mass of the vector meson [JMW95]. In this case a derivative on the Goldstone bosons counts as small, whereas a derivative on the vector mesons does not influence the order. We encounter this situation for example by determining the lowest order contribution to the scattering of a Goldstone boson off a vector meson. This term is given by the WT term, which is $\mathcal{O}(q)$, since there is only one 'soft' derivative (see Appendix D.1).

In our calculation the requirement of small energies is not fulfilled, and therefore we have to be careful in applying the power counting. The assumption is that considering the lowest order terms, which are dictated by either one of the above power counting schemes, the calculation is also applicable at higher energies. In addition, for the final state interactions we will see in Chapter 5 how we extend the applicability of our calculation to higher energies by applying the power counting to the kernel of the Bethe-Salpeter equation instead of applying it to the scattering amplitude. This is of course where the model starts and the theory ends. However, in Chapter 7 we will see that our model is well behaved and can be systematically improved, which are two very promising properties.

3.1.3. Axial-vector meson couplings

Now we also introduce the relevant terms, describing the interactions of the a_1, into the Lagrangian. We recall that we will investigate two scenarios describing the τ decay, where in one of them the a_1 field is included explicitly. Thus, for this scenario we will need the Lagrangian which we are going to discuss in the following. The axial-vector nonet A_μ is given by

$$A_\mu = \begin{pmatrix} a_1^0 + f_1(1285) & \sqrt{2}a_1^+ & \sqrt{2}K_{1A}^+ \\ \sqrt{2}a_1^- & -a_1^0 + f_1(1285) & \sqrt{2}K_{1A}^0 \\ \sqrt{2}K_{1A}^- & \sqrt{2}K_{1A}^0 & \sqrt{2}f_1(1420) \end{pmatrix}_\mu . \qquad (3.26)$$

Before we write down the interaction terms, we want to comment on the troublesome term $\mathrm{Tr}[A_\mu u^\mu]$, which appears in the Lagrangian when one uses the four-vector field formalism instead of the antisymmetric tensor description [EGPdR89]. This interaction couples the unphysical spin 0 component of the a_1 to the Goldstone bosons. In our approach, we can of course just set the coupling to zero, but it is instructive to have a closer look at the spin 0 component of the a_1.
The problem is that the condition

$$\partial_\mu V^\mu = \partial_\mu A^\mu = 0 , \qquad (3.27)$$

which eliminates the extra component, does not remain valid in the presence of the interactions, as long as the fields do not couple to conserved currents. If the fields couple to conserved currents, the unwanted spin 0 component will be projected out at the vertex. However the axial-vector mesons are not treated as gauge particles in our scheme, and there is no reason why they should couple to a conserved current. The only thing which should be assured is that the unphysical spin 0 component is not propagated. That is already taken care of since the projectors, which we will introduce in Chapter 5, project on the $J = 1$ state, and therefore eliminate the spin 0 part.. The coupling of the a_1 to the W, which we will write down below, also projects out the unwanted part, as can be seen in the explicit expression for the vertex in Appendix D. Therefore, the question of how to treat the spin 0 component is only academical in that case.
A different way to assure the elimination of the spin 0 component is using the tensor representation, where the interactions project automatically on transverse states [Leu07]. We will comment on the use of the tensor formalism at the end of the chapter.

The Lagrangian, we are going to use, to describe the interactions of the a_1 is

$$\mathcal{L}_{axial} = -\frac{f_A}{4}\,\mathrm{Tr}[A_{\mu\nu}f_-^{\mu\nu}] + ic_1\,\mathrm{Tr}[V^{\mu\nu}[A_\mu, u_\nu]] + ic_2\mathrm{Tr}[A^{\mu\nu}[V_\mu, u_\nu]] , \qquad (3.28)$$

where the first term describes the coupling of the a_1 to the W and the last two terms describe the decay of the a_1 into Goldstone boson and vector meson with the unknown constants c_1 and c_2. According to the power counting discussions in the previous section, the first term is $\mathcal{O}(q^3)$ (situation 1) and the two other terms are $\mathcal{O}(q)$ (situation 2). The i in front of these constants is chosen such that c_1 and c_2 are real, which follows from hermiticity

$$(i\,\mathrm{Tr}[V^{\mu\nu}[A_\mu, u_\nu]])^* = -i\,\mathrm{Tr}[(V^{\mu\nu})^T[(A_\mu)^T, (u_\nu)^T]] = -i\,\mathrm{Tr}[V^{\mu\nu}[u_\nu, A_\mu]] = i\,\mathrm{Tr}[V^{\mu\nu}[A_\mu, u_\nu]] . \qquad (3.29)$$

While the first term on the right hand side of Eq.(3.28) has again already been written down in [EGL$^+$89], one can find different approaches in the literature in order to describe the a_1 decay vertex. Before we will comment on the other works, we will first explain the structure of our terms. Since we want to describe the decay of an axial-vector meson into a Goldston boson and a vector meson, we need one axial-vector field, one vector field and u_μ, which contains the Goldstone boson fields. Demanding a minimum number of derivatives, one is led to the terms above without the specific ordering. In addition the term has to be C-invariant, which leads to the commutator, which can be seen as follows

$$\mathrm{Tr}[V^{\mu\nu}A_\mu u_\nu] \xrightarrow{C} \mathrm{Tr}[(-V^{\mu\nu T})A_\mu^T u_\nu^T] = -\mathrm{Tr}[u_\nu A_\mu V^{\mu\nu}] = -\mathrm{Tr}[V^{\mu\nu}u_\nu A_\mu]\,. \tag{3.30}$$

Since u_μ transforms as an axial-vector under parity, the invariance under parity transformations can also be seen directly.

Looking at Eq.(3.28) we see that both terms describing the decay into vector and pseudoscalar meson contain a u^μ. This means that integrating out the a_1 would generate to lowest order an interaction term of vector mesons and Goldstone bosons, which contains two u^μ and therefore leads to an expression of order $\mathcal{O}(q^2)$. Since the WT term is $\mathcal{O}(q^1)$ including both interactions is not double counting. This will become important in the discussion of the results in Chapter 7.

In [RPO04] the authors propose a phenomenological Lagrangian in terms of tensor fields, which is successful in reproducing the decay branching ratios. In [KM90] the hidden symmetry formalism was used to derive the pertinent terms, which yields the same results as the phenomenological approach. Comparing our Lagrangian to these works, we find agreement by choosing

$$c_1 = -\frac{1}{4}\,, \quad c_2 = -\frac{1}{8}\,. \tag{3.31}$$

We will come back to that relation, when we discuss the calculation using an explicit a_1 in Section 6.5 and when we look at the results in Section 7.3.

In [GDPP04] the WCCWZ scheme with tensor fields is used to write down the most general Lagrangian including axial-vector fields. Using tensor fields, one is led to terms with more derivatives in that case and more possible terms, namely five terms. Therefore it is more useful to compare directly the matrix elements and see if nevertheless the same structures appear. This is done in Chapter 6 and we find that their choice of parameters corresponds to

$$c_1 = 0\,, \quad c_2 = -\frac{1}{4}\,. \tag{3.32}$$

These values, however, have to be handled with care, since due to the additional structures in [GDPP04] a one-to-one comparison is not possible (see Chapter 6).

3.2. Vector vs tensor formulation

As already mentioned, power counting in the presence of vector mesons depends on the choice of interpolating fields, in particular whether one uses vector or tensor fields [EGL$^+$89]. This issue will be discussed in the present section. The tensor field Lagrangian, fitting our needs, is

$$\mathcal{L}_{tensor} = \frac{M^2}{8}\,\mathrm{Tr}[W_{\mu\nu}W^{\mu\nu}] - \frac{1}{4}\,\mathrm{Tr}[\partial^\lambda W_{\lambda\mu}\partial_\nu W^{\nu\mu}] + \mathrm{Tr}[W_{\mu\nu}\tilde{j}^{\mu\nu}] \tag{3.33}$$

with

$$\tilde{j}^{\mu\nu} = \frac{F_V}{4} f_+^{\mu\nu} + \frac{iG_V}{4}[u^\mu, u^\nu] \,. \tag{3.34}$$

According to the power counting considerations before, we see that for example the contribution to pion scattering from this Lagrangian contributes already at $\mathcal{O}(q^4)$, since the vertex for the ρ decay into two pions appears with one derivative less. In principle, one could also introduce $\mathcal{O}(q^4)$ contact terms, but using arguments concerning the high-energy behaviour of the pion form factor, these terms are discussed away [EGL$^+$89]. In the vector field formalism, where the contributions to pion scattering even started at $\mathcal{O}(q^6)$, one can of course also introduce additional $\mathcal{O}(q^4)$ contact terms. In the following, we will see that this is even necessary in order to connect to the tensor field Lagrangian.

In order to show the relation between the vector and the tensor formulation, we will transform the vector meson Lagrangian into a Lagrangian using antisymmetric tensor fields. We start with a Lagrangian of the form

$$\mathcal{L} = -\frac{1}{8} \operatorname{Tr}[V_{\mu\nu} V^{\mu\nu}] + \frac{M^2}{4} \operatorname{Tr}[V_\mu V^\mu] + \operatorname{Tr}[V_{\mu\nu} j^{\mu\nu}] \tag{3.35}$$

with

$$j^{\mu\nu} = -\frac{f_V}{4} f_+^{\mu\nu} - \frac{ig_V}{4}[u^\mu, u^\nu], \tag{3.36}$$

which of course corresponds to the Lagrangian we are going to use (cf. Eq.(3.18)). The masses M^2 of the vector mesons in the octet were chosen to be the same for simplicity. In principle, one can write down a separate mass term for every vector particle, but since we are mainly interested in the higher order term resulting from the transformation, choosing one average mass is sufficient. The transformation, which follows, is suitable especially for that kind of interaction. The coupling of the current to the vector meson can also be written as

$$\operatorname{Tr}[V_{\mu\nu} j^{\mu\nu}] = \operatorname{Tr}[\partial_\mu V_\nu (j^{\mu\nu} - j^{\nu\mu})] \to -\operatorname{Tr}[V_\nu \partial_\mu (j^{\mu\nu} - j^{\nu\mu})] = \operatorname{Tr}[V_\nu \tilde{j}^\nu] \tag{3.37}$$

with

$$\tilde{j}^\nu = \partial_\mu (j^{\mu\nu} - j^{\nu\mu}) \,. \tag{3.38}$$

Thus, we can also assume the general form of the coupling to be $\operatorname{Tr}[V^\mu j_\mu]$ and then transform the Lagrangian. That procedure is chosen in [Leu07] and works in principle the same way. However, in that way one introduces additional derivatives, which ruins the high-energy behaviour. In case the interactions can be written as $\operatorname{Tr}[V^\mu j_\mu]$ without partial integration, the vector field formalism will produce less derivatives, and therefore it will have the better high-energy behaviour. Thus, by choosing the interpolating fields, one should also consider the kind of interactions, one is dealing with. One should not blindly argue with the better high-energy behaviour of the tensor field formalism for any kind of Lagrangian. Nevertheless, an argument for favouring the tensor field formalism, which is always valid, is the inherent projection on transverse states.

The transformation, which follows, is only suited for terms including one vector field. A discussion on transformations covering a broader spectrum of interaction terms can be found in [KNT07]. We start with the introduction of an antisymmetric tensor field $W'_{\mu\nu}$ by adding $\frac{1}{8} W'_{\mu\nu} W^{\mu\nu\prime}$ to the Lagrangian. Then we replace the field by the shifted tensor field $W_{\mu\nu}$

$$W_{\mu\nu} = W'_{\mu\nu} - V_{\mu\nu} - \alpha j^{\mu\nu} \,, \tag{3.39}$$

which leads to the following Lagrangian

$$
\begin{aligned}
\mathcal{L}' = {} & \frac{1}{8} \operatorname{Tr}[W_{\mu\nu} W^{\mu\nu}] + \frac{M^2}{4} \operatorname{Tr}[V_\mu V^\mu] + \operatorname{Tr}[V_{\mu\nu} j^{\mu\nu} (1 + \frac{1}{4}\alpha)] \\
& + \frac{1}{4}\alpha \operatorname{Tr}[W_{\mu\nu} j^{\mu\nu}] + \frac{1}{8}\alpha^2 \operatorname{Tr}[j_{\mu\nu} j^{\mu\nu}] + \frac{1}{2} \operatorname{Tr}[W_{\mu\nu} \partial^\mu V^\nu]
\end{aligned} \tag{3.40}
$$

Now we want to choose α such that $V_{\mu\nu}$ decouples from the other fields, i.e. from $j^{\mu\nu}$, which is the case for $\alpha = -4$. Using partial integration, we move the derivative in the last term on the tensor field and arrive at

$$
\mathcal{L}' = \frac{1}{8} \operatorname{Tr}[W_{\mu\nu} W^{\mu\nu}] + \frac{M^2}{4} \operatorname{Tr}[V_\mu V^\mu] - \operatorname{Tr}[W_{\mu\nu} j^{\mu\nu}] - \frac{1}{2} \operatorname{Tr}[\partial^\nu W_{\nu\mu} V^\mu] + 2 \operatorname{Tr}[j_{\mu\nu} j^{\mu\nu}] \tag{3.41}
$$

Now we introduce V_μ'

$$
V_\mu' = V_\mu - \frac{1}{M^2} \partial^\lambda W_{\lambda\mu} \,,
$$

and we see that we can integrate out V_μ' easily, since it does not interact with any other particle. Thus, we get

$$
\mathcal{L}'' = \frac{1}{8} \operatorname{Tr}[W_{\mu\nu} W^{\mu\nu}] - \frac{1}{4M^2} \operatorname{Tr}[\partial^\lambda W_{\lambda\mu} \partial_\nu W^{\nu\mu}] - \operatorname{Tr}[W_{\mu\nu} j^{\mu\nu}] + 2 \operatorname{Tr}[j_{\mu\nu} j^{\mu\nu}] \,. \tag{3.42}
$$

We renormalise the tensor field such that it describes a proper spin 1 particle

$$
W_{\mu\nu} = M \tilde{W}_{\mu\nu} \,, \tag{3.43}
$$

and arrive at the final Lagrangian

$$
\mathcal{L}'' = \frac{M^2}{8} \operatorname{Tr}[\tilde{W}_{\mu\nu} \tilde{W}^{\mu\nu}] - \frac{1}{4} \operatorname{Tr}[\partial^\lambda \tilde{W}_{\lambda\mu} \partial_\nu \tilde{W}^{\nu\mu}] - M \operatorname{Tr}[\tilde{W}_{\mu\nu} j^{\mu\nu}] + 2 \operatorname{Tr}[j_{\mu\nu} j^{\mu\nu}] \,. \tag{3.44}
$$

We can make contact to the tensor field Lagrangian of Eq.(3.33) by identifying $f_V = \frac{F_V}{M}$ and $g_V = \frac{G_V}{M}$. However, there is one difference, namely the contact terms contained in $\operatorname{Tr}[j_{\mu\nu} j^{\mu\nu}]$. The contribution of these terms to our calculation is discussed in Chapter 6. It will turn out that these contact terms are necessary to get a reasonable high-energy behaviour.

The entire Lagrangian we are going to use in the bound-state scenario is

$$
\mathcal{L} = \mathcal{L}_{vec} + \mathcal{L}_2 - 2 \operatorname{Tr}[j_{\mu\nu} j^{\mu\nu}] \,, \tag{3.45}
$$

where $\mathcal{L}_2$ is lowest order CHPT Lagrangian defined in Eq.(2.41) and $\mathcal{L}_{vec}$ is defined in Eq.(3.18). This Lagrangian (3.45) is equivalent to $\mathcal{L}_2$ plus the corresponding tensor field Lagrangian (3.33). In case we explicitly include the a_1, we have an additional term

$$
\mathcal{L}_{a1} = \mathcal{L}_{vec} + \mathcal{L}_2 - 2 \operatorname{Tr}[j_{\mu\nu} j^{\mu\nu}] + \mathcal{L}_{axial} \tag{3.46}
$$

with $\mathcal{L}_{axial}$ given in Eq.(3.28).

3.3. Renormalisation in the presence of spin-1 fields

As we will discuss in Chapter 5, the treatment of the final state interactions in the τ decay involves a summation of loop diagrams. These loops lead to divergent expressions, which need to be renormalised. While this is a straightforward procedure in CHPT, the renormalisation in the presence of vector mesons, or heavy particles in general, requires some explanation.
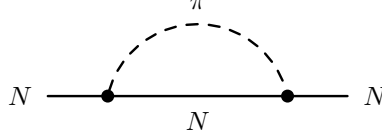
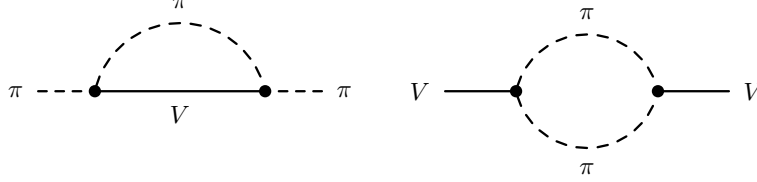**Figure 3.1.:** Pion-loop contribution to the nucleon self energy.

Figure 3.2.: Example of self-energy graphs including vector mesons, which have no analog in the meson-baryon sector.

3.3.1. Powercounting for loop diagrams

In CHPT the expansion in momentum can be mapped onto an expansion in terms of tree and loop graphs, with the chiral order of a graph given by [Sch03]

$$D = \sum_n V_n(n - 2) + 2L + 2 \tag{3.47}$$

with L the number of loops and V_n the number of vertices of order $\mathcal{O}(p^n)$. In the presence of a heavy mass scale in the loops this power counting breaks down. The problem was first tackled in the meson-baryon sector [GSS88], where one found that loop graphs might start at the same order as the corresponding tree graphs. In particular, it was found that the nucleon mass requires renormalisation at every order in the loop expansion. The loop in Fig. 3.1 already generates an infinite contribution to the nucleon mass, even in the chiral limit. Several solutions have been proposed, as the infrared regularization scheme (IR) [BL99], the Extended On-Mass-Shell Renormalization (EOMS) [FGJS03] and the χ-BS(3) approach [LK02]. We do not want to discuss the different methods in detail, since that has been done in the references quoted above, but we will address the consequences for the renormalisation of the loop diagrams in the present calculation.

When dealing with vector mesons instead of baryons, one encounters in general an additional complication. Due to baryon number conservation a baryon in the loop is always connected to an external baryon. In that case the momentum w in the loop, as for example in Eq.(3.48) below, belongs to a heavy particle. For vector mesons new classes of graphs might appear (see Fig. 3.2), where an external Goldstone boson can be connected to a heavy particle in the loop or two Goldstone bosons in the loop can be connected to a vector meson. For a discussion of these diagrams and an extension of the IR scheme, we refer to [BM05]. The loops appearing in our work, however, can be treated in analogy to the meson-baryon sector.

The basic idea to restore power counting in the above prescriptions is to perform additional subtractions in the renormalisation of the diagrams. These subtractions are chosen such that the diagrams contribute to the desired order. These additional subtractions have to be analytic in the small variables in order to be realisable by counterterms of the Lagrangian. That this is indeed the case has been shown in the references quoted above. In the χ-BS(3) scheme the additional subtractions are realised in dimensional regularisation through the subtraction of

a pole appearing in three dimensions. In IR the loop integrals are split in a so called infrared singular part and a regular part, where the regular part is the power counting violating term associated with the heavy mass scale in the loop, which is dropped. In EOMS the power counting violating terms are identified and shown to be analytic by a suitable expansion of the loop integrals. All prescription agree to the desired order but may differ in additional contributions from higher orders. This is due to the fact that the loop integrals, which contain a heavy mass scale, might contribute to all orders and since one only demands to be accurate to a certain order, there is some freedom in dealing with the higher order terms.

The easiest example and also the divergent loop integral, we encounter in our work, is the scalar loop integral including one vector meson (or one heavy particle)

$$I_{\phi V}(w) = i \int \frac{d^4 l}{(2\pi)^4} \frac{1}{(l-w)^2 - M_\phi^2 + i\epsilon} \frac{1}{l^2 - M_V^2 + i\epsilon} \, . \tag{3.48}$$

The expected order of this integral is determinded as follows: The integration in 4 dimensions counts as $\mathcal{O}(q^4)$, the Goldstone boson propagator as $\mathcal{O}(q^{-2})$ and the vector meson propagator as $\mathcal{O}(q^{-1})$. The order of the vector meson propagator stems from the fact that in case the internal lines are connected to a heavy particle, this means

$$w^2 - M_V^2 = \mathcal{O}(q) \, . \tag{3.49}$$

This counting shows that in the presence of a heavy particle Eq.(3.47) cannot hold anymore and the integral in Eq.(3.48) is expected to have chiral order $\mathcal{O}(q)$. Without additional subtractions, however, it contributes already at $\mathcal{O}(q^0)$. In all the above schemes that contribution would be subtracted with the argument that it already has been included in the most general chiral Lagrangian, and therefore it is taken care of by a suitable counterterm. In our scheme we only include the Weinberg-Tomozawa term and that term is not the suitable counter-term, which can take care of the additional subtraction. Thus by choosing the subtraction for the loop diagram, we simulate part of the higher order terms, which we do not include. In particular, that means it is not a hard constraint to choose the renormalisation such that $I_{\phi V} \sim \mathcal{O}(q)$. Of course, it would be unreasonable to use arbitrarily big subtractions, but one has the freedom to vary the renormalisation parameter in a suitable range. We will come back to that point in Chapter 7.

3.3.2. Crossing symmetry

Since we do not include the suitable counterterms in our calculation, the renormalisation parameter, which could be for example a subtraction point, is a free parameter. We now want to look at an argument, which puts a constraint on the parameter, which renormalises the amplitude of a Goldstone boson scattering off a vector meson. More details about this renormalisation condition can be found in [LK02, LK04].

In an exact theory the amplitude, which one calculates, should be crossing symmetric. Since in our calculation, we neglect the *u*-channel cut (left-handed cut [OO99]) and consider only the *s*-channel cut, as will be explained in detail in Chapter 4, our amplitudes will not be crossing symmetric by construction. The basic assumption, which that approximation relies on, is that in an energy region where the loop diagrams do not develop a cut, the loops can be neglected. This means our calculation is reliable in the region of the *s*-channel cut and in the low-energy region, where no cut is present. An analogous calculation could be done by summing the *u*-channel diagrams, which should then be valid in the region of the *u*-channel

cut and again in the low-energy region. Thus, the amplitudes should match in the region between the cuts. If we choose our subtraction scheme such that

$$T_{\mu\nu}(s_0) = K_{\mu\nu}(s_0) \tag{3.50}$$

for an s_0 in the region of no cuts, i.e. $s_{left} < s_0 < s_{right}$, then the matching is guaranteed. In Eq.(3.50) $T_{\mu\nu}$ is the unitarised scattering amplitude and $K_{\mu\nu}$ the lowest order expression. Furthermore $s_{left/right}$ is the threshold for the appearance of the left-/right-handed cut. That means, we match the unitarised scattering amplitude with the perturbative amplitude at sub-threshold energies. Of course, it also automatically recovers the perturbative nature of the amplitude near threshold.

Another way to put the last constraint is that the one-loop correction should not be unnaturally large by choosing a peculiar renormalisation. In other words the one-loop correction should not be larger than the lowest order result itself.

Chapter 4.

Chiral Unitarity

In this chapter we discuss the framework for describing the final state interactions of the hadrons. The final state is dominated by resonance structures, and therefore a perturbative calculation can not describe the process. Assuming that the resonance structure is generated dynamically, one needs a proper way of resumming the strong rescattering effects. A prominent way of treating these interactions is to impose unitarity constraints together with constraints from chiral symmetry on the scattering amplitude. The success of that approach seems to indicate that unitarity is responsible for the structures appearing in the final state. We will show how to derive the most general form of a partial wave amplitude fulfilling unitarity, when the left-hand cut is neglected, by using the N/D method [OO99]. That amplitude will then be matched to the lowest order expression of a chiral expansion. Another common scheme to describe the rescattering is to solve a Lippmann-Schwinger equation or a Bethe-Salpeter equation with potentials fixed from chiral symmetry breaking [OO97, RPO04, LK04]. We will also discuss that approach and comment on the equivalence of that method to the N/D prescription. We will also address briefly the inverse amplitude method and describe its relation to the other methods.

4.1. Unitarity and helicity amplitudes

As already mentioned, we want to use unitarity to constrain the scattering amplitude. Since we are dealing with spin-1 particles, we will briefly derive the unitarity condition for helicity amplitudes. Defining the T-matrix as $S = \mathbb{1} + iT$, the unitarity condition reads

$$-i(T - T^\dagger) = TT^\dagger \,. \tag{4.1}$$

Now we sandwich the T-matrix between two two-particle states with momenta p_1, p_2 and k_1, k_2 and insert a complete set of states between $T^\dagger T$. Thus we get

$$-i\langle p_1, p_2|T|k_1, k_2\rangle + i\langle p_1, p_2|T^\dagger|k_1, k_2\rangle = \sum_n \left(\prod_{i=1}^n \int \frac{d^3 q_i}{(2\pi)^3} \frac{1}{2E_i}\right) \langle p_1 p_2|T^\dagger|\{q_i\}\rangle\langle\{q_i\}|T|k_1 k_2\rangle \,. \tag{4.2}$$

The only intermediate states we consider are two-particle states (which is the first simplification), and for the moment we also omit the coupled channels, which we will talk about later. Therefore, we can write

$$- i(M(k_1 k_2 \to p_1 p_2) - M^*(p_1 p_2 \to k_1 k_2))$$
$$= (2\pi)^4 \left(\prod_{i=1}^2 \int \frac{dq_i^3}{(2\pi)^3} \frac{1}{2E_i}\right) M^*(p_1 p_2 \to q_1 q_2) M(k_1 k_2 \to q_1 q_2)\delta(k_1 + k_2 - \sum q_i) \tag{4.3}$$

times an overall $\delta(k_1 + k_2 - p_1 - p_2)$. The invariant matrix element M is defined in Eq.(A.26). Since in our case one particle is a vector meson, we have to take into account the polarisation of the states. The matrix element can be expanded in the centre-of-mass system (CMS) in helicity amplitudes as follows (see Appendix A and [JW59])

$$M(k_1 k_2, \lambda \to p_1 p_2, \overline{\lambda}) = \sum_{JM} \frac{2J+1}{4\pi} D^*_{M\overline{\lambda}}(\overline{\phi}, \overline{\theta}, -\overline{\phi}) D_{M\lambda}(\phi, \theta, -\phi) M^{JM}_{\overline{\lambda}\lambda}. \tag{4.4}$$

For the left hand side of Eq.(4.3) we can choose $\phi = \overline{\theta} = \overline{\phi} = 0$ and θ to be the angle between the incoming and outgoing vector particle. On the right hand side, we have to integrate over arbitrary angles and we will use the orthogonality relation of the Wigner functions Eq.(A.46). Plugging in everything, we get

$$2\sum_J \frac{2J+1}{4\pi} d^J_{\overline{\lambda}\lambda} \Im M^J_{\overline{\lambda}\lambda} = \frac{p_{cm}}{16\pi^2\sqrt{s}} \sum_J \sum_{\lambda'} \frac{(2J+1)}{4\pi} d^J_{\overline{\lambda}\lambda}(\theta) M^{*J}_{\lambda'\overline{\lambda}} M^J_{\lambda'\lambda}, \tag{4.5}$$

where the d-functions are the simplified Wigner functions, defined in Appendix A.3 and s is the total invariant energy. p_{cm} is the centre-of-mass momentum given by

$$p_{cm} = \frac{1}{2\sqrt{s}} \sqrt{(s - (M_V + m_\phi)^2)(s - (M_V - m_\phi^2)^2)} \tag{4.6}$$

with the vector meson mass M_V and the Goldstone boson mass m_ϕ. Comparing coefficients, we get

$$2\Im M^J_{\overline{\lambda}\lambda} = \frac{p_{cm}}{16\pi^2\sqrt{s}} \sum_{\lambda'} M^{*J}_{\lambda'\overline{\lambda}} M^J_{\lambda'\lambda}. \tag{4.7}$$

So far we have nine equations for nine unknown matrix elements. From parity invariance, however, we know

$$M_{\overline{\lambda}\lambda} = M_{-\overline{\lambda}-\lambda}, \tag{4.8}$$

which reduces the independent matrix elements to five. Using

$$M^+_{00} = M_{00} \tag{4.9}$$

$$M^+_{01} = \frac{1}{\sqrt{2}}(M_{01} + M_{0-1}) = \sqrt{2}M_{01} \tag{4.10}$$

$$M^+_{10} = \frac{1}{\sqrt{2}}(M_{10} + M_{-10}) = \sqrt{2}M_{10} \tag{4.11}$$

$$M^+_{11} = M_{11} + M_{1-1} \tag{4.12}$$

$$M^-_{11} = M_{11} - M_{1-1} \tag{4.13}$$

the problem decouples to a problem involving the four matrix elements with the index $+$ and to an equation involving only M^-_{11}. M^-_{11} is the coefficient of the negative parity part (see Chapter 5 for more details), which we are not interested in, since we want to investigate the a_1, which has positive parity. Writing the helicity structure in matrix notation the positive parity part becomes

$$\Im M = M^*\sigma M, \tag{4.14}$$

with

$$\sigma = \frac{p}{32\pi^2\sqrt{s}}, \tag{4.15}$$

which is proportional to the two-particle phase space, and

$$M = \begin{pmatrix} M_{11} & M_{10} \\ M_{01} & M_{00} \end{pmatrix}, \tag{4.16}$$

where we dropped the index $+$, since it would just appear everywhere.

Including coupled channels, we only have to make slight changes. Looking at Eq.(4.2) or Eq.(4.3) we see that the matrix elements basically get another index indicating the channel. When we integrate over the phase space we also have to distinguish between the different channels. In our case we are dealing with two channels, and we get

$$\Im M = M^* \Sigma M \,, \tag{4.17}$$

where Σ is given by

$$\Sigma = \begin{pmatrix} \sigma_{\rho\pi} & 0 & 0 & 0 \\ 0 & \sigma_{KK^*} & 0 & 0 \\ 0 & 0 & \sigma_{\rho\pi} & 0 \\ 0 & 0 & 0 & \sigma_{KK^*} \end{pmatrix} \,, \tag{4.18}$$

and M reads

$$M = \begin{pmatrix} M_{1111} & M_{1211} & M_{1110} & M_{1210} \\ M_{2111} & M_{2211} & M_{2110} & M_{2210} \\ M_{1101} & M_{1201} & M_{1100} & M_{1200} \\ M_{2101} & M_{2201} & M_{2100} & M_{2200} \end{pmatrix} \,, \tag{4.19}$$

where the first two indices indicate the channel with

$$\text{channel } 1 : \ \rho\pi \tag{4.20}$$

$$\text{channel } 2 : \ KK^* \tag{4.21}$$

and the last two indices determine the helicity of the incoming and outgoing channel. The notation is chosen such that the indices denoting the outgoing channel always appear on the left, e.g. M_{1210} denotes the scattering amplitude for $(KK^*, \lambda = 0) \rightarrow (\pi\rho, \bar{\lambda} = 1)$. Note that $M = M^T$, since

$$M_{abij} = \langle a, i | T | b, j \rangle = \langle b, j | T | a, i \rangle = M_{baji} \,, \tag{4.22}$$

where $|a, i\rangle$ is a state of particles in channel a with the helicity of the vector meson i. The relation above relies on time reversal invariance, which is excellently discussed in e.g. [Tun85].

These equations only hold for $s > s_{threshold}$ and the cut is called the right-hand cut. We know from crossing symmetry that there is another cut on the left hand side. For $s < s_{left}$ we have

$$M_l(s + i\epsilon) - M_l(s - i\epsilon) = 2i\Im M_l(s). \tag{4.23}$$

4.2. N/D method

In this section we derive the most general structure of a partial wave amplitude, when the left-hand cut is neglected, by making use of the N/D method. The derivation is based upon [OO99].

In order to focus on the principles, we leave out the helicity and the coupled-channel structure for the moment. We will discuss the differences and modifications in that case afterwards. Dealing with one channel and scalar particles Eq.(4.14) can be written as

$$\Im T_L^{-1} = -\sigma(s) \,. \tag{4.24}$$

Here L is the angular momentum and T_L are the expansion coefficients of the expansion of the scattering amplitude in Legendre Polynomials P_L

$$T_L = \frac{2L+1}{2} \int M(s, \cos\theta) P_L(\cos\theta) d\cos\theta \tag{4.25}$$

and

$$M = \sum_L T_L(s) P_L(\cos\theta) \,. \tag{4.26}$$

We start by writing the partial wave amplitude as a quotient of two functions

$$T_L = \frac{N_L}{D_L} \,. \tag{4.27}$$

These functions are chosen such that N_L carries the left-hand cut and D_L bears the right-hand cut. Then we know that the imaginary parts obey the following equations

$$\begin{aligned} \Im D_L &= \Im T_L^{-1} N_L = -\sigma(s) N_L \,, \quad s > s_{th} \\ \Im D_L &= 0 \,, \quad s < s_{th} \end{aligned} \tag{4.28}$$

and

$$\begin{aligned} \Im N_L &= \Im T_L D_L \,, \quad s < s_{left} \\ \Im N_L &= 0 \,, \quad s > s_{left} \end{aligned} \tag{4.29}$$

Since we want to neglect the left-hand cut, we set $N_L = 1$ and describe the amplitude by D_L alone. Using a dispersion relation, we can write

$$D_L = \sum_{k=0}^{n-1} s^k a_k + \frac{s^n}{\pi} \int_{s_{th}}^{\infty} \frac{-\sigma(\zeta)}{\zeta^n(\zeta-s)} d\zeta \,, \tag{4.30}$$

where n is chosen such that

$$\left| \frac{D_L(s)}{s^n} \right| \overset{|s|\to\infty}{\longrightarrow} 0 \,. \tag{4.31}$$

This function describes the most general structure, when the left-hand cut is neglected, except in the case of the existence of zeros in T_L, which are not covered by Eq.(4.30). At these points $\Im D_L$ and therefore D_L is not known. In [CDD56] that problem is studied and solved by introducing the function α, which satisfies

$$\frac{d\alpha}{ds} = \Im D_L \,. \tag{4.32}$$

For the existence and properties of α see [CDD56] and references within. The imaginary part of D_L is known and continuous except at the zeros of T_L and therefore α is known between two zeros only up to a constant. Thus, it can be written as

$$\alpha(s) = -\int_{s_{th}}^{s} \sigma(\zeta) d\zeta + \sum_i \alpha(s_i) \Theta(s - s_i) \,. \tag{4.33}$$

Plugging Eq.(4.33) together with Eq.(4.32) into Eq.(4.30), we find

$$D_L = \sum_{k=0}^{n-1} s^k a_k + \frac{s^n}{\pi} \int_{s_{th}}^{\infty} \frac{-\sigma(\zeta))}{\zeta^n(\zeta-s)} d\zeta + \sum_i \frac{\alpha(s_i)}{\pi} \frac{s^n}{s_i^n} \frac{1}{s_i - s} \,. \tag{4.34}$$

Using

$$\frac{s^n}{s_i^n} \frac{1}{s_i - s} = -\frac{1}{s_i^n} \sum_{j=0}^{n-1} s^{n-1-j} s_i^j + \frac{1}{s_i - s} \, , \tag{4.35}$$

we see that we can absorb the first part into $\sum_{k=0}^{n-1} s^k a_k$ and change $a_k \to \tilde{a}_k$. Replacing $\frac{\alpha(s_i)}{\pi} = \gamma_i$, we get

$$D_L = \sum_{k=0}^{n-1} s^k \tilde{a}_k + \frac{s^n}{\pi} \int_{s_{th}}^{\infty} \frac{-\sigma(\zeta)}{\zeta^n(\zeta - s)} d\zeta + \sum_i \frac{\gamma_i}{s_i - s} \, . \tag{4.36}$$

Thus, the most general partial wave amplitude becomes

$$T_L = D_L^{-1} \tag{4.37}$$

$$D_L = \sum_{k=0}^{n-1} s^k \tilde{a}_k + \frac{s^n}{\pi} \int_{s_{th}}^{\infty} \frac{-\sigma(\zeta)}{\zeta^n(\zeta - s)} d\zeta + \sum_i \frac{\gamma_i}{s_i - s} \, . \tag{4.38}$$

The terms which appear in the last sum on the right hand side of Eq.(4.38) are usually called CDD-poles, named after the authors of [CDD56]. In [Gas75] these terms were linked to the existence of preexistent particles. These poles can also mimic the presence of zeros required by the underlying symmetries, as for example the Adler zeros of meson-meson scattering (see [OO99] and references within), which are however not of interest in our case.

Assuming that D_L is described by a once subtracted dispersion relation, we get

$$T_L = D_L^{-1}$$
$$D_L = \tilde{a}_0 + \frac{s}{\pi} \int_{s_{th}}^{\infty} \frac{-\sigma(\zeta)}{\zeta(\zeta - s)} d\zeta + \sum_i \frac{\gamma_i}{s_i - s} \, . \tag{4.39}$$

We split the constant $\tilde{a}$ in two parts $\tilde{a} = a_{tree} + a_{loop}$ and define

$$g(s) = a_{loop} + \frac{s}{\pi} \int_{s_{th}}^{\infty} \frac{-\sigma(\zeta)}{\zeta(\zeta - s)} d\zeta \, . \tag{4.40}$$

The function $g(s)$ can be associated with the scalar loop function $I_{\phi V}(s)$ given in Eq.(3.48) since both have the same cut and the same imaginary part along the cut, which can be deduced from the optical theorem [PS95]. The dependence of the loop function on the regularisation scale or the subtraction point is translated into the free choice of the constant a_{loop}. After that association one is pushed to identify the remaining terms as the tree contributions of the scattering amplitude. One could use large-N_C (N_C=number of colours in QCD) arguments to make the argument sound more fancy, but in principle one also just identifies the integral in Eq.(4.40) with the loops, which would then be suppressed and the remaining terms correspond again to contact and pole terms, which remain in the large-N_C limit. Defining

$$K = \left(a_{tree} + \sum_i \frac{\gamma_i}{s_i - s} \right)^{-1} , \tag{4.41}$$

we get

$$T_L = \left[\frac{1}{K} + g(s) \right]^{-1} = \frac{K}{1 + Kg(s)} \, , \tag{4.42}$$

which is identical with the solution of the Bethe-Salpeter equation, in case the kernel K factorises out of the integral (see Section 4.4).

Now we turn to the full problem by also including the coupled-channel and helicity structure. Including the helicity structure and coupled channels the unitarity relation was given in Eq.(4.17). The equation can be rewritten in the form

$$\Im M^{-1} = -\Sigma\,.\tag{4.43}$$

Thus, we have a dispersion relation for every entry of M^{-1}, where the imaginary parts only appear on the diagonals. Using a once subtracted dispersion relation, we get

$$T_{ij}^{-1} = -\delta_{ij}\left(a_i + \frac{s}{\pi}\int_{s_{th_i}}^{\infty}\frac{\rho_i(\zeta)}{\zeta(\zeta - s)}d\zeta\right) + K_{ij}^{-1}\,,\tag{4.44}$$

where $\rho_1 = \rho_3 = \sigma_{\pi\rho}$ and $\rho_2 = \rho_4 = \sigma_{K^*K}$. K_{ij}^{-1} contains all the subtraction constants and contributions from CDD-poles. Using matrix notation the formula looks more familiar

$$T = (1 + KG)^{-1}K\tag{4.45}$$

with

$$G_{ij} = \delta_{ij}i\int\frac{d^4l}{(2\pi)^4}\frac{1}{l^2 - M_i^2 + i\epsilon}\frac{1}{(w - l)^2 - m_i^2 + i\epsilon} = -\delta_{ij}\left(a_i + \frac{s}{\pi}\int_{s_{th_i}}^{\infty}\frac{\rho_i(\zeta)}{\zeta(\zeta - s)}d\zeta\right)\,.\tag{4.46}$$

Again, we can make the identification of K with the contact and pole terms present before unitarisation and remaining in the Large N_C limit. Expanding that equation, we get

$$T = K - KGK \pm \dots\,.\tag{4.47}$$

We note that we can match that expression to lowest order CHPT, in which case K is nothing but the lowest order scattering contribution and the remaining terms correspond to the sum of loop diagrams resulting from the iteration of the lowest order interaction (see Section 4.4).

4.3. Inverse amplitude method

There is another method, which is capable of extending CHPT to higher energies, the inverse amplitude method (IAM). We will briefly review the derivation of that method [GNP02] in order to be able to pin down the differences to the N/D method. We will write everything in a matrix notation, which includes the helicity and the coupled-channel structure. We start by looking at the inverse amplitude, which after using the unitarity constraint to substitute the imaginary part of the inverse amplitude, can be written as

$$T^{-1} = \Re T^{-1} - i\Sigma\,.\tag{4.48}$$

The crucial step is now to approximate the inverse of the real part by an expansion scheme, e.g. by chiral perturbation theory, as follows

$$\Re T^{-1} = \Re(T_1 + T_2 + \dots)^{-1} = \Re(T_1^{-1}(1 + (T_2 + \dots)T_1^{-1})^{-1}) = T_1^{-1}(1 - \Re(T_2)T_1^{-1}) + \dots\,,\tag{4.49}$$

where we used that the lowest order contribution T_1 consists of tree graphs, i.e. $\Im T_1 = 0$. Pluggin this equation into Eq.(4.48), yields

$$T \simeq (T_1^{-1}(1 - \Re(T_2)T_1^{-1}) - i\Sigma)^{-1} = T_1(T_1 - T_2)^{-1}T_1\,.\tag{4.50}$$

We used that

$$\Im T_2 = T_1 \Im G T_1 \,, \tag{4.51}$$

which is the perturbative unitarity relation. By comparing Eq.(4.50) and Eq.(4.45), we see that the methods in general will produce different results, which is of course not a big surprise, since the approximations, which have been used, are not the same. However, if

$$\Re T_2 = T_1 \Re G T_1 \tag{4.52}$$

and $K = T_1$, the methods agree. Using CHPT, the IAM includes in addition to the loop diagrams, also the contact terms of higher order, which might be partly simulated through the regularisation parameter but not completely and not in general. In [OO99], for instance, using the N/D method, the ρ could not be generated dynamically with a suitable cutoff. It has to be included as a preexistent particle. On the other hand the IAM method can reproduce the ρ [GNP02], if one uses CHPT up to order $\mathcal{O}(q^4)$. As we have briefly discussed in Section 3.2, the ρ can be understood to mediate the $\mathcal{O}(q^4)$ contact terms (at least in the tensor formulation) [EGL$^+$89]. Thus the IAM is capable to reconstruct a resonance from its low-energy appearance.

In the following we will explain how the inverse amplitude method works by looking at a toy model [OOP99]. We assume the amplitude has the following structure

$$T = \frac{ap^2}{q^2 - M^2 + i2M\Gamma} \,, \tag{4.53}$$

where q^2 is the total invariant energy squared of, for example, a meson pair, p^2 is an invariant quantity of dimension momentum squared related to the momenta and masses of the mesons, and $2M\Gamma = -ap^2\Im G$, where G is the two-meson propagator defined in Eq.(4.46). Using the IAM formalism with

$$T_1 = -a\frac{p^2}{M^2} \tag{4.54}$$

and

$$\Re T_2 = -\frac{ap^2 q^2}{M^4} = T_1 \frac{q^2}{M^2} \,, \tag{4.55}$$

we get

$$T = \frac{T_1^2}{T_1 - \Re T_2 - iT_1\Im G T_1} = \frac{ap^2}{q^2 - M^2 + i2M\Gamma} \,, \tag{4.56}$$

which is the exact result. That explains of course why the method is successful in describing the resonance structure, but it does not tell us anything about the nature of the resonances. The method is able to produce the kind of structure in Eq.(4.53), but that structure could be present because of a real resonance or it could be produced by some rescattering mechanism. Since our aim is to figure out the nature of a resonance, we will not use the IAM. The N/D method offers a cleaner interpretation of the structure, which appears, since it can be connected to the Bethe-Salpeter equation and therefore to potential scattering, with the potential given by the lowest order interaction. Especially when we use the WT term as the driving force, we can be sure that no preexistent resonance has its footprints in that process. In the next section, we will see the connection of the N/D method to the Bethe-Salpeter equation in detail.
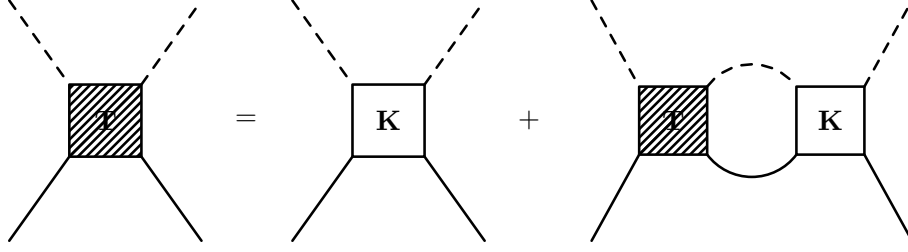
Figure 4.1.: Diagrammatic form of the Bethe-Salpeter equation.

4.4. The Bethe-Salpeter equation

The Bethe-Salpeter equation was originally derived in [SB51]. It is the relativistic analogon to the integral form of the two-body Schrödinger equation. We do not want to derive the equation, but we want to say a few words on its structure, which in principle is enough to convince oneself that the equation is correct. Before we write down the equation, we define a class of diagrams, namely the two-particle irreducible diagrams. We will define these diagrams in the case of Goldstone boson vector-meson scattering, but it should be obvious how to extend the definition to other processes. This class exists of all diagrams with two external pseudoscalar meson and two external vector meson lines with the exception of two classes of diagrams. The first kind of diagrams, which are excluded, are the ones which fall apart by an equal-time cut of one vector meson propagator and one Goldstone boson propagator. The other kind of diagrams, which are excluded, are the disconnected diagrams. The equation which expresses the scattering amplitude in terms of the kernel K, which is given by the two-particle irreducible diagrams, is called the Bethe-Salpeter equation (Fig. 4.1)

$$T^{\mu\nu}(\bar{p}, p, w) = K^{\mu\nu}(\bar{p}, p, w) + \int \frac{d^4l}{(2\pi)^4} K^{\mu\alpha}(\bar{p}, l, w) G_{\alpha\beta}(l, w) T^{\beta\nu}(l, p, w) \,, \qquad (4.57)$$

where $p\,(\bar{p})$ is the incoming (outgoing) momentum of the vector meson, w the total four-momentum and

$$G_{\alpha\beta} = i \frac{1}{(w-l)^2 - m_\phi^2 + i\epsilon} \frac{g_{\alpha\beta} - \frac{l_\alpha l_\beta}{M_V^2}}{l^2 - M_V^2 + i\epsilon} \qquad (4.58)$$

the product of propagators. M_V is the mass of the vector meson and m_ϕ is the mass of the Goldstone boson. For the moment, we leave out the coupled-channel structure. The full coupled-channel version of the Bethe-Salpeter equation is given in Eq.(4.70) below.

So far that equation is just a shift of the problem of evaluating the scattering amplitude to the problem of evaluating the kernel. However, that equation offers another kind of approximation for the purpose of practical calculations. Instead of doing perturbation theory for the scattering amplitude, one can do it for the kernel. That amounts to the summation of a certain kind of loop diagrams, namely the ones which have a right-hand cut. In Fig. 4.2 one can see the kind of diagrams, which are summed up, if the lowest order approximation to the kernel is just a contact term.

Calculating the kernel in perturbation theory, we can write down the equation easily but in general the equation is still not easily solvable for non-separable kernels, i.e. $K(p, \bar{p}) \neq K_1(p)K_2(\bar{p})$. In addition, the tensor structure leads to complications. However, since we are usually only interested in the lowest partial waves of the scattering, a partial wave expansion is reasonable.
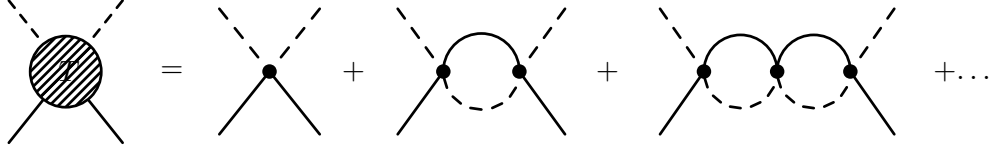
Figure 4.2.: Iteration of loop diagrams by using lowest order interaction for the kernel.

In order to establish a closer relationship to potential scattering, we shortly recall the analogous formulas in non-relativistic scattering theory. In quantum mechanics one usually deals with a Hamiltonian of the form

$$H = H_0 + V \,, \tag{4.59}$$

where the eigenstates ϕ_a of H_0 are known and V is a potential between, for example, two particles. The Lippmann-Schwinger equation then reads

$$|\psi_a^\pm\rangle = |\phi_a\rangle + G^\pm V |\psi_a^\pm\rangle \,, \tag{4.60}$$

where $|\psi_a^\pm\rangle$ are the unknown eigenstates of the total Hamiltonian and

$$G_a^\pm = \frac{1}{E_a - H_0 \pm i\epsilon} \,. \tag{4.61}$$

The epsilon prescription guarantees that G is well defined, $|\psi_a^+\rangle$ corresponds to a state propagating away from the scattering region and $|\psi_a^-\rangle$ denotes a state propagating towards the scattering region. The S matrix is defined as

$$S(a,b) \equiv \langle \psi_a^- | \psi_b^+ \rangle = \delta(a-b) - 2\pi i \delta(E_a - E_b) T(a,b) \tag{4.62}$$

where T contains the interesting part of the scattering process. Using Eq.(4.60) and Eq.(4.62) one finds that the T matrix is given by

$$T(a,b) = \langle \phi_a | V | \Psi_b^+ \rangle \tag{4.63}$$

or

$$T |\phi_a\rangle = V |\psi_a^+\rangle \,. \tag{4.64}$$

Using again Eq.(4.60) and Eq.(4.64) one finds the following equation for T

$$T = V + V G^+ T \,, \tag{4.65}$$

which obviously is very similar to the Bethe-Salpeter equation.

4.4.1. Partial wave expansion

A partial wave expansion of the scattering amplitude and the kernel leads to two complications. First of all, one has to make sense of the expansion of an object with Lorentz indices, and secondly, the particles in the loops are offshell. We will discuss these problems in detail in Chapter 5 and also in Appendix B.

For the moment we assume that we can expand the kernel and the scattering amplitude into projectors $Y_{ij}^{\mu\nu(JMP)}$

$$K_{ab}^{\mu\nu}(q, \overline{q}, w) = \sum_{J,M,P,i,j} V_{abij}^{(JMP)}(s) Y_{ij}^{\mu\nu(JMP)}(q, \overline{q}, w) \,, \tag{4.66}$$

31

$$T_{ab}^{\mu\nu}(q,\overline{q},w) = \sum_{J,M,P,i,j} M_{abij}^{(JMP)}(s) Y_{ij}^{\mu\nu(JMP)}(q,\overline{q},w) \,, \tag{4.67}$$

which fulfil the following orthogonality relation

$$\int \frac{d^4l}{(2\pi)^4} Y_{\lambda_1\lambda_2\mu\alpha}^{JMP}(\overline{q},l,w) G^{\alpha\beta}(l,w) Y_{\lambda_3\lambda_4\beta\nu}^{J'M'P'}(l,q,w)$$
$$= \delta_{\lambda_2\lambda_3}\delta_{PP'}\delta_{JJ'}\delta_{MM'} Y_{\lambda_1\lambda_4\mu\nu}^{JMP}(\overline{q},q,w)(-I_{\phi V}) \,. \tag{4.68}$$

We recall that $I_{\phi V}$ is given by

$$I_{\phi V} = i \int \frac{d^4l}{(2\pi)^4} \frac{1}{(l-w)^2 - M_\phi^2 + i\epsilon} \frac{1}{l^2 - M_V^2 + i\epsilon} \,. \tag{4.69}$$

The indices a,b correspond to the channels $\pi\rho$ and KK^*, where T^{ab} denotes a scattering $b \to a$, J is the total angular momentum, M its projection, P the parity and i,j are the helicities of the incoming and outgoing channel. The coupled-channel version of the Bethe-Salpeter equation for a Goldstone boson and a vector meson reads

$$T_{\mu\nu}^{ab}(\overline{q},q,w) = K_{\mu\nu}^{ab}(\overline{q},q,w) + \sum_{c,d} \int \frac{d^4l}{(2\pi)^4} K_{\mu\beta}^{ad}(\overline{q},l,w) G_{dc}^{\alpha\beta}(l,w) T_{\alpha\nu}^{cb}(l,q,w) \tag{4.70}$$

with

$$G_{cd}^{\alpha\beta}(l,w) = \frac{i}{(w-l)^2 - m_c^2 + i\epsilon} \frac{g^{\alpha\beta} - l^\alpha l^\beta / M_c^2}{l^2 - M_c^2 + i\epsilon} \delta_{cd} \,. \tag{4.71}$$

Note that the expansion coefficients in Eq.(4.66) and Eq.(4.67) only depend on $s = w^2$ ($w = (\sqrt{s}, \vec{0})$), which means they are onshell. In principle these coefficients can also depend on $w \cdot l$ and l^2, which we discuss at the end of this section. Plugging in the expansions Eq.(4.66) and Eq.(4.67) in Eq.(4.70) yields

$$\sum_{JMP,ij} M_{abij}^{(JMP)} Y_{ij}^{\mu\nu(JMP)} = \sum_{JMP,ij} V_{abij}^{(JMP)} Y_{ij}^{\mu\nu(JMP)}$$
$$+ \sum_{c,d} \sum_{J,M,P,i,j} \sum_{J',M',P',i',j'} \int \frac{d^4l}{(2\pi)^4} V_{acij}^{(JMP)} Y_{ij}^{\mu\beta(JMP)} G_{\alpha\beta}^{dc} M_{dbi'j'}^{(J'M'P')} Y_{i'j'}^{\alpha\nu(J'M'P')} \,. \tag{4.72}$$

Using the orthogonality relation, one gets

$$\sum_{J,M,P,i,j} M_{abij}^{(JMP)} Y_{ij}^{\mu\nu(JMP)} = \sum_{J,M,P,i,j} V_{abij}^{(JMP)} Y_{ij}^{\mu\nu(JMP)}$$
$$+ \sum_{c} \sum_{J,M,P,i,j} \sum_{j'} V_{acij}^{(JMP)} M_{dbjj'}^{(JMP)} Y_{ij'}^{\mu\nu(JMP)}(-I_c) \,. \tag{4.73}$$

Since the projectors are linearly independent with respect to J, M, P, i, j, we get rid of the sum over J, M, P, i, j and we will omit the indices JMP from now on. So we are left with

$$M_{abij} = V_{abij} + \sum_{c}\sum_{k} V_{acik} M_{cbkj}(-I_c) \tag{4.74}$$

which can be solved algebraically. Note that this is identical to the N/D method. We introduce the renormalised quantity $J_{\phi V}(s,\mu)$

$$J_{\phi V}(s,\mu) = I_{\phi V}(s) - I_{\phi V}(\mu) \,, \tag{4.75}$$

which depends on the subtraction point μ. In order to render Eq.(4.74) finite we substitute

$$I_{\phi V}(s) \rightarrow J_{\phi V}(s, \mu_1), \tag{4.76}$$

which introduces the unknown parameter μ_1.

In case the coefficients would depend also on the loop momentum l, we could still use the orthogonality relation, but Eq.(4.73) would read

$$\sum_{J,M,P,i,j} M_{abij}^{(JMP)} Y_{ij}^{\mu\nu(JMP)} = \sum_{J,M,P,i,j} V_{abij}^{(JMP)} Y_{ij}^{\mu\nu(JMP)}$$

$$+ \sum_c \sum_{J,M,P,i,j} \sum_{j'} \int \frac{\vec{l}^2 d|\vec{l}| dl^0}{(2\pi)^4} (-i) \frac{V_{acij}^{(JMP)}(w,l) M_{cbjj'}^{(JMP)}(w,l)}{((w-l)^2 - m_c^2 + i\epsilon)(l^2 - M_c^2 + i\epsilon)} Y_{ij'}^{\mu\nu(JMP)}. \tag{4.77}$$

We could use the orthogonality of the projectors, since it follows from the integration over the angles, which can be seen in Appendix B. Using again the linear independence of the projectors and omitting J, M, P, one gets

$$M_{abij} = V_{abij} + \sum_c \sum_k \int \frac{d^4l}{(2\pi)^4} V_{acik}(w,l) M_{cbkj}(w,l) \frac{-i}{(w-l)^2 - m_c^2 + i\epsilon} \frac{1}{l^2 - M_c^2 + i\epsilon}. \tag{4.78}$$

Eq.(4.78) is obviously not the same as Eq.(4.74) and can not be solved algebraically. In the next section, we will discuss why, nevertheless, it is reasonable to put the coefficients onshell.

4.4.2. Onshell reduction

In the last section we saw that due to the dependence of the kernel and the scattering amplitude on the loop momentum, the Bethe-Salpeter equation will not be easily solvable. We will now discuss the difference between Eq.(4.74) and Eq.(4.78). For simplicity, we leave out the coupled-channel and the helicity structure, which does not affect the general arguments. Thus, we are dealing with an equation of the form

$$M = V + \int \frac{d^4}{(2\pi)^4} V(w,l) M(w,l) \frac{-i}{(w-l)^2 - m^2 + i\epsilon} \frac{1}{l^2 - M^2 + i\epsilon}, \tag{4.79}$$

which is just a Bethe-Salpeter equation for scalar particles. There are different explanations in the literature why it is justified to use the Bethe-Salpeter equation with the kernel taken onshell, e.g. [LK02, OO97]. One of the explanations is of course given in section 4.2, which says that the N/D method is equivalent to the Bethe-Salpeter equation with the kernel taken onshell. We will also look at two other explanations in order to see the problem from different sides. One should mention that it has been shown in [KLF01] that using kernels which just differ offshell will lead to different results in the solution of the Bethe-Salpeter equation. Thus, we do not want to show that the result will not change, but we want to see what kind of differences we can expect.

The idea of the justification of the onshell reduction in [OO97] is based on the following observation

$$\int \frac{d^4l}{(2\pi)^4} \frac{l^2}{l^2 - m_1^2} \frac{1}{(w-l)^2 - m_2^2} = \int \frac{d^4l}{(2\pi)^4} \frac{m_1^2}{l^2 - m_1^2} \frac{1}{(w-l)^2 - m_2^2} + \int \frac{d^4l}{(2\pi)^4} \frac{1}{(w-l)^2 - m_2^2}. \tag{4.80}$$

Figure 4.3.: Two examples of tadpole diagrams.

We see that we can split an integral with a momentum squared in the numerator into the same integral using the onshell condition for the momentum plus a tadpole. Originally the name tadpole was introduced for diagrams with one external leg due to its striking similarity to an actual tadpole, as can be seen by looking at the left diagram in Fig. 4.3. The name tadpole is also used for one-loop diagrams with a propagator which connects back to its originating vertex (e.g. right diagram in Fig. 4.3). A tadpole is an analytic function of $s = w^2$, i.e. it has no cuts. It is straightforward to use Eq.(4.80) to write in general

$$\int \frac{d^4l}{(2\pi)^4} K(w,l)G(l)K(w,l) = \int \frac{d^4l}{(2\pi)^4} K_{on}(s)G(l)K_{on}(s) + tadpoles\,, \qquad (4.81)$$

where $K_{on}(s)$ is the function $K(w,l)$ onshell. It is also straightforward to imagine, that for higher loops the equation looks similar and instead of having just a sum of tadpoles, they might appear in powers. Since the tadpoles have no cuts, they will contribute in a similar way to the real part as higher order contact terms. Thus, neglecting the tadpoles is a simplification on the same level as neglecting the higher order contact terms.

In [LK02] the authors give a formula how one can modify the kernel and still get the same onshell result for the scattering amplitude. In a few examples it is shown, how that formula is able to reduce the Bethe-Salpeter equation to an algebraic equation. We will derive that formula and also show two examples.
We begin by splitting the kernel into 4 parts

$$K = \overline{K} + K_L + K_R + K_{LR}\,, \qquad (4.82)$$

where K_L vanishes for onshell kinematics in the outgoing channel, K_R vanishes for onshell kinematics in the incoming channel and K_{LR} vanishes in both cases. Now we rewrite the onshell scattering amplitude using that decomposition. We will use an index i if the incoming momenta are onshell and an index o if the outgoing momenta are onshell.

$$T^{io} = \overline{K}^{io} + \overline{K}^{o}GT^i + K_R^o GT^i \qquad (4.83)$$

and T^i is given by

$$T^i = \overline{K}^i + K_L^i + KGT^i\,. \qquad (4.84)$$

If we put the scattering amplitudes back offshell, we calculate an onshell equivalent amplitude, which we call W. Looking at Eq.(4.84), we see

$$W - KGW = \overline{K} + K_L\,. \qquad (4.85)$$

The left hand side can be written as

$$W - K_L GW - K_R GW - K_{LR}GW - \overline{K}GW = W - K_R GW - K_{LR}GW - (K_L + \overline{K})GW$$
$$= W - K_R GW - K_{LR}GW - (1 - K_R G - K_{LR}G)(1 - K_R G - K_{LR}G)^{-1}(K_L + \overline{K})GW\,.$$

Introducing

$$X = (1 - K_R G - K_{LR} G)^{-1}(K_L + \overline{K}),$$ (4.86)

Eq.(4.85) becomes

$$(1 - K_R G - K_{LR} G)W - (1 - K_R G - K_{LR} G)XGW = K_L + \overline{K}$$ (4.87)

or

$$W - XGW = X \quad \Longleftrightarrow \quad W = (1 - XG)^{-1}X.$$ (4.88)

If we denote the offshell extension of T^{io} by $\overline{T}$, we see by looking at Eq.(4.83) that

$$\overline{T} = \overline{K} + \overline{K}G(1 - XG)^{-1}X + K_R G(1 - XG)^{-1}X.$$ (4.89)

We note that

$$X(1 - GX) = (1 - XG)X$$ (4.90)

and multiply $\overline{T}$ with $(1 - GX)$ from the right to get

$$\overline{T}(1 - GX) = \overline{K}(1 - GX) + \overline{K}GX + K_R GX = \overline{K} + K_R GX.$$ (4.91)

That can be written as

$$\overline{T}(1 - GX + G\overline{K} + GK_R GX) - \overline{T}G(\overline{K} + K_R GX) = \overline{K} + K_R GX.$$ (4.92)

Introducing the abbreviation

$$V = (\overline{K} + K_R GX)(1 - GX + G\overline{K} + GK_R GX)^{-1},$$ (4.93)

we get

$$\begin{aligned} \overline{T} - \overline{T}GV &= V \\ \overline{T} &= V(1 - GV)^{-1} \\ \overline{T} - VG\overline{T} &= (1 - VG)V(1 - GV)^{-1} = V \\ \overline{T} &= (1 - VG)^{-1}V \end{aligned}$$ (4.94)

This formula tells us how one can change a kernel and still get the same onshell result. We will illustrate how it works, first on an easy example, which can be also found in [LK02] and then on the WT term, which we use in our calculation.

Example 1

The first example employs the WT term for pion-nucleon scattering as kernel, which is given by

$$K = C(\slashed{q} + \slashed{\overline{q}}) = C(2\slashed{w} - \slashed{p} - \slashed{\overline{p}}).$$ (4.95)

The Bethe-Salpeter equation for this case is

$$T = K + \int \frac{d^4l}{(2\pi)^4} K(l, w) \frac{-i}{\slashed{p} - M_N + i\epsilon} \frac{1}{(w - l)^2 - m_\pi^2 + i\epsilon} T(l, w).$$ (4.96)

The decomposition into the 4 kernels can be directly seen

$$\begin{aligned} \overline{K} &= C(2\slashed{w} - 2M_N) \\ K_{LR} &= 0 \\ K_R &= -C(\slashed{p} - M_N) \\ K_L &= -C(\slashed{\overline{p}} - M_N). \end{aligned}$$ (4.97)

So the equation for X becomes

$$X = C(2\psi - M_N - \bar{\slashed{p}}) + iC \int \frac{d^4l}{(2\pi)^4} X(l) G_\pi(w - l) \,, \tag{4.98}$$

where $G_\pi(q) = 1/(q^2 - m_\pi^2 + i\epsilon)$ is the pion propagator. The solution to that equation is

$$X = C(2\psi - M_N - \bar{\slashed{p}}) + \frac{C^2(I_\pi^l + (\psi - m_N)I_\pi)}{1 - CI_\pi} = C(2\psi - M_N - \bar{\slashed{p}}) + \frac{C^2(\psi - m_N)I_\pi}{1 - CI_\pi} \,, \tag{4.99}$$

where we used

$$I_\pi = i \int \frac{d^4l}{(2\pi)^4} G_\pi(l) \,, \quad I_\pi^l = i \int \frac{d^4l}{(2\pi)^4} l \, G_\pi(l) = 0 \,. \tag{4.100}$$

Knowing X we can evaluate V

$$V = (\overline{K} + K_R G X) + V G K_L \,, \tag{4.101}$$

which is in that case

$$V = 2C(\psi - m_N) + C^2(\psi - m_N)I_\pi + \frac{C^3 I_\pi^2(\psi - m_N)}{1 - CI_\pi} + iC \int \frac{d^4l}{(2\pi)^4} V G_\pi(l) \,. \tag{4.102}$$

We notice that the external momenta are gone and we get

$$\begin{aligned}
V &= \frac{1}{1 - CI_\pi} \left(2C(\psi - m_N) + C^2(\psi - m_N)I_\pi + \frac{C^3 I_\pi^2(\psi - m_N)}{1 - CI_\pi} \right) \\
&= \frac{\psi - m_N}{(1 - CI_\pi)^2} (2C(1 - CI_\pi) + C^2 I_\pi(1 - CI_\pi) + C^3 I_\pi^2) \\
&= C \frac{\psi - m_N}{(1 + CI_\pi)^2} (2 - CI_\pi) \,.
\end{aligned} \tag{4.103}$$

Thus, using the kernel V, we can easily solve the Bethe-Salpeter equation. Besides the tadpoles, we get the same result for the onshell scattering amplitude, which we would have got by simply using the kernel onshell.

Example 2

In this example we will consider the kernel which appears in our calculation after the projection on $J = 1^+$ (see Section 5.1). For simplicity, we will leave out the helicity and coupled-channel structure and assume that the scattering amplitude is determined by the following equation

$$T = K + \int \frac{d^4l}{(2\pi)^4} K(w, l) T(w, l) \frac{-i}{(w - l)^2 - m^2 + i\epsilon} \frac{1}{l^2 - M^2 + i\epsilon} \,. \tag{4.104}$$

The kernel in this simplified case is

$$K = C \left(2w \cdot q + 2w \cdot \bar{q} - q^2 - \bar{q}^2 - 2 \frac{(w \cdot q)(w \cdot \bar{q})}{s} \right) \,. \tag{4.105}$$

We turn that expression into a form, where one easily can read off the different parts of the kernel K_{on}, K_L, K_R and K_{LR}

$$K = \frac{C}{2} \left(3s - p^2 - \bar{p}^2 - \frac{1}{s} p^2 \bar{p}^2 - \frac{1}{s} q^2 \bar{q}^2 + \frac{1}{s} p^2 \bar{q}^2 + \frac{1}{s} q^2 \bar{p}^2 - q^2 - \bar{q}^2 \right) \,. \tag{4.106}$$

Thus, the four parts are given by

$$
\overline{K} = \frac{C}{2}\left(3s - 2M_\rho^2 - \frac{M_\rho^4}{s} - \frac{M_\pi^4}{s} + \frac{2}{s}M_\pi^2 M_\rho^2 - 2M_\pi^2\right)
$$
$$
K_L = (\overline{p}^2 - M_\rho^2)a(s) + (\overline{q}^2 - M_\pi^2)a(s)
$$
$$
K_R = (p^2 - M_\rho^2)a(s) + (q^2 - M_\pi^2)a(s)
$$
$$
K_{LR} = -\frac{C}{2s}\big((p^2 - M_\rho^2)(\overline{p}^2 - M_\rho^2) + (q^2 - M_\pi^2)(\overline{q}^2 - M_\pi^2)
$$
$$
+ (p^2 - M_\rho^2)(\overline{q}^2 - M_\pi^2) + (q^2 - M_\pi^2)(\overline{p}^2 - M_\rho^2)\big)\,,
$$

$$(4.107)$$

where we introduced

$$
a(s) = -\frac{C}{2s}(s + M_\rho^2 - M_\pi^2) \tag{4.108}
$$

This yields the following equation for X

$$
X + ia(s)\int \frac{d^4l}{(2\pi)^4}G_\pi X + ia(s)\int \frac{d^4l}{(2\pi)^4}G_\rho X
$$
$$
- \frac{iC}{2s}(\overline{p}^2 - M_\rho^2)\left(\int \frac{d^4l}{(2\pi)^4}G_\pi X + \int \frac{d^4l}{(2\pi)^4}G_\rho X\right)
$$
$$
- \frac{iC}{2s}(\overline{q}^2 - M_\pi^2)\left(\frac{d^4l}{(2\pi)^4}G_\pi X + \frac{d^4l}{(2\pi)^4}G_\rho X\right) = K_L + \overline{K}\,,
$$

$$(4.109)$$

with

$$
G_\rho = \frac{1}{(w - l)^2 - M_\rho^2 + i\epsilon}\,. \tag{4.110}
$$

Introducing

$$
I(s, X) = -i\int \frac{d^4l}{(2\pi)^4}G_\pi X - i\int \frac{d^4l}{(2\pi)^4}G_\rho X\,, \tag{4.111}
$$

this becomes

$$
X + \left(\frac{C}{2s}(\overline{p}^2 - M_\rho^2) + \frac{C}{2s}(\overline{q}^2 - M_\pi^2) - a(s)\right)I(s, X) = \overline{K} + (\overline{p}^2 - M_\rho^2)a(s) + (\overline{q}^2 - M_\pi^2)a(s)\,.
$$

$$(4.112)$$

With the ansatz

$$
X = f_1(s) + f_2(s)(\overline{p}^2 - M_\rho^2) + f_3(s)(\overline{q}^2 - M_\pi^2)\,, \tag{4.113}
$$

the equation can be solved, and the determination of the f_i is in principle straightforward, but a bit lengthy. Since the explicit form of the f_i is not of interest for our purposes, we will skip the calculation and solve for V. Knowing the structure of X, we can already write down the equation for V, which is

$$
V = \overline{K} + a(s)I(s, X) - ia(s)\int \frac{d^4l}{(2\pi)^4}V(G_\pi + G_\rho) + VGK_{LR}GX\,, \tag{4.114}
$$

where we used that

$$
X - K_RGX - \overline{K} = K_L + K_{LR}GX\,. \tag{4.115}
$$

We can simplify the last term of Eq.(4.114) as follows

$$
VGK_{LR}GX = \frac{C}{2s}\int \frac{d^4l}{(2\pi)^4}\int \frac{d^4l'}{(2\pi)^4}V(G_\pi(l) + G_\rho(l))(G_\pi(l') + G_\rho(l'))X(l')
$$
$$
\equiv b(s)\int \frac{d^4l}{(2\pi)^4}V(G_\pi(l) + G_\rho(l))\,,
$$

$$(4.116)$$

where $b(s)$ is some function of tadpoles and only depends on s. Then Eq.(4.114) becomes

$$V = \overline{K} + a(s)I(s, X) - (ia(s) - b(s)) \int \frac{d^4l}{(2\pi)^4} V(G_\pi + G_\rho), \qquad (4.117)$$

and therefore

$$V = \frac{\overline{K} + a(s)I(s, X)}{1 + (a(s) + ib(s))(I_\pi + I_\rho)}. \qquad (4.118)$$

Thus, we see that again the problem reduces to an algebraic one by the modification of the kernel. Although we did not explicitly calculate $I(s, X)$, we know that it is a function of tadpoles. In other words, dropping all tadpoles in Eq.(4.118) would lead to $V = \overline{K}$.

4.4.3. The kernel

The kernel of the Bethe-Salpeter equation can consist of parts, which are analytic in the energy region, one is interested in, and parts which are non-analytic. The non-analytic parts are possible s-channel resonances, which have a pole in the physical region. The analytic part consists of contact terms, as well as t- and u-channel processes, since they do not have any singularities in the physical energy region. The analytic parts can be expanded in powers of the momenta of the involved particles (and in powers of the Goldstone boson masses). This leads to contact terms, which can equivalently and systematically be expressed in terms of a chiral Lagrangian. The approach we take is to consider the relevant s-channel resonances in the kernel and keep contact terms up to a specific order. This approximation is a model assumption, and it is not guaranteed that it works for the quite large energy region, we are interested in. However, it is certainly worthwhile to study its properties. Following this strategy, one has to avoid double counting between the s-channel processes and the contact terms, since for $s < m_{res}^2$ these s-channel resonance terms can also contribute to the analytic part.

Now we want to become specific and discuss the present case. Here the problem is that one is not sure whether there is a relevant preexisting resonance (i.e. a quark-antiquark state at about 1260 MeV with quantum numbers $J^P = 1^+$). Therefore, we calculate two different scenarios, one with explicit a_1 and one without explicit a_1. Comparing to experiment, we determine which scenario is favoured by the data. As already mentioned, we have to be careful with double counting. Restricting the contact terms to the WT term, there is no problem, since the WT term contributes at $\mathcal{O}(q)$ and the elementary a_1 at $\mathcal{O}(q^2)$. Thus, there can be no double counting. In particular, this means that only considering an a_1 and neglecting the WT term is very questionable. The focus in discussing the results will therefore be on the interplay between the a_1 and the WT term.

In order to check the systematics of our model, we will also study the influence of keeping contact terms up to order $\mathcal{O}(q^2)$ instead of $\mathcal{O}(q)$ in the scenario without explicit a_1.

Chapter 5.

Partial Wave Projectors

A very useful tool in scattering theory is the partial wave expansion, being so valuable because for low energies only the lowest angular momentum modes are excited. In a relativistic framework, including particles with spin, the orbital angular momentum is not a good quantum number anymore and neither is the spin. Instead one uses states with definite helicity and total angular momentum, which have been first employed in [JW59]. Similar to the partial wave decomposition one expands the scattering amplitude into helicity amplitudes. In our case we want to expand a kernel with a tensor structure in objects with definite total angular momentum and helicity, which we call projectors. By total angular momentum and helicity of a tensor we mean that after multiplying with the polarisation vectors, the resulting scalar object has the appropriate quantum numbers (see Eq.(5.29)).

In the following we will derive the explicit form of the projectors. A similar derivation can be found in [LK04], which, however, deals different with the offshell extrapolation of the objects, and therefore also ends up with different projectors. We will discuss the differences in detail in Section 5.3.

The general form of a scattering amplitude for the scattering of a pseudoscalar meson ϕ off a vector meson V with polarisation λ is given by

$$\langle \phi(\overline{q}) V(\overline{p}, \overline{\lambda}) | T | \phi(q) V(p, \lambda) \rangle = (2\pi)^4 \delta^4(q + p - \overline{q} - \overline{p}) \epsilon^\dagger_\mu(\overline{p}, \overline{\lambda}) T^{\mu\nu}(\overline{q}, q, w) \epsilon_\nu(p, \lambda) , \qquad (5.1)$$

where $w = p + q = \overline{q} + \overline{p}$ is the total four-momentum, ϵ_μ is the polarisation vector of a vector meson (see Appendix A.2), q $(\overline{q})$ is the momentum of the incoming (outgoing) meson and p $(\overline{p})$ is the momentum of the incoming (outgoing) vector meson. Due to Lorentz invariance the most general form of $T^{\mu\nu}$ is given in terms of five scalar amplitudes

$$T_{\mu\nu} = \sum_i F_i L^i_{\mu\nu} , \qquad (5.2)$$

with

$$L^{\mu\nu}_1 = g^{\mu\nu} - \frac{w^\mu w^\nu}{s}, \quad L^{\mu\nu}_2 = w^\mu w^\nu, \quad L^{\mu\nu}_3 = w^\mu \overline{q}^\nu - w^\mu w^\nu \frac{\overline{q} \cdot w}{s}$$
$$L^{\mu\nu}_4 = q^\mu w^\nu - w^\mu w^\nu \frac{q \cdot w}{s}, \quad L^{\mu\nu}_5 = \left(q^\mu - w^\mu \frac{(q \cdot w)}{s} \right) \left(\overline{q}^\nu - w^\nu \frac{\overline{q} \cdot w}{s} \right) . \qquad (5.3)$$

The L_i can of course be chosen differently as long as they contain all possible Lorentz structures in a linearly independent way. We note that there are only five independent terms, since p and $\overline{p}$ can be expressed in terms of $w, q, \overline{q}$. In addition, structures containing e.g. $\overline{q}^\mu$ are not independent since

$$\epsilon^\dagger_\mu(\overline{p}, \overline{\lambda}) \overline{q}^\mu = \epsilon^\dagger_\mu(\overline{p}, \overline{\lambda})(w - \overline{p})^\mu = \epsilon^\dagger_\mu(\overline{p}, \overline{\lambda}) w^\mu \qquad (5.4)$$

due to $\epsilon_\mu^\dagger(\overline{p})\overline{p}^\mu = 0$.

After multiplying with polarisation vectors, the amplitude can be expanded in the centre-of-mass system (CMS) as follows

$$\epsilon_\mu^\dagger(\overline{p}, \overline{\lambda}) T^{\mu\nu} \epsilon_\nu(p, \lambda) = \sum_{JM} \frac{2J+1}{4\pi} D_{M\overline{\lambda}}^*(\overline{\phi}, \overline{\theta}, -\overline{\phi}) D_{M\lambda}(\phi, \theta, -\phi) \langle JM\overline{\lambda}|T|JM\lambda \rangle, \qquad (5.5)$$

which we already used in Eq.(4.4). The Wigner functions D are given in Appendix A.3, as well as the simplified Wigner functions d, which we will need below. $|JM\lambda\rangle$ is a state with total angular momentum J, its projection M and helicity λ. In two-particle scattering one usually chooses the incoming particles flying along the z-axis and the outgoing particles moving in the xz-plane with an angle θ to the z-axis, which corresponds to the choice

$$q_\mu = (q_0, 0, 0, -p_{cm}), \quad w_\mu = (\sqrt{s}, 0, 0, 0), \quad \overline{q}_\mu = (\overline{q}_0, -\overline{p}_{cm}\sin\theta, 0, -\overline{p}_{cm}\cos\theta), \qquad (5.6)$$

where $p_{cm} = |\vec{p}|$ is the centre-of-mass momentum. In that case Eq.(5.5) reduces to

$$\epsilon_\mu^\dagger(\overline{p}, \overline{\lambda}) T^{\mu\nu} \epsilon_\nu(p, \lambda) = \sum_J (2J+1) \langle \overline{\lambda}|T^J|\lambda \rangle d_{\lambda\overline{\lambda}}^J(\theta), \qquad (5.7)$$

where we abbreviated $|JM\lambda\rangle = |\lambda\rangle$. From Eq.(5.5) we would expect a factor of 4π, which we put into the definition of the matrix element. The sum over M is cancelled by $d_{\lambda M}(0) = \delta_{M\lambda}$, which reflects the fact that there is no orbital angular momentum along the direction of motion.

We abbreviate the nine possible (and five independent) helicity combinations as follows

$$\begin{aligned} \phi_1 &= \epsilon_\mu^\dagger(\overline{p}, 1) T^{\mu\nu} \epsilon_\nu(p, 1) + \epsilon_\mu^\dagger(\overline{p}, 1) T^{\mu\nu} \epsilon_\nu(p, -1) \\ &= \epsilon_\mu^\dagger(\overline{p}, -1) T^{\mu\nu} \epsilon_\nu(p, -1) + \epsilon_\mu^\dagger(\overline{p}, -1) T^{\mu\nu} \epsilon_\nu(p, 1) \end{aligned} \qquad (5.8)$$

$$\begin{aligned} \phi_2 &= \epsilon_\mu^\dagger(\overline{p}, 1) T^{\mu\nu} \epsilon_\nu(p, 1) - \epsilon_\mu^\dagger(\overline{p}, 1) T^{\mu\nu} \epsilon_\nu(p, -1) \\ &= \epsilon_\mu^\dagger(\overline{p}, -1) T^{\mu\nu} \epsilon_\nu(p, -1) - \epsilon_\mu^\dagger(\overline{p}, -1) T^{\mu\nu} \epsilon_\nu(p, 1) \end{aligned} \qquad (5.9)$$

$$\phi_3 = \frac{\overline{M}_V \sqrt{2}}{\sin\theta} \epsilon_\mu^\dagger(\overline{p}, 0) T^{\mu\nu} \epsilon_\nu(p, 1) = -\frac{\overline{M}_V \sqrt{2}}{\sin\theta} \epsilon_\mu^\dagger(\overline{p}, 0) T^{\mu\nu} \epsilon_\nu(p, -1) \qquad (5.10)$$

$$\phi_4 = \frac{M_V \sqrt{2}}{\sin\theta} \epsilon_\mu^\dagger(\overline{p}, 1) T^{\mu\nu} \epsilon_\nu(p, 0) = -\frac{M_V \sqrt{2}}{\sin\theta} \epsilon_\mu^\dagger(\overline{p}, -1) T^{\mu\nu} \epsilon_\nu(p, 0) \qquad (5.11)$$

$$\phi_5 = M_V \overline{M}_V \epsilon_\mu^\dagger(\overline{p}, 0) T^{\mu\nu} \epsilon_\nu(p, 0), \qquad (5.12)$$

where M_V ($\overline{M}_V$) is the mass of the incoming (outgoing) vector meson.

Next we want to find a connection between ϕ_i and F_i, which can be calculated by multiplying Eq.(5.2) with the explicit expression for the polarisation vectors given in Appendix A.2. This yields

$$\begin{pmatrix} \phi_1 \\ \phi_2 \\ \phi_3 \\ \phi_4 \\ \phi_5 \end{pmatrix} = \begin{pmatrix} -1 & 0 & 0 & 0 & 0 \\ -x & 0 & 0 & 0 & -p_{cm}\overline{p}_{cm}(1-x^2) \\ \overline{\omega} & 0 & -\sqrt{s}\overline{p}_{cm}^2 & 0 & -p_{cm}\overline{p}_{cm}\overline{\omega}x \\ -\omega & 0 & 0 & p_{cm}^2\sqrt{s} & \omega\overline{p}_{cm}p_{cm}x \\ -\omega\overline{\omega}x & p_{cm}\overline{p}_{cm}s & \overline{p}_{cm}^2\sqrt{s}\omega x & p_{cm}^2\sqrt{s}\overline{\omega}x & p_{cm}\overline{p}_{cm}\omega\overline{\omega}x^2 \end{pmatrix} \cdot \begin{pmatrix} F_1 \\ F_2 \\ F_3 \\ F_4 \\ F_5 \end{pmatrix}, \qquad (5.13)$$

where $\omega = p_0 = \frac{w \cdot p}{\sqrt{s}}$ is the energy of the vector meson in the CMS and $x = \cos\theta$. The inverse of that equation is

$$
\begin{pmatrix} F_1 \\ F_2 \\ F_3 \\ F_4 \\ F_5 \end{pmatrix} = \begin{pmatrix} -1 & 0 & 0 & 0 & 0 \\ \frac{\omega\overline{\omega}x}{p_{cm}\overline{p}_{cm}s(1-x^2)} & -\frac{\omega\overline{\omega}x^2}{p_{cm}\overline{p}_{cm}s(1-x^2)} & \frac{\omega x}{p_{cm}\overline{p}_{cm}s} & -\frac{\overline{\omega}x}{p_{cm}\overline{p}_{cm}s} & \frac{1}{p_{cm}\overline{p}_{cm}s} \\ -\frac{\overline{\omega}}{\sqrt{s}\overline{p}_{cm}^2(1-x^2)} & \frac{\overline{\omega}x}{\sqrt{s}\overline{p}_{cm}^2(1-x^2)} & -\frac{1}{\overline{p}_{cm}^2\sqrt{s}} & 0 & 0 \\ -\frac{\omega}{\sqrt{s}p_{cm}^2(1-x^2)} & \frac{\omega x}{\sqrt{s}p_{cm}^2(1-x^2)} & 0 & \frac{1}{p_{cm}^2\sqrt{s}} & 0 \\ \frac{x}{\overline{p}_{cm}p_{cm}(1-x^2)} & -\frac{1}{\overline{p}_{cm}p_{cm}(1-x^2)} & 0 & 0 & 0 \end{pmatrix} \cdot \begin{pmatrix} \phi_1 \\ \phi_2 \\ \phi_3 \\ \phi_4 \\ \phi_5 \end{pmatrix}. \quad (5.14)
$$

Thus, we can express the scalar amplitudes F_i in terms of the helicity matrix elements, which yields

$$
\begin{aligned}
T_{\mu\nu}(q,\overline{q},w) = {} & -\phi_1 L^1_{\mu\nu} \\
& + L^2_{\mu\nu}\frac{1}{p_{cm}\overline{p}_{cm}s}\left(\frac{\omega\overline{\omega}x}{1-x^2}\phi_1 - \frac{\omega\overline{\omega}x^2}{1-x^2}\phi_2 + \omega x\phi_3 - \overline{\omega}x\phi_4 + \phi_5\right) \\
& + L^3_{\mu\nu}\frac{1}{\overline{p}_{cm}^2\sqrt{s}}\left(-\frac{\overline{\omega}}{1-x^2}\phi_1 + \frac{\overline{\omega}x}{1-x^2}\phi_2 - \phi_3\right) \\
& + L^4_{\mu\nu}\frac{1}{p_{cm}^2\sqrt{s}}\left(-\frac{\omega}{1-x^2}\phi_1 + \frac{\omega x}{1-x^2}\phi_2 + \phi_4\right) \\
& + L^5_{\mu\nu}\frac{1}{p_{cm}\overline{p}_{cm}(1-x^2)}(x\phi_1 - \phi_2).
\end{aligned} \quad (5.15)
$$

We introduce parity eigenstates, which are given by

$$
\langle 1_\pm| = \frac{1}{\sqrt{2}}(\langle -1| \pm \langle 1|). \quad (5.16)
$$

Using the symmetry relations for the d-functions Eq.(A.48) and Eq.(A.49), we can express the ϕ_i as

$$
\phi_1 = \frac{1}{2}\sum_J(2J+1)(\langle 1_+|T^J|1_+\rangle(d^J_{11}+d^J_{1-1}) + \langle 1_-|T^J|1_-\rangle(d^J_{11}-d^J_{1-1})) \quad (5.17)
$$

$$
\phi_2 = \frac{1}{2}\sum_J(2J+1)(\langle 1_+|T^J|1_+\rangle(d^J_{11}-d^J_{1-1}) + \langle 1_-|T^J|1_-\rangle(d^J_{11}+d^J_{1-1})) \quad (5.18)
$$

$$
\phi_3 = \frac{\overline{M}_V\sqrt{2}}{\sin\theta}\frac{1}{\sqrt{2}}\sum_J(2J+1)d^J_{10}\langle 0|T^J|1_+\rangle \quad (5.19)
$$

$$
\phi_4 = \frac{M_V\sqrt{2}}{\sin\theta}\frac{1}{\sqrt{2}}\sum_J(2J+1)d^J_{01}\langle 1_+|T^J|0\rangle \quad (5.20)
$$

$$
\phi_5 = M_V\overline{M}_V\sum_J(2J+1)d^J_{00}\langle 0|T^J|0\rangle. \quad (5.21)
$$

If one plugs these expressions into Eq.(5.15), one can read off the projectors, which are the prefactors in front of the matrix elements. For $J = 1$ the projector with negative parity is

$$
Y^{1^-}_{11\mu\nu} = \frac{3}{2}x\left(-L^1_{\mu\nu} - L^5_{\mu\nu}\frac{1}{\overline{p}p}\right) \quad (5.22)
$$

and the projectors with positive parity are

$$Y^{1+}_{11\mu\nu} = \frac{3}{2}\left(-L^1_{\mu\nu} + L^2_{\mu\nu}\frac{\omega\overline{\omega}x}{p_{cm}\overline{p}_{cm}s} + L^3_{\mu\nu}\frac{-\overline{\omega}}{\overline{p}^2_{cm}\sqrt{s}} + L^4_{\mu\nu}\frac{-\omega}{p^2_{cm}\sqrt{s}}\right) \tag{5.23}$$

$$Y^{1+}_{10\mu\nu} = M_V\frac{3}{\sqrt{2}}\left(-\frac{\overline{\omega}x}{p_{cm}\overline{p}_{cm}s}L^2_{\mu\nu} + L^4_{\mu\nu}\frac{1}{p^2_{cm}\sqrt{s}}\right) \tag{5.24}$$

$$Y^{1+}_{01\mu\nu} = -\overline{M}_V\frac{3}{\sqrt{2}}\left(\frac{\omega x}{p_{cm}\overline{p}_{cm}s}L^2_{\mu\nu} - L^3_{\mu\nu}\frac{1}{\overline{p}^2_{cm}\sqrt{s}}\right) \tag{5.25}$$

$$Y^{1+}_{00\mu\nu} = \frac{3M_V\overline{M}_V x L^2_{\mu\nu}}{p_{cm}\overline{p}_{cm}s}\,. \tag{5.26}$$

We usually do not need the explicit form of the projectors, which will become clear in the rest of the chapter. The projectors are of course defined for the kinematics given in Eq.(5.6). In general the projectors can also depend on the z-projection of the angular momentum, which is not the case for this choice of coordinate system, as explained above.

The quantity, which is of more interest and which does not depend on the coordinate system is the matrix element in front of the projector. We calculate these coefficients in terms of F_i by using

$$\epsilon^\dagger_\mu(\overline{p},\overline{\lambda})\left(\sum_i F_i L^{\mu\nu}_i\right)\epsilon_\nu(p,\lambda) = \sum_J (2J+1)\langle\overline{\lambda}|T^J|\lambda\rangle d^J_{\lambda\overline{\lambda}}(\theta) \tag{5.27}$$

and the orthogonality relation Eq.(A.45) in order to get

$$\langle\overline{\lambda}|T^J|\lambda\rangle = \frac{1}{2}\int_0^\pi \epsilon^\dagger_\mu(\overline{p},\overline{\lambda})\left(\sum_i F_i L^{\mu\nu}_i\right)\epsilon_\nu(p,\lambda)d^J_{\lambda\overline{\lambda}}\sin\theta d\theta\,. \tag{5.28}$$

As already mentioned, the projectors are chosen such that when they are multiplied with the respective polarisation vectors, the appropriate terms of the expansion of the scattering amplitude remain. To be more precise, the projectors fulfil

$$\epsilon^{\mu\dagger}(\overline{p},\lambda_1)Y^{JM^P}_{\lambda_2\lambda_3\mu\nu}(\overline{p},l,s)\epsilon^\nu(l,\lambda_4) = \delta_{|\lambda_1|\lambda_2}\delta_{\lambda_3|\lambda_4|}(2J+1)D^{*J}_{M\lambda_1}(\overline{\Omega})D^J_{M\lambda_4}(\Omega)$$
$$\cdot\left(\frac{1}{\sqrt{2}}\right)^{\lambda_2+\lambda_3}P^{(\lambda_1-\lambda_4)/2}\,. \tag{5.29}$$

In our derivation we chose the coordinate system which is best suited to derive the expansion coefficients, which are independent of the frame. In principle it is enough to know the property Eq.(5.29) and the expansion coefficients in order to perform calculations.

We also need the projectors for particles, which are off the mass shell, since the vector meson appears in our calculation as an intermediate particle. Since we did not use the mass shell condition at any point of the derivation, the offshell form of the projectors one can easily get by substituting the polarisation vectors by their offshell form. The expansion coefficients will then in general also depend on the momenta, but the expansion into projectors can still be done. The reason is that using spherical coordinates, which introduces the angles, can be done for particles being onshell or offshell. There is one subtlety concerning the polarisation vectors, since the vector meson propagator also contains a spin 0 part. That issue will be discussed in Appendix B, where we derive the orthogonality relation for the projectors.

5.1. Projection of the WT term

Now we want to use the machinery, we just developed, to project the WT term (see Appendix D.1) on $J^P = 1^+$. We first have to determine the F_i, which is easily done by writing

$$K^{\mu\nu} = -\frac{C_{WT}}{4F_0^2}(p + \overline{p})(q + \overline{q})g^{\mu\nu} = -\frac{C_{WT}}{4F_0^2}(p + \overline{p})(q + \overline{q})\left(L_1^{\mu\nu} + \frac{L_2^{\mu\nu}}{s}\right), \tag{5.30}$$

and therefore

$$F_1 = -\frac{C_{WT}}{4F_0^2}(p + \overline{p})(q + \overline{q}) = sF_2, \quad F_3 = F_4 = F_5 = 0. \tag{5.31}$$

We introduce the auxiliary function $g(s)$

$$g(s) = \frac{1}{6}\frac{C_{WT}}{F_0^2}(2w \cdot q + 2w \cdot \overline{q} - q^2 - 2q_0\overline{q}_0 - \overline{q}^2), \tag{5.32}$$

where $q_0 = \frac{q \cdot w}{\sqrt{s}}$ is the energy of the Goldstone boson in the CMS. $g(s)$ is $\mathcal{O}(q)$ as one can see from the appearance of one Goldstone boson derivative. We note that $g(s)$ as well as F_i have a matrix structure reflecting the coupled channels. This structure is encoded in C_{WT} and in the different masses. The function $g(s)$ depends only on s since the expansion coefficients are taken onshell. Using $g(s)$, F_1 reads

$$F_1 = -\frac{3}{2}g - \frac{C_{WT}}{2F_0^2}\overline{p}_{cm}p_{cm}x. \tag{5.33}$$

Next we will determine the expansion coefficients $V_{abij}^P = (V_{ij}^P)_{ab}$. We note that

$$\phi_1 + \phi_2 = \sum_J (2J + 1)(V_{11}^{J^+} + V_{11}^{J^-})d_{11}^J \tag{5.34}$$

and

$$\phi_1 - \phi_2 = \sum_J (2J + 1)(V_{11}^{J^+} - V_{11}^{J^-})d_{1-1}^J. \tag{5.35}$$

Using the explicit expressions and the orthogonality relation for the d-functions in Appendix A.3, the connection between F_i and ϕ_i from Eq.(5.13) and Eq.(5.17), we get

$$\begin{aligned} V_{11}^{1^+} + V_{11}^{1^-} &= \int_{-1}^{1}\frac{1}{2}(\phi_1(x) + \phi_2(x))d_{11}^1(x)dx \\ &= \int_{-1}^{1}\left(F_1\left(-\frac{1}{2}x - \frac{1}{2}\right) - F_5\frac{p\overline{p}(1 - x^2)}{2}\right)\frac{1 + x}{2}dx = -\frac{1}{4}\int_{-1}^{1}F_1(1 + x)^2dx \\ &= g + \frac{C_{WT}}{16f^2}\frac{8}{3}p\overline{p}, \end{aligned} \tag{5.36}$$

$$\begin{aligned} V_{11}^{1^+} - V_{11}^{1^-} &= \int_{-1}^{1}\frac{1}{2}(\phi_1(x) - \phi_2(x))d_{1-1}^1(x)dx \\ &= \int_{-1}^{1}\left(F_1\left(\frac{1}{2}x - \frac{1}{2}\right) + F_5\frac{p\overline{p}(1 - x^2)}{2}\right)\frac{1 - x}{2}dx = -\frac{1}{4}\int_{-1}^{1}F_1(1 - x)^2dx \\ &= g - \frac{C_{WT}}{16f^2}\frac{8}{3}p\overline{p}, \end{aligned} \tag{5.37}$$

and therefore

$$V_{11}^{1^+} = g. \tag{5.38}$$

Furthermore

$$
V_{01}^{1^+} = \frac{1}{2\overline{M}} \int_{-1}^{1} \sin\theta \phi_3(x) d_{10}^1(x) dx =
$$

$$
= -\frac{1}{2\sqrt{2\overline{M}}} \int_{-1}^{1} (1-x^2)(F_1\overline{\omega} - F_3\sqrt{s}\overline{p}^2 - F_5\overline{\omega}p\overline{p}x) dx \qquad (5.39)
$$

$$
= -\frac{1}{2\sqrt{2\overline{M}}} \int_{-1}^{1} (1-x^2)F_1\overline{\omega}\, dx = \frac{\overline{\omega}}{\sqrt{2}\,\overline{M}} g \,,
$$

$$
V_{10}^{1^+} = \frac{1}{2M} \int_{-1}^{1} \sin\theta \phi_4(x) d_{01}^1(x) dx =
$$

$$
= \frac{1}{2\sqrt{2}M} \int_{-1}^{1} (1-x^2)(-\omega F_1 + F_4 p^2\sqrt{s} + F_5\omega\overline{p}px) dx \qquad (5.40)
$$

$$
= -\frac{1}{2\sqrt{2}M} \int_{-1}^{1} (1-x^2)\omega F_1\, dx = \frac{\omega}{\sqrt{2}M} g \,,
$$

and finally

$$
V_{00}^{1^+} = \frac{1}{2M\overline{M}} \int_{-1}^{1} \phi_5(x) d_{00}^1(x) dx
$$

$$
= \frac{1}{2M\overline{M}} \int_{-1}^{1} (-\omega\overline{\omega}xF_1 + F_2 s\overline{p}p + F_3\sqrt{s}\overline{p}^2\omega x + F_4\overline{\omega}p^2x\sqrt{s} + F_5\omega\overline{\omega}\overline{p}px^2)x\, dx
$$

$$
= \frac{1}{2M\overline{M}} \int_{-1}^{1} (-\omega\overline{\omega}x^2 F_1 + F_2 sp\overline{p}x) dx = \frac{1}{2M\overline{M}} \int_{-1}^{1} (-\omega\overline{\omega}x^2 + p\overline{p}x)F_1\, dx \qquad (5.41)
$$

$$
= \frac{\omega\overline{\omega}}{2M\overline{M}} g - \frac{C_{WT}p_{cm}^2\overline{p}_{cm}^2}{6F_0^2 M\overline{M}} \,.
$$

We abbreviate the last term by introducing another auxiliary function $h(s)$

$$
h(s) = \frac{C_{WT}p_{cm}^2\overline{p}_{cm}^2}{6F_0^2 M\overline{M}} \,. \qquad (5.42)
$$

Since $h(s)$ is $\mathcal{O}(q^4)$, whereas g is $\mathcal{O}(q)$, it is higher order and we neglect it for the moment. We explicitly checked the influence of this term, and there was no visible difference in the results by including the term. With these coefficients the lowest partial wave takes an easy form

$$
K_{\mu\nu}^{J^P=1^+} = gY_{11\mu\nu}^{1^+} + g\frac{\overline{\omega}}{\sqrt{2}\,\overline{M}}Y_{01\mu\nu}^{1^+} + g\frac{\omega}{\sqrt{2}M}Y_{10\mu\nu}^{1^+} + g\frac{\omega\overline{\omega}}{2M\overline{M}}Y_{00\mu\nu}^{1^+}
$$

$$
= -\frac{3}{2}gL_{\mu\nu}^1 = -g\frac{3}{2}\left(g_{\mu\nu} - \frac{w_\mu w_\nu}{w^2}\right) \,. \qquad (5.43)
$$

Next we want to connect to the calculation in [LK04], which also yields a handy simplification, if we neglect $h(s)$. Rewriting $g(s)$ yields

$$
g_{ab}(s) = \frac{C_{ab}^{WT}}{12F_0^2}\left(3s - (M_{\phi a}^2 + M_{\phi b}^2 + M_{Va}^2 + M_{Vb}^2) - \frac{1}{s}(M_{Vb}^2 - M_{\phi b}^2)(M_{Va}^2 - M_{\phi a}^2)\right) \,. \quad (5.44)
$$

and for convenience we assign numbers to the channels as we did in Chapter 4

$$
\text{channel } 1 = \pi\rho
$$
$$
\text{channel } 2 = KK^* \,. \qquad (5.45)
$$

The equation we have to solve is (see Section 4.4.1)

$$M_{abij} = V_{abij} + \sum_c \sum_k V_{acik} M_{cbkj}(-I_{V\phi}).$$

(5.46)

In matrix notation and using the renormalised loop integral the equation is

$$
\begin{pmatrix} M_{1111} \\ M_{2111} \\ M_{1101} \\ M_{2101} \end{pmatrix} = \begin{pmatrix} V_{1111} \\ V_{2111} \\ V_{1101} \\ V_{2101} \end{pmatrix}
$$
$$
+ \begin{pmatrix} V_{1111}(-J_{\pi\rho}) & V_{1211}(-J_{KK^*}) & V_{1110}(-J_{\pi\rho}) & V_{1210}(-J_{KK^*}) \\ V_{2111}(-J_{\pi\rho}) & V_{2211}(-J_{KK^*}) & V_{2110}(-J_{\pi\rho}) & V_{2210}(-J_{KK^*}) \\ V_{1101}(-J_{\pi\rho}) & V_{1201}(-J_{KK^*}) & V_{1100}(-J_{\pi\rho}) & V_{1200}(-J_{KK^*}) \\ V_{2101}(-J_{\pi\rho}) & V_{2201}(-J_{KK^*}) & V_{2100}(-J_{\pi\rho}) & V_{2200}(-J_{KK^*}) \end{pmatrix} \cdot \begin{pmatrix} M_{1111} \\ M_{2111} \\ M_{1101} \\ M_{2101} \end{pmatrix},
$$

(5.47)

where we recall the definition of $J_{\phi V}$

$$J_{\phi V}(s, \mu) = I_{\phi V}(s) - I_{\phi V}(\mu).$$

(5.48)

We abbreviate the matrix by VJ and write down the equation for the other M's

$$
\begin{pmatrix} M_{1110} \\ M_{2110} \\ M_{1100} \\ M_{2100} \end{pmatrix} = \begin{pmatrix} V_{1110} \\ V_{2110} \\ V_{1100} \\ V_{2100} \end{pmatrix} + VJ \cdot \begin{pmatrix} M_{1110} \\ M_{2110} \\ M_{1100} \\ M_{2100} \end{pmatrix}.
$$

(5.49)

Altogether there are 16 unknown expansion coefficients, which are determined by four equations each with four unknowns. It should be obvious how the equations for the remaining expansion coefficients look like. For the WT term we see that the third row is a multiple of the first row of VJ and the second row is a multiple of the fourth row. This can be seen by looking at the explicit expressions for V_{abij}, which we calculated in Eq.(5.36)-Eq.(5.41). We will call the proportionality factors v_1 and v_2. For the first matrix equation, for example, we have

$$v_1 M_{1111} = M_{1101}, \quad v_2 M_{2111} = M_{2101}$$

(5.50)

with

$$v_1 = \frac{\omega_{\pi\rho}}{\sqrt{2} M_\rho}$$

(5.51)

$$v_2 = \frac{\omega_{KK^*}}{\sqrt{2} M_{K^*}}.$$

(5.52)

Thus, the equations for four unknowns reduce to equations with two unknowns, and we are left with

$$
\begin{pmatrix} M_{1111} \\ M_{2111} \end{pmatrix} = \begin{pmatrix} V_{1111} \\ V_{2111} \end{pmatrix} + \begin{pmatrix} V_{1111}J_1 + v_1 V_{1110}J_1 & V_{1211}J_2 + v_2 V_{1210}J_2 \\ V_{2111}J_1 + v_1 V_{2110}J_1 & V_{2211}J_2 + v_2 V_{2210}J_2 \end{pmatrix} \cdot \begin{pmatrix} M_{1111} \\ M_{2111} \end{pmatrix}
$$
$$
= \begin{pmatrix} V_{1111} \\ V_{2111} \end{pmatrix} + \begin{pmatrix} (1+v_1^2)V_{1111}J_1 & (1+v_2^2)V_{1211}J_2 \\ (1+v_1^2)V_{2111}J_1 & (1+v_2^2)V_{2211}J_2 \end{pmatrix} \cdot \begin{pmatrix} M_{1111} \\ M_{2111} \end{pmatrix}.
$$

(5.53)

The solution for the other equations can be seen as follows

$$
\begin{pmatrix} M_{1110} \\ M_{2110} \\ M_{1100} \\ M_{2100} \end{pmatrix} = (1 - VJ)^{-1} \begin{pmatrix} V_{1110} \\ V_{2110} \\ V_{1100} \\ V_{2100} \end{pmatrix} = (1 - VJ)^{-1} v_1 \begin{pmatrix} V_{1111} \\ V_{2111} \\ V_{1101} \\ V_{2101} \end{pmatrix} = v_1 \begin{pmatrix} M_{1111} \\ M_{2111} \\ M_{1101} \\ M_{2101} \end{pmatrix} \tag{5.54}
$$

and analogous for the remaining unknown expansion coefficients. We see that the helicity structure completely decouples in case we neglect $h(s)$. The final results for $T^{\mu\nu}$ in the channels, we are interested in, are given by

$$
\begin{aligned}
T^{\mu\nu}_{\pi\rho\pi\rho} &= M_{1111} Y^{\mu\nu}_{11} + M_{1110} Y^{\mu\nu}_{10} + M_{1101} Y^{\mu\nu}_{01} + M_{1100} Y^{\mu\nu}_{00} \\
&= M_{1111}(Y^{\mu}_{11} + c_1 Y^{\mu\nu}_{10} + c_1 Y^{\mu\nu}_{01} + c_1 c_1 Y^{\mu\nu}_{00}) = -M_{1111} \frac{3}{2} \left(g^{\mu\nu} - \frac{w^\mu w^\nu}{w^2} \right)
\end{aligned} \tag{5.55}
$$

and

$$
\begin{aligned}
T^{\mu\nu}_{KK^*\pi\rho} &= M_{2111} Y^{\mu\nu}_{11} + M_{2110} Y^{\mu\nu}_{10} + M_{2101} Y^{\mu\nu}_{01} + M_{2100} Y^{\mu\nu}_{00} \\
&= M_{21211}(Y^{\mu}_{11} + c_1 Y^{\mu\nu}_{10} + c_2 Y^{\mu\nu}_{01} + c_1 c_2 Y^{\mu\nu}_{00}) = -M_{2111} \frac{3}{2} \left(g^{\mu\nu} - \frac{w^\mu w^\nu}{w^2} \right) .
\end{aligned} \tag{5.56}
$$

These are the same results as in [LK04].

5.2. Connection between helicity states and orbital angular momentum

In order to determine the s and d-wave component of the vector-meson Goldstone boson two-particle state, we need to know the relation between the helicity states and the orbital angular momentum l. In particular, we first want to determine the following overlap

$$
\langle J, M; l, s = 1 | J, M, \lambda \rangle = ? . \tag{5.57}
$$

In order to do so, we express both states in Eq.(5.57) in terms of orbital angular momentum and spin states, which is pretty simple for the left hand side. The states of total angular momentum J can be written as a combination of states with definite orbital angular momentum l and spin s

$$
|J, M; l, s\rangle = \sum_{m_s} C(m m_s (ls) J M) |l, m\rangle |s, m_s\rangle , \tag{5.58}
$$

where $s = 1$ is the spin of the vector meson, m_s the z-projection of the spin, m the z-projection of the orbital angular momentum, $M = m + m_s$ and C is a Clebsch-Gordan coefficient. We choose the following notation for the Clebsch-Gordan coefficients

$$
\langle j_1 j_2, m_1 m_2 | j_1 j_2, jm \rangle = C(m_1 m_2 (j_1 j_2) jm) \delta_{m, m_1 + m_2} . \tag{5.59}
$$

Next we want to express the helicity states of the moving system in terms of the spin and orbital angular momentum states. Since the spin and the orbital angular momentum are not conserved quantum numbers in a relativistic framework, the helicity states will be a mixture of different states. We need the following relations

$$
|l, m\rangle = \sqrt{\frac{2l + 1}{4\pi}} \int d\Omega |\theta, \phi\rangle D^{l*}_{m,0}(\phi, \theta, 0) , \tag{5.60}
$$

and the inverse of that equation, which is

$$|\theta, \phi\rangle = \sum_{l,m} |l, m\rangle \sqrt{\frac{2l+1}{4\pi}} D_{m0}^l(\phi, \theta, 0) \,. \tag{5.61}$$

At the same time we can write for a helicity state moving along the z axis $|\hat{z}, \lambda >$

$$|\hat{z}, \lambda >= |\hat{z}\rangle |s, \lambda\rangle \,, \tag{5.62}$$

where $|s, \lambda\rangle$ is the usual spin state with $m_s = \lambda$. Although the spin is not a conserved quantum number, it coincides with the helicity state in the rest frame of the particle. Since one can not produce any orbital angular momentum along the direction of motion, after a boost the z-projection of the total angular momentum is still given by the spin projection of the particle, which is the same as the helicity. Thus, we can use the above decomposition. Next we apply the rotation operator $U(\phi, \theta, 0)$ to the state. After the rotation the spin and helicity states will not be the same anymore, but the connection is given by the Wigner rotation functions. We have to rotate each factor on the right hand side of Eq.(5.62) separately, which gives

$$|\theta, \phi, \lambda\rangle = U(\phi, \theta, 0)|\hat{z}, \lambda\rangle = \sum_{m_S} |\theta, \phi\rangle D_{m_S \lambda}^1(\phi, \theta, 0)|1, m_S\rangle \,. \tag{5.63}$$

Applying the projection operator (see [Tun85] or [JW59]) on definite total angular momentum states, we get

$$
\begin{aligned}
|J, M, \lambda\rangle &= \sqrt{\frac{2J+1}{4\pi}} \int D_{M\lambda}^{J*}(\phi, \theta, 0)|\theta, \phi, \lambda\rangle d\Omega \\
&= \sum_{m_S} \sqrt{\frac{2J+1}{4\pi}} \int D_{M\lambda}^{J*}(\phi, \theta, 0)|\theta, \phi\rangle D_{m_S\lambda}^1(\phi, \theta, 0)|1, m_S\rangle d\Omega \\
&= \sum_{m_S, l, m} \sqrt{\frac{2l+1}{4\pi}} \sqrt{\frac{2J+1}{4\pi}} \int D_{M\lambda}^{J*}(\phi, \theta, 0)|l, m\rangle D_{m0}^l(\phi, \theta, 0) D_{m_S\lambda}^1(\phi, \theta, 0)|1, m_S\rangle d\Omega \,.
\end{aligned} \tag{5.64}
$$

We use the following relation for the Wigner rotation functions

$$D_{mn}^j(R) D_{m'n'}^{j'}(R) = \sum_{J,M,N} C(mm'(jj')JM)\rangle D_{MN}^J(R) C(nn'(jj')JN) \,, \tag{5.65}$$

which yields

$$
\begin{aligned}
|J, M, \lambda\rangle &= \sum_{m_S, l, m, l'} \sqrt{\frac{2l+1}{4\pi}} \sqrt{\frac{2J+1}{4\pi}} \int D_{M\lambda}^{J*}(\phi, \theta, 0) D_{m+m_S, \lambda}^{l'}(\phi, \theta, 0) d\Omega |l, m\rangle |m1\rangle \\
&\quad \cdot C(m_S m(l1)l'm_S + m) C(0\lambda(l1)l'\lambda) \\
&= \sum_{m_S, l, m, l'} \sqrt{\frac{2l+1}{4\pi}} \sqrt{\frac{2J+1}{4\pi}} 2\pi \delta_{M, m+m_S} \int d_{M\lambda}^J(x) d_{M\lambda}^{l'}(x) dx |l, m\rangle |1, m_S\rangle \\
&\quad \cdot C(m_S m(l1)l'm_s + m) C(0\lambda(l1)l'\lambda) \\
&= \sum_{l, m_S} \sqrt{\frac{2l+1}{2J+1}} C(m_S(M - m_S)(l1)JM) C(0\lambda(l1)J\lambda)|l, M - m_S\rangle |1, m_S\rangle \,.
\end{aligned} \tag{5.66}
$$

Therefore, we get from Eq.(5.58) and Eq.(5.66)

$$\langle J, M; l, 1|J, M, \lambda\rangle = \sqrt{\frac{2l+1}{2J+1}} C(0\lambda(l1)J\lambda) \,, \tag{5.67}$$

where we used

$$\sum_{m_S, m_{s'}} C(m_S(M - m_S)(l1)JM)C((M' - m_{s'})m_{s'}(l1)J'M') = \delta_{JJ'}\delta_{MM'} \,. \tag{5.68}$$

Now we will connect the helicity projectors to angular momentum projectors. In order to do so we notice that

$$M_{\lambda\bar{\lambda}} = \langle J, M, \bar{\lambda}|T|J, M, \lambda\rangle = \sum_{l,l'}\langle J, M, \bar{\lambda}|J, M; l', 1\rangle\langle J, M; l', 1|T|J, M; l, 1\rangle\langle J, M; l, 1|J, M, \lambda\rangle$$

$$= \sum_{l,l'}\langle J, M; l', 1|T|J, M; l, 1\rangle\frac{\sqrt{(2l+1)(2l'+1)}}{2J+1}C(0\lambda(l1)J\lambda)C(0\bar{\lambda}(l'1)J\bar{\lambda}) \,,$$

$$\tag{5.69}$$

where we used that also the orbital angular momentum states build a complete basis. By building quotients of the respective amplitudes, we can pin down constraints. If we only consider $J^P = 1^+$ and therefore only deal with s- and d-waves, we know for all possible combinations of l

$$\frac{M_{11}}{M_{1-1}} = \frac{M_{11}}{M_{-1-1}} = \frac{M_{11}}{M_{-11}} = \frac{M_{10}}{M_{-10}} = \frac{M_{01}}{M_{0-1}} = 1 \,, \tag{5.70}$$

which we knew in principle already from Eq.(4.8). Therefore, we can use (again)

$$M_{11}^+ = M_{11} + M_{1-1} = 2M_{11} \tag{5.71}$$

$$M_{10}^+ = \frac{1}{\sqrt{2}}(M_{10} + M_{-10}) = \sqrt{2}M_{10} \tag{5.72}$$

$$M_{01}^+ = \frac{1}{\sqrt{2}}(M_{01} + M_{0-1}) = \sqrt{2}M_{01} \,. \tag{5.73}$$

Looking up the Clebsch-Gordan coefficients of Eq.(5.69), we get the following relations for the respective transitions

$$s - \text{wave} \rightarrow s - \text{wave}: \quad \frac{M_{11}^+}{M_{10}^+} = \sqrt{2} \quad, \quad \frac{M_{11}^+}{M_{01}^+} = \sqrt{2} \quad, \quad \frac{M_{11}^+}{M_{00}^+} = 2 \tag{5.74}$$

$$s - \text{wave} \rightarrow d - \text{wave}: \quad \frac{M_{11}^+}{M_{10}^+} = -\frac{\sqrt{2}}{2}, \quad \frac{M_{11}^+}{M_{01}^+} = \sqrt{2} \quad, \quad \frac{M_{11}^+}{M_{00}^+} = -1 \tag{5.75}$$

$$d - \text{wave} \rightarrow s - \text{wave}: \quad \frac{M_{11}^+}{M_{10}^+} = \sqrt{2} \quad, \quad \frac{M_{11}^+}{M_{01}^+} = -\frac{\sqrt{2}}{2}, \quad \frac{M_{11}^+}{M_{00}^+} = -1 \tag{5.76}$$

$$d - \text{wave} \rightarrow d - \text{wave}: \quad \frac{M_{11}^+}{M_{10}^+} = -\frac{\sqrt{2}}{2}, \quad \frac{M_{11}^+}{M_{01}^+} = -\frac{\sqrt{2}}{2}, \quad \frac{M_{11}^+}{M_{00}^+} = \frac{1}{2} \,. \tag{5.77}$$

Calling the transitions with definite angular momentum D_{ab}, where $a, b \in \{s, d\}$ and supressing the Lorentz indices, we get

$$D_{ss} = Y_{11} + \frac{1}{\sqrt{2}}Y_{10} + \frac{1}{\sqrt{2}}Y_{01} + \frac{1}{2}Y_{00} \tag{5.78}$$

$$D_{sd} = Y_{11} - \frac{2}{\sqrt{2}}Y_{10} + \frac{1}{\sqrt{2}}Y_{01} - Y_{00} \tag{5.79}$$

$$D_{ds} = Y_{11} + \frac{1}{\sqrt{2}}Y_{10} - \frac{2}{\sqrt{2}}Y_{01} - Y_{00} \tag{5.80}$$

$$D_{dd} = Y_{11} - \frac{2}{\sqrt{2}}Y_{10} - \frac{2}{\sqrt{2}}Y_{01} + 2Y_{00} \,. \tag{5.81}$$

In principle we can multiply each of these expressions by an arbitrary normalisation constant, which we chose to be one, which means we use the above expressions. If we want to express our amplitude in terms of orbital angular momentum

$$
\begin{aligned}
T^{\mu\nu} &= M_{11}^+ Y_{11}^{\mu\nu} + M_{10}^+ Y_{10}^{\mu\nu} + M_{01}^+ Y_{01}^{\mu\nu} + M_{00}^+ Y_{00}^{\mu\nu} \\
&= c_{ss} D_{ss}^{\mu\nu} + c_{sd} D_{sd}^{\mu\nu} + c_{ds} D_{ds}^{\mu\nu} + c_{dd} D_{dd}^{\mu\nu} ,
\end{aligned}
\tag{5.82}
$$

we have to solve the following equations

$$
\begin{pmatrix}
1 & 1 & 1 & 1 \\
\frac{1}{\sqrt{2}} & -\frac{2}{\sqrt{2}} & \frac{1}{\sqrt{2}} & -\frac{2}{\sqrt{2}} \\
\frac{1}{\sqrt{2}} & \frac{1}{\sqrt{2}} & -\frac{2}{\sqrt{2}} & -\frac{2}{\sqrt{2}} \\
\frac{1}{2} & -1 & -1 & 2
\end{pmatrix}
\cdot
\begin{pmatrix}
c_{ss} \\ c_{sd} \\ c_{ds} \\ c_{dd}
\end{pmatrix}
=
\begin{pmatrix}
M_{11}^+ \\ M_{10}^+ \\ M_{01}^+ \\ M_{00}
\end{pmatrix} .
\tag{5.83}
$$

The solution to that equation is

$$
\frac{1}{9}
\begin{pmatrix}
4 & 2\sqrt{2} & 2\sqrt{2} & 2 \\
2 & -2\sqrt{2} & \sqrt{2} & -2 \\
2 & \sqrt{2} & -2\sqrt{2} & -2 \\
1 & -\sqrt{2} & -\sqrt{2} & 2
\end{pmatrix}
\cdot
\begin{pmatrix}
M_{11}^+ \\ M_{10}^+ \\ M_{01}^+ \\ M_{00}
\end{pmatrix}
=
\begin{pmatrix}
c_{ss} \\ c_{sd} \\ c_{ds} \\ c_{dd}
\end{pmatrix} .
\tag{5.84}
$$

It is interesting to note, that only for a particle at rest, the Weinberg-Tomozawa term is a pure s-wave, while for moving particles, factors of $\frac{\omega}{M}$ reduce the s-wave part. In Chapter 7 Fig. 7.22 we will look at that quantitatively and show the ratios of the coefficients c_{ab} for different kernels.

If one goes beyond WT and includes higher corrections to the kernel, it will not be obvious, which terms in the Lagrangian will contribute at which order to a given coefficient c. Since one is interested in determining the leading order contribution to the coefficients, we investigate this issue in more detail. We can not expect the WT term to be the leading order term for all transitions. It clearly is the leading order term for an s-wave to s-wave transition, since the contribution from the WT term is $\mathcal{O}(q)$, as one can see by looking at Eq.(5.84) and the expansion coefficients Eq.(5.36)-Eq.(5.41). Since the higher order terms can only contribute terms of order equal or higher $\mathcal{O}(q^2)$, the WT term is the leading term. For transitions involving d-waves we have to look closer. In the following we will show in which order the scalar coefficients F_i from Eq.(5.2) contribute to the respective transitions. For simplicity we only consider the $\pi\rho$ channel.

We start by investigating the WT term. As already mentioned, it yields an $\mathcal{O}(q)$ contribution to c_{ss}, which is obviously the leading term, since the WT term is the only term at that order. To determine the order of the other transitions, we expand in powers of $\frac{p_{cm}}{M_\rho}$, which yields

$$
c_{sd} = c_{ds} = \frac{g(s)}{9}\left(2 - 2\frac{\omega}{M_\rho} + \frac{\omega}{M_\rho} - \frac{\omega^2}{M_\rho^2}\right) = \frac{g(s)}{9}\left(-\frac{p_{cm}^2}{M_\rho^2} + \frac{1}{2}\frac{p_{cm}^2}{M_\rho^2} - \frac{p_{cm}^2}{M_\rho^2} + \mathcal{O}(q^4)\right),
\tag{5.85}
$$

where we used

$$
\frac{\omega}{M} = 1 + \frac{p_{cm}^2}{2M_\rho^2} + \mathcal{O}(q^4) .
\tag{5.86}
$$

Therefore, altogether the expression is $\mathcal{O}(q^3)$, since $g(s)$ is $\mathcal{O}(q)$. The relatively high order is not surprising, since the occurrence of the mixed transition c_{sd} is a relativistic effect, which leads to an additional factor of p_{cm}^2/M_ρ^2. Expanding c_{dd} yields

$$
c_{dd} = \frac{g(s)}{9}\left(1 - \frac{\omega}{M_\rho} - \frac{\omega}{M_\rho} + \frac{\omega^2}{M_\rho^2}\right) = \frac{g(s)}{9}\left(-\frac{1}{2}\frac{p_{cm}^2}{M_\rho^2} - \frac{1}{2}\frac{p_{cm}^2}{M_\rho^2} + \frac{p_{cm}^2}{M_\rho^2} + \mathcal{O}(q^4)\right) .
\tag{5.87}
$$

Thus, we see that even the $\mathcal{O}(q^3)$ terms cancel and the final order of the expression is $\mathcal{O}(q^5)$. Here the order is even higher as for c_{sd} although the appearance of a d-wave transition in general is not a pure relativistic effect. However, a d-wave transition stemming from the WT with its specific energy dependence is a relativistic effect, and therefore suppressed by further powers of p_{cm}^2/M_ρ^2. We will not discuss the coefficient c_{dd} further, since in a rigorous treatment, we would also have to check for example the contributions stemming from $J = 2$ and $J = 3$ terms of the expansion.

Next we want to see at which order the higher order terms might contribute to c_{sd}. Since the WT term contributes at $\mathcal{O}(q^3)$ to c_{sd} and c_{ds}, there might be terms of higher order in the Lagrangian (cf. Section 6.6 below), which contribute at the same order to the respective coefficients. Thus, we investigate, how the scalar coefficients F_i appear in c_{sd} and c_{ds}. We can see from Eq.(5.36-5.41) that F_2 will only yield nonzero contributions to $J = 1^+$, if it is proportional to x. In case it is proportional to x it also has to come with a factor of p_{cm}^2. Together with the factor p_{cm}^2 in Eq.(5.41) a contribution from F_2 is always at least $\mathcal{O}(q^4)$. We also do not have to consider F_1, since an F_1 stemming from the higher order terms would always be of higher order than the F_1 from the WT term. In case the only nonzero F_i would be F_3, we can read off the expansion coefficient from Eq.(5.36-5.41) to be

$$V_{11}^{1^+} = V_{10}^{1^+} = 0, \quad V_{01}^{1^+} = \frac{2\sqrt{s}p_{cm}^2}{\sqrt{2}3M_\rho}F_3, \quad V_{00}^{1^+} = \frac{\omega\sqrt{s}p_{cm}^2}{3M_\rho^2}F_3. \tag{5.88}$$

Here we assumed that an F_3 can exist which is not proportional to x. Indeed an example will be given in Eq.(6.100). We also see from Eq.(6.100) that the leading order term in F_3 is $\mathcal{O}(q)$. The above coefficients lead to

$$c_{ss} = \frac{2\sqrt{s}p_{cm}^2}{\sqrt{2}3M_\rho}F_3\left(2\sqrt{2} + 2\frac{\omega}{\sqrt{2}M}\right), \tag{5.89}$$

which is obviously $\mathcal{O}(q^3)$,

$$c_{ds} = \frac{2\sqrt{s}p_{cm}^2}{\sqrt{2}3M_\rho}F_3\left(-2\sqrt{2} - 2\frac{\omega}{\sqrt{2}M}\right), \tag{5.90}$$

which is also $\mathcal{O}(q^3)$ and

$$c_{sd} = \frac{2\sqrt{s}p_{cm}^2}{\sqrt{2}3M_\rho}F_3\left(\sqrt{2} - 2\frac{\omega}{\sqrt{2}M}\right) = \frac{2\sqrt{s}p_{cm}^2}{\sqrt{2}3M_\rho}F_3\left(-\frac{p_{cm}^2}{\sqrt{2}M^2} + \mathcal{O}(q^4)\right), \tag{5.91}$$

which is $\mathcal{O}(q^5)$. Looking at F_4 one only has to switch the roles of c_{sd} and c_{ds}. Any contribution stemming from F_5 would be at least $\mathcal{O}(q^4)$, which can be concluded with the same arguments we used for F_2. Thus, we can make the following statements :

- The leading order contribution to c_{ss} is given by the WT term only and is $\mathcal{O}(q)$.

- The leading order contribution to c_{sd} (c_{ds}) is $\mathcal{O}(q^3)$ and stems from the WT term and from any term proportional to $L_3^{\mu\nu}$ ($L_4^{\mu\nu}$) with the scalar factor F_3 in front of it being $\mathcal{O}(q)$. (These terms can be found in the $\mathcal{O}(q^2)$ Lagrangian in Eq.(6.94) below.)

It is not surprising that the coefficient c_{sd} is higher order than the coefficient c_{ss}, since the appearance of the mixed transitions is a pure relativistic effect, which leads to an additional increase in the order.

5.3. Covariant projectors

The projectors, we have constructed, are especially suited for the calculation we want to do. The task, we set out in the beginning, was to solve the Bethe-Salpeter equation with the use of projectors and then implement that solution in the context of the τ decay. Since we can explicitly work in the CMS of the Goldstone boson and the vector meson, we only need the projectors in that frame. In this frame the projectors written down in the preceding sections are perfectly well defined and the most straightforward thing one can write down. However, there are applications, where one needs the projectors in a general frame, as for example in in-medium calculations, where the frame of reference is the heat bath and not the CMS. One can not make sense of the angular expansion outside the CMS, but we can express everything in terms of covariant objects and call that object the covariant projector, which would then be defined in any frame [LK04].

Another issue, which has to be addressed, is that in our calculation the outgoing ρ meson is offshell. In order to derive the explicit form of the projectors, we considered the particles to be on their mass shell. Thus, in order to use the explicit form in our case, we have to define an offshell extrapolation of the projectors. In principle this extrapolation is arbitrary, since there is no definite argument to constrain the extrapolation. The covariant projectors offer a possibility to define the offshell extrapolation, which is also arbitrary in the sense that there is no reason for us to use the covariant projectors, but at least we have chosen the offshell extrapolation according to some 'higher' principle, namely covariance. We will discuss that issue again in Section 6.8.

In the following we will define the covariant projectors for $J^P = 1^+$ and show their relation to the projectors we have calculated before. As noted in [LK04], problems will arise, if one wants to express for example $\cos\theta$ in terms of four-vector products

$$\cos\theta \leftrightarrow \frac{Y_{q\bar{q}}}{\sqrt{Y_{qq}Y_{\bar{q}\bar{q}}}}\,, \tag{5.92}$$

with

$$Y_{xy} = \frac{(w \cdot x)(w \cdot y)}{w^2} - x \cdot y\,, \tag{5.93}$$

because of the square root singularities, which spoil the analytic properties of the projector in an arbitrary frame. Thus, we take linear combinations of the CMS projectors in order to avoid such terms. The linear combinations, which one can use for $J^P = 1^+$ are

$$\mathcal{Y}_1^{\mu\nu} = Y_{11\mu\nu}^{1^+} + \frac{\overline{\omega}}{\sqrt{2}\,\overline{M}}Y_{01\mu\nu}^{1^+} + \frac{\omega}{\sqrt{2}M}Y_{10\mu\nu}^{1^+} + \frac{\omega\overline{\omega}}{2M\overline{M}}Y_{00\mu\nu}^{1^+} = -\frac{3}{2}\left(g_{\mu\nu} - \frac{w_\mu w_\nu}{w^2}\right) \tag{5.94}$$

$$\mathcal{Y}_2^{\mu\nu} = \frac{p_{cm}^2\overline{p}_{cm}^2}{M\overline{M}}Y_{22}^{\mu\nu} = 3\left(\frac{(w \cdot q)(w \cdot \bar{q})}{s} - q \cdot \bar{q}\right)\frac{w^\mu w^\nu}{s} \tag{5.95}$$

$$\mathcal{Y}_3^{\mu\nu} = \frac{\overline{p}_{cm}^2}{\overline{M}}\left(Y_{01}^{\mu\nu} + \frac{\omega}{\sqrt{2}M}Y_{00}^{\mu\nu}\right) = \frac{3}{\sqrt{2}\sqrt{s}}\left(w^\mu\overline{q}^\nu - w^\mu w^\nu\frac{\overline{q} \cdot w}{s}\right) \tag{5.96}$$

$$\mathcal{Y}_4^{\mu\nu} = \frac{p_{cm}^2}{M}\left(Y_{10}^{\mu\nu} + \frac{\overline{\omega}}{\sqrt{2}\,\overline{M}}Y_{00}^{\mu\nu}\right) = \frac{3}{\sqrt{2}\sqrt{s}}\left(q^\mu w^\nu - w^\mu w^\nu\frac{q \cdot w}{s}\right)\,, \tag{5.97}$$

which are exactly the projectors for $J^P = 1^+$ in [LK04]. Note that the projectors are very similar to $L_1^{\mu\nu} - L_4^{\mu\nu}$.

Next we want to investigate, if there are any differences, when we use the covariant projectors. We first rename the CMS projectors and omit the Lorentz indices

$$Y_{11}^{\mu\nu} = Y_1, \quad Y_{00}^{\mu\nu} = Y_2, \quad Y_{01}^{\mu\nu} = Y_3, \quad Y_{10}^{\mu\nu} = Y_4. \tag{5.98}$$

The orthogonality relation Eq.(B.1) for the same parity $(P = +)$ part, the same J and the same M (i.e. just the helicity structure) is abbreviated as

$$(Y_i, Y_j) = o_{ijk} Y_k \tag{5.99}$$

with o_{ijk} given by

$$o_{ijk} = \begin{cases} -I_{V\phi} & \text{for} \quad ijk \in \{111, 144, 222, 233, 313, 342, 424, 431\} \\ 0 & \text{otherwise} \end{cases}. \tag{5.100}$$

We can expand the scattering amplitude for $J^P = 1^+$ into both projectors as

$$T = \sum_i t_i Y_i, \tag{5.101}$$

$$T = \sum_i t_i' \mathcal{Y}_i. \tag{5.102}$$

The matrix A, which gives the transformation between the coefficients

$$A \cdot t' = t \tag{5.103}$$

and between the projectors

$$A^T Y = \mathcal{Y} \tag{5.104}$$

is given by

$$A = \begin{pmatrix} 1 & 0 & 0 & 0 \\ \frac{\omega\overline{\omega}}{2M\overline{M}} & \frac{p_{cm}^2 \overline{p}_{cm}^2}{M\overline{M}} & \frac{\omega\overline{p}_{cm}^2}{\sqrt{2}M\overline{M}} & \frac{\overline{\omega}p_{cm}^2}{\sqrt{2}M\overline{M}} \\ \frac{\overline{\omega}}{\sqrt{2M}} & 0 & \frac{\overline{p}_{cm}^2}{M} & 0 \\ \frac{\omega}{\sqrt{2M}} & 0 & 0 & \frac{p_{cm}^2}{M} \end{pmatrix}. \tag{5.105}$$

We call the inverse $B = A^{-1}$. We calculate the orthogonality relation for the covariant projectors by using Eq.(5.99), which gives

$$(\mathcal{Y}_i, \mathcal{Y}_j) = a_{ki} a_{lj} (Y_k, Y_l) = a_{ki} a_{lj} o_{klm} Y_m = a_{ki} a_{lj} o_{klm} b_{nm} \mathcal{Y}_n. \tag{5.106}$$

Calculating the orthogonality relation for the covariant projectors in the CMS is justified, since the covariant projectors are defined in any frame.

Next we will show explicitly that for the applications of the projectors in the present work, it does not matter whether we perform the calculation with the CMS projectors or with the covariant ones. We will solve the Bethe-Salpeter equation with both projectors and afterwards show, that one can transform the results into each other. In particular this means that in any calculation in the CMS it does not matter which projectors one uses. We can expand the scattering amplitude as in Eq.(5.101) and Eq.(5.102) and the kernel as

$$K = \sum_i k_i Y_i, \tag{5.107}$$

$$K = \sum_i k_i' \mathcal{Y}_i \,. \tag{5.108}$$

The two expansions differ offshell, but onshell they are of course the same. This difference can be seen by noting that in Eq.(5.94)-Eq.(5.97) everything is expressed in terms of four-vectors, whereas in Eq.(5.23)-Eq.(5.26) the 'onshell quantities' p_{cm} and ω appear. Omitting the Lorentz indices, the Bethe-Salpeter equation in the first case is

$$t_i Y_i = k_i Y_i + k_i t_j o_{ijk} Y_k \,, \tag{5.109}$$

which we write as

$$t = k + G \cdot t \tag{5.110}$$

with $(G)_{ij} = k_l o_{lji}$. In the second case we have

$$t_i' \mathcal{Y}_i = k_i' \mathcal{Y}_i + k_i' t_j' a_{ki} a_{lj} o_{klm} b_{nm} \mathcal{Y}_n \,, \tag{5.111}$$

which we write as

$$t' = k' + G' \cdot t' \,, \tag{5.112}$$

with $(G')_{ij} = k_n a_{lj} o_{nlm} b_{im}$. Next we want to show that multiplying t' by A really gives t, which would show that it does not matter how we perform the calculation and that we can transform the results also afterwards. In order to do so, we first note that

$$(AG')_{ij} = a_{ik} k_n a_{lj} o_{nlm} b_{km} = k_n a_{lj} o_{nli} = (GA)_{ij} \,, \tag{5.113}$$

and therefore also

$$A \cdot G'^n = G^n A \tag{5.114}$$

from which it follows that

$$A \cdot t' = A(1 - G')^{-1} k' = A \sum_{n=0}^{\infty} G'^n k' = \sum_{n=0}^{\infty} G^n A k' = (1 - G)^{-1} k = t \,. \tag{5.115}$$

The crucial step in the derivation is that the orthogonality relation and therefore the loop integrals for the covariant projectors are actually calculated in the CMS, which means that even when we use the covariant projectors the calculations will be the same.

Differences might appear through the different offshell extrapolations of the projectors, which can be seen best for $\mathcal{Y}_2$ since it is directly proportional to Y_2. The following example shows the differences, which might appear offshell, for a simple case.

Example

The kernel we want to consider is

$$K = Y_2 \tag{5.116}$$

or expressed in covariant projectors

$$K = k' \mathcal{Y}_2 \tag{5.117}$$

with $k' = \frac{M\overline{M}}{\overline{p}_{cm}^2 p_{cm}^2}$. The result for T in the first case is

$$T = (1 - I_{\phi V})^{-1} Y_2 \tag{5.118}$$

and in the second case

$$T' = \left(1 - k' \frac{\overline{p}_{cm}^2 p_{cm}^2}{M\overline{M}} I_{\phi V}\right)^{-1} k' \mathcal{Y}_2 = (1 - I_{V\phi})^{-1} k' \mathcal{Y}_2 \,. \tag{5.119}$$

Onshell the results are the same, but they differ offshell. We can see this by looking at Eq.(5.95), where we see that instead of factors of p_{cm} covariant expressions in terms of four-vectors appear, which are not onshell. We also see that there would not have been a difference if we had transformed the projectors into covariant projectors before or after the calculation, since the results only differ by the use of the different projectors. In other words, if we tried to express the result from Eq.(5.118) in covariant projectors, we would as well end up with Eq.(5.119). Thus, calculating in the CMS system and afterwards transforming into covariant projectors would have let to the same results as calculating with the covariant projectors from the beginning.

For our calculations in all scenarios even the offshell extrapolation is the same, as we will see in Chapter 6.

Chapter 6.

τ Decay

The present chapter is structured as follows: after spending a few words on the weak interactions, we use the tools we discussed before to calculate the τ decay. First, we calculate the τ decay without a_1, which is the shortest part due to the simple form of the WT term. Including the a_1 is in principle straightforward after the discussions in the last chapters, but leads to some lengthy calculations, which the interested reader can find in the appendices B.1 and E.3. Finally, we calculate the decay again without a_1, but include higher order corrections to the WT term. We recall that performing the calculation with *and* without explicit a_1 is important in order to see how decisive the τ decay actual is. In addition, including the higher order terms is a reliable method in order to test the systematics of our model and study possible improvements.

6.1. Weak interactions

So far we have not yet discussed the weak process, which is the starting point of the τ decay. The weak decay of the τ into a neutrino and a W boson is part of the standard model, which is subject of many textbooks. We only summarise the properties which are relevant for the τ decay and refer to [PS95] for details.

The weak and the electromagnetic interactions are described by a spontaneously broken gauge theory, the so called Glashow-Weinberg-Salam Theory of weak interactions. It is based on an SU(2)×U(1) gauge theory, which is broken down to U(1). The interaction part of the Lagrangian, which couples the W bosons to the τ lepton is given by

$$\mathcal{L}_W = g(W_\mu^+ J_W^{\mu+} + W_\mu^- J_W^{\mu-}) \tag{6.1}$$

with

$$J_W^{\mu+} = \frac{1}{\sqrt{2}}(\bar{\nu}_L \gamma^\mu \tau_L)\,, \quad J_W^{\mu-} = \frac{1}{\sqrt{2}}(\bar{\tau}_L \gamma^\mu \nu_L)\,, \tag{6.2}$$

where the index L denotes the projection on left-handed states, as in Eq.(2.6). The weak coupling g is related to the Fermi constant G_F by

$$G_F = \sqrt{2}\frac{g^2}{8M_W^2}\,. \tag{6.3}$$

The decay of the W boson to mesons is part of the chiral Lagrangian Eq.(2.41). The decay vertex, which is given in Appendix D, includes an entry of the Cabibbo-Kobayashi-Maskawa matrix, namely V_{ud}. That matrix describes the relation between the quark mass eigenstates

and the weak eigenstates, which are not the same. In the SU(3) case the mixing can be described by a single parameter

$$\begin{pmatrix} d' \\ s' \end{pmatrix} = \begin{pmatrix} \cos\theta_C & \sin\theta_C \\ -\sin\theta_C & \cos\theta_C \end{pmatrix} = \begin{pmatrix} d \\ s \end{pmatrix}, \tag{6.4}$$

which is the so called Cabibbo angle θ_C

$$\cos\theta_C = V_{ud} = 0.974. \tag{6.5}$$

6.2. The decay width

Since the weak decay vertex is common in all diagrams (cf. Fig. 6.2 and Fig. 6.8 below), we can separate it from the hadronic information by writing the invariant matrix element as

$$i\mathcal{M} = C(s)S_\mu \left(g^{\mu\nu} - \frac{w^\mu w^\nu}{M_W^2} \right) W_\nu, \tag{6.6}$$

where we used the following abbreviations

$$S_\mu = \bar{v}(p_\nu)\gamma_\mu(1 - \gamma_5)u(p_\tau) \tag{6.7}$$

and

$$C(s) = \left(\sqrt{\frac{G_F M_W^2}{\sqrt{2}}} \right) \frac{1}{s - M_W^2} \simeq -\sqrt{\frac{G_F}{\sqrt{2}M_W^2}} = C. \tag{6.8}$$

W_ν denotes the hadronic tensor, which we will calculate in detail below. Since the mass of the W boson is much bigger than the energy region we are interested in, the last approximation is well justified. The observable quantity we want to determine is the decay width for $\tau^- \rightarrow \pi^-\pi^0\pi^0\nu_\tau$, which is given by

$$d\Gamma = \frac{(2\pi)^4}{2M_\tau}|\mathcal{M}|^2 d\phi_4, \tag{6.9}$$

where $d\phi_4$ is the four-body phase space, which we can write as a product of a three-body and two-body phase space [PDG06]

$$d\phi_4(p_\tau, q_1, q_2, q_3, p_\nu) = d\phi_3(w, q_1, q_2, q_3)d\phi_2(p_\tau, w, p_\nu)(2\pi)^3 ds. \tag{6.10}$$

In Chapter 7 we actually compare the spectral function with the data, which is related to the decay width. The exact relation is given in Eq.(7.21), where one can see that the two quantities differ basically by some kinematical factors.
We notice that S_μ in Eq.(6.7) depends only on p_τ and p_ν and the hadronic part depends only on w, q_1, q_2, q_3 (which can be seen explicitly below). Rewriting the width yields

$$\frac{d\Gamma}{ds} = \int_{\phi_3} \int_{\phi_2} \frac{(2\pi)^7}{2M_\tau}|C|^2 \frac{1}{4} \sum_{spins} S_\mu^* S_\nu \left(g^{\mu\alpha} - \frac{w^\mu w^\alpha}{M_W^2} \right) \left(g^{\nu\beta} - \frac{w^\nu w^\beta}{M_W^2} \right) W_\alpha^* W_\beta d\phi_3 d\phi_2. \tag{6.11}$$

Note the additional factor of $\frac{1}{2}$ in Eq.(6.11) due to two identical particles in the final state.

We see that we can treat

$$W_{\mu\nu} \equiv \int_{\phi_3} W_\mu^* W_\nu d\phi_3 \tag{6.12}$$

separately and by Lorentz invariance it must have the following structure

$$W^{\mu\nu}(s) = W_1(s)\left(g^{\mu\nu} - \frac{w^\mu w^\nu}{w^2}\right) + W_2(s)\frac{w^\mu w^\nu}{w^2}. \tag{6.13}$$

W_1 and W_2 can then be calculated from the following two equations

$$3W_1(s) + W_2(s) = \int_{\phi_3} W^* \cdot W \, d\phi_3 \tag{6.14}$$

$$W_2(s) = \frac{1}{s}\int_{\phi_3} w \cdot W^* w \cdot W \, d\phi_3 \tag{6.15}$$

The three-body phase space can be written as

$$d\phi_3 = \frac{1}{(2\pi)^7}\frac{1}{16s}dm_{12}^2 dm_{23}^2, \tag{6.16}$$

with the following kinematical borders

$$(m_{23}^2)_{\text{max}} = (E_2^* + E_3^*)^2 - \left(\sqrt{E_2^{*2} - m_\pi^2} - \sqrt{E_3^{*2} - m_\pi^2}\right)^2, \tag{6.17}$$

$$(m_{23}^2)_{\text{min}} = (E_2^* + E_3^*)^2 - \left(\sqrt{E_2^{*2} - m_\pi^2} + \sqrt{E_3^{*2} - m_\pi^2}\right)^2. \tag{6.18}$$

These are the values when particle 2 and 3 fly parallel or antiparallel to each other. Since m_{23}^2 is a Lorentz invariant quantity, we can calculate it in any frame, and for convenience we choose the m_{12} rest frame, where $E_2^* = \frac{\sqrt{m_{12}^2}}{2}$ and $E_3^* = \frac{s - m_\pi^2 - m_{12}^2}{2\sqrt{m_{12}^2}}$. Therefore,

$$(m_{23}^2)_{\text{max}} = \frac{(s - m_\pi^2)^2}{4m_{12}^2} - \left(\sqrt{\frac{m_{12}^2}{4} - m_\pi^2} - \sqrt{\frac{(s - m_\pi^2 - m_{12}^2)^2}{4m_{12}^2} - m_\pi^2}\right)^2, \tag{6.19}$$

$$(m_{23}^2)_{\text{min}} = \frac{(s - m_\pi^2)^2}{4m_{12}^2} - \left(\sqrt{\frac{m_{12}^2}{4} - m_\pi^2} + \sqrt{\frac{(s - m_\pi^2 - m_{12}^2)^2}{4m_{12}^2} - m_\pi^2}\right)^2 \tag{6.20}$$

and

$$(m_{12}^2)_{\text{max}} = (\sqrt{s} - m_\pi)^2, \tag{6.21}$$

$$(m_{12}^2)_{\text{min}} = 4m_\pi^2. \tag{6.22}$$

Using the above formulas, the calculation of W_1 and W_2 is straightforward. Thus, it only remains to bring Eq.(6.11) in a suitable shape.

The sum over the spin matrices is

$$\begin{aligned}
\sum S^\mu S^{\beta *} &= \sum \overline{v}(p_{\nu_\tau})\gamma^\mu(1 - \gamma_5)u(p_\tau)\overline{u}(p_\tau)(1 + \gamma_5)\gamma^\beta v(p_{\nu_\tau}) \\
&= \text{Tr}[\slashed{p}_\nu \gamma^\mu(1 - \gamma_5)(\slashed{p}_\tau + m_\tau)(1 + \gamma_5)\gamma^\beta] \\
&= \text{Tr}[\slashed{p}_\nu \gamma^\mu \slashed{p}_\tau \gamma^\beta + \slashed{p}_\nu \gamma^\mu \slashed{p}_\tau \gamma_5 \gamma^\beta - \slashed{p}_\nu \gamma^\mu \gamma_5 \slashed{p}_\tau \gamma^\beta + \slashed{p}_\nu \gamma^\mu \slashed{p}_\tau \gamma^\beta] \\
&= 2\,\text{Tr}[\slashed{p}_\nu \gamma^\mu \slashed{p}_\tau \gamma^\beta - \slashed{p}_\nu \gamma^\mu \slashed{p}_\tau \gamma^\beta \gamma_5] \\
&= 8(p_{\nu_\tau}^\mu p_\tau^\beta - p_{\nu_\tau} \cdot p_\tau g^{\mu\beta} + p_{\nu_\tau}^\beta p_\tau^\mu + i\epsilon^{\mu\beta\alpha\sigma}p_{\nu\sigma}p_{\tau\alpha}),
\end{aligned} \tag{6.23}$$

where we used the properties of the γ matrices from Appendix .A.

The decay width becomes

$$\frac{d\Gamma}{ds} = \int_{\phi_2} \frac{(2\pi)^7}{8M} |C|^2 8(2p_{\nu_\tau}^\alpha p_\tau^\beta - p_\tau \cdot p_{\nu_\tau} g^{\alpha\beta}) \left(\frac{w_\alpha w_\delta}{M_W^2} - g_{\alpha\delta} \right) \left(\frac{w_\beta w_\sigma}{M_W^2} - g_{\beta\sigma} \right)$$
$$\left(W_1(s) \left(g^{\delta\sigma} - \frac{w^\delta w^\sigma}{w^2} \right) + W_2(s) \frac{w^\delta w^\sigma}{w^2} \right) d\phi_2 \,, \tag{6.24}$$

where we used that the expression in front of $S_\mu S_\nu$ is symmetric in μ, ν, and therefore the term including the ϵ tensor vanishes. The expression can be further simplified

$$\frac{d\Gamma}{ds} = \frac{(2\pi)^7}{M} |C|^2 \int_{\phi_2} (2p_{\nu_\tau}^\alpha p_\tau^\beta - p_\tau \cdot p_{\nu_\tau} g^{\alpha\beta}) \Bigg(W_1(s) \left(g_{\alpha\beta} - \frac{w_\alpha w_\beta}{w^2} \right)$$
$$+ W_2(s) \frac{1}{s} w^\alpha w^\beta \left(1 - 2 \frac{w^2}{M_W^2} + \frac{w^4}{M_W^4} \right) \Bigg) d\phi_2 \,. \tag{6.25}$$

Neglecting terms of $\mathcal{O}(\frac{s}{M_W^2})$ (as we did already in Eq.(6.8)), we get

$$\frac{d\Gamma}{ds} = 2 \frac{(2\pi)^7}{M_\tau} |C|^2 (W_2(s) - W_1(s)) \frac{1}{s} \int_{\phi_2} (w \cdot p_{\nu_\tau})(w \cdot p_\tau) d\phi_2$$
$$- \frac{(2\pi)^7}{M_\tau} |C|^2 (W_1(s) + W_2(s)) \int_{\phi_2} (p_{\nu_\tau} \cdot p_\tau) d\phi_2 \,. \tag{6.26}$$

Neglecting the neutrino mass, we know

$$w \cdot p_{\nu_\tau} = \frac{1}{2}((w + p_{\nu_\tau})^2 - s) = \frac{1}{2}(M_\tau^2 - s) \tag{6.27}$$

$$w \cdot p_\tau = \frac{1}{2}(-(p_\tau - w)^2 + s + M_\tau^2) = \frac{1}{2}(M_\tau^2 + s) \tag{6.28}$$

$$p_{\nu_\tau} \cdot p_\tau = \frac{1}{2}(-(p_\tau - p_{\nu_\tau}) + M_\tau^2) = \frac{1}{2}(M_\tau^2 - s) \tag{6.29}$$

and

$$\int_{\phi_2} d\phi_2 = \frac{1}{2(2\pi)^5} p_{cm} \frac{1}{M_\tau} \,, \tag{6.30}$$

with $p_{cm} = \frac{1}{2M_\tau}(M_\tau^2 - s)$. Thus, we finally get

$$\frac{d\Gamma}{ds} = \frac{\pi^2}{2M_\tau s} |C|^2 (M_\tau^2 - s)^2 \left(W_2 - W_1 \left(1 + \frac{2s}{M_\tau^2} \right) \right) \,. \tag{6.31}$$

6.3. Which diagrams to include?

One can not expect chiral perturbation theory to describe the τ decay in the whole energy region (see [CFU96] for pure CHPT calculations), since the energies, which are involved are beyond $1\,\text{GeV}$ and the decay is dominated by resonance structures. Including vector mesons at tree level will certainly improve the calculation, but still one can not expect to find a satisfying description of the data due to the strong correlations in the final state. In particular, the vector
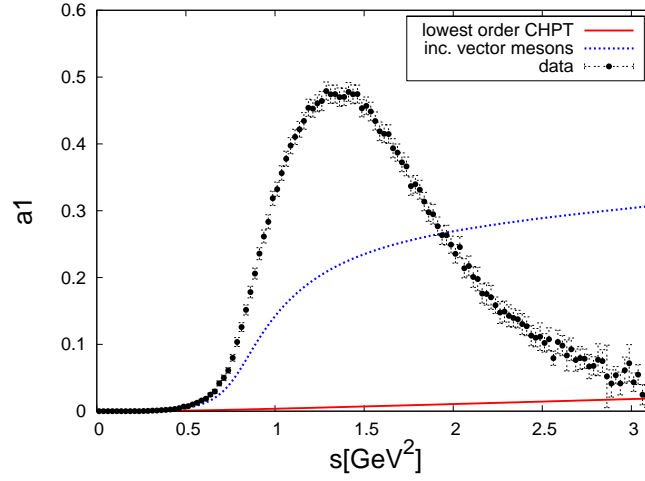
Figure 6.1.: Spectral function for the decay $\tau^- \to \pi^- \pi^0 \pi^0 \nu_\tau$ without including rescattering diagrams in comparison to data from [S$^+$05]. The lowest order CHPT calculation corresponds to the diagrams Fig. 6.2a, 6.2b and the second curve additionally includes the diagrams Fig. 6.2c, 6.2d.
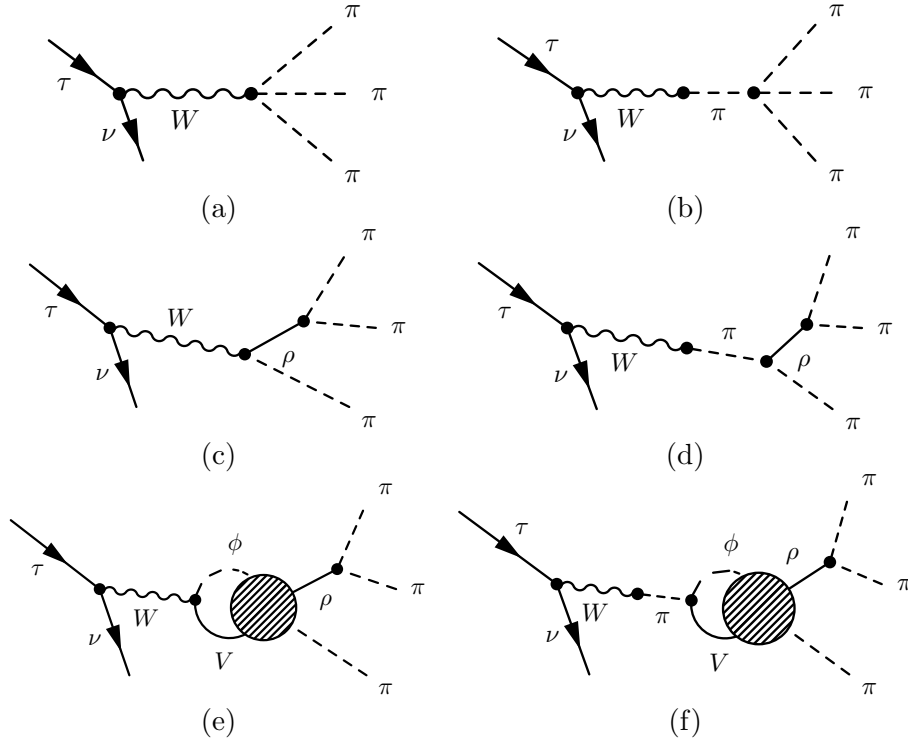

Figure 6.2.: Relevant diagrams for the decay $\tau^- \to \pi^- \pi^0 \pi^0 \nu_\tau$ without including the a_1. ϕ and V correspond to intermediate Goldstone boson and vector meson ($\pi\rho$ or KK^*). The blob represents the final state interaction obtained from the solution of the Bethe-Salpeter equation (see Fig. 4.2).
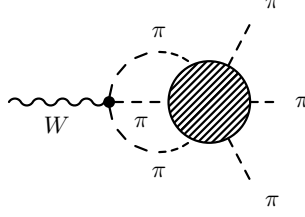
Figure 6.3.: Diagram describing pion correlations, which we do *not* include in our calculation. The blob denotes the final state interactions of the pions.

mesons at tree level can not produce an axial-vector resonance. In Fig. 6.1 we see the spectral function calculated in lowest order CHPT and by including vector mesons in comparison to data. The CHPT calculation (Fig. 6.2a, 6.2b) can only describe the lowest data points, which are far below the $\pi\rho$ threshold. The onset of the rise in the region $0.5 - 0.7\,\mathrm{GeV}^2$ is described much better if one includes the tree-level vector-meson diagrams Fig. 6.2c, 6.2d. Nonetheless, the main bump in the data at about $1.5\,\mathrm{GeV}^2$ is clearly out of reach. The philosophy in the present work is that the final state is dominated by the coupled-channel dynamics of the $\pi\rho$ state. That point of view is suggested by the improvement when we include the ρ in the calculation and the height of the amplitude, which we can see in Fig. 6.1. The deviation from the data for higher energies can then be explained by the increasing importance of the rescattering diagrams, describing the final state interactions (Fig. 6.2e, 6.2f). We neglect further correlations between the pions, as for example the diagram in Fig. 6.3, which we expect to have only a minor influence, since the tree level result for the three-pion process is much smaller than the tree-level result for the process including vector mesons (see Fig. 6.1). When we include the a_1 we expect, of course, also the a_1 to have a major influence on the result, but we still include the WT term in the calculation, as already mentioned.

In Chapter 7 we will also look at Dalitz projections, where one can see the clearly dominating ρ in the final state, which gives another justification for the processes, which we include.

6.4. Calculation of τ decay without a_1

In this version of the calculation, the a_1 is assumed to be generated dynamically. Therefore, we have to include strong final state effects, which we do by iterating the loop diagrams, as described in the previous chapters. In Fig. 6.2 we see the processes, which we take into account. The diagrams Fig. 6.2a, 6.2b are the lowest order CHPT processes, Fig. 6.2c, 6.2d are the tree-level processes including vector mesons and the diagrams Fig. 6.2e, 6.2f describe the rescattering. W_μ from Eq.(6.6) is split into the following contributions

$$W^\mu = W^\mu_{3\pi} + W^\mu_{vec} + W^\mu_{\pi\rho} + W^\mu_{KK^*}\,, \tag{6.32}$$

where $W^\mu_{3\pi}$ corresponds to the processes in Fig. 6.2a, 6.2b, W^μ_{vec} to the diagrams Fig. 6.2c, 6.2d and $W^\mu_{\phi V}$ to Fig. 6.2e, 6.2f. Using the rules from Appendix D, these functions are given

by

$$W_\mu^{3\pi} = \frac{gV_{ud}}{3F_0}(q_1 + q_3 - 2q_2)_\mu + \frac{F_0 gV_{ud}}{2}w_\mu \frac{1}{s - m_\pi^2}\frac{1}{6F_0^2}(-4w(q_1 + q_3 - 2q_2) - 2m_\pi^2)\,, \quad (6.33)$$

$$W_\mu^{vec} = \left[-\frac{gV_{ud}}{2F_0}(f_V(w \cdot m_{12}g_{\mu\alpha} - m_{12\nu}w_\alpha) - 2g_V(q_3 \cdot m_{12}g_{\mu\alpha} - m_{12\mu}q_{3\alpha}))\right.$$

$$\left. - \frac{F_0 gV_{ud}}{2}\frac{2g_V}{F_0^2}w_\mu\frac{1}{s - m_\pi^2}(m_{12} \cdot q_3 w_\alpha - w \cdot m_{12}q_{3\alpha})\right]\frac{g_V}{F_0^2}\frac{m_{12}^2}{m_{12}^2 - M_\rho^2 - \Pi}(q_1 - q_2)^\alpha$$

$$+ (q_1 \leftrightarrow q_3)\,, \quad (6.34)$$

$$W_\mu^{V\phi} = \left[\frac{-c_{\phi V}gV_{ud}}{2\sqrt{2}F_0}\int\frac{d^4l}{(2\pi)^4}(f_V(w \cdot lg_\mu^\alpha - l_\mu w^\alpha) - 2g_V((w - l) \cdot lg_\mu^\alpha - l_\mu(w - l)^\alpha))G_{\alpha\beta}^{V\phi}(l)\right.$$

$$\left. - \frac{1}{s - m_\pi^2}\frac{F_0 gV_{ud}}{2}w_\mu\int\frac{d^4l}{(2\pi)^4}c_{\phi V}\frac{\sqrt{2}g_V}{F_0^2}(l(w - l)w^\alpha - lw(w - l)^\alpha)G_{\alpha\beta}^{V\phi}(l)\right]$$

$$\cdot\frac{ig_V}{F_0^2}T_{V\phi}^{\beta\gamma}\frac{m_{12}^2}{m_{12}^2 - M_\rho^2 - \Pi}(q_1 - q_2)_\gamma \quad + \quad (q_1 \leftrightarrow q_3)\,, \quad (6.35)$$

where q_1 and q_3 are the momenta of the likewise non-charged pions, q_2 is the momentum of the charged pion, $w = q_1 + q_2 + q_3$, $m_{ij} = q_i + q_j$ and

$$G_{\alpha\beta}^{V\phi}(l) = \frac{1}{(w - l)^2 - m_\phi^2 + i\epsilon}\frac{g_{\alpha\beta} - \frac{l_\alpha l_\beta}{M_V^2}}{l^2 - M_V^2 + i\epsilon}\,. \quad (6.36)$$

$(q_1 \leftrightarrow q_3)$ denotes the same amplitude with the momenta of the likewise pions q_1 and q_3 exchanged. The self energy of the ρ meson is taken from [GK91] and given by

$$\Pi(p^2) = \frac{g_\rho^2}{48\pi^2}p^2\left(\left(1 - \frac{4m_\pi^2}{p^2}\right)^{\frac{3}{2}}\left(\ln\left|\frac{\sqrt{1 - \frac{4m_\pi^2}{p^2}} + 1}{\sqrt{1 - \frac{4m_\pi^2}{p^2}} - 1}\right| - i\pi\theta(p^2 - 4m_\pi^2)\right) + \frac{8m_\pi^2}{p^2} + C_{sub}\right)\,,$$
$$(6.37)$$

where $g_\rho = 6.05$ and the subtraction constant C_{sub} is given such that $\Re\Pi(p^2 = M_\rho^2) = 0$, which leads to

$$C_{sub} = -\frac{8m_\pi^2}{M_\rho^2} - 2\left(1 - \frac{4m_\pi^2}{M_\rho^2}\right)^{3/2}\ln\frac{M_\rho + \sqrt{M_\rho^2 - 4m_\pi^2}}{2m_\pi}\,. \quad (6.38)$$

All other constants appearing can be found in Appendix D and Tab. E.1. In most calculations the spectral distribution of the vector mesons ia also considered in the loop integral. This is done by folding the loop integral with the spectral function as follows

$$I_{\phi V} \to I_{\phi V} = i\int dx\left(\frac{-1}{\pi}\frac{\Im\Pi_V(x)}{(x - M_V^2 - \Re\Pi_V(x))^2 + \Im\Pi_V(x)^2}\right.$$
$$\left.\int\frac{d^4l}{(2\pi)^4}\frac{1}{(w - l)^2 - M_\phi^2 + i\epsilon}\frac{1}{l^2 - x + i\epsilon}\right)\,, \quad (6.39)$$

where the index V on the self energy indicates the different self energies for K^* and ρ. The self energy of K^* is calculated analogous to the one for the ρ.

The rescattering is encoded in $T_{\phi V}^{\mu\nu}$ in Eq.(6.35), which describes the scattering amplitude for the process $\phi V \to \pi\rho$. We note that $T_{\phi V}^{\mu\nu}$ factors out of the integral, since in case we take the Weinberg-Tomozawa term as the kernel, $T_{\phi V}^{\mu\nu}$ is given by Eq.(5.55) and Eq.(5.56), which only depends on w.

Evaluating the integral in Eq.(6.35), doing some algebra and introducing some abbreviations, the above functions take the following form

$$W_{3\pi}^{\mu} = -\left(g^{\mu\nu} - \frac{w^{\mu}w^{\nu}}{w^2}\right)\frac{gV_{ud}}{F_0}q_{2\nu} - \frac{gV_{ud}}{F_0}\frac{w^{\mu}}{s}\frac{m_{\pi}^2}{s - m_{\pi}^2}\left(\frac{1}{2}s - (q_2 \cdot w)\right), \tag{6.40}$$

$$W_{vec}^{\mu} = \left(g^{\mu\nu} - \frac{w^{\mu}w^{\nu}}{w^2}\right)\frac{gV_{ud}g_V}{F_0^3}\frac{m_{12}^2}{m_{12}^2 - M_V^2 - \Pi}\Big(f_V(m_{12}^2 q_{2\nu} - (m_{12} \cdot q_2)m_{12\nu})$$

$$+ (f_V - 2g_V)((m_{12}q_3)q_{2\nu} - m_{12\nu}(q_3 \cdot q_2))\Big)$$

$$+ \frac{w^{\mu}}{s}\frac{m_{\pi}^2}{s - m_{\pi}^2}\frac{2gV_{ud}g_V^2}{F_0^3}\big((m_{12} \cdot q_3)(w \cdot q_2) - (w \cdot m_{12})(q_3 \cdot q_2)\big)\frac{m_{12}^2}{m_{12}^2 - M_V^2 - \Pi}$$

$$+ (q_1 \leftrightarrow q_3), \tag{6.41}$$

$$W_T^{\mu} = W_{\pi\rho}^{\mu} + W_{KK^*}^{\mu} = \left(g^{\mu\nu} - \frac{w^{\mu}w^{\nu}}{w^2}\right)b_T\frac{m_{12}^2}{m_{12}^2 - M_{\rho}^2 - \Pi}(q_1 - q_2)_{\nu} \quad + \quad (q_1 \leftrightarrow q_3). \tag{6.42}$$

Whereas the simplifications leading to Eq.(6.40) and Eq.(6.41) are straightforward, Eq.(6.35) contains an additional loop diagram, which needs to be renormalised. The simplification of this expression corresponds to a special case of the calculation shown in Appendix B.1. In order to get to the simple form shown in Eq.(6.42), we dropped tadpoles in the renormalisation of the divergent integrals, which has been explained in the previous chapters. The nontrivial part of W_{μ}^T is contained in b_T and given by

$$b_T = \frac{3g_V gV_{ud}}{4F_0^3}M_{1111}J_{\pi\rho}(\mu_2)\Big((f_V - 2g_V)\frac{1}{2}(s - m_{\pi}^2 + M_{\rho}^2)$$

$$+ 2g_V\left(\frac{2}{3}M_{\rho}^2 + \frac{1}{12s}(m_{\pi}^2 - M_{\rho}^2 - s)^2\right)\Big)$$

$$- \frac{3g_V gV_{ud}}{4\sqrt{2}F_0^3}M_{1211}J_{KK^*}(\mu_2)\Big((f_V - 2g_V)\frac{1}{2}(s - m_K^2 + M_{K^*}^2)$$

$$+ 2g_V\left(\frac{2}{3}M_{K^*}^2 + \frac{1}{12s}(m_K^2 - M_{K^*}^2 - s)^2\right)\Big). \tag{6.43}$$

We recall that M_{1111} and M_{1211} are the expansion coefficients of the scattering amplitude, which in general can be determined by Eq.(4.74) and which are explicitly calculated in Section 5.1. We note that the renormalised loop integral $J_{\phi V}(\mu_2)$ appearing in b_T does not have to depend on the same subtraction point as the loop integrals in the scattering amplitude. Therefore we denote the subtraction point of this loop with μ_2 and the subtraction point appearing in the scattering amplitude with μ_1. We will discuss the appearance of two subtraction points and their relation in more detail later.
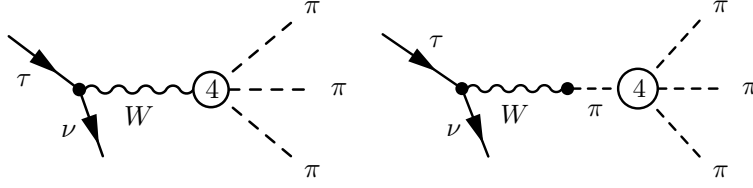
Figure 6.4.: Higher order contribution to the decay $\tau^- \to \pi^- \pi^0 \pi^0 \nu$.

Choice of interpolating fields

In Chapter 3 we discussed the differences in using vector fields or antisymmetric tensor fields to describe the interactions. In order to transform from vector fields to antisymmetric tensor fields, one had to include the following higher order interactions

$$\mathcal{L}_{3\pi ho} = -2 \operatorname{Tr}[j_{\mu\nu} j^{\mu\nu}] \tag{6.44}$$

with

$$j^{\mu\nu} = -\frac{f_V}{4} f_+^{\mu\nu} - \frac{ig_V}{4}[u^\mu, u^\nu]. \tag{6.45}$$

Assuming that CHPT is given at $\mathcal{O}(q^4)$ solely by the vector-meson tensor field Lagrangian without further point interactions, one needs the interaction term in Eq.(6.44), if one works in the vector-field realisation. We will show that the inclusion of Eq.(6.44) yields indeed a decent high-energy behaviour. Dropping terms, which are not of interest for the τ decay, we get

$$-2 \operatorname{Tr}[j_{\mu\nu} j^{\mu\nu}] \longrightarrow \frac{g_V^2}{8} \operatorname{Tr}[[u^\mu, u^\nu][u_\mu, u_\nu]] - \frac{if_V g_V}{4} \operatorname{Tr}[f_+^{\mu\nu}[u_\mu, u_\nu]]. \tag{6.46}$$

The vertices with the corresponding Feynman rules can be found in Appendix D. Perturbatively, they yield the additional contribution, which is shown diagrammatically in Fig. 6.4. Below we will show that one can even resum contributions generated from Eq.(6.44) and the $\rho\pi\pi$ coupling. The contribution from Fig. 6.4 reads

$$i\mathcal{M}_{ho} = C S_\mu \left(g^{\mu\nu} - \frac{w^\mu w^\nu}{M_W^2} \right) W_\nu^{3\pi ho}, \tag{6.47}$$

with

$$
\begin{aligned}
W_{3\pi ho}^\mu = &-\left(g^{\mu\nu} - \frac{w^\mu w^\nu}{s} \right) \left[\frac{gV_{ud} g_V}{F_0^3} (f_V - 2g_V)(q_{2\nu}(m_{12} \cdot q_3) - m_{12\nu}(q_2 \cdot q_3)) \right. \\
&\left. + \frac{gV_{ud} g_V f_V}{F_0^3} \left(m_{12}^2 q_{2\nu} - \frac{m_{12}^2}{2} m_{12\nu} \right) \right] \\
&- \frac{2gV_{ud} g_V^2}{F_0^3} \frac{m_\pi^2}{s(s - m_\pi^2)} w^\mu((w \cdot q_2)(m_{12} \cdot q_3) - (q_2 \cdot q_3)(w \cdot m_{12})) \quad + \quad (q_1 \leftrightarrow q_3).
\end{aligned}
\tag{6.48}
$$

We will show that the net effect of adding this contribution (in a resummed way) is the replacement

$$\frac{p^2}{p^2 - M_\rho^2 - \Pi} \to \frac{M_\rho^2}{p^2 - M_\rho^2 - \Pi} \tag{6.49}$$

in W_{vec}^μ (Eq.(6.41)). Superficially, it seems like we actually have to replace $p^2 \to M_\rho^2 + \Pi$. In order to show the validity of Eq.(6.49), we look at the sums of diagrams, which build up

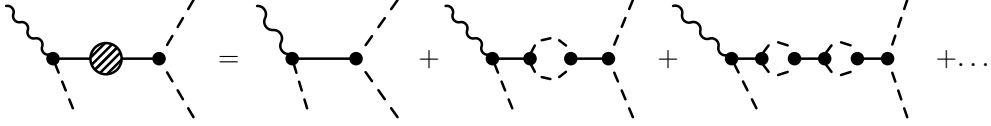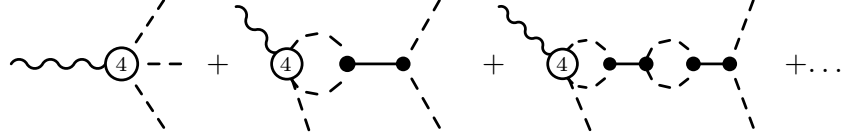**Figure 6.5.:** Sum of diagrams, which build up the full ρ propagator.

Figure 6.6.: Sum of higher order diagrams, contributing to the τ decay.

the full ρ propagator, which are shown in Fig. 6.5. So far we have just included additionally the two diagrams, which can be seen in Fig. 6.4. But looking at the sum in Fig. 6.5, it would be reasonable to also include the diagrams in Fig. 6.6, which we call W_{sum}^{μ}. In the following we will show that by including this sum, the replacement in Eq.(6.49) is justified. The central relation is that the higher order contact term is proportional to the lowest order diagram including the ρ, which is stated more precise in Fig. 6.7. This relation guarantees that one can split off the $\rho\pi\pi$ vertex in the higher order contact term in the same way as for the resonance diagram. Thus, using the relation in Fig. 6.7, both sums together yield

$$W_{vec}^{\mu} + W_{sum}^{\mu} = W_{vec}^{\mu} \left(1 - \frac{p^2 - M^2}{p^2} \right) = W_{vec}^{\mu} \frac{M^2}{p^2} \, , \tag{6.50}$$

which leads exactly to the replacement advocated in Eq.(6.49). We will not explicitly mention the inclusion of the higher order terms anymore in the following, but only perform the replacement in W_{vec}^{μ}.

We omitted the diagrams with the π intermediate state (right diagram Fig. 6.4) in the discussion, since the arguments follow exactly the same lines.

6.5. Calculation of the τ decay with explicit a_1

Next we include the a_1 explicitly. We introduce it as a bare resonance and generate the width by summing up the self-energy contributions from the decay of the a_1 into Goldstone boson and vector meson. As already mentioned, there is no good reason to drop the WT term when we include the a_1, and therefore we keep it. The choice for the kernel has been discussed in detail in Section 4.4.3. We have to calculate the diagrams shown in Fig. 6.8. In comparison
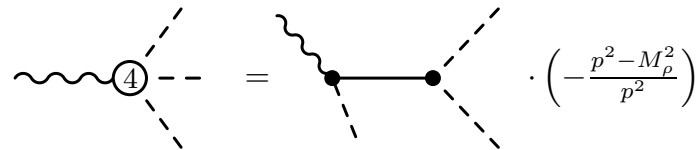

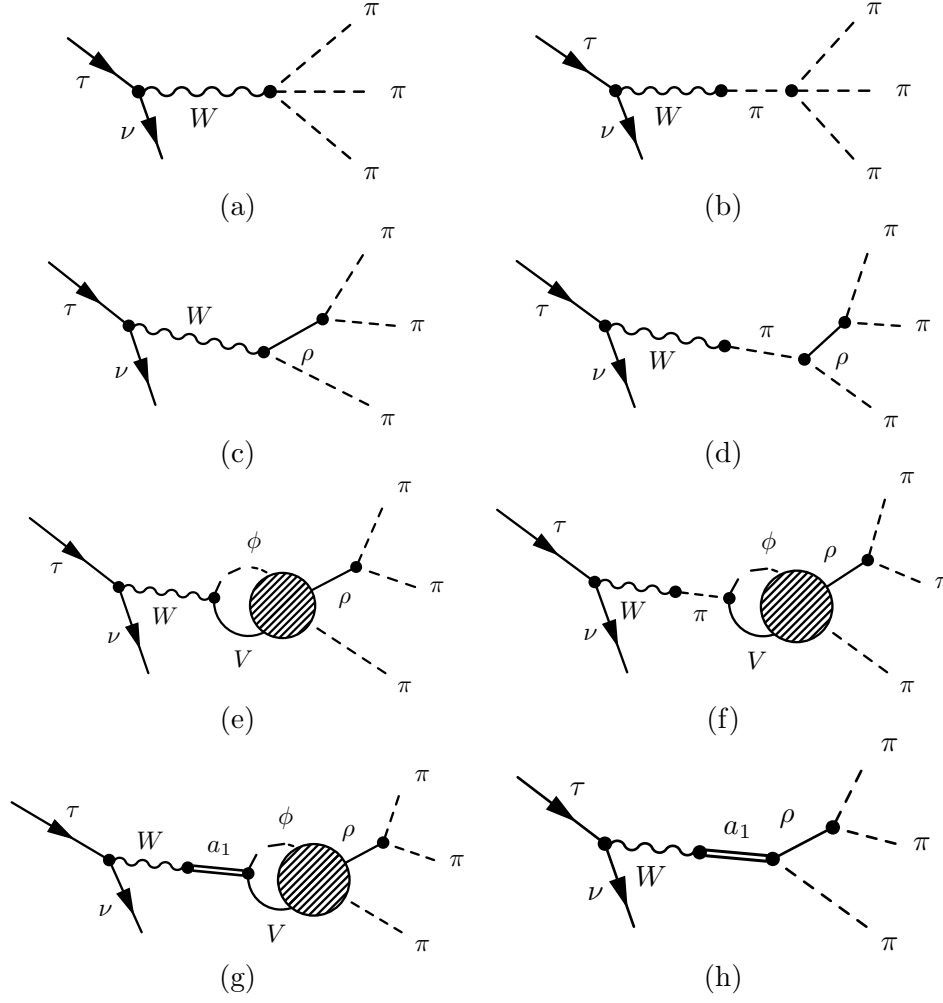**Figure 6.7.:** Relation between higher order contact term and lowest order resonance diagram.

Figure 6.8.: Relevant diagrams for the decay $\tau^- \to \pi^-\pi^0\pi^0\nu$ including the a_1.
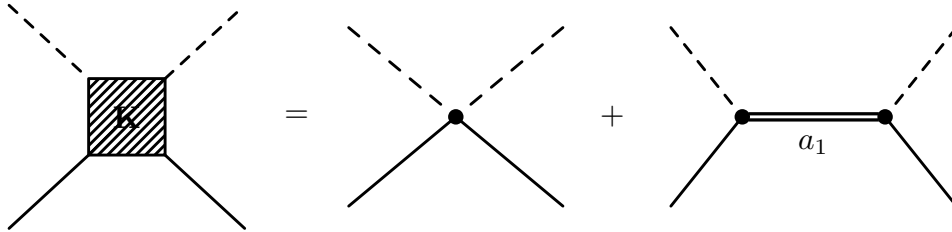

Figure 6.9.: Kernel of the Bethe-Salpeter equation when including the a_1 explicitly (see also Fig. 4.1); i.e. one has to replace the point interaction in Fig. 4.2 by the two diagrams on the right hand side.

to Fig. 6.2, there are two additional diagrams, where the W merges into the a_1. Furthermore the blobs, indicating the resummation, are not the same as in the calculation before, since we also include the a_1 interaction in the kernel. The additional diagram in the kernel is shown in Fig. 6.9, and it leads to the following expression

$$K_{a_1}^{\mu\nu} = c_{V\phi}c_{V'\phi'}\frac{16}{F_0^2}\frac{(-i)}{s - M_a^2}\left(g_{\alpha\beta} - \frac{w_\alpha w_\beta}{M_a^2}\right)(-i)(-1)$$
$$(c_1(q^\nu p^\alpha - pqg^{\alpha\nu}) + c_2(w^\nu q^\alpha - qwg^{\alpha\nu}))(c_1(\overline{q}^\mu\overline{p}^\beta - \overline{pq}g^{\beta\mu}) + c_2(w^\mu\overline{q}^\beta - \overline{q}wg^{\beta\mu})).$$

(6.51)

Note the additional factor of $(-i)$ due to the definition of the kernel in the Bethe-Salpeter equation and a factor of two due to the normalisation of the states (see also Section D.1). We rewrite this expression in a form, from which it is easy to read off the F_i

$$K_{a_1}^{\mu\nu} = \frac{16C_{WT}}{F_0^2}\frac{1}{s - M_a^2}\left[w^\mu w^\nu\left(c_1^2\left(\overline{p}p - \overline{pq} - pq - \frac{(w\overline{p})(wp)}{M_a^2} + \frac{(\overline{pq})(wp)}{M_a^2} + \frac{(pq)(w\overline{p})}{M_a^2}\right.\right.\right.$$
$$\left.\left.- \frac{(pq)(\overline{pq})}{M_a^2}\right) + c_1c_2(\overline{q}p - \overline{q}w) + c_1c_2(\overline{p}q - qw) + c_2^2(q\overline{q})\right)$$
$$+ w^\mu\overline{q}^\nu(c_1^2 pq - c_1c_2 pq + c_1c_2 qw - c_2^2 qw)$$
$$+ w^\nu q^\mu(c_1^2\overline{pq} + c_1c_2\overline{q}w - c_1c_2\overline{pq} - c_2^2\overline{q}w)$$
$$\left.+ g^{\mu\nu}(c_1^2(\overline{pq})(pq) + c_1c_2(\overline{q}w)(pq) + c_1c_2(\overline{pq})(qw) + c_2^2(\overline{q}w)(qw))\right],$$

(6.52)

where we used the Weinberg-Tomozawa matrix C_{WT} to describe the isospin structure, since it turned out to be the same.

Looking at Eq.(5.41), we see that terms proportional to x in F_2 vanish, and therefore we leave them out in F_2 already. Thus, we can write

$$F_1 = \frac{16C_{WT}}{F_0^2}\frac{1}{s - M_a^2}(c_1^2(\overline{pq})(pq) + c_1c_2(\overline{q}w)(pq) + c_1c_2(\overline{pq})(qw) + c_2^2(\overline{q}w)(qw))$$

(6.53)

$$F_2 = \frac{16C_{WT}}{F_0^2}\frac{1}{s - M_a^2}((c_1^2(\overline{p}p) + c_1c_2\overline{q}p + c_1c_2\overline{p}q + c_2^2(q\overline{q}))$$

(6.54)

$$F_3 = \frac{16C_{WT}}{F_0^2}\frac{1}{s - M_a^2}((c_1^2 - c_1c_2)pq + (c_1c_2 - c_2^2)qw)$$

(6.55)

$$F_4 = \frac{16C_{WT}}{F_0^2}\frac{1}{s - M_a^2}((c_1^2 - c_1c_2)\overline{pq} + (c_1c_2 - c_2^2)\overline{q}w)),$$

(6.56)

Using Eq.(5.28) and performing the same steps as in Section 5.1, the coefficients of the projected kernel are given by

$$V_{ab11}^{1^+} = -\frac{2}{3}F_{1ab} + g_{ab}$$

(6.57)

$$V_{ab01}^{1^+} = -\frac{2}{3\sqrt{2}M_a}(F_{1ab}\omega_a - F_{3ab}\sqrt{s}p_a^2) + \frac{\omega_a}{\sqrt{2}M_{Va}}g_{ab}$$

(6.58)

$$V_{ab10}^{1^+} = \frac{2}{3\sqrt{2}M_b}(-\omega_b F_{1ab} + F_{4ab}p_b^2\sqrt{s}) + \frac{\omega_b}{\sqrt{2}M_{Vb}}g_{ab}$$

(6.59)

$$V_{ab00}^{1^+} = \frac{1}{3M_a M_b}\left(-\omega_a\omega_b F_{1ab} - sp_b^2 p_a^2(c_1 - c_2)^2\frac{16C_{WT}}{F_0^2}\frac{1}{s - M_a^2} + F_{3ab}\omega_b p_a^2\sqrt{s}\right.$$
$$\left.+ F_{4ab}\omega_a p_b^2\sqrt{s}\right) + \frac{\omega_a\omega_b}{2M_{Va}M_{Vb}}g_{ab}.$$

(6.60)

We note again that the coefficients F_i possess a matrix structure, since C_{WT} is a matrix, and the indices a, b denote the respective channels.

The whole matrix element can be written similar to Eq.(6.6)

$$i\mathcal{M}_{a1} = CS_\mu \left(g^{\mu\nu} - \frac{w^\mu w^\nu}{M_W^2} \right) W_\nu \,, \tag{6.61}$$

but this time with

$$W_\nu = W_\nu'^{\pi\rho} + W_\nu'^{KK^*} + W_\nu^{3\pi} + W_\nu^{vec} + W_\nu^{tree} + W_\nu^{a1\pi\rho} + W_\nu^{a1KK^*} \,. \tag{6.62}$$

W_ν^{tree} corresponds to Fig. 6.8h, W_ν^{a1} to Fig. 6.8g and $W_\nu'^{V\phi}$ differ from $W_\nu^{V\phi}$ because of the different kernel. Due to the non-vanishing of F_3 and F_4 the solution of the Bethe-Salpeter equation will not take the simple form of Eq.(5.55), and in contrast to the calculation before $T_{V\phi}^{\mu\nu}$ will not factor out of the integral. Therefore, we can not take over the calculation for $W_\nu^{V\phi}$ from before, and we have to do some more algebra. Using the rules from Appendix D, we get

$$
\begin{aligned}
W_\mu'^{\phi V} =& \left[\frac{-c_{\phi V} g V_{ud}}{2\sqrt{2}F_0} \int \frac{d^4 l}{(2\pi)^4} (f_V (w \cdot l g_\mu^\alpha - l_\mu w^\alpha) \right. \\
& \qquad - 2g_V ((w-l)\cdot l g_\mu^\alpha - l_\mu (w-l)^\alpha)) G_{\alpha\beta}^{\phi V}(l) T_{\phi V}^{\beta\gamma}(l) \\
& \left. - \frac{1}{s - m_\pi^2} \frac{F_0 g V_{ud}}{2} w_\mu \int \frac{d^4 l}{(2\pi)^4} c_{\phi V} \frac{\sqrt{2}g_V}{F_0^2} (l(w-l)w^\alpha - lw(w-l)^\alpha) G_{\alpha\beta}^{\phi V}(l) T_{\phi V}^{\beta\gamma}(l) \right] \\
& \cdot \frac{ig_V}{F_0^2} \frac{m_{12}^2}{m_{12}^2 - M_\rho^2 - \Pi}(q_1 - q_2)_\gamma \quad + \quad (q_1 \leftrightarrow q_3) \\
=& \left[-c_{\phi V}\frac{g V_{ud}}{2\sqrt{2}F_0} \int \frac{d^4 l}{(2\pi)^4} \left(f_V (w \cdot l g_\mu^\alpha - l_\mu w^\alpha) \right. \right. \\
& \left. - 2g_V ((w-l)\cdot l g_\mu^\alpha - l_\mu (w-l)^\alpha - \frac{w_\mu w^\alpha}{s} l(w-l) + (w-l)^\alpha w_\mu \frac{lw}{s}) \right) G_{\alpha\beta}^{\phi V}(l) T_{\phi V}^{\gamma\beta}(l) \\
& \left. - c_{\phi V}\frac{g V_{ud}}{2\sqrt{2}F_0} 2g_V \frac{m_\pi^2}{s-m_\pi^2} \frac{w_\mu}{s} \int \frac{d^4 l}{(2\pi)^4}(l(w-l)w^\alpha - lw(w-l)^\alpha) G_{\alpha\beta}^{\phi V}(l) T_{\phi V}^{\gamma\beta}(l) \right] \\
& \cdot \frac{ig_V}{F_0^2} \frac{m_{12}^2}{m_{12}^2 - M_\rho^2 - \Pi}(q_1 - q_2)_\gamma \quad + \quad (q_1 \leftrightarrow q_3) \,.
\end{aligned}
\tag{6.63}
$$

We evaluate that expression explicitly in Appendix B.1, where it is shown to take the form

$$
\begin{aligned}
W_{\phi V}'^\mu =& \frac{c_{\phi V} g V_{ud} g_V}{2\sqrt{2}F_0^3} J_{\phi V}(\mu_2) \left(g_V(\alpha_1^{\phi V} L_1^{\gamma\mu} + \alpha_3^{\phi V} L_3^{\gamma\mu}) \frac{m_{12}^2}{m_{12}^2 - M_\rho^2 - \Pi}(q_1 - q_2)_\gamma \right. \\
& \left. + \frac{1}{2}(f_V - 2g_V)(\alpha_2^{\phi V} L_1^{\gamma\mu} + \alpha_4^{\phi V} L_3^{\gamma\mu}) \frac{m_{12}^2}{m_{12}^2 - M_\rho^2 - \Pi}(q_1 - q_2)_\gamma \right) \quad + \quad (q_1 \leftrightarrow q_3) \,.
\end{aligned}
$$

The coefficients α_i can be found in Appendix B.1. We see that the result is proportional to $L_1^{\mu\nu}$ and $L_3^{\mu\nu}$, which means that we can express the result easily in terms of the covariant projectors from Section 5.3. Thus, due to the explicit form of the result, the offshell extension will not change by this replacement.

The contribution from the additional diagram in Fig. 6.8g is given by

$$
W^\mu_{a1\phi V} = \frac{if_A}{2} g V_{ud} s \left(g^{\mu\nu} - \frac{w^\mu w^\nu}{w^2} \right) \frac{g_{\nu\alpha}}{s - M^2_{a1}} c_{\phi V} \frac{2\sqrt{2}}{F_0}
$$
$$
\left(c_1 \int \frac{d^4l}{(2\pi)^4} ((w-l)^\beta l^\alpha - (w-l)lg^{\alpha\beta}) G^{\phi V}_{\beta\gamma} T^{\gamma\delta}_{\phi V} \right.
$$
$$
\left. + c_2 \int \frac{d^4l}{(2\pi)^4} ((w-l)^\alpha w^\beta - (w-l)wg^{\alpha\beta}) G^{\phi V}_{\beta\gamma} T^{\delta\gamma}_{\phi V} \right) \frac{g_V}{F_0^2} \frac{m^2_{12}}{m^2_{12} - M^2_\rho - \Pi} (q_1 - q_2)_\delta
$$
$$
+ \quad (q_1 \leftrightarrow q_3)
$$
$$
= \frac{2ic_{\phi V} f_A g V_{ud} g_V s}{\sqrt{2} F_0^3} \left(g^{\mu\alpha} - \frac{w^\mu w^\alpha}{w^2} \right) \frac{1}{s - M^2_{a1}} \left(c_1 \int \frac{d^4l}{(2\pi)^4} ((w-l)^\beta l_\alpha - (w-l)lg^\beta_\alpha) G^{\phi V}_{\beta\gamma} T^{\gamma\delta}_{\phi V} \right.
$$
$$
\left. + c_2 \int \frac{d^4l}{(2\pi)^4} ((w-l)_\alpha w^\beta - (w-l)wg^\beta_\alpha) G^{\phi V}_{\beta\gamma} T^{\delta\gamma}_{\phi V} \right) \frac{m^2_{12}}{m^2_{12} - M^2_\rho - \Pi} (q_1 - q_2)_\delta
$$
$$
+ \quad (q_1 \leftrightarrow q_3) .
$$
(6.64)

This expression can be simplified in a similar way as $W'^\mu_{\phi V}$, which yields

$$
W^\mu_{a1\phi V} = \frac{c_{\phi V} f_A g V_{ud} g_V}{\sqrt{2} F_0^3} \frac{s}{s - M^2_a} J_{\phi V}(\mu_1) \left(g^\mu_\alpha - \frac{w^\mu w_\alpha}{w^2} \right)
$$
$$
\cdot \left((c_1 \beta^{\phi V}_1 + c_2 \beta^{\phi V}_2) L^{\delta\alpha}_1 + (c_1 \beta^{\phi V}_3 + c_2 \beta^{\phi V}_4) L^{\delta\alpha}_3 \right) \frac{m^2_{12}}{m^2_{12} - M^2_\rho - \Pi} (q_1 - q_2)_\delta
$$
$$
+ \quad (q_1 \leftrightarrow q_3) .
$$
(6.65)

The coefficients $\beta^{\phi V}_i$ are again functions of s and are given by

$$
\beta^{\phi V}_1 = (s - m^2_\phi - M^2_V) M_{11} + \frac{M_V}{\sqrt{2}\sqrt{s}} (s + m^2_\phi - M^2_V) M_{10} ,
$$
(6.66)

$$
\beta'^{\phi V}_1 = (s - m^2_\phi - M^2_V) M_{01} + \frac{M_V}{\sqrt{2}\sqrt{s}} (s + m^2_\phi - M^2_V) M_{00} ,
$$
(6.67)

$$
\beta^{\phi V}_2 = (s + m^2_\phi - M^2_V) M_{11} + \frac{\sqrt{s}}{\sqrt{2} M_V} (s - m^2_\phi - M^2_V) M_{10} ,
$$
(6.68)

$$
\beta'^{\phi V}_2 = (s + m^2_\phi - M^2_V) M_{01} + \frac{\sqrt{s}}{\sqrt{2} M_V} (s - m^2_\phi - M^2_V) M_{00} ,
$$
(6.69)

$$
\beta^{\phi V}_3 = \beta^{\phi V}_1 \frac{\overline{\omega}}{\overline{p}^2 \sqrt{s}} - \beta'^{\phi V}_1 \frac{\sqrt{2} M_\rho}{\overline{p}^2 \sqrt{s}} ,
$$
(6.70)

$$
\beta^{\phi V}_4 = \beta^{\phi V}_2 \frac{\overline{\omega}}{\overline{p}^2 \sqrt{s}} - \beta'^{\phi V}_2 \frac{\sqrt{2} M_\rho}{\overline{p}^2 \sqrt{s}} .
$$
(6.71)

Note that the indices on the expansion coefficients M_{ij} of the scattering amplitude indicating the channels are suppressed, as explained in Appendix B.1.

The last new diagram, we have to evaluate, is the new tree level diagram in Fig. 6.8h, which leads to the following expression

$$
W^\mu_{tree} = \frac{2 f_A g V_{ud} g_V}{F_0^3} \frac{s}{s - M^2_a} \left(g^{\mu\alpha} - \frac{w^\mu w^\alpha}{w^2} \right) \frac{m^2_{12}}{m^2_{12} - M^2_\rho - \Pi} (q_1 - q_2)^\beta
$$
$$
(c_1 (q_{3\beta} m_{12\alpha} - q_3 m_{12} g_{\alpha\beta}) + c_2 (w_\beta q_{3\alpha} - w q_3 g_{\alpha\beta}) \quad + \quad (q_1 \leftrightarrow q_3) .
$$
(6.72)

In order to compare the resulting matrix element to the one in [GDPP04], we write

$$
i\mathcal{M}_{tree} = \frac{4G_F V_{ud} f_A g_V}{3F_0^3} \frac{s}{s - M_A^2} \frac{m_{12}^2}{m_{12}^2 - M_\rho^2} S^\mu \left(g_{\mu\nu} - \frac{w_\mu w_\nu}{s} \right)
$$

$$
\cdot \left[(q_1 - q_2)^\nu \left(c_2(-2s + 2m_{12}^2 + m_{23}^2 - 3m_\pi^2) - c_1 m_{12}^2 (s - m_{12}^2 + m_{23}^2 - 3m_\pi^2) \right) \right. \tag{6.73}
$$

$$
\left. + (q_3 - q_2)^\nu (c_2 - c_1)(u - m_{23}^2) \right] \quad + \quad (q_1 \leftrightarrow q_3).
$$

In [GDPP04] an additional constant λ_0 appears, which we consider to be negligible due to an additional factor of m_π^2. Neglecting λ_0, the matrix element obtained in [GDPP04] can be written as

$$
i\mathcal{M} = \frac{4G_F V_{ud} F_A G_V}{\sqrt{2} 3 F_0^3} \frac{s}{s - M_A^2} \frac{m_{12}^2}{m_{12}^2 - M_\rho^2} S^\mu \left(g_{\mu\nu} - \frac{w_\mu w_\nu}{s} \right)
$$

$$
\cdot \left[(q_1 - q_2)^\nu \left(\frac{\lambda'}{s}(-2s + 2m_{12}^2 + m_{23}^2 - 3m_\pi^2) + \frac{\lambda''}{m_{12}^2}(s - m_{12}^2 + m_{23}^2 - 3m_\pi^2) \right) \right. \tag{6.74}
$$

$$
\left. + (q_3 - q_2)^\nu \left(\frac{\lambda'}{s} + \frac{\lambda''}{m_{12}^2} \right)(u - m_{23}^2) \right] \quad + \quad (q_1 \leftrightarrow q_3).
$$

This means we can identify

$$
\mp \frac{\sqrt{2}}{M_A M_\rho} c_1 \leftrightarrow \frac{\lambda''}{m_{12}^2}, \quad \pm \frac{\sqrt{2}}{M_A M_\rho} c_2 \leftrightarrow \frac{\lambda'}{s}, \tag{6.75}
$$

where the additional dependence on s and m_{12}^2 stems from the choice of fields. In [GDPP04] high-energy constraints are used to constrain the parameters, which results in

$$
\lambda'' = 0, \quad \lambda' = \frac{1}{2}. \tag{6.76}
$$

This leads to the values for c_1 and c_2, which have been given in Eq.(3.32). A direct comparison, however, is ambiguous due to the higher order terms and the additional energy dependence. Although, for example, the influence of λ_0 should be small, by using the values obtained in [GDPP04] one finds that this is not the case. In addition, in [GDPP04] the width of the a_1 is parametrised, whereas we will generate it by the decay into vector meson and Goldstone boson, which also makes a comparison troublesome. The sign for c_2 was chosen by comparing the relative minus sign to the expressions for the other diagrams in [GDPP04].

$W_{a1\phi V}^\mu$ as well as the new tree level diagram W_{tree}^μ are singular at $s = M_{a_1}$. The reason for this is that the bare a_1 does not have a width. This width is generated by the Bethe-Salpeter equation and only the sum of *all* diagrams yields a well defined result. Thus we have to add the diagrams Fig. 6.8g and Fig. 6.8h in order to get a non-singular result. Adding the diagrams leads to

$$
W_\mu^{tree} + W_\mu^{a1\pi\rho} + W_\mu^{a1KK^*} = \frac{f_A g V_{ud} g_V s}{\sqrt{2} F_0^3} \left(g_{\mu\alpha} - \frac{w_\mu w_\alpha}{w^2} \right) \frac{m_{12}^2}{m_{12}^2 - M_\rho^2 - \Pi}(q_1 - q_2)_\beta
$$

$$
\left(c_1 \left(-(M_1^{a1})_1 L_1^{\alpha\beta} + \left(-\frac{\omega_{\pi\rho}}{\sqrt{s}p_{cm\pi\rho}^2}(M_1^{a1})_1 + \frac{\sqrt{2}M_\rho}{\sqrt{s}p_{cm\pi\rho}^2}(M_1^{a1})_3 \right) L_3^{\beta\alpha} \right) \right.
$$

$$
\left. + c_2 \left(-(M_2^{a1})_1 L_1^{\alpha\beta} + \left(-\frac{\omega_{\pi\rho}}{\sqrt{s}p_{cm\pi\rho}^2}(M_2^{a1})_1 + \frac{\sqrt{2}M_\rho}{\sqrt{s}p_{cm\pi\rho}^2}(M_2^{a1})_3 \right) L_3^{\beta\alpha} \right) \right) \tag{6.77}
$$

$$
+ \quad (q_1 \leftrightarrow q_3).
$$

The details of calculation as well as the definition of M_i^{a1} can be found in Appendix E.3. Looking at Eq.(6.77), it is still not explicit that the expression does not contain a singularity anymore, but it should be clear from the explanation above. In order to get a feeling for the expression and see its connection to the a_1 propagator including the self-energy, we neglect the WT term for the moment. Then the sum of these diagrams should be equal to a tree diagram including the self energy Π_{a_1} of the a_1. This means that without the WT term the a_1 propagator is given by

$$
\frac{1}{s - M_a^2 - \Pi_{a1}} \overset{!}{=} \frac{c_1(M_1^{a1})_1 + c_2(M_2^{a1})_1}{(c_1(s - m_\pi^2 - M_\rho^2) + c_2(s + m_\pi^2 - M_\rho^2))\sqrt{2}}
$$
$$
\overset{!}{=} \left(-(c_1(M_1^{a1})_1 + c_2(M_2^{a1})_1)\omega_{\pi\rho} + (c_1(M_1^{a1})_3 + c_2(M_2^{a1})_3)\sqrt{2}M_\rho\right) \frac{1}{2\sqrt{2}\sqrt{s}p_{cm\pi\rho}^2(c2 - c1)} .
$$
(6.78)

Showing this equality analytically is cumbersome and therefore we checked it numerically by explicitly calculating both sides. Including the WT term, however, the above formula does not hold anymore.

We see that we can add $W_\mu'^{\phi V}$ and $W_\mu^{tree} + W_\mu^{a1\phi V}$ easily and get

$$
W_\mu^{Ta1} \equiv W_\mu^{tree} + \sum_{\phi V}(W_\mu^{a1\phi V} + W_\mu'^{\phi V}) = \left(g_{\mu\alpha} - \frac{w_\mu w_\alpha}{w^2}\right) \frac{m_{12}^2}{m_{12}^2 - M_\rho^2 - \Pi}(q_1 - q_2)_\delta
$$
$$
(A_1 L_1^{\delta\alpha} + A_2 L_3^{\delta\alpha}) \quad + \quad (q_1 \leftrightarrow q_3)
$$
(6.79)

with

$$
A_1 = -\frac{f_A g V_{ud} g_V s}{\sqrt{2}F_0^3}(c_1(M_1^{a1})_1 + c_2(M_2^{a1})_1) + \sum_{\phi V} \frac{c_{\phi V} g V_{ud} g_V}{2\sqrt{2}F_0^3} J_{\phi V}(\mu_2)\left(g_V \alpha_1^{\phi V} + \frac{1}{2}(f_V - 2g_V)\alpha_2^{\phi V}\right)
$$
(6.80)

and

$$
A_2 = -\frac{f_A g V_{ud} g_V s}{\sqrt{2}F_0^3}\left(c_1\left(\frac{\omega_{\pi\rho}}{\sqrt{s}p_{cm\pi\rho}^2}(M_1^{a1})_1 - \frac{\sqrt{2}M_\rho}{\sqrt{s}p_{cm\pi\rho}^2}(M_1^{a1})_3\right)\right.
$$
$$
\left. + c_2\left(\frac{\omega_{\pi\rho}}{\sqrt{s}p_{cm\pi\rho}^2}(M_2^{a1})_1 - \frac{\sqrt{2}M_\rho}{\sqrt{s}p_{cm\pi\rho}^2}(M_2^{a1})_3\right)\right)
$$
$$
+ \sum_{\phi V} \frac{c_{\phi V} g V_{ud} g_V}{2\sqrt{2}F_0^3} J_{\phi V}(\mu_2)\left(g_V \alpha_3^{\phi V} + \frac{1}{2}(f_V - 2g_V)\alpha_4^{\phi V}\right) .
$$
(6.81)

The remaining part is now straightforward and follows the same lines as in the calculation before. We only have to substitute W_T^μ with W_{Ta1}^μ in the calculation of W_1. W_2 does not change, because neither $W_{\phi V}^\mu$ nor $W_{\phi Va1}^\mu$ contribute to W_2.

At the beginning of this section we used that the a_1 vertex, which results from the Lagrangian Eq.(3.28), is given by

$$
\Gamma_{a1}^{\mu\nu} = -\frac{2\sqrt{2}c_{\phi V}}{F_0}c_1(q^\nu p^\mu - p \cdot q g^{\mu\nu}) - \frac{2\sqrt{2}c_{\phi V}}{F_0}c_2(w^\nu q^\mu - w \cdot q g^{\mu\nu}) .
$$
(6.82)

Using $\epsilon_\nu(p)p^\nu = 0$, $s = M_a^2$, $M_a^2 = 2M_\rho^2$ and $c_1 = 2c_2$ the vertex can be cast into a different form

$$
\Gamma_{a1}^{\mu\nu} = \frac{2\sqrt{2}c_{\phi V}}{F_0}c_2(2q^\nu p^\mu - (2pq + wq)g^{\mu\nu} + w^\nu q^\mu) = \frac{2\sqrt{2}c_{\phi V}}{F_0}c_2(w^\nu p^\mu - wp g^{\mu\nu}) .
$$
(6.83)

The last expression is the vertex, which is used in [RPO04]. We see that only with the simplifications above, the vertex is the same as the one we use. These simplifications, however, basically mean to put certain momenta onshell and apply Weinberg's relation between the ρ and a_1 mass [Wei67], as well as a relation between c_1 and c_2, which are anyway free parameters. Using explicitly the vertex from Eq.(6.83), the formulas slightly change and we have to replace

$$A_1 = -\frac{f_A g V_{ud} g_V s}{\sqrt{2} F_0^3} c_2 (M_3^{a1})_1 + \sum_{\phi V} \frac{c_{\phi V} g V_{ud} g_V}{2\sqrt{2} F_0^3} J_{\phi V}(\mu_2) \left(g_V \alpha_1^{\phi V} + \frac{1}{2}(f_V - 2g_V)\alpha_2^{\phi V} \right) \quad (6.84)$$

and

$$
\begin{aligned}
A_2 = & -\frac{f_A g V_{ud} g_V s}{\sqrt{2} F_0^3} c_2 \left(\frac{\omega_{\pi\rho}}{\sqrt{s} p_{cm\pi\rho}^2} (M_3^{a1})_1 - \frac{\sqrt{2} M_\rho}{\sqrt{s} p_{cm\pi\rho}^2} (M_3^{a1})_3 \right) \\
& + \sum_{\phi V} \frac{c_{\phi V} g V_{ud} g_V}{2\sqrt{2} F_0^3} J_{\phi V}(\mu_2) \left(g_V \alpha_3^{\phi V} + \frac{1}{2}(f_V - 2g_V)\alpha_4^{\phi V} \right),
\end{aligned}
\quad (6.85)
$$

with

$$M_3^{a1} = \frac{1}{s - M_a^2}(1 - VJ)^{-1} \begin{pmatrix} \sqrt{2}(s - m_\pi^2 + M_\rho^2) \\ -(s - M_K^2 + M_{K^*}^2) \\ 2M_\rho\sqrt{s} \\ -\sqrt{2}M_{K^*}\sqrt{s} \end{pmatrix}. \quad (6.86)$$

In addition, the kernel changes, which is taken care of by using

$$F_1 = \frac{16 C_{WT}}{F_0^2} \frac{1}{s - M_a^2} c_2^2 (w \cdot p)(w \cdot \bar{p}) \quad (6.87)$$

$$F_2 = \frac{16 C_{WT}}{F_0^2} \frac{1}{s - M_a^2} c_2^2 (q\bar{q}) \quad (6.88)$$

$$F_3 = \frac{16 C_{WT}}{F_0^2} \frac{1}{s - M_a^2} c_2^2 (w \cdot p) \quad (6.89)$$

$$F_4 = \frac{16 C_{WT}}{F_0^2} \frac{1}{s - M_a^2} c_2^2 (w \cdot \bar{p}). \quad (6.90)$$

In Section 7.3 we will show the influence of these modifications on the results.

6.6. Calculation of τ decay including higher order terms

This time we again assume that the a_1 is generated dynamically. In addition to the WT term, we consider higher order corrections to the kernel of the Bethe-Salpeter equation. One part of the higher order correction, as the WT term itself, is contained in the kinetic part of the Lagrangian Eq.(3.18). As long as we were only interested in the lowest order, we dropped it in the derivation of the WT term because it is higher order (see Eq.(D.1) and the comment afterwards). This term reads

$$\frac{1}{2}\,\mathrm{Tr}[[V^\mu, \partial_\mu V_\nu]\Gamma^\nu] \to \frac{1}{16 F_0^2}\,\mathrm{Tr}[[V^\mu, \partial_\mu V_\nu][\phi, \partial^\nu \phi]], \quad (6.91)$$

where we dropped terms containing more than two Goldstone boson fields. A partial integration leads to

$$-\frac{1}{16 F_0^2}\,\mathrm{Tr}[[V^\mu, V^\nu][\partial_\mu \phi, \partial_\nu \phi] - \underbrace{[V^\mu, V^\nu][\phi, \partial_\mu \partial_\nu \phi]}_{=0} - \underbrace{[\partial_\mu V^\mu, V^\nu][\phi, \partial_\nu \phi]}_{=0}], \quad (6.92)$$

where one sees that the second part is zero by exchanging $\mu \leftrightarrow \nu$ and the third part is zero because of $\partial_\mu V^\mu = 0$. The first term in Eq.(6.92) has a similar structure as the WT term, and we can evaluate it by looking closely at the result of the WT term. The new contribution to the kernel reads

$$K_1^{\mu\nu} = \frac{C_{WT}}{2F_0^2}(q^\nu \bar{q}^\mu - q^\mu \bar{q}^\nu).$$
(6.93)

Next we write down all terms with two pion momenta, which one can construct, taking care of parity, C-invariance, hermiticity and of course chiral symmetry (see Appendix C for details)

$$
\begin{aligned}
\mathcal{L}_{ho} = {} & \lambda_1' \operatorname{Tr}[V_\mu V^\mu u_\nu u^\nu] + \lambda_2' \operatorname{Tr}[V_\mu u_\nu V^\mu u^\nu] \\
& + \lambda_3' \operatorname{Tr}[V_\mu V_\nu u^\mu u^\nu] + \lambda_4' \operatorname{Tr}[V_\mu V^\nu u_\nu u^\mu] + \lambda_5' \operatorname{Tr}[V_\mu u^\mu V_\nu u^\nu + V_\mu u^\nu V_\nu u^\mu] \\
& + \lambda_6' \operatorname{Tr}[V_{\mu\nu} V^{\nu\alpha} u_\alpha u^\mu] + \lambda_7' \operatorname{Tr}[V_{\mu\nu} V^{\nu\alpha} u^\mu u_\alpha] + \lambda_8' \operatorname{Tr}[V_{\mu\nu} u_\alpha V^{\nu\alpha} u^\mu + V_{\mu\nu} u^\mu V^{\nu\alpha} u_\alpha] \quad (6.94) \\
& + \lambda_9' \operatorname{Tr}[V_\mu u^\nu] \operatorname{Tr}[V^\mu u_\nu] + \lambda_{10}' \operatorname{Tr}[V_\mu u^\mu] \operatorname{Tr}[V_\nu u^\nu] + \lambda_{11}' \operatorname{Tr}[V_\mu u_\nu] \operatorname{Tr}[V^\nu u^\mu] \\
& + \lambda_{12}' \operatorname{Tr}[V_\mu^\alpha u^\mu] \operatorname{Tr}[V_{\nu\alpha} u^\nu] + \lambda_{13}' \operatorname{Tr}[V_{\mu\alpha} u_\nu] \operatorname{Tr}[V^{\nu\alpha} u^\mu].
\end{aligned}
$$

The thirteen new terms are evaluated in Appendix D and lead to the following kernel in addition to the WT-term

$$
\begin{aligned}
K_{ho}^{\mu\nu} = {} & \frac{4C_{WT}}{F_0^2}\Big((\bar{q} \cdot q)g^{\mu\nu}(\lambda_1' - 2\lambda_2') + \bar{q}^\nu q^\mu(\lambda_3' - 2\lambda_5' - \frac{1}{2}) \\
& + \bar{q}^\mu q^\nu(\lambda_4' - 2\lambda_5' + \frac{1}{2}) - (w \cdot q)(w \cdot \bar{q})g^{\mu\nu}(\lambda_6' + \lambda_7' - 2\lambda_8')\Big) \\
& - \frac{8\mathbb{1}_2}{F_0^2}\Big((\lambda_9'(q \cdot \bar{q}) + (\lambda_{12}' + \lambda_{13}')(w \cdot q)(w \cdot \bar{q}))g^{\mu\nu} + \lambda_{10}' q^\mu \bar{q}^\nu + \lambda_{11}' \bar{q}^\mu q^\nu\Big).
\end{aligned}
$$
(6.95)

Thus, we see that there are actually only eight independent variables contributing to the kernel. Using $p^\nu e_\nu(p) = 0$, we can replace $q^\nu \bar{q}^\mu \to w^\nu w^\mu$ and use that only terms proportional to x will contribute to F_2. Thus, the term proportional to $w^\mu w^\nu$ does not contribute at all, and we are down to six independent variables, which we call $\lambda_1, \lambda_2, \ldots \lambda_6$. Therefore the kernel can be written as

$$
\begin{aligned}
K_{ho}^{\mu\nu} = {} & \frac{C_{WT}}{F_0^2}\Big(g^{\mu\nu}\big(\lambda_1(q \cdot \bar{q}) + \lambda_2(w \cdot q)(w \cdot \bar{q})\big) + q^\mu \bar{q}^\nu \lambda_3\Big) \\
& - \frac{\mathbb{1}_2}{F_0^2}\Big(\big(\lambda_4(q \cdot \bar{q}) + \lambda_5(w \cdot q)(w \cdot \bar{q})\big)g^{\mu\nu} + \lambda_6 q^\mu \bar{q}^\nu\Big).
\end{aligned}
$$
(6.96)

We express $q^\mu \bar{q}^\nu$ in terms of the covariant structures $L_i^{\mu\nu}$ as follows

$$q^\mu \bar{q}^\nu = L_5^{\mu\nu} + \frac{q \cdot w}{s}L_3^{\mu\nu} + \frac{\bar{q} \cdot w}{s}L_4^{\mu\nu} + \frac{(q \cdot w)(\bar{q} \cdot w)}{s^2}L_2^{\mu\nu},$$
(6.97)

in order to read off the coefficients F_i, which are

$$F_1 = \frac{C_{WT}}{F_0^2}(q_0 \bar{q}_0)(\lambda_1 + s\lambda_2) - \frac{\mathbb{1}_2}{F_0^2}(q_0 \bar{q}_0)(\lambda_4 + s\lambda_5)$$
(6.98)

$$F_2 = -\lambda_1 \frac{C_{WT}}{F_0^2}\frac{1}{s}p_{cm}\bar{p}_{cm}x + \lambda_4 \frac{\mathbb{1}_2}{F_0^2}\frac{1}{s}p_{cm}\bar{p}_{cm}x$$
(6.99)

$$F_3 = \frac{C_{WT}}{F_0^2}\frac{q \cdot w}{s}\lambda_3 - \frac{\mathbb{1}_2}{F_0^2}\frac{q \cdot w}{s}\lambda_6$$
(6.100)

$$F_4 = \frac{C_{WT}}{F_0^2}\frac{\bar{q} \cdot w}{s}\lambda_3 - \frac{\mathbb{1}_2}{F_0^2}\frac{\bar{q} \cdot w}{s}\lambda_6.$$
(6.101)

We already dropped terms proportional to x in F_1 and we dropped terms not proportional to an even or no power of x in F_2 and F_5, because they do not contribute to the channel $J^P = 1^+$. This leads to the following expansion coefficients for the kernel

$$V_{ab11}^{1^+} = -\frac{2}{3}F_{1ab} + g_{ab} \tag{6.102}$$

$$V_{ab01}^{J^+} = -\frac{2}{3\sqrt{2}M_a}(F_{1ab}\omega_a - F_{3ab}\sqrt{s}p_a^2) + \frac{\omega_a}{\sqrt{2}M_{Va}}g_{ab} \tag{6.103}$$

$$V_{ab10}^{J^+} = \frac{2}{3\sqrt{2}M_b}(-\omega_b F_{1ab} + F_{4ab}p_b^2\sqrt{s}) + \frac{\omega_b}{\sqrt{2}M_{Vb}}g_{ab} \tag{6.104}$$

$$V_{ab00}^{J^+} = \frac{1}{3M_aM_b}\left(-\omega_a\omega_b F_{1ab} - (\lambda_1 C_{WT} - \lambda_4 \mathbb{1}_2)_{ab}\frac{1}{F_0^2}p_b^2p_a^2 + F_{3ab}\omega_b p_a^2\sqrt{s}\right.$$
$$\left. + F_{4ab}\omega_a p_b^2\sqrt{s}\right) + \frac{\omega_a\omega_b}{2M_{Va}M_{Vb}}g_{ab}\,. \tag{6.105}$$

The diagrams, we have to include are the same as in Fig. 6.2 with a different scattering amplitude. As in the case including the a_1, the scattering amplitude will not take the simple form of Eq.(5.43), but we can use the results from the last section and write similar to before

$$i\mathcal{M}^{ho} = CS_\mu\left(g^{\mu\nu} - \frac{w^\mu w^\nu}{M_W^2}\right)W_\nu\,, \tag{6.106}$$

with

$$W_\nu = W_\nu''^{\rho\pi} + W_\nu''^{KK^*} + W_\nu^{3\pi} + W_\nu^{vec}\,, \tag{6.107}$$

where

$$W_\mu''^{\phi V} = \frac{c_{\phi V}gV_{ud}g_V}{2\sqrt{2}F_0^3}J_{\phi V}(\mu_2)\left(g_{\mu\alpha} - \frac{w_\mu w_\alpha}{w^2}\right)\left(\left(g_V\alpha_1^{\phi V} + \frac{1}{2}(f_V - 2g_V)\alpha_2^{\phi V}\right)L_1^{\gamma\alpha}\right.$$
$$\left. + \left(g_V\alpha_3^{\phi V} + \frac{1}{2}(f_V - 2g_V)\alpha_4^{\phi V}\right)L_3^{\gamma\alpha}\right)\frac{m_{12}^2}{m_{12}^2 - M_\rho^2 - \Pi}(q_1 - q_2)_\gamma$$
$$+ \quad (q_1 \leftrightarrow q_3)\,. \tag{6.108}$$

$W_\mu''^{\phi V}$ is calculated the same way as $W_\mu'^{\phi V}$ in Appendix B.1 and the coefficients $\alpha_i^{\phi V}$ are also the same except that one has to replace the coefficients of the scattering amplitude, since the kernel has changed. The remaining part for calculating the width works the same way as before.

6.7. W form factor

Instead of first calculating the scattering amplitude, one could introduce the W form factor to determine the decay. Leaving out some details and only considering the WT term, it is possible to work out the decay width in a few lines. It is instructive to look at this simple calculation, since here the intermediate steps are not clouded by lengthy algebra and the core of the calculation is better visible.
The details we leave out are

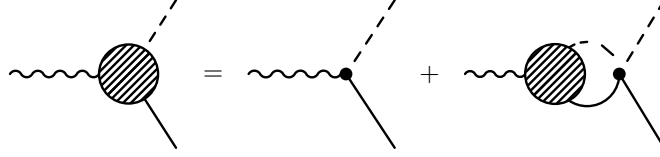- neglect longitudinal part of the hadronic tensor proportional to m_π^2

Figure 6.10.: Diagrammatic form of the equation to determine the form factor of the W boson. The dashed lines represent pions, the solid lines the ρ meson and the wiggly line the W boson. The bare vertex includes also the diagram with the intermediate pion (see Eq.(6.111)).

- $f_V - 2g_V = 0$

- neglect lowest order CHPT diagrams (direct three-pion decays)

- only $\pi\rho$ channel, no coupled channels

The first simplification actually has no visible influence on the result. The second simplification is numerically almost fulfilled, i.e.

$$\frac{f_V - 2g_V}{f_V} \approx 0.1 \quad \rightarrow \quad f_V >> (f_V - 2g_V) \tag{6.109}$$

The third approximation will only influence the very low-energy region of the decay. The only serious simplification is the last one, which we will later also see to have a minor influence on the results. Therefore, we can expect this slimmed down version to be pretty close to the full calculation.
The equation, determining the W form factor, is

$$V^{\mu\nu}(q,w) = V_0^{\mu\nu}(q,w) + \int \frac{d^4l}{(2\pi)^4} V^{\mu\alpha}(l,w) G_{\alpha\beta}(l,w) K^{\beta\nu}(l,q,w)\,, \tag{6.110}$$

which can be seen in pictorial form in Fig. 6.10. With the simplifications above, $V_0^{\mu\nu}$ is given by

$$
\begin{aligned}
V_0^{\mu\nu} &= \frac{-igV_{ud}}{2F_0}\left(f_V(w\cdot pg^{\mu\nu} - p^\mu w^\nu) - g_V(2q\cdot pg^{\mu\nu} - 2p^\mu q^\nu)\right) \\
&\quad + i\frac{F_0 gV_{ud}}{2}w^\mu \frac{i}{s-m_\pi^2}\frac{i2g_V}{F_0^2}((q\cdot p)w^\nu - (w\cdot p)q^\nu) \\
&= \frac{-igV_{ud}f_V}{2F_0}\left(wpg^{\mu\nu} - p^\mu w^\nu - qpg^{\mu\nu} + p^\mu q^\nu + w^\mu w^\nu \frac{pq}{s} - w^\mu q^\nu \frac{wq}{s}\right) + (\sim m_\pi^2) \\
&\rightarrow \frac{-igV_{ud}f_V}{2F_0}\left(g^{\mu\alpha} - \frac{w^\mu w^\alpha}{s}\right)(g_\alpha^\nu wp - p_\alpha w^\nu - g_\alpha^\nu qp + p_\alpha q^\nu) \\
&= \frac{-igV_{ud}f_V p^2}{2F_0}\left(g^{\mu\alpha} - \frac{w^\mu w^\alpha}{s}\right)(g_\alpha^\nu - \frac{p_\alpha p^\nu}{p^2})\,,
\end{aligned}
\tag{6.111}
$$

where p is the momentum of the vector meson. We drop the term proportional to p^ν, since it will not contribute due to the form of the $\rho\pi\pi$ vertex $(\sim (q_1 - q_2)^\mu)$ and the renormalisation scheme, in which tadpoles are dropped. Thus, we get

$$V_0^{\mu\nu} = \frac{-igV_{ud}f_V M_\rho^2}{2F_0}\left(g^{\mu\nu} - \frac{w^\mu w^\nu}{s}\right) \equiv V_0 L_1^{\mu\nu} \tag{6.112}$$

with $L_1^{\mu\nu}$ defined in Eq.(5.3). The kernel $K^{\mu\nu}$ is already known to be (see Eq.(5.43))

$$K^{\mu\nu} = K_0 L_1^{\mu\nu} \tag{6.113}$$

with

$$K_0 = -\frac{1}{4F_0^2}\left(3s - (2m_\pi^2 + 2M_\rho^2) - \frac{1}{s}(M_\rho^2 - m_\pi^2)^2\right). \tag{6.114}$$

Looking at Eq.(6.110) and the form of the kernel, i.e. that it does not depend on q, we can write down a reasonable ansatz for $V_{\mu\nu}$

$$V^{\mu\nu} = V(s)L_1^{\mu\nu}. \tag{6.115}$$

Plugging in this ansatz in Eq.(6.110) we get

$$VL_1^{\mu\nu} = V_0 L_1^{\mu\nu} + K_0 V I_{\pi\rho}\left(\frac{2}{3} + \frac{1}{12M_\rho^2 s}(m_\pi^2 - M_\rho^2 - s)^2\right)L_1^{\mu\nu}, \tag{6.116}$$

and we can easily read off V to be

$$V = \frac{V_0}{1 - K_0\left(\frac{2}{3} + \frac{1}{12M_\rho^2 s}(m_\pi^2 - M_\rho^2 - s)^2\right)I_{\pi\rho}}. \tag{6.117}$$

The result is rendered finite by substituting $I_{\pi\rho} \to J_{\pi\rho}(\mu_1)$. The above calculation seems to employ only one subtraction point μ_1. This is in contrast to our derivation in Section 6.4, where we argued that two different subtraction points can appear, namely one to renormalise the Bethe-Salpeter equation and one for the entrance loop from the W boson into the rescattering process. We will show in the following how the second subtraction point can also be recovered in the present calculation.

Omitting the Lorentz structure for the moment, the full W decay vertex can be written as

$$V = V_0 + V_0 GT. \tag{6.118}$$

In the solution of the Bethe-Salpeter equation for the scattering matrix, we will use G' in the following, in order to indicate a possibly different subtraction point. Using $T = (1 - KG')^{-1}K$ the form factor V can be written as

$$\begin{aligned} V &= V_0 + V_0 G(1 - KG')^{-1}K = V_0(1 - G'K)(1 - G'K)^{-1} + V_0 GK(1 - G'K)^{-1} \\ &= V_0(1 - G'K + GK)(1 - G'K)^{-1}, \end{aligned} \tag{6.119}$$

which corresponds to an equation of the form shown in Fig. 6.10, provided one takes the bare W form factor as

$$V_0' = V_0(1 - G'K + GK). \tag{6.120}$$

We see that in the vertex we can effectively include a change in the subtraction point of the first loop relative to the subtraction point of the Bethe-Salpeter equation. We note that the change in the subtraction point is at least one order higher in a chiral counting, since the kernel K is already $\mathcal{O}(q)$. We recall that Eq.(3.18) contains only the lowest order $W \to \phi V$ vertex. Using different renormalisation points for the loops G and G' gives us the possibility to account for modifications of this lowest order expression.

For the calculation of the whole decay, we only use one diagram, which is shown Fig. 6.11. Thus, we get

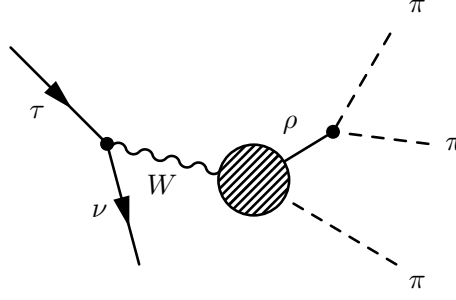$$i\mathcal{M} = CS_\mu\left(g^{\mu\nu} - \frac{w^\mu w^\nu}{M_W^2}\right)W_{form}^\nu \tag{6.121}$$

Figure 6.11.: Diagram describing the τ decay in the simplified version.

with

$$W^\mu_{form} = -\frac{iVg_V}{F_0^2}\frac{m_{12}^2}{m_{12}^2 - M_\rho^2 - \Pi}L_1^{\mu\alpha}(q_{1\alpha} - q_{2\alpha}) \quad + \quad (q_1 \leftrightarrow q_3). \tag{6.122}$$

It is instructive to check whether the full calculation from Section 6.4 with the simplifications above yield the same result. Thus we write Eq.(6.32) (including the higher order corrections Eq.(6.44)) with the simplifications above, which yields

$$
\begin{aligned}
W^\mu = -\frac{gV_{ud}g_V f_V M_\rho^2}{2F_0^3}\frac{m_{12}^2}{m_{12}^2 - M_\rho^2 - \Pi}L_1^{\mu\nu}(q_1 - q_2)_\nu \\
\left(1 - \frac{3}{2}M_{11}J(\mu_2)\left(\frac{2}{3} + \frac{1}{12sM_\rho^2}(s + M_\rho^2 - m_\pi^2)^2\right)\right).
\end{aligned}
\tag{6.123}
$$

M_{11} can be deduced from Eq.(5.53) to be

$$M_{11} = \frac{-\frac{2}{3}K_0}{1 - \frac{2}{3}K_0 J_{\pi\rho}(\mu_2)(1 + \frac{\omega_{\pi\rho}^2}{2M_\rho^2})} \tag{6.124}$$

with

$$\frac{2}{3} + \frac{1}{12sM_\rho^2}(s + M_\rho^2 - m_\pi^2)^2 = \frac{2}{3}\left(1 + \frac{\omega_{\pi\rho}^2}{2M_\rho^2}\right). \tag{6.125}$$

Thus we get

$$
\begin{aligned}
W^\mu &= -\frac{gV_{ud}g_V f_V M_\rho^2}{2F_0^3}\frac{m_{12}^2}{m_{12}^2 - M_\rho^2 - \Pi}L_1^{\mu\nu}(q_1 - q_2)_\nu \\
&\quad \cdot \left(1 + \frac{K_0 J_{\pi\rho}(\mu_2)\left(\frac{2}{3} + \frac{1}{12sM_\rho^2}(s + M_\rho^2 - m_\pi^2)^2\right)}{1 - K_0 J_{\pi\rho}(\mu_1)\left(\frac{2}{3} + \frac{1}{12sM_\rho^2}(s + M_\rho^2 - m_\pi^2)^2\right)}\right) \\
&= \frac{-iV_0 g_V}{F_0^2}\frac{m_{12}^2}{m_{12}^2 - M_\rho^2 - \Pi}L_1^{\mu\nu}(q_1 - q_2)_\nu \\
&\quad \cdot \left(\frac{1 - K_0\left(\frac{2}{3} + \frac{1}{12sM_\rho^2}(s + M_\rho^2 - m_\pi^2)^2\right)(J_{\pi\rho}(\mu_1) - J_{\pi\rho}(\mu_2))}{1 - K_0 J_{\pi\rho}(\mu_1)\left(\frac{2}{3} + \frac{1}{12sM_\rho^2}(s + M_\rho^2 - m_\pi^2)^2\right)}\right).
\end{aligned}
\tag{6.126}
$$

Remembering Eq.(6.120), this is obviously the same as the result in Eq.(6.122).
It is interesting and also important to investigate the size of the correction induced from applying different subtraction points. Therefore, we plot $\left|\frac{V_0'}{V_0}\right|$ for $\mu_1 = M_\rho^2$ and $\mu_2 = 8.5M_\rho^2$,
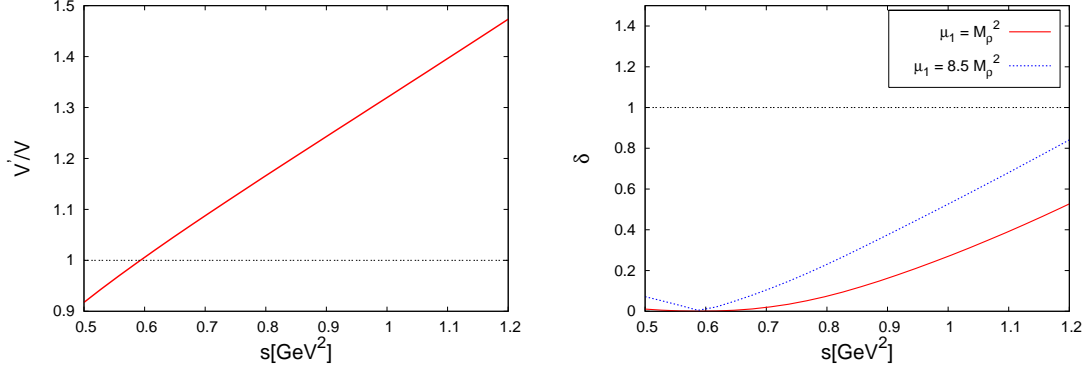
Figure 6.12.: The left plot shows the ratio V_0'/V_0 for $\mu_1 = M_\rho^2$ and $\mu_2 = 8.5M_\rho^2$. The right plot shows the relative strength $\delta = \left|\frac{V_1}{V_0}\right|$ of the one-loop correction to the lowest order vertex for the decay $W \to \pi\rho$.

which will turn out to be the best choice (see Chapter 7). The ratio can be seen in the left plot of Fig. 6.12. We only plotted the ratio up to $1.2\,\text{GeV}$, since at higher energies the power counting is not expected to work anyway. We see that around the threshold for the decay into $\pi\rho$ the correction is indeed reasonably sized and comparable to the correction for the subtraction point at $\mu_1 = M_\rho^2$. Since K_0 changes sign at around $s \approx 0.6\,\text{GeV}$, a change in the subtraction point leads to a decrease of V_0' below that energy.

Another way to check the size of the correction is to demand that the contribution from the first loop should not be bigger than the lowest order term itself. Thus, we compare the lowest order vertex for the decay $W \to \rho\pi$, with the one-loop correction, i.e. we have to compare V_0 with

$$V_{1loop}^{\mu\nu} = V_0 K_0 I_{\pi\rho} \left(\frac{2}{3} + \frac{1}{12M_\rho^2 s}(m_\pi^2 - M_\rho^2 - s)^2\right) L_1^{\mu\nu} \equiv V_1 L_1^{\mu\nu}. \tag{6.127}$$

We note that by comparing only the first loop, there can only be one subtraction point, since we only have one loop integral. Of course, this is the case, which can be seen for example by expanding Eq.(6.126) up to one loop. In the right plot of Fig. 6.12 we see the relative strength $\delta = \left|\frac{V_1}{V_0}\right|$ of the one-loop correction to the lowest order vertex for two choices of the subtraction point. We see that for both subtraction points the corrections for low energies are not too big. Choosing $\mu_2 \simeq 8.5M_\rho^2$ seems like a big change, but since the real part of the loop integral increases slowly (see Fig. E.1), the subtraction is not very big.

We do not show the results of the simplified calculations explicitly, since one can anticipate the outcome by looking at the discussions in Chapter 7. In particular, in Fig. 7.8 we will see that neglecting the strangeness channel does not have a big effect. The other simplification have already been estimated at the beginning of the chapter to be less important.

6.8. Onshell, offshell?

During the last chapters we met several situations, where we encountered so called offshell effects. In order not to get confused, we briefly recall and summarise the situation. Although, in principle, offshell effects are not measurable [FS00], we mentioned possible influences on the results. The reasons for the possible effects on the results originate in certain approximations

we made. In the following we recall the different situations and explain in detail the possible effects and the reasons for them. There are basically three occurrences:

- In the discussion on the choice between vector and tensor fields (Section 6.4 and Section 3.2) we encountered the prototype of an offshell effect. We saw that both descriptions differ by additional contact terms. Thus, choosing one of the representations, the other one yields the same results, as long as one also includes the additional terms in the calculation. Not including these additional terms would lead to a difference in the matrix element of a factor of p^2/M_ρ^2. Putting the ρ on the mass shell, the matrix elements would be the same, but since the ρ meson is offshell (we look at a two-pion final state emerging from the ρ) in our calculation, there is a difference. A very similar situation has been discussed in [FS00]. Thus choosing different interpolating fields, we might have to consider additional or less diagrams in order to get the same result. This raises the question, which diagrams one has to include in the calculations. In our case we choose the relevant processes such that we get a decent high-energy behaviour.

- In Section 4.4.2 we discussed in much detail, why it is justified to take the kernel in the Bethe-Salpeter equation onshell. We showed that this simplification is on the same level as neglecting higher order contact terms and therefore putting the kernel onshell is not a severe additional approximation. Again we see that the offshell effect is connected to higher order contact terms and in principle this situation is connected to the one we discussed before. Here, however, the situation is mixed up with the approximation, we do by calculating the kernel of the Bethe-Salpeter equation perturbatively, which corresponds to summing only a certain class of diagrams. Since we expect the higher order corrections to the kernel to play a minor role, we do not expect severe problems. However, this is a model assumption and we will test it by investigating the influence on the result by including corrections to the kernel. In case these terms induce systematic corrections in the result, there is an indication that the model assumption is reasonable.

- In order to expand the kernel and the scattering amplitude in partial waves, we have to put the particles onshell. However, as already mentioned, the vector mesons in our calculation are not onshell. Therefore, we have to put the projectors back offshell, which is ambiguous and which has been discussed in Section 5.3. This uncertainty in the offshell extrapolation is of different nature as the ones before, since here the uncertainty originates in the question, how to define a partial wave expansion for virtual particles. In Chapter 7 we will show the results by assuming the ρ to be stable, in which case this problem does not appear. This means we consider $\pi\rho$ to be the final state instead of three pions. In this way we can estimate the possible influence induced by this effect.

Chapter 7.

Results

The quantity, we want to compare most of our calculations with, is the hadronic spectral function which enters the decay $\tau^- \to 2\pi^0 \pi^- \nu_\tau$. The data, we use, were measured by the ALEPH collaboration and can be found in [S$^+$05]. Since the spectral function is the central quantity, we will first discuss its relation to our calculation in detail.

7.1. Spectral function

The definition of the spectral function, which one finds in [S$^+$05], is

$$a_1 = -\frac{2\pi}{s} \Im\Pi_T(s) \,, \tag{7.1}$$

with the hadronic vacuum polarisation

$$\Pi_{\mu\nu} = \Pi_T \left(g_{\mu\nu} - \frac{w_\mu w_\nu}{s} \right) + \Pi_L \frac{w_\mu w_\nu}{s} \,. \tag{7.2}$$

defined by

$$\Pi_{\mu\nu} = i \int d^4x \, e^{iwx} \langle 0 | T A_\mu(x) A_\nu(0)^\dagger | 0 \rangle \,, \tag{7.3}$$

where T is the time ordering symbol and A^μ is the charged axial current

$$A_\mu = \overline{u} \gamma_\mu \gamma_5 d \,. \tag{7.4}$$

The definition in Eq.(7.3) is especially suited to express the spectral function in terms of the generating functional, which we will show next. We recall that in the presence of external fields the QCD Lagrangian reads

$$\mathcal{L} = \mathcal{L}_{QCD}^0 + \mathcal{L}_{ext} = \mathcal{L}_{QCD}^0 + \overline{q}\gamma_\mu \left(v^\mu + \frac{1}{3} v_{(s)}^\mu + \gamma^5 a^\mu \right) q - \overline{q}(s - i\gamma^5 p)q \,, \tag{7.5}$$

and we define the generating functional as

$$\exp(iZ(v, a, s, p)) = \langle 0 | T e^{i \int d^4x \mathcal{L}_{ext}(x)} | 0 \rangle \,. \tag{7.6}$$

Then we can write

$$\langle 0 | T A_\mu(x) A_\nu(0)^\dagger | 0 \rangle = (-i)^2 \frac{\delta}{\delta a_\mu^+(x) \delta a_\nu^-(0)} \exp(iZ)|_{v=a=p=0, s=diag(m_u, m_d, m_s)} \,. \tag{7.7}$$

In order to connect to the weak interactions, we identify

$$a_\mu^+ = \frac{gV_{ud}}{2\sqrt{2}}W_\mu^+ \,. \tag{7.8}$$

Using the generating functional of the hadronic Lagrangian in Eq.(7.7), we can connect the spectral function to the effective theory we use.

In principle the spectral function is chosen such that it contains the hadronic information of the process of interest, which can be seen in the above formulas. For an exact relation to the previous calculation, however, it will be easier to start with the decay, one actually calculates. The decay width of the W can be written as

$$\Gamma(W \to X) = \frac{1}{3}\sum_\lambda \epsilon_\mu^\dagger(\lambda)\epsilon_\nu(\lambda)\frac{1}{2\sqrt{s}}(-i)\frac{g^2V_{ud}^2}{8}H_{\mu\nu}\,, \tag{7.9}$$

where the hadronic tensor $H_{\mu\nu}$ is given by

$$\begin{aligned}
H_{\mu\nu} &= i\sum_n \int \prod_{i=1}^n \left(\frac{d^3p_i}{(2\pi)^3 2E_i}\right)\langle 0|A_\mu(0)|n\rangle\langle n|A_\nu^\dagger(0)|0\rangle(2\pi)^4\delta^4(w - p_n) \\
&= i\sum_n \int \prod_{i=1}^n \left(\frac{d^3p_i}{(2\pi)^3 2E_i}\right)\int d^4x\, e^{ix(w-p_n)}\langle 0|A_\mu(0)|n\rangle\langle n|A_\nu^\dagger(0)|0\rangle \\
&= i\sum_n \int \prod_{i=1}^n \left(\frac{d^3p_i}{(2\pi)^3 2E_i}\right)\int d^4x\, e^{iwx}\langle 0|e^{i\hat{p}x}A_\mu(0)e^{-i\hat{p}x}|n\rangle\langle n|A_\nu(0)^\dagger|0\rangle \\
&= i\int d^4x\, e^{iwx}\langle 0|A_\mu(x)A_\nu(0)^\dagger|0\rangle\,,
\end{aligned} \tag{7.10}$$

where $p_n = \sum_i p_i$. From the lines above we can also see that

$$\int d^4x\, e^{iwx}\langle 0|A_\nu(0)^\dagger A_\mu(x)|0\rangle \ = 0\,, \tag{7.11}$$

since the term would lead to $\delta^4(w + p_n)$, which can not be fulfilled due to energy-momentum conservation. Next we want to bring the time ordering symbol into the game as follows

$$\begin{aligned}
H_{\mu\nu} &= i\int d^4x\,\theta(x_0)e^{iwx}\langle 0|A_\mu(x)A_\nu^\dagger(0)|0\rangle + i\int d^4x\,\theta(-x_0)e^{iwx}\langle 0|A_\mu(x)A_\nu^\dagger(0)|0\rangle \\
&= i\int d^4x\,\theta(x_0)e^{iwx}\langle 0|A_\mu(x)A_\nu^\dagger(0)|0\rangle + i\int d^4x\,\theta(-x_0)e^{iwx}\langle 0|A_\mu(0)A_\nu^\dagger(-x)|0\rangle \\
&= i\int d^4x\,\theta(x_0)e^{iwx}\langle 0|A_\mu(x)A_\nu^\dagger(0)|0\rangle + i\int d^4x\,\theta(x_0)e^{-iwx}\langle 0|A_\mu(0)A_\nu^\dagger(x)|0\rangle \\
&= i\int d^4x\, e^{iwx}\langle 0|TA_\mu(x)A_\nu^\dagger(0)|0\rangle + i\int d^4x\, e^{-iwx}\langle 0|TA_\mu(0)A_\nu^\dagger(x)|0\rangle\,,
\end{aligned} \tag{7.12}$$

where we used that

$$\langle 0|A_\mu(x)A_\nu(0)|0\rangle = \langle 0|e^{-i\hat{p}x}A_\mu(x)e^{i\hat{p}x}e^{-i\hat{p}x}A_\nu(0)e^{i\hat{p}x}|0\rangle = \langle 0|A_\mu(0)A_\nu(-x)|0\rangle\,. \tag{7.13}$$

We could introduce the time ordering symbol for the θ function, since the contribution for negative times is zero, which we know from Eq.(7.11).
From Lorentz invariance, we know that $H_{\mu\nu}$ must have the following structure

$$H_{\mu\nu} = H_1\left(g_{\mu\nu} - \frac{w_\mu w_\nu}{s}\right) + H_2\frac{w_\mu w_\nu}{s}\,. \tag{7.14}$$

This means that $H_{\mu\nu}$ is symmetric under the exchange of $\mu \leftrightarrow \nu$, which leads to

$$\int d^4x\, e^{iwx}\langle 0|A_\mu(x)A_\nu^\dagger(0)|0\rangle = \int d^4x\, e^{iwx}\langle 0|A_\nu(x)A_\mu^\dagger(0)|0\rangle\,. \tag{7.15}$$

Therefore, we get

$$H_{\mu\nu} = \Pi_{\mu\nu} - \Pi_{\mu\nu}^* = 2i\Im\Pi_{\mu\nu}\,. \tag{7.16}$$

Plugging this expression into Eq.(7.9) yields

$$\Gamma(W \to X) = \frac{1}{3}\sum_\lambda \epsilon_\mu^\dagger(\lambda)\epsilon_\nu(\lambda)\frac{1}{2\sqrt{s}}(-i)\frac{g^2V_{ud}^2}{8}2i\Im\Pi^{\mu\nu} = -\frac{g^2V_{ud}^2}{8\sqrt{s}}\Im\Pi_T\,, \tag{7.17}$$

where we used Eq.(7.2) and $\epsilon(w)\cdot w = 0$. Thus, with the definition of the spectral function $a_1(s)$ in Eq.(7.1) we get

$$a_1(s) = \frac{2\pi}{s}\frac{8\sqrt{s}}{g^2V_{ud}^2}\Gamma \tag{7.18}$$

In order to determine the spectral function for the decay of $\tau^- \to 2\pi^0\pi^-\nu_\tau$, we replace the total decay width by $\Gamma(W \to 3\pi)$. This width has in principle been calculated already in Chapter 6 and is given by

$$\Gamma(W \to 3\pi) = W^{\mu\nu}\frac{1}{6}\sum \epsilon_\mu^\dagger\epsilon_\nu\frac{(2\pi)^4}{2\sqrt{s}} = -\frac{(2\pi)^4}{4\sqrt{s}}W_1\,, \tag{7.19}$$

where we expressed the decay width in terms of W_1 (see Eq.(6.13); W_2 does not appear since $\epsilon_\mu w^\mu = 0$). Note the factor of $\frac{1}{2}$ due to the identical particles in the final state. Thus, the spectral function in terms of W_1 is

$$a_1(s) = -(2\pi)^5\left(\frac{2}{gV_{ud}}\right)^2\frac{1}{2s}W_1 = -\frac{2^6\pi^5}{g^2V_{ud}^2s}W_1\,. \tag{7.20}$$

In [S$^+$05] the spectral function is given in a different form

$$a_1(s) = \frac{m_\tau^8}{6V_{ud}^2}\frac{B_{3\pi}}{B(\tau^- \to e^-\overline{\nu}_\tau\nu_\tau)}\frac{1}{N}\frac{dN}{ds}\left((m_\tau^2 - s)^2(m_\tau^2 + 2s)\right)^{-1}\,, \tag{7.21}$$

which can be seen to be the same by using

$$\Gamma(\tau^- \to e^-\nu_\tau\overline{\nu}_e) = \frac{m_\tau^5 G_F^2}{192\pi^3} \tag{7.22}$$

and

$$\frac{1}{N}\frac{dN}{ds} = \frac{1}{\Gamma_{tot}B_{3\pi}}\frac{d\Gamma}{ds} \tag{7.23}$$

together with our expression for $\frac{d\Gamma}{ds}$ in Eq.(6.31), when we neglect W_2. The two expressions Eq.(7.20) and Eq.(7.21) differ by the appearance of W_2, which would be zero, if the axial-vector current was conserved. The contribution from W_2, however, is very small since it is suppressed by a factor of m_π^2, which is negligible from a practical point of view.

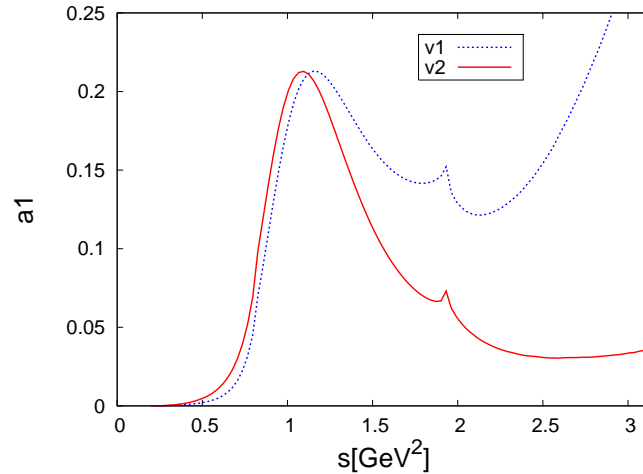**Figure 7.1.:** Spectral function for the decay $\tau^- \to 2\pi^0\pi^-\nu_\tau$ calculated with different choices for the interpolating fields. v1 only uses the vector field Lagrangian Eq.(3.18), whereas v2 additionally includes the contact terms from Eq.(3.45).

7.2. Calculation without a_1

First we want to investigate the spectral function for the decay $\tau^- \to 2\pi^0\pi^-\nu_\tau$ calculated by iterating the WT term in order to dynamically generate the a_1. We will discuss the influence of different aspects of the calculation on the results in detail and determine the values of the subtraction points.

- Influence of interpolating fields and spectral distribution

We discussed the different possibilities to describe vector particles, namely in terms of vector fields and in terms of antisymmetric tensor fields. We introduced higher order corrections in order to account for the difference stemming from the choice of fields. For the present calculation we note that using the antisymmetric tensor fields, leads to the appearance of less derivatives, and therefore we expect a better high-energy behaviour. Instead of explicitly using the antisymmetric tensor fields, we use the vector representation but also include the higher order terms given in Eq.(3.45). Fig. 7.1 shows the spectral function calculated with vector fields (v1) and with vector fields including the higher order terms (v2). One clearly sees the better high-energy behaviour. In Fig. 7.1 we used dimensional regularisation with $\mu_1 = \mu_2 = M_\rho^2$, which is the value from [LK04]. We will discuss the influence of the subtraction points in detail below. The kink which can be seen at about $1.9\,\mathrm{GeV}^2$ results from the threshold of the KK^* channel. Using spectral distributions for the vector mesons, taken from [GK91], smoothes the curve, which can be seen in Fig. 7.2. The curve also gets a little broader and moves to the right, but the overall structure is unchanged. If we do not state otherwise, the following calculations will always contain the higher order corrections (i.e. v2) and the spectral function for the vector mesons in the loop.
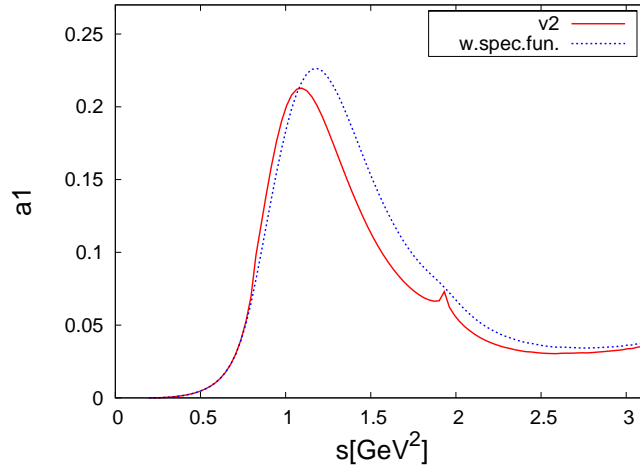
- Influence of renormalisation

Figure 7.2.: Spectral function for the decay $\tau^- \to 2\pi^0\pi^-\nu_\tau$ calculated with and without including the width of the vector mesons in the loop integral. The curve labeled v2 is the same as in Fig. 7.1.

In Chapter 6 we encountered two subtraction points in our calculation. In the following we will investigate the influence of these two parameters. We start by setting $\mu_1 = \mu_2$ and vary them simultaneously. In perturbation theory physical quantities do not depend on the renormalisation scale or the cutoff, which one is using in the respective regularisation scheme. Since we are summing only certain diagrams in our approach, and we do not include the counter terms accompanying the divergent loop integrals, our results will depend on the renormalisation parameter. This parameter simulates parts of the counter terms, which are of higher order in a chiral counting. In the left plot of Fig. 7.3 we see the spectral function for the decay $\tau^- \to 2\pi^0\pi^-\nu_\tau$ calculated with different renormalisation schemes in comparison to data from [S$^+$05]. The various schemes are explained in Appendix E. The different curves clearly differ in the height of the peak, but the position of the peak is not influenced. The width of the peak turns out to be too small in all prescriptions. The cutoffs cut_{three} in the three-dimensional cutoff scheme and cut_{euc} in the euclidian cutoff scheme are chosen at $1\,\mathrm{GeV}$, the subtraction constant a_0 in the dispersion relation is $a_0 = -0.001$ and the subtraction point in dimensional regularisation is chosen at $\mu_1 = M_\rho^2$ again. We see that a cutoff of natural size leads to a much higher and sharper peak than the subtraction point, which was motivated by crossing symmetry. It is hard to say what the natural size of a subtraction constant a_0 is and we chose it such that it lies in between the other curves. Since including the spectral function for the vector mesons in the cutoff schemes is more complicated and does not lead to new insights for this comparison, we did not include the spectral distribution in the loops in the calculations shown in the left plot of Fig. 7.3. In the right plot of Fig. 7.3 we calculated the spectral function using dimensional regularisation with different subtraction points in order to see how the subtraction point is connected to the other renormalisation parameters. The figure shows that we end up with pretty much the same results as in the left plot. Thus, using dimensional regularisation and varying the subtraction point, we cover the full discussion on the renormalisation parameter.

It is also instructive to look directly at the scattering amplitudes, which describe the rescattering. We note that the scattering amplitude only depends on μ_1 and is independent of μ_2. In Fig. 7.4 we see the real and imaginary part of the scattering amplitude for $\pi\rho$ scattering (corresponding to M_{1111}) for different renormalisation descriptions. The curves shown in Fig.
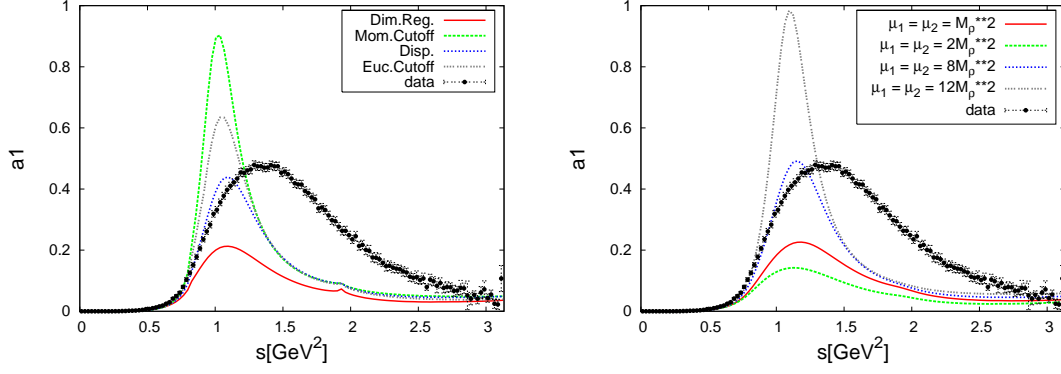
Figure 7.3.: The left plot shows the spectral function for the decay $\tau^- \to 2\pi^0\pi^-\nu_\tau$ calculated with different renormalisation schemes in comparison to data from [S$^+$05]. For the values of the renormalisation parameters see the text. The right plot shows the spectral function calculated with dimensional regularisation for different subtraction points.
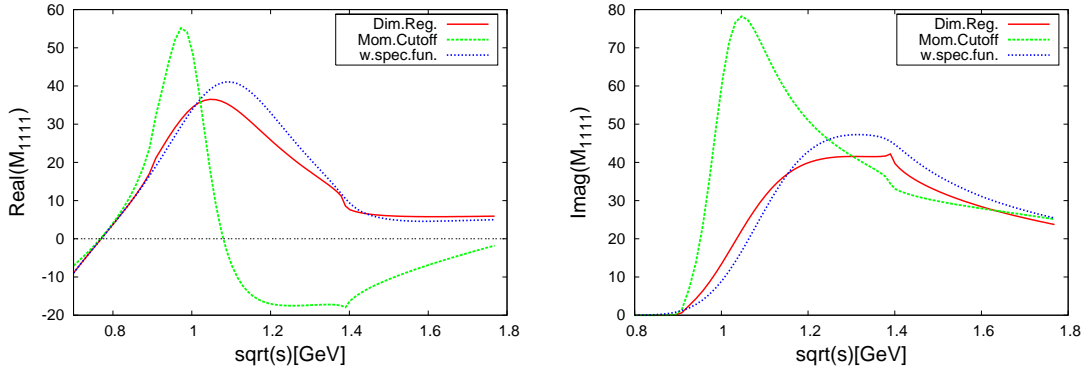

Figure 7.4.: Real (left) and imaginary (right) part of the scattering amplitude for $\pi\rho$ scattering. The curves correspond to the highest curve in the left plot of Fig. 7.3 and to the two curves shown in Fig. 7.2.

7.4 correspond to the highest and lowest curve in the left plot of Fig. 7.3. In addition, we plotted the lowest curve using a spectral distribution for vector mesons in the loop, which corresponds to the result in Fig. 7.2. We see that the scattering amplitude hardly shows a resonance structure by using the subtraction point at M_ρ^2. The resonant structure is more pronounced for the cutoff scheme. Including the spectral function of the ρ basically smoothes the curve. The bump in the imaginary part is moved to the left in the cutoff scheme, whereas in Fig. 7.3 one could hardly see a difference in the position of the peak. This shows that it is not so obvious to translate the structure seen in the scattering amplitude to the spectral function of the τ decay. In other words, interferences between the tree level diagrams and the rescattering diagrams (cf. Fig. 6.2) play an important role.

Next we want to investigate the effect of changing μ_2 while keeping μ_1 fixed. We will use $\mu_1 = M_\rho^2$, which in [LK04] was determined by using crossing symmetry arguments. Thus, using these arguments to fix one subtraction point, we are in principle left with only one free parameter. The results for different choices of μ_2 can be seen in Fig. 7.5. We see that we can describe the data very well by varying only that subtraction point and keeping $\mu_1 = M_\rho^2$ fixed in the scattering amplitude. We note that choosing the subtraction point at $\mu_2 = 8.5M_\rho^2$,
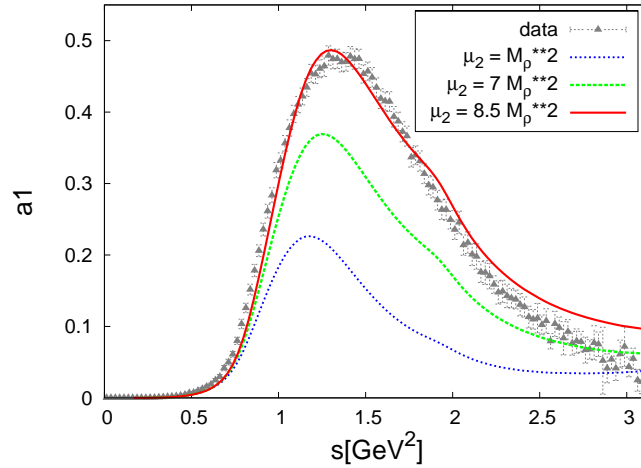
Figure 7.5.: Spectral function for the decay $\tau^- \to 2\pi^0\pi^-\nu_\tau$, calculated by varying the subtraction point μ_2 of the first loop and keeping the subtraction point in the scattering amplitude fixed at $\mu_1 = M_\rho^2$, in comparison to data from [S+05].

which describes the data best, corresponds approximately to a cutoff of $1\,\mathrm{GeV}$ in a cutoff scheme. Obviously this value is very reasonable.

For completeness, we also investigate the dependence on μ_1 while keeping μ_2 fixed. In Fig. 7.6 we see the spectral function for different values of μ_1 and $\mu_2 = 8.5M_\rho^2$. Raising the subtraction point to $\mu_1 = 2M_\rho^2$ broadens the curve and the peak is moved a little to the right. Further raising the subtraction point leads to a smaller width and the peak is shifted to the left. We note in passing that the maximum in the width of the peak is connected to the minimum of the real part of the loop function, which can be seen in Fig. E.1.

In Fig. 7.7 we see the spectral function for $\mu_1 = M_\rho^2$ and $\mu_2 = 8.5M_\rho^2$ (see Fig. 7.5) split into the different contributions from the diagrams shown in Fig. 6.2. We see that the bump is partly created by the negative interference of the rescattering diagrams and the diagrams including the vector mesons at tree level. The little bump, we see in the rescattering contribution alone appears at the wrong position and only the sum of all diagrams gives the pronounced peak, which is of course the only quantity that can be measured.

- Influence of coupled channels

The spectral function calculated with and without including the strangeness channel is shown in Fig. 7.8, which shows that the bump also appears without the kaon channel. The height is a little less by leaving out the kaons, but that could be compensated by varying the subtraction point μ_2. The rise in the data in the energy region up to about $1.1\,\mathrm{GeV}^2$ can also be described by leaving out the kaons, but the width of the peak is better described by including both channels. However, the effect is pretty small and one can safely say that the $\rho\pi$ channel plays the dominant role.
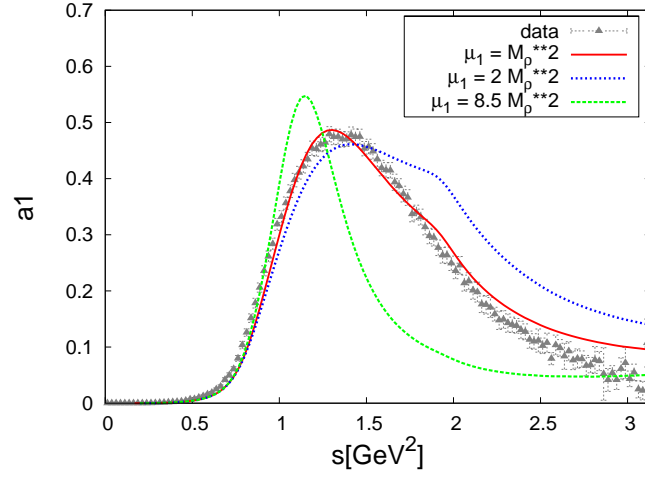
- Varying g_V and f_V

Figure 7.6.: Spectral function for the decay $\tau^- \to 2\pi^0\pi^-\nu_\tau$, calculated by varying the subtraction point μ_1 of the scattering amplitude, while keeping μ_2 fixed at $\mu_2 = 8.5M_\rho^2$, in comparison to data from [S+05].
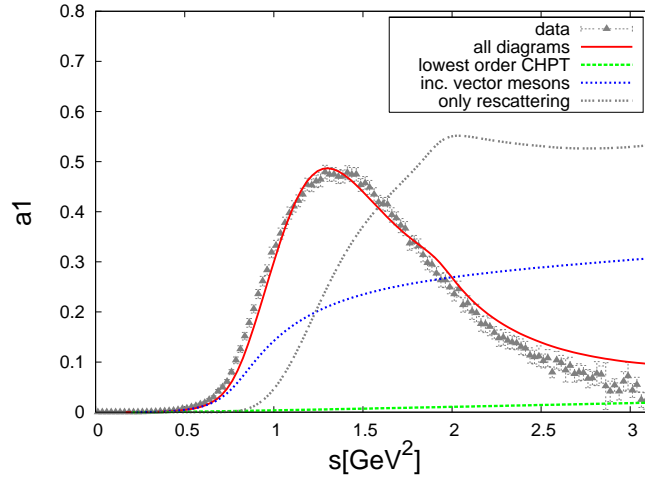

Figure 7.7.: Spectral function for $\mu_1 = M_\rho^2$ and $\mu_2 = 8.5M_\rho^2$ (see Fig. 7.5) splitted up into the different contributions from the diagrams in Fig. 6.2 in comparison to data from [S+05]. The 'lowest order CHPT' curve corresponds to Fig. 6.2a,b, 'inc. vector mesons' to Fig. 6.2c,d and 'only rescattering' to Fig. 6.2e,f.
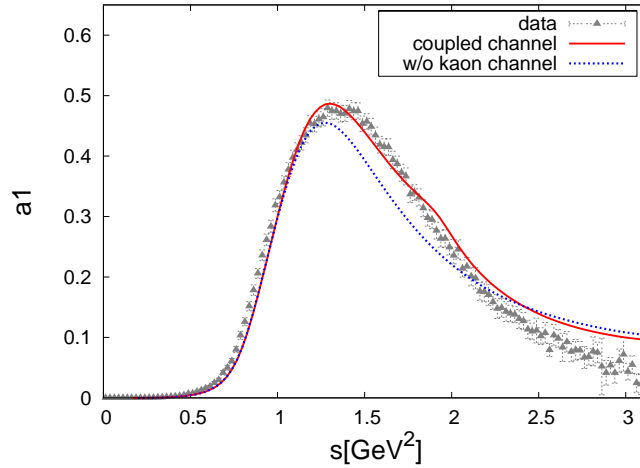
Figure 7.8.: Spectral function for the decay $\tau^- \to 2\pi^0\pi^-\nu_\tau$ calculated with and without including the kaon channel in comparison to data from [S$^+$05].

So far we used the experimentally measured values for f_V and g_V, which are given by

$$ f_V = \frac{0.154\,\text{GeV}}{M_\rho}\,, \quad g_V = \frac{0.069\,\text{GeV}}{M_\rho}\,. \tag{7.24} $$

As already noted in Chapter 3, these values slightly differ from

$$ f_V = 2g_V\,, \quad g_V = \frac{F_0}{\sqrt{2}M_\rho}\,, \tag{7.25} $$

which are the values, obtained by theoretical considerations and approximations in [EGL$^+$89]. In order to show the influence of these parameters on the results, we show in Fig. 7.9 the spectral function calculated with different values for g_V and f_V. 'g1' corresponds to the theoretical motivated values of f_V and g_V according to Eq.(7.25) with the subtraction points $\mu_1 = M_\rho^2$ and $\mu_2 = 8.5M_\rho^2$. 'g2' uses the same parameters as 'g1', except for μ_2, which is chosen to be $\mu_2 = 14M_\rho^2$ in order to fit the height of the peak. We see that the moderate difference in f_V and g_V has a sizeable impact on the results, which is due to the fact that the combination $f_V g_V$ appears quadratically in the final formulas. The change in the height of the peak can be compensated by a readjustment of the subtraction point μ_2, but the spectral function in this case seems to be shifted to the right. We note that there is no other parameter, which potentially can influence the spectral function up to about $s \approx 0.7\,\text{GeV}^2$, as can be seen from the discussions before.

Except of the influence at low energies and the resulting small shift, varying f_V and g_V seems to have a similar effect as varying μ_2. This is not too surprising, since changing f_V and g_V changes also the W decay vertex and leaves the scattering amplitude untouched.

- Stable ρ

In Section 6.3 we discussed which diagrams we should include in our calculation, and we assumed that the contribution from the pion final state interactions are small. In order to show that this a reasonable assumption, we compare our previous calculations with one, where
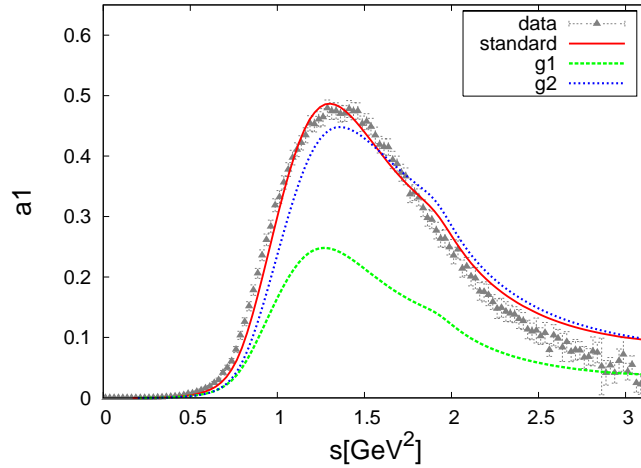
Figure 7.9.: Spectral function for the decay $\tau^- \to 2\pi^0\pi^-\nu_\tau$ calculated with different values for g_V and f_V in comparison to data from [S+05]. 'g1' corresponds to the theoretically motivated values of f_V and g_V according to Eq.(7.25) with the subtraction points $\mu_1 = M_\rho^2$ and $\mu_2 = 8.5M_\rho^2$. 'g2' uses the same parameters as 'g1', except μ_2, which is chosen to be $\mu_2 = 14M_\rho^2$.

the ρ is assumed to be stable. This means we look at a spectral function obtained from the final state $\rho\pi$ instead of 3π. With the notation from Chapter 6 and neglecting the longitudinal part proportional to m_π^2, we get

$$W_{stable}^\mu = -\left(g^{\mu\nu} - \frac{w^\mu w^\nu}{s}\right) b_T \frac{F_0^2}{g_V}\epsilon_\nu^\rho(p) + \left(g^{\mu\nu} - \frac{w^\mu w^\nu}{s}\right)\frac{gV_{ud}f_V}{2F_0}(p^2 g_{\nu\alpha} - p_\alpha p_\nu)\epsilon_\rho^\alpha(p)\,, \quad (7.26)$$

and therefore

$$W_1 = -\frac{1}{3}\frac{p_{cm}}{2(2\pi)^5\sqrt{s}}\left(|b_T|^2\frac{F_0^4}{g_V^2} + \frac{g^2 V_{ud}^2 f_V^2}{4F_0^2}M_\rho^4 - \frac{f_V}{g_V}F_0 g V_{ud}M_\rho^2\Re(b_T)\right)$$
$$\cdot\left(2 + \frac{1}{4sM_\rho^2}(s + M_\rho^2 - m_\pi^2)^2\right)\,. \quad (7.27)$$

For simplicity, we also neglected terms $\sim (f_V - 2g_V)$ in the tree level diagram (W_{vec}^μ). We checked explicitly, that these terms influence the results by less than 10%, and therefore they would only lengthen the formulas above. The negligible influence is of course expected from Eq.(6.109). In order to see the net effect of assuming a stable ρ, we do not include the spectral function for the vector mesons in the loops. When the ρ is stable, the threshold for the decay of the τ is of course sharper and moved to the right, which can be seen in Fig. 7.10. We see that besides these differences, the structure is the same as before and there is not much room for a big contribution from pion final state interactions.

Using the projectors defined in Chapter 5 or in [LK04] implies a certain offshell extrapolation. In our calculation we describe a ρ, which is not on the mass shell, and therefore a specific offshell extrapolation might influence the result. Using a stable ρ, that problem does not appear. Since the result with a stable ρ shows the same structures, this also helps in gaining trust in the offshell extrapolation, which we chose.

We want to summarise shortly what we saw so far. In a scenario where the a_1 is generated dynamically we employ two parameters μ_1 and μ_2. Varying both simultaneously with $\mu_1 = \mu_2$,

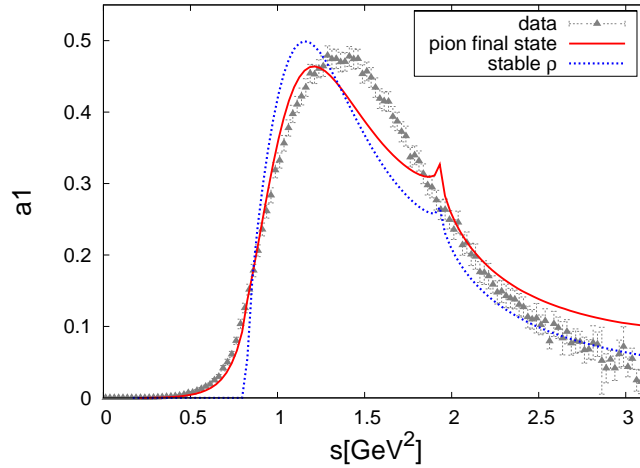**Figure 7.10.:** The plot shows the spectral function for the decay $\tau^- \to 2\pi^0\pi^-\nu_\tau$ calculated by assuming $\rho\pi$ to be the final state ('stable ρ') and using the usual three-pion final state ('pion final state') in comparison to data from [S$^+$05]. In order to see the mere difference by assuming the different final state, we do not use a spectral distribution for the vector mesons in the loop. The subtraction points are chosen according to the best choice at $\mu_1 = M_\rho^2$ and $\mu_2 = 8.5 M_\rho^2$.

we saw that we always got a peak at the same position with varying height and a too small width. Using the value from [LK04] to fix μ_1, we describe the data very well by choosing the only remaining free parameter μ_2 at $8.5 M_\rho^2$. We also saw that in the process under consideration the main contribution came from the $\rho\pi$ channel, while the kaon channel plays a minor role. In addition, we investigated the influence of the parameters f_V and g_V and found that the results are quite sensitive to these parameters. In particular, the low-energy behaviour is best described by using the values, which are directly determined from experiment. Finally we assumed the ρ to be stable, which yields a qualitatively similar result. This eliminates concerns about possibly large final state interactions of the pions (cf. Fig. 6.3).

7.3. Calculation with explicit a_1

Now we want to look at the results of the calculation when we include the a_1 explicitly. A very small coupling of the a_1 together with the values from the calculations before will of course reproduce the results from before and will give a good description of the data. To check whether a scenario with an explicit a_1 can also describe the data reasonably well, we have to demand that the coupling is not almost zero, and we expect the value of the coupling to be comparable to the values found in [RPO04, KM90, GDPP04]. In order to get non zero couplings and still be reasonably close to the data, we have to keep the contribution from the WT term small. We start by choosing $\mu_1 = \mu_2 = M_\rho^2$ according to [LK04], which we can expect to be a good choice by looking at Fig. 7.3. Scanning through the parameter space, it turned out that in most cases a two bump structure is observed. We show an example of this in Fig. 7.11 (set 3). By finetuning the parameters, it is possible to merge these two bumps into one, which can also be seen in Fig. 7.11 (set 1 or set 2). The parameters leading to these curves are given in Tab. 7.1. From set 1 and set 2, we see that there are different possible
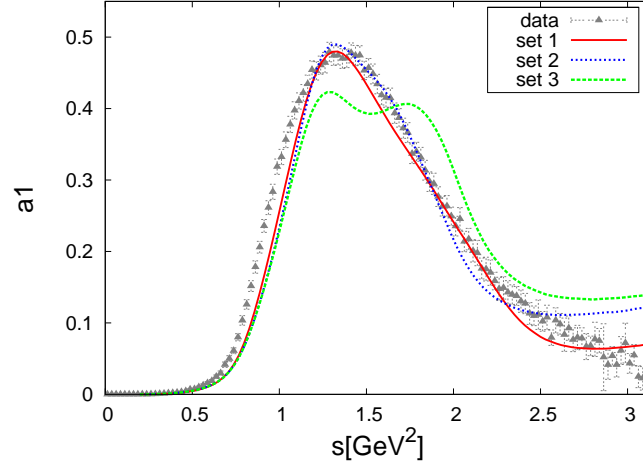
Figure 7.11.: Spectral function for the decay $\tau^- \to 2\pi^0\pi^-\nu_\tau$ including the a_1 with different sets of paramaters in comparison to data from [S$^+$05]. The parameter sets are given in Tab. 7.1.

	M_{a_1} [GeV]	f_A	c_1	c_2	μ_1 $[M_\rho^2]$	μ_2 $[M_\rho^2]$	remark
set 1	1.23	$\frac{F_0}{\sqrt{2}M_\rho}\cdot 1.05$	$-\frac{1}{4}\frac{1}{1.65}$	$-\frac{1}{8}\frac{1}{1.6}$	2	1.05	
set 2	1.195	$\frac{F_0}{\sqrt{2}M_\rho}\cdot 1.45$	$-\frac{1}{4}\frac{1}{2.6}$	$-\frac{1}{8}\frac{1}{1.6}$	1	2.5	
set 3	1.21	$\frac{F_0}{\sqrt{2}M_\rho}\cdot 1.45$	$-\frac{1}{4}\frac{1}{2.4}$	$-\frac{1}{8}\frac{1}{1.6}$	1	2.5	
set 4	1.5	$\frac{F_0}{\sqrt{2}M_\rho}$	$-\frac{1}{4}$	$-\frac{1}{8}$	2	5.5	w/o WT
set 5	1.5	$\frac{F_0}{\sqrt{2}M_\rho}$	-	$-\frac{1.4}{8}$	2	5.8	w/o WT, Eq.(6.83)
set 6	1.2	$\frac{F_0}{\sqrt{2}M_\rho}\cdot 1.05$	$-\frac{1}{4}\frac{1}{1.7}$	$-\frac{1}{8}\frac{1}{1.6}$	2	6	f_V, g_V Eq.(7.25)

Table 7.1.: Different sets of parameters for the calculations with explicit a_1. The remark 'w/o WT' means that the WT term is not included, the additional remark 'Eq.(6.83)' means that the a_1 decay vertex from Eq.(6.83) is used (which does not employ the parameter c_1) and 'f_V, g_V Eq.(7.25)' means that we choose the values from Eq.(7.25) for f_V and g_V.
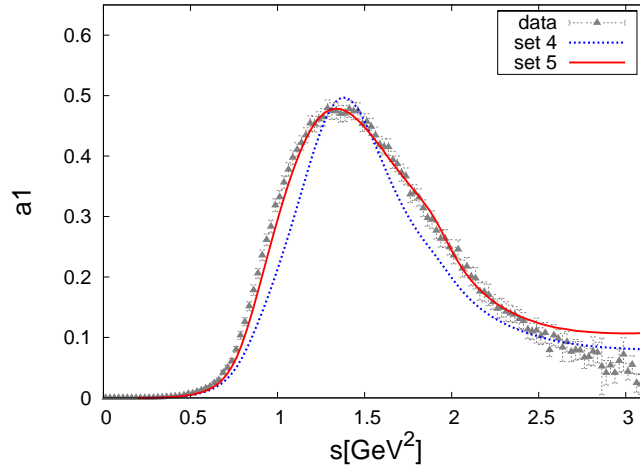
Figure 7.12.: Spectral function for the decay $\tau^- \to 2\pi^0\pi^-\nu_\tau$ including the a_1 with different sets of paramaters in comparison to data from [S$^+$05]. The WT was not included in these calculations. In addition, the curve labelled 'set 5' uses a different energy dependence to describe the a_1 decay (see text).

choices for the parameters, which can (more or less) describe the data. A deviation is only seen for $0.8\,\mathrm{GeV}^2 \lesssim s \lesssim 1.1\,\mathrm{GeV}^2$.

Next we want to see, how far we get by switching off the WT term. We perform such an analysis without the WT term for completeness. We recall our strategy discussed in Section 4.4.3 to approximate the ϕV scattering kernel by possible resonances (here the a_1) plus contact terms of lowest order. In that strategy there is no justification to neglect even the lowest order contact term, which is just the WT term with its strength fixed model independently by chiral symmetry breaking. In Fig. 7.12 we see the spectral function calculated with explicit a_1 but without the WT term in the kernel (set 4). In that case the second bump disappears and by changing the parameters, one can determine the position and the height of the peak. Although one might expect that the width of the peak can be adjusted by the choice of c_1 and c_2, this is not the case, since there is a more complex interplay between the position and the width of the peak. There are lots of parameter choices which give a qualitatively similar curve. The curve labelled set 4 represents the best fit to the data by varying all parameters and we see that it agrees with the choice for c_1 and c_2 from [KM90] and [RPO04] (cf. Eq.(3.31)). For the curve labelled 'set 5', we used the a_1 decay vertex from Eq.(6.83) and we see that in this case the shape of the peak is described very well. This shows the uncertainties in the shape of the width and how it is influenced by the energy dependence of the a_1 decay vertex. Therefore, we have to be careful to draw conclusions from the exact shape of the width.
From Fig. 7.12 (set 4) and Fig. 7.11 one should not conclude that the WT term is a correction, which improves the shape of the width, since one does not simply switch on the WT term in order to get from Fig. 7.12 to Fig. 7.11. Instead the parameter sets are quite different and one has to finetune the parameters in order to arrive at a single reasonable peak, when one includes the WT term.
Looking at 'set 4' in Fig. 7.12 one might criticise that we do not have the most sophisticated model describing the explicit a_1 and that other models describe the data better (e.g. [UBW02, GDPP04]). However, our description of the a_1 is completely sufficient to show the strong influence of the WT term and has the advantage to be elementary and transparent.
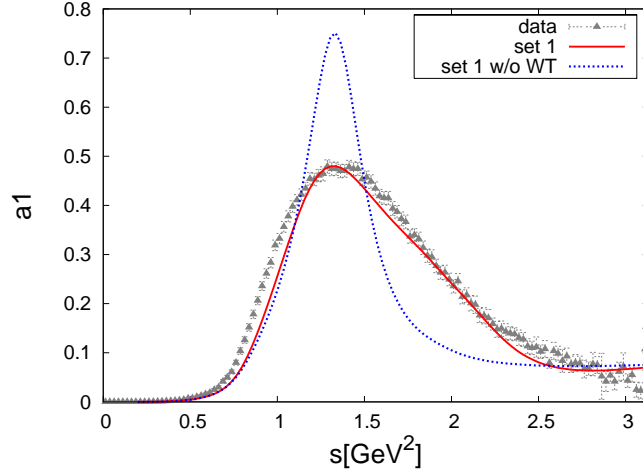
Figure 7.13.: Spectral function for the decay $\tau^- \to 2\pi^0\pi^-\nu_\tau$ including the a_1 using parameter set 1 with and without including the WT term in comparison to data from [S$^+$05].
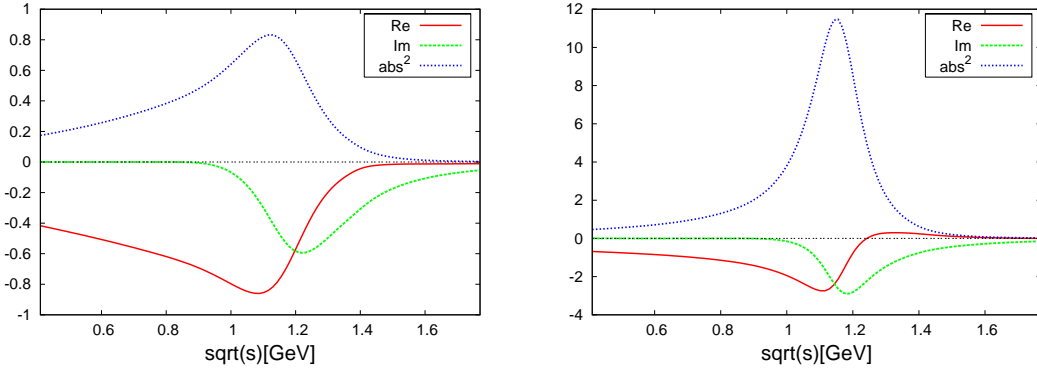

Figure 7.14.: Real part (Re), imaginary part (Im) and absolute value squared (abs^2) of the a_1 propagators resulting from parameter set 4 (left plot) and parameter set 1 without WT term (right plot).

Next, we want to see the role of the WT played in the best result, which was shown in Fig. 7.11 (set 1). In Fig. 7.13 we plotted the result from parameter set 1 with and without including the WT term. Although with this choice of subtraction points the WT term is suppressed very strongly, it obviously still has a major influence on the result.

Looking at the parameters for the calculations, which do not include the WT term, one might wonder why the mass of the a_1 is that high, although the peak clearly is at the right position of $\sqrt{s} \approx 1.26\,\mathrm{GeV}$. The first guess would be that the parameter in Tab. 7.1 is a bare parameter and that together with the real part of the self energy, one gets the physical mass. However, the subtraction point μ_1 is chosen to be $\mu_1 = 2M_\rho^2$, and therefore the real part of the renormalised loop function is almost zero at the physical mass of the hypothetical a_1. From Eq.(6.78) we know that a shift of the bare mass has to be proportional to $\Re J_{\phi V}(\mu_1)$ and therefore is almost zero. In order to see why the spectral function nevertheless peaks at the right position, we look at the a_1 propagators, which result from 'set 4' in Fig. 7.12 and 'set 1 w/o WT' in Fig. 7.13. In Fig. 7.14 we see the real part (Re), imaginary part (Im)
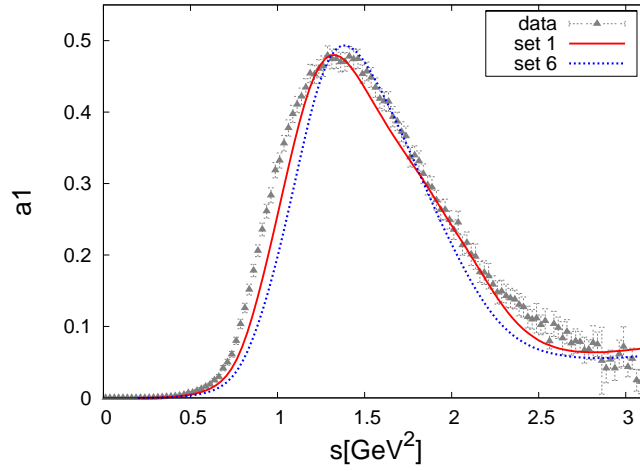
Figure 7.15.: Spectral function for the decay $\tau^- \to 2\pi^0\pi^-\nu_\tau$ including the a_1 using different sets of paramaters in comparison to data from [S+05].

and absolute value squared (abs^2) of the a_1 propagator resulting from parameter set 4 (left plot) and parameter set 1 without WT term (right plot). In the left plot the zero in the real part does obviously not coincide with the maximum in the imaginary part. Thus, defining the physical mass as either the zero of the real part or the maximum of the imaginary part leads to different values. If one chooses the bare mass around 1.2 GeV without including the WT term, the width will turn out too small, which has been seen in Fig. 7.13 already. In the right plot of Fig. 7.14 we see the propagator corresponding to set 1 without WT term, which clearly has a smaller width than the one in the left plot. Again, one might argue that the model does not properly describe the width of the a_1. On the other hand, it can also be used as another sign that the a_1 is just not necessary to describe the data. The shape of the spectral function seems to be driven by the $\pi\rho$ loop function and the energy dependence in front of it. The pole structure of the propagator is shifted to the right of the region, where the interesting structure appears. Therefore the actual pole structure of the propagator seems to be redundant. A point interaction, which is sufficiently attractive and yields the proper phase space (width) is all one needs. We saw already in the previous section that the WT term alone without explicit a_1 can also reproduce the peak.

In the discussion of the results without the explicit a_1, we showed results for the theoretically motivated values of f_V and g_V. Using the theoretical values, it is possible to further suppress the WT term in comparison to the explicit a_1. In Fig. 7.15 we see the best result, which we found in this case. In Fig. 7.9 we found that the rise in the data for energies between about $0.7\,\mathrm{Gev}^2 \lesssim s \lesssim 1.2\,\mathrm{GeV}^2$ is described worse. Here, we find the same problem in the case of the a_1. However, we note that using the theoretically motivated parameters, one can hardly call it finetuning anymore, since it is much easier to get rid of the second bump.

Looking at the results including the a_1 it is not so easy to draw an immediate conclusion. For sure, one can say that the WT term has a major influence on the result. The second bump structure can be recovered in almost every calculation including the a_1 together with the WT term. An important point is that the inclusion of the WT term leads to very strong effects, although we already kept the contribution very small. Only by finetuning one can merge the two appearing bumps. However, merging two bumps by finetuning the parameters does not
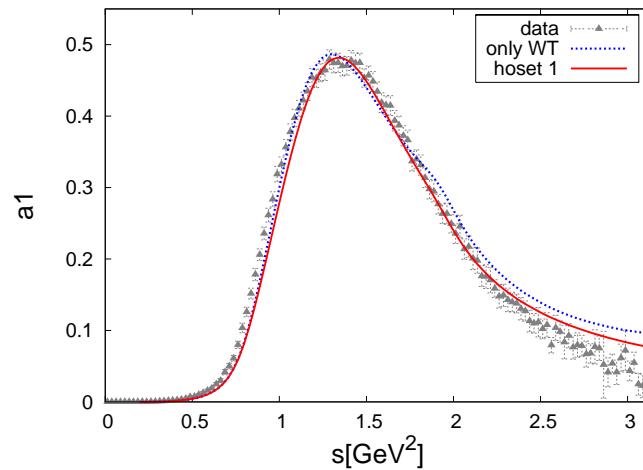
Figure 7.16.: Spectral function for the decay $\tau^- \to 2\pi^0 \pi^- \nu_\tau$ including higher order terms in the kernel in comparison to data from [S$^+$05]. For the choice of the parameters see Tab. 7.2.

seem to be a natural way of reproducing the data. In other words: Why should an elementary state appear right at the position, where an attractive potential already created a peak? We note again that the strength of the WT term is model independently fixed by chiral symmetry breaking. Since the WT alone already produces a peak at the right position, one could already expect that a description of the data including the a_1 has to be accompanied by a delicate choice of the parameters. Still, it would be too much to talk about a definite sign that there is no explicit a_1. However, the peculiarities with explicit a_1 together with the success of the description without the a_1 should be regarded as a good indication. In the next section, we will show that adding higher order corrections to the WT term it is possible to systematically improve the situation in the molecule scenario and that the ordering of diagrams makes sense in this scenario without the explicit a_1.

7.4. Higher order terms

In Section 6.6 we determined the corrections to the kernel at $\mathcal{O}(q^2)$, which led to six new unknown parameters. In the following we leave out the explicit a_1 again and show the influence of these corrections on the results. In Fig. 7.16 we show the spectral function with and without including the higher order correction. There are several parameter sets (Tab. 7.2), which can describe the data in a qualitatively similar way. We see that the higher order terms can be chosen such that they systematically improve the agreement with the data. Note that the size of the higher order terms is *not* constrained by chiral symmetry (except that they should be of natural size - a demand of every effective field theory).

Next we investigate the connection between the higher order terms and the subtraction points. Changing μ_2 can hardly be compensated by the higher order terms, which is expected, since the μ_2 acts as a higher oder correction to the W decay vertex and not to the scattering amplitude. However, a slight raise in μ_2 can be compensated, as can be seen in Fig. 7.17. It can also be seen that the higher order terms do not touch the energy region up to about $s \approx 1\,\mathrm{GeV}^2$.

	λ_1	$\lambda_2 \, [\text{GeV}^{-1}]$	λ_3	λ_4	$\lambda_5 \, [\text{GeV}^{-1}]$	λ_6	$\mu_1 \, [\text{GeV}^2]$	$\mu_2 \, [\text{GeV}^2]$
hoset 1	0	0	1.5	-1.4	0	0	M_ρ^2	$8.5 M_\rho^2$
hoset 2	0.6	0.3	2.5	0	0	0	M_ρ^2	$9 M_\rho^2$
hoset 3	0	-0.3	0	-1.4	0	0	M_ρ^2	$8.5 M_\rho^2$
hoset 4	0.85	0	0	-0.45	0	0	$8.5 M_\rho^2$	$8.5 M_\rho^2$

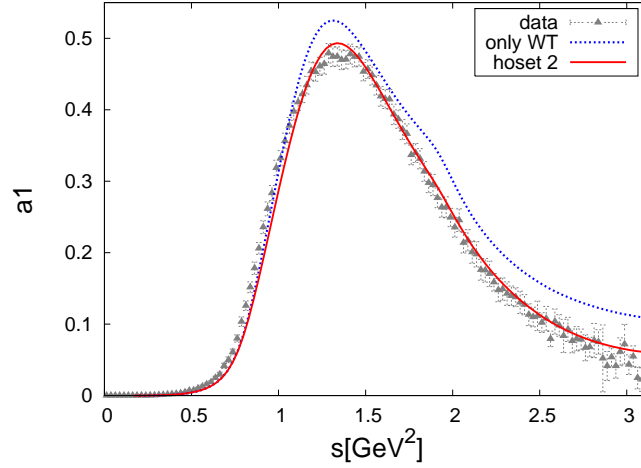**Table 7.2.:** Different sets of parameters, which yield a good description of the spectral function.

Figure 7.17.: Spectral function for the decay $\tau^- \to 2\pi^0 \pi^- \nu_\tau$ including higher order terms in the kernel in comparison to data from [S$^+$05]. For the choice of the parameters see Tab. 7.2. In the calculation including only the WT term we employ the same subtraction point $\mu_2 = 9 \, M_\rho^2$ as in the calculation including the higher order terms.
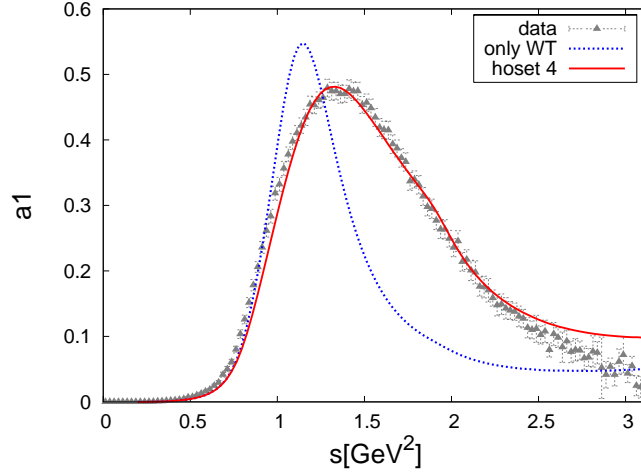
Figure 7.18.: Spectral function for the decay $\tau^- \to 2\pi^0\pi^-\nu_\tau$ with and without higher order terms using $\mu_1 = \mu_2 = 8.5M_\rho^2$ in comparison to data. The parameters for the higher order corrections are given in Tab. 7.2.

Next we want to discuss the connection to μ_1. Here we can expect that the higher order terms are at least to some extent able to compensate for changes. In Fig. 7.18 we can see that we can account for moving the subtraction point μ_1 by changing the parameters of the higher order terms. The parameters are again given in Tab. 7.2. We see that the compensation is even better than expected, since the corrections up to order $\mathcal{O}(q^2)$ do not have to carry all the structures, which might be influenced by moving the subtraction point.

It is also interesting to look directly at the changes induced in the scattering amplitude. In Fig. 7.19 we see the real and imaginary part of the scattering amplitude for the different parameter sets given in Tab. 7.2 in comparison to the calculation without higher order corrections. In order not to overload the figures, we show four different plots. Figs. 7.19(a) and (b) show the scattering amplitudes for the first three parameters sets in comparison to a calculation without higher order corrections and $\mu_1 = M_\rho^2$. We see that the scattering amplitude is not modified much. Only 'hoset 2' shows a different structure, which becomes most obvious in the imaginary part. This change in the scattering amplitude seems to be correlated with the parameter λ_3, which we will further investigate, when we look at the Dalitz plot projections in Section 7.5. Fig. 7.19(c) and (d) show the scattering amplitudes for the 'hoset 4', which was chosen to compensate for the change in the subtraction point μ_1. The figure shows the scattering amplitude for $\mu_1 = M_\rho^2$ and $\mu_1 = 8.5M_\rho^2$ without higher order terms in comparison to $\mu_1 = 8.5M_\rho^2$ with higher order corrections. We see that the corrections bring the scattering amplitudes for $\mu_1 = 8.5M_\rho^2$ back into the shape they had before, when we used $\mu_1 = M_\rho^2$ without higher order corrections. In other words, changes in the renormalisation point can be replaced by changes in the higher order terms. The renormalisation scale dependence is reduced as it should, when including higher order terms.

One might argue that including the higher order corrections was unnecessary and describing the data with 6 parameters is no success. However, the point in including the higher order corrections is not that we can describe the data with seven parameters, but that they systematically improve the result. In case of the inclusion of an explicit a_1, we saw that adding the WT term to the a_1 interaction worsened the results. Here, however, adding the higher order terms to the kernel behaves as a correction. Note that the calculations are not ordered
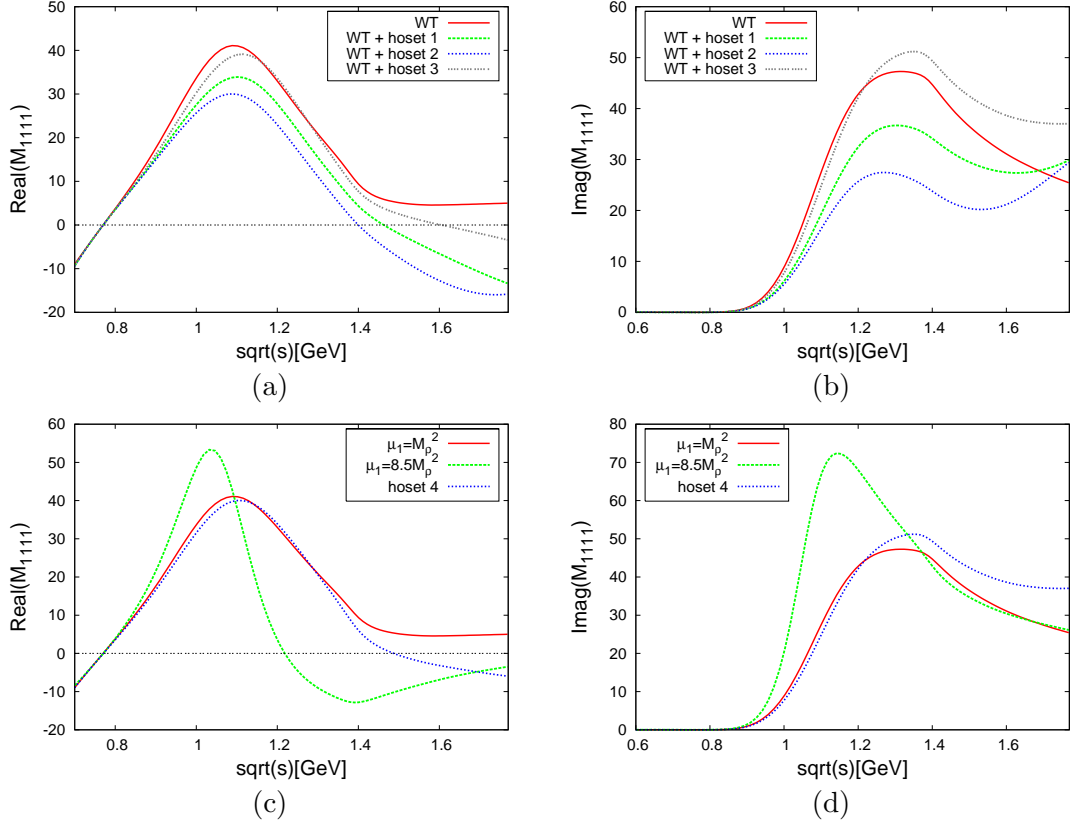
Figure 7.19.: Real (left) and imaginary (right) part of the scattering amplitude for $\pi\rho$ scattering with and without higher order corrections. The upper two plots show the scattering amplitudes for hoset 1-3 in comparison to a calculation without higher order terms and $\mu_1 = M_\rho^2$. The lower two plots show the scattering amplitude for hoset 4 in comparison to a calculation without higher order corrections and $\mu_1 = M_\rho^2$ and $\mu_1 = 8.5 M_\rho^2$, respectively.

according to usual perturbation theory. Instead the kernel of the Bethe-Salpeter equation is calculated in perturbation theory. The convergence of that kind of perturbative expansion is not guaranteed. Therefore it is encouraging to see that the next to leading order terms behave as a correction and are even able to improve the agreement with the data.

We note that there are many possible choices for the parameters, which describe the data. In Section 7.5 we will see that the different sets can be further discriminated by looking at the Dalitz plot projections.

7.5. Dalitz plot projections

In Fig. 7.20 we show the Dalitz plot projections in m_{12}^2 or m_{23}^2 for the calculation using the WT term only and for the calculation including the higher order terms in comparison to data from [A$^+$00]. We determined the normalisation of the theoretical curve such that the area under all curves, corresponding to different slices of $\sqrt{s}$, agrees with the area under the data points. We also subtracted the contribution to the data, which was identified as background in [A$^+$00]. Using this normalisation, we do not really lose any information, since we already saw before that the spectral function was well reproduced for all invariant masses, which implies a proper total decay width and therefore a proper normalisation. Fig. 7.20 clearly shows that the final state is dominated by the ρ meson, and the data are described quite well by all parameter sets. The last two plots seem to show an improvement by including the higher order corrections. The improvement in the last two plots is most pronounced for hoset 2. But since we overshoot at lower m_{12}^2 and the error bars are pretty large for these invariant masses, the advantage is not very stringent. We recall that q_1 and q_3 are the momenta of the likewise pions and that the amplitude is symmetric under the exchange $q_1 \rightarrow q_3$. Thus, m_{12}^2 and m_{23}^2 are the invariant mass of the intermediate ρ, which we clearly see in the Dalitz plot projections.

In Fig. 7.21 we plot the number of decays versus m_{13}^2, which is the invariant mass of the likewise pions. These pions do not build up the ρ and therefore the structure in these plots is completely different from Fig. 7.20. When we look at Fig. 7.21, we also find that the calculations including the higher order corrections describe the data better, which again is more pronounced for hoset 2. The steep rise at small m_{13}^2 is much better reproduced by hoset2 and also the additional structure at higher invariant masses is reproduced better with hoset 2, although we overshoot that structure. We note that using hoset 3 and hoset 4, we do not get a noteworthy difference in the Dalitz plot projections in comparison to a calculation without higher order corrections. Thus, the improvement in the Dalitz plots seems to be correlated with the parameter λ_3, which is non-vanishing for hoset 1 and hoset 2 (cf. Tab. 7.2).

It is interesting to see the amount of d-wave contributions from the different parameter sets. In Fig. 7.22 we plotted the absolute value of the ratio of the respective coefficient c_{ss} and c_{ds} to the sum of all coefficients (see Section 5.2). We see, that the parameter sets, which describe the Dalitz plot projections better, clearly have a higher d-wave contribution. Thus, our calculation indicates a population of d-waves in the τ decay in the amount, which is shown in Fig. 7.22. We note that the leading order contribution to c_{sd} is given by the terms proportional to λ_3 and λ_6 in Eq.(6.96). A statement about pure d-wave transitions given by c_{dd} would be more complicated, since terms of higher chiral order than q^2 would contribute at leading order.
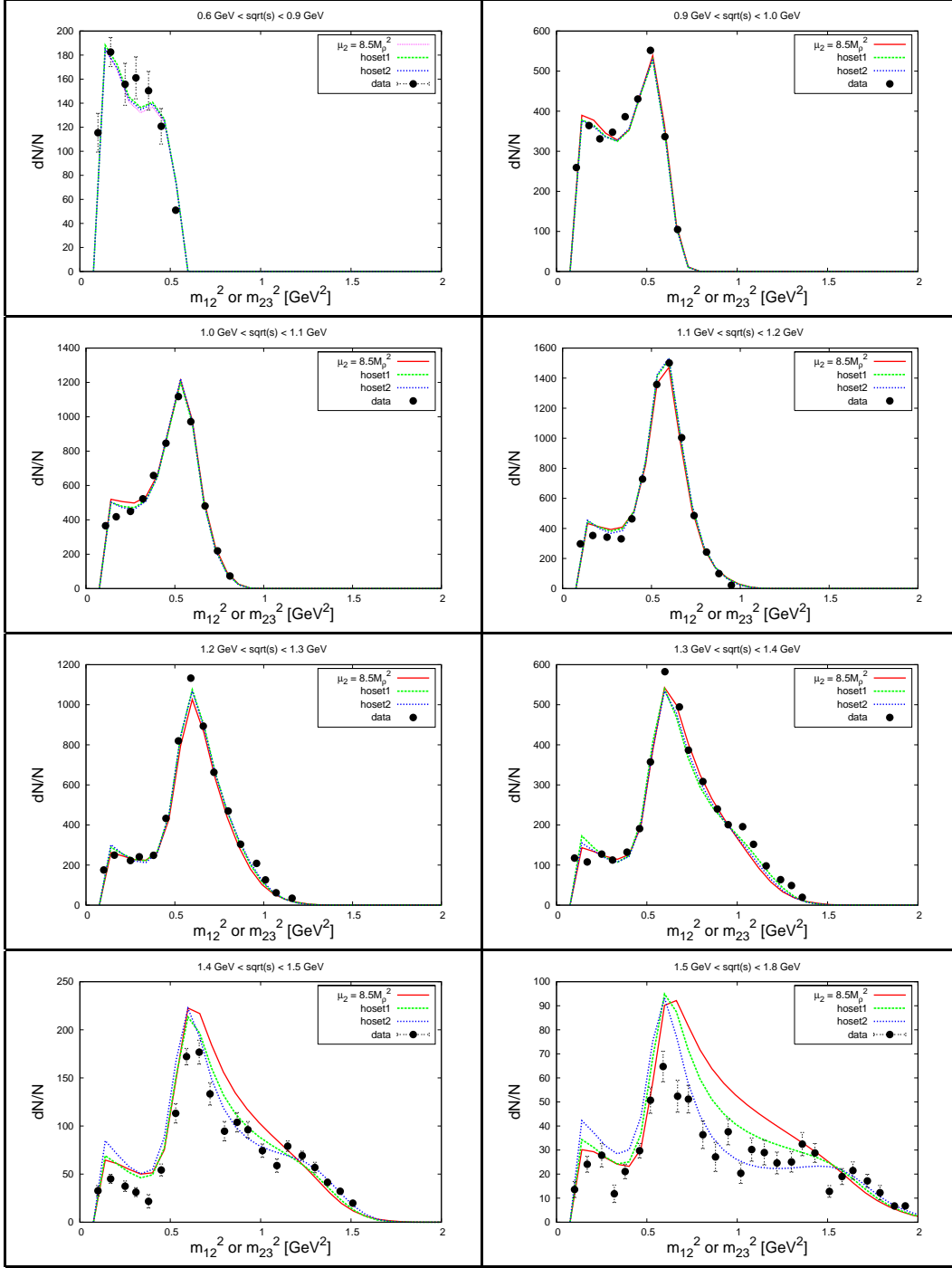
Figure 7.20.: Dalitz plot projections in m_{12}^2 or m_{23}^2 with and without higher order corrections in comparison to data from [A$^+$00]. The different parameter sets can be found in Tab. 7.2. The curve labelled $\mu_2 = 8.5M_\rho^2$ corresponds to a calculation using the WT term only, $\mu_1 = M_\rho^2$ and $\mu_2 = 8.5M_\rho^2$.

Figure 7.21.: Dalitz plot projections in m_{13}^2 with and without higher order corrections in comparison to data from [A$^+$00]. The different parameter sets can be found in Tab. 7.2. The curve labelled $\mu_2 = 8.5M_\rho^2$ corresponds to a calculation using the WT term only, $\mu_1 = M_\rho^2$ and $\mu_2 = 8.5M_\rho^2$.
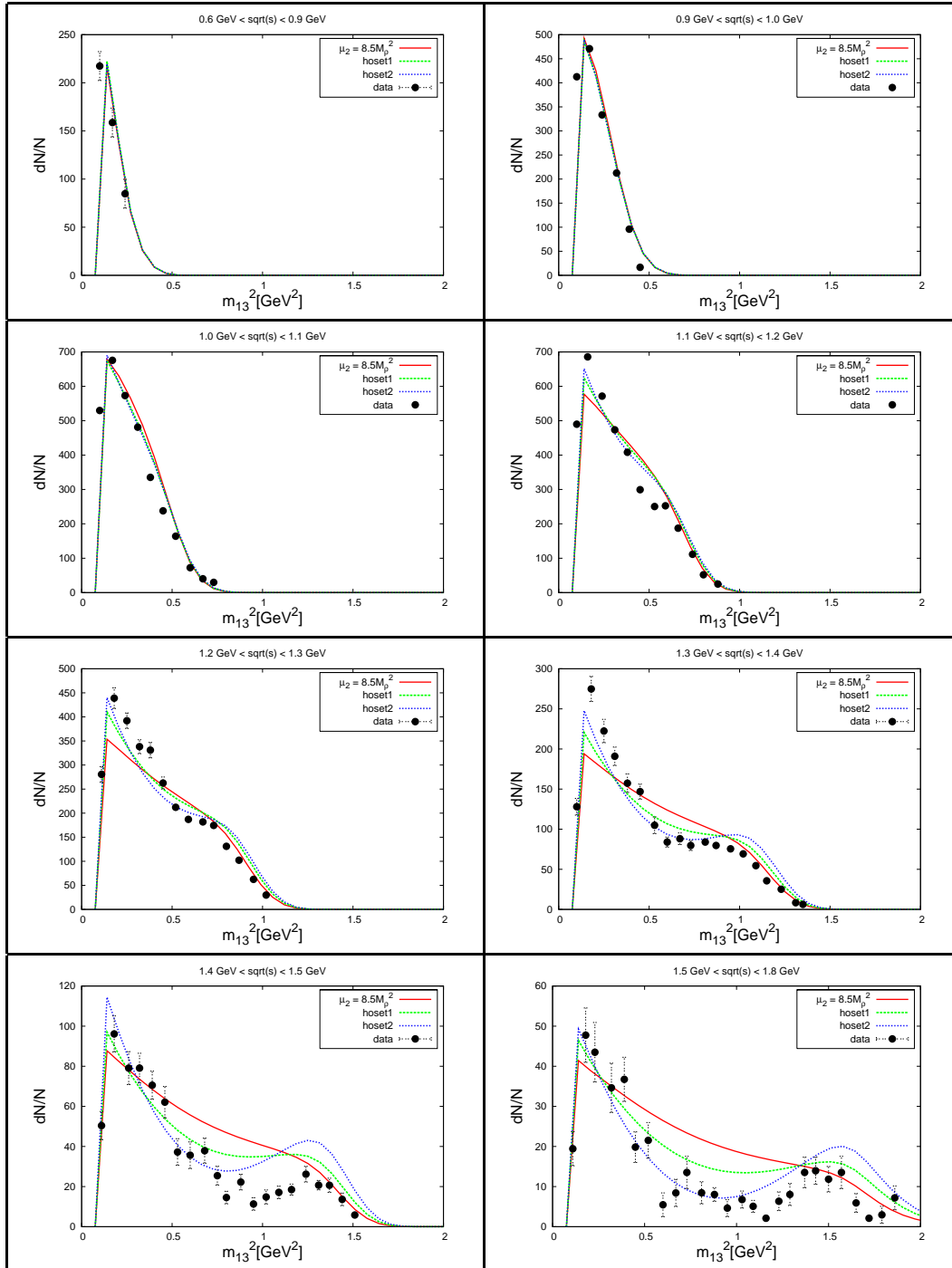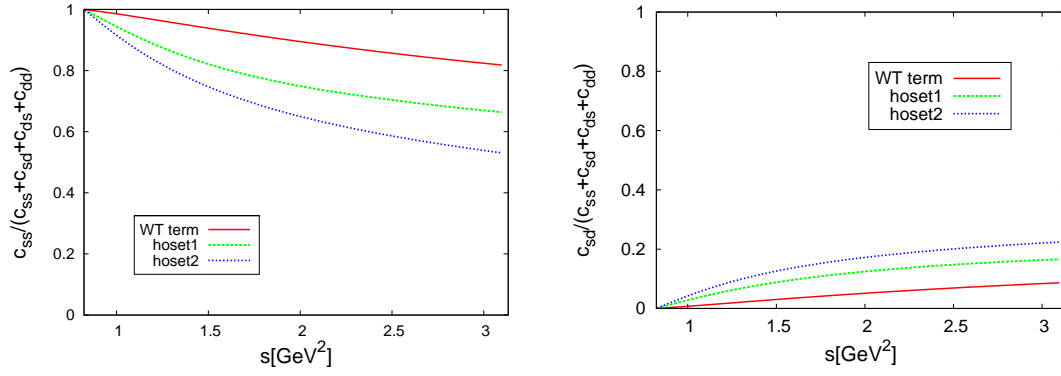
Figure 7.22.: Population of angular momentum states expressed in $c_{ss}/(c_{ss} + 2c_{sd} + c_{dd})$ (left) and $c_{sd}/(c_{ss} + 2c_{sd} + c_{dd})$ (right). The curve labelled 'WT term' shows the population for the WT term only, whereas the other kernels include higher order corrections with the parameters given in Tab. 7.2.

Chapter 8.

Summary and Outlook

We presented in this thesis a new way to calculate the process $\tau^- \to 2\pi^0\pi^-\nu_\tau$. We performed the calculation under different assumptions and we emphasise that in the simplest scenario, which describes the data already very well, we only used one free parameter. In this scenario the resonant structure seen in the data essentially is caused by an attractive final state interaction between π and ρ. In order to set the stage, the first chapters were devoted to the explanation of the ingredients of our model describing the decay process, which are essentially chiral symmetry and unitarity. We discussed the most important facts and issues which appear by implementing vector mesons in the chiral Lagrangian and showed their effects on our calculation. In one scenario the strong final state correlations which appear in the τ decay are taken into account by iterating the lowest order interaction in a Bethe-Salpeter equation. The connection of the Bethe-Salpeter equation to the unitarisation methods has been reviewed in detail. In order to solve the Bethe Salpeter equation we used the so called partial wave projectors. We presented an exact relation to the covariant projectors used in [LK04] and showed a proof of their orthogonality. We also gave the exact connection between the helicity states and states of orbital angular momentum. Afterwards we performed the calculation in different ways, namely with and without including an explicit a_1. All relevant formulas to retrace the calculation have been given in Chapter 6. The calculations were essentially split in three parts:

1. In one scenario we described the final state correlations in the τ decay solely by iterating the WT term (molecule scenario). The picture we promote is that the process is dominated by $\rho\pi$ final state interactions, which are described by iterating the WT term. The weak decay is part of the standard model and the WT term is predicted parameter free from chiral symmetry. The remaining coupling constants (f_V, g_V), which describe the interaction of the vector mesons are determined by the properties of the ρ [EGL+89]. The only unknown parameters in the calculation entered through the renormalisation of the loop integrals. We introduced two subtraction points to render the loop integrals finite. One subtraction point (μ_1) renormalises the loops in the scattering amplitude describing the final state interactions. This parameter was already introduced in [LK04] and fixed by crossing symmetry arguments. The other subtraction point (μ_2) enters in the renormalisation of the first loop, which contains the W decay vertex. We investigated the influence of these parameters on the results. First, we set $\mu_1 = \mu_2$ and varied them simultaneously. In particular, we compared the different values used in [LK04] and [ROS05]. We found that all choices produce a peak at the same position with a different height. The position of this peak was in the region of the resonant structure seen in the data, but the width always turned out to be too small. Afterwards we investigated the influence of μ_2 by keeping μ_1 fixed. Using the crossing symmetry argument from [LK04] in order to determine μ_1, we were left with one parameter. Fitting this parameter, we reproduced the spectral function for the decay $\tau^- \to 2\pi^0\pi^-\nu_\tau$ quite well.

2. In a second scenario, we explicitly introduced the a_1 in the calculation. This introduced

new parameters, namely the mass of the a_1, its coupling to the W boson f_A and the couplings to the vector-meson Goldstone boson states c_1 and c_2. The most obvious feature in that calculation has been, that due to the strong influence of the WT term, a second bump appeared. Finetuning the parameters, one could merge the two bumps into one and the data were described more or less satisfying. However, the results of these calculations are peculiar. An important point is that the inclusion of the WT term leads to very strong effects, although we already kept the contribution very small. Merging two bumps by finetuning the parameters does not seem to be a natural way of reproducing the data. Since the WT alone already produces a peak at the right position, one could expect already that a description of the data including the a_1 has to be accompanied by a delicate choice of the parameters. Thus, recalling the success of the model without explicit a_1, the scenario with explicit a_1 seems to be artificial.

3. In the third part we left out the explicit a_1 again and included higher order corrections to the kernel. These additional terms further improved the molecule scenario, and we found an almost perfect agreement with the data. These corrections introduced six new parameters and many combinations of these parameters were found, which fit the spectral function very well. However, the intention in introducing the higher order terms was not only to describe the spectral function, which was already described quite well without the corrections, but to show the possibility of a systematic improvement. The corrections induced by these terms behaved as higher order corrections are supposed to behave. That was not clear from the beginning, since we calculated the kernel of the Bethe-Salpeter equation perturbatively, which does not automatically guarantee that we picked up the most important contributions for the scattering amplitude itself. Therefore, this is an encouraging fact, which puts further foundation to the molecule scenario and shows its systematic nature.

Comparing our calculation to the Dalitz projections, we found that including higher order terms, which carry d-wave components, describe the data better. In a relativistic framework one first has to make sense of what one means with a d-wave component. This task has been fulfilled in Chapter 5. We defined the coefficient c_{sd}, which describes the transition from an s-wave to a d-wave state, and pointed out that the leading contribution to this term is given by the WT term and the higher order correction, which we included in the third part of the calculation. The size of this coefficient is clearly correlated with the quality to describe the Dalitz plot data.

We also discussed possible uncertainties in the model. We discussed the influence of pion final state correlations and the influence of the offshell behaviour of the ρ. In order to judge the uncertainties, we performed the calculation under the assumption that the ρ is stable, which led to very similar results. In addition, we note that the clear sign of the peak was seen with almost any choice for the free parameters and the importance of the WT term is not questionable.

To summarise, one finds that without the explicit a_1 one has a well behaved model, which can be systematically improved and which describes the data very well. Most parameters (in the simplest scenario, all but one) are fixed by chiral symmetry breaking and the well known properties of the ρ. An explicit a_1 leads to peculiar properties, if one generates the width consistently from the Bethe-Salpeter equation and additionally includes the WT term. Although it is possible to find parameter sets, which describe the data more or less satisfying, the scenario seems artificial. When we try to describe the data with an explicit a_1, the strength of the WT interaction causes problems. On the other hand, this strength is fixed by chiral symmetry breaking and we note again that including the WT term and the explicit a_1 is not double counting. For sure one can claim that the WT term should not be disregarded, as however, has been done in many previous approaches.

These indications point towards a dynamical nature of the a_1 as a coupled-channel meson-molecule.

As an outlook we note that a further step in the calculation would be to include medium effects in order to see what happens to the a_1 in case we approach the chiral symmetry restoration [RW00]. In principle, when the restoration happens, the axial-vector spectral function defined in Section 7.1 must be degenerate with the corresponding vector spectral function. In the latter the ρ meson prominently appears at least in the vacuum [S$^+$05]. It is, however, not so clear what chiral restoration implies for the specific part of the spectral function with a three-pion final state. In any case one would expect a drastic reshaping of both the vector and the axial-vector spectral function.

It would also be interesting to figure out how well the molecule scenario agrees with QCD lattice calculations [Kog83] of the axial-vector current-current correlator (in the specific region accessible by lattice QCD). Here one has to perform the calculations with a higher pion mass in order to connect to lattice QCD calculations. This also brings into play pion mass corrections to the involved coupling constants as for example F_0, f_V, g_V. Still one can expect that the presented framework offers enough predictive power to obtain a valuable comparison to lattice QCD [Leu06].

Appendix A.

Notation and Normalisation

A.1. Conventions and γ matrices

The notation and the conventions in this work correspond mainly to those in the book of Peskin and Schroeder [PS95].

Units

We work in natural units, i.e.,

$$\hbar = c = 1 \,. \tag{A.1}$$

This yields the relations

$$[\text{length}] = [\text{time}] = [\text{energy}]^{-1} = [\text{mass}]^{-1} \,.$$

The only unit conversion that will be needed throughout this work is given by

$$197.327 \,\text{MeV} = 1 \,\text{fm}^{-1} \,.$$

Metric tensor and four-vectors

We use the metric tensor in the form,

$$g_{\mu\nu} = g^{\mu\nu} = \begin{pmatrix} 1 & 0 & 0 & 0 \\ 0 & -1 & 0 & 0 \\ 0 & 0 & -1 & 0 \\ 0 & 0 & 0 & -1 \end{pmatrix} \,.$$

Four-vectors are denoted by italic letters (x), three-vectors are marked by arrows $(\vec{x})$. Greek indices denote the components of a four-vector and run from 0 to 3 (where the zeroth component is the time or energy component of the four-vector). Following the Einstein summation convention, we sum over all indices that appear twice in a term.
We distinguish between four-vectors with upper (contravariant) and lower (covariant) indices,

$$x^\mu = (x^0, \vec{x}) \qquad\qquad (\text{contravariant}) \,,$$
$$x_\mu = g_{\mu\nu} x^\nu = (x^0, -\vec{x}) \qquad\qquad (\text{covariant}) \,.$$

The scalar product of two four-vectors is defined by

$$x \cdot p = x_\mu x^\mu = g_{\mu\nu} x^\mu p^\nu = x^0 p^0 - \vec{x} \cdot \vec{p} \,.$$

Pauli matrices

The Pauli matrices are given by

$$\sigma^1 = \begin{pmatrix} 0 & 1 \\ 1 & 0 \end{pmatrix}, \qquad \sigma^2 = \begin{pmatrix} 0 & -i \\ i & 0 \end{pmatrix}, \qquad \sigma^3 = \begin{pmatrix} 1 & 0 \\ 0 & -1 \end{pmatrix}. \tag{A.2}$$

The Pauli matrices obey the (anti-)commutation relations

$$\{\sigma_i, \sigma_j\} = 2\delta_{ij} \qquad \text{and} \qquad [\sigma_i, \sigma_j] = 2i\epsilon_{ijk}\tau_k, \tag{A.3}$$

where δ_{ij} is the Kronecker delta and ϵ_{ijk} is the totally antisymmetric tensor (Levi-Civita symbol) in three dimensions. The (anti-)commutation relations above lead to the following helpful relation

$$\sigma^i \sigma^j = \delta^{ij} + i\epsilon^{ijk}\sigma^k. \tag{A.4}$$

Dirac matrices

The Dirac matrices (or γ matrices) satisfy – independently of the chosen representation – the anticommutation relations

$$\{\gamma^\mu, \gamma^\nu\} = 2g^{\mu\nu}. \tag{A.5}$$

There exist several explicit representations of the Dirac matrices. In this work, we will use the so-called chiral (or Weyl) representation that can be constructed from the Pauli matrices in a 2×2 block form:

$$\gamma^0 = \begin{pmatrix} 0 & \mathbb{1}_{2\times2} \\ \mathbb{1}_{2\times2} & 0 \end{pmatrix}, \qquad \gamma^i = \begin{pmatrix} 0 & \tau^i \\ -\tau^i & 0 \end{pmatrix}, \qquad \gamma^5 = \begin{pmatrix} -\mathbb{1}_{2\times2} & 0 \\ 0 & \mathbb{1}_{2\times2} \end{pmatrix}. \tag{A.6}$$

Products of γ matrices and four-vectors are denoted in the Feynman slash notation,

$$p \cdot \gamma = p_\mu \gamma^\mu = \slashed{p}.$$

In addition, we use

$$\gamma^5 = i\gamma^0\gamma^1\gamma^2\gamma^3. \tag{A.7}$$

By construction, the matrix γ^5 has the following properties,

$$(\gamma^5)^2 = \mathbb{1}_{4\times4}, \qquad (\gamma^5)^\dagger = \gamma^5, \qquad \{\gamma^5, \gamma^\mu\} = 0.$$

The γ matrices also fulfil

$$\gamma^{\mu\dagger}\gamma_0 = \gamma_0\gamma^\mu,$$

which assures the hermiticity of the Dirac Lagrangian.

Traces of γ matrices

We will encounter traces of γ matrices. For further reference, we list some helpful relations below:

$$\text{Tr}[\mathbb{1}_{4\times4}] = 4, \tag{A.8}$$

$$\text{Tr}[\gamma^\mu\gamma^\nu] = 4g^{\mu\nu}, \tag{A.9}$$

$$\text{Tr}[\gamma^\mu\gamma^\nu\gamma^\rho\gamma^\sigma] = 4(g^{\mu\nu}g^{\rho\sigma} - g^{\mu\rho}g^{\nu\sigma} + g^{\mu\sigma}g^{\nu\rho}), \tag{A.10}$$

$$\text{Tr}[\gamma^5] = 0, \tag{A.11}$$

$$\text{Tr}[\gamma^\mu\gamma^\nu\gamma^5] = 0, \tag{A.12}$$

$$\text{Tr}[\gamma^\mu\gamma^\nu\gamma^\rho\gamma^\sigma\gamma^5] = -4i\epsilon^{\mu\nu\rho\sigma}. \tag{A.13}$$

Note that the trace of an odd number of γ matrices is always zero.

Gell-Mann matrices

The elements of SU(3) can be written in terms of the eight generators λ_a

$$U(\theta) = \exp\left(-i\sum_{a=1}^{8} \theta_a \frac{\lambda_a}{2}\right), \tag{A.14}$$

with real parameters θ_a. One possible representation for the generators is the one chosen by Gell-Mann, which is given by

$$\lambda_1 = \begin{pmatrix} 0 & 1 & 0 \\ 1 & 0 & 0 \\ 0 & 0 & 0 \end{pmatrix}, \quad \lambda_2 = \begin{pmatrix} 0 & -i & 0 \\ i & 0 & 0 \\ 0 & 0 & 0 \end{pmatrix}, \quad \lambda_3 = \begin{pmatrix} 1 & 0 & 0 \\ 0 & -1 & 0 \\ 0 & 0 & 0 \end{pmatrix},$$

$$\lambda_4 = \begin{pmatrix} 0 & 0 & 1 \\ 0 & 0 & 0 \\ 1 & 0 & 0 \end{pmatrix}, \quad \lambda_5 = \begin{pmatrix} 0 & 0 & -i \\ 0 & 0 & 0 \\ i & 0 & 0 \end{pmatrix}, \quad \lambda_6 = \begin{pmatrix} 0 & 0 & 0 \\ 0 & 0 & 1 \\ 0 & 1 & 0 \end{pmatrix}, \tag{A.15}$$

$$\lambda_7 = \begin{pmatrix} 0 & 0 & 0 \\ 0 & 0 & -1 \\ 0 & i & 0 \end{pmatrix}, \quad \lambda_8 = \frac{1}{\sqrt{3}}\begin{pmatrix} 1 & 0 & 0 \\ 0 & 1 & 0 \\ 0 & 0 & -2 \end{pmatrix}.$$

Some useful properties are

$$\lambda_a = \lambda_a^{\dagger}, \tag{A.16}$$
$$\mathrm{Tr}[\lambda_a \lambda_b] = 2\delta_{ab}, \tag{A.17}$$
$$\mathrm{Tr}[\lambda_a] = 0. \tag{A.18}$$

Trace relations

In [EFS02] one can find the following formula concerning 3×3 matrices, which follows from the Cayley-Hamilton theorem

$$\begin{aligned}
&A_1\{A_2, A_3\} + A_2\{A_3, A_1\} + A_3\{A_1, A_2\} - \mathrm{Tr}[A_1]\{A_2, A_3\} - \mathrm{Tr}[A_2]\{A_3, A_1\} \\
&- \mathrm{Tr}[A_3]\{A_1, A_2\} + \mathrm{Tr}[A_1]\,\mathrm{Tr}[A_2]A_3 + \mathrm{Tr}[A_2]\,\mathrm{Tr}[A_3]A_1 + \mathrm{Tr}[A_3]\,\mathrm{Tr}[A_1]A_2 - \mathrm{Tr}[A_1 A_2]A_3 \\
&- \mathrm{Tr}[A_2 A_3]A_1 - \mathrm{Tr}[A_3 A_1]A_2 - \mathrm{Tr}[A_1 A_2 A_3]\mathbb{1}_3 - \mathrm{Tr}[A_1 A_3 A_2]\mathbb{1}_3 + \mathrm{Tr}[A_1 A_2]\,\mathrm{Tr}[A_3]\mathbb{1}_3 \\
&+ \mathrm{Tr}[A_3 A_1]\,\mathrm{Tr}[A_2]\mathbb{1}_3 + \mathrm{Tr}[A_2 A_3]\,\mathrm{Tr}[A_1]\mathbb{1}_3 - \mathrm{Tr}[A_1]\,\mathrm{Tr}[A_2]\,\mathrm{Tr}[A_3]\mathbb{1}_3 = 0.
\end{aligned} \tag{A.19}$$

Multiplying this equation with another matrix and taking the trace, one can derive trace relations. In our case, we want to find trace relations for terms constructed out of two V_μ and two u_μ (see Appendix C below). Using the above formula, we find the following relations

$$2\,\mathrm{Tr}[V_\mu u_\nu u^\nu V^\mu] + 2\,\mathrm{Tr}[V_\mu u_\nu V^\mu u^\nu] + 2\,\mathrm{Tr}[V_\mu V^\mu u_\nu u^\nu] = \mathrm{Tr}[V_\mu V^\mu]\,\mathrm{Tr}[u_\nu u^\nu] + 2\,\mathrm{Tr}[V_\mu u_\nu]\,\mathrm{Tr}[V^\mu u^\nu] \tag{A.20}$$

and

$$\begin{aligned}
&2\,\mathrm{Tr}[V_\mu V_\nu u^\mu u^\nu] + 2\,\mathrm{Tr}[V_\mu V_\nu u^\mu u^\nu] + \mathrm{Tr}[V_\mu u^\mu V_\nu u^\nu] + \mathrm{Tr}[V_\mu u_\nu V^\nu u^\mu] \\
&= \mathrm{Tr}[V_\mu u^\nu]\,\mathrm{Tr}[V_\nu u^\mu] + \mathrm{Tr}[V_\mu u^\mu]\,\mathrm{Tr}[V^\nu u_\nu] + \mathrm{Tr}[V_\mu V_\nu]\,\mathrm{Tr}[u^\mu u^\nu].
\end{aligned} \tag{A.21}$$

A.2. Momentum states, helicity states and normalisation

One-particle momentum states with three-momentum $\vec{p}$ and helicity λ are normalised such that their inner product is Lorentz invariant, i.e.

$$\langle \overline{p}, \overline{\lambda} | p, \lambda \rangle = 2E_p (2\pi)^3 \delta^{(3)}(\vec{p} - \vec{\overline{p}}) \delta_{\lambda\overline{\lambda}} \tag{A.22}$$

Thus, we can deduce the normalisation for a two-particle state. We choose the second particle to be a scalar since we encounter these states in our calculation, but it should be obvious how one can extend the description to two particles with spin.

$$\langle \overline{p}, \overline{q}, \overline{\lambda} | p, q, \lambda \rangle = 4E_p E_q (2\pi)^6 \delta^{(3)}(\vec{p} - \vec{\overline{p}}) \delta^{(3)}(\vec{q} - \vec{\overline{q}}) \delta_{\lambda\overline{\lambda}} . \tag{A.23}$$

Using the total four-momentum $w^\mu = p^\mu + q^\mu$ we can rewrite the above equation

$$
\begin{aligned}
\langle \overline{p}, \overline{q}, \overline{\lambda} | p, q, \lambda \rangle &= 4E_p E_q (2\pi)^6 \delta^{(3)}(\vec{w} - \vec{\overline{w}}) \delta^{(3)}(\vec{q} - \vec{\overline{q}}) \delta_{\lambda\overline{\lambda}} \\
&= 4E_p E_q (2\pi)^6 \delta^{(3)}(\vec{w} - \vec{\overline{w}}) \frac{1}{\vec{q}^2} \delta(|\vec{q}| - |\vec{\overline{q}}|) \delta(\Omega - \overline{\Omega}) \delta_{\lambda\overline{\lambda}} \\
&= 4\frac{\sqrt{s}}{|\vec{q}|} (2\pi)^6 \delta^{(4)}(w - \overline{w}) \langle \overline{\theta}, \overline{\phi}, \overline{\lambda} | \theta, \phi, \lambda \rangle \\
&= 4\frac{\sqrt{s}}{|\vec{q}|} (2\pi)^6 \langle \overline{w}, \overline{\theta}, \overline{\phi}, \overline{\lambda} | w, \theta, \phi, \lambda \rangle ,
\end{aligned}
$$

and thus

$$|p, q, \lambda \rangle = 2(2\pi)^3 \sqrt{\frac{\sqrt{s}}{|\vec{q}|}} |w, \theta, \phi, \lambda \rangle . \tag{A.24}$$

Scattering matrix

In order to isolate the interesting part of the scattering matrix, one defines the T-matrix

$$S = \mathbb{1} + iT . \tag{A.25}$$

The invariant matrix element M is introduced as

$$\langle \overline{p}, \overline{q}, \overline{\lambda} | T | p, q, \lambda \rangle = (2\pi)^4 \delta^4(\overline{p} + \overline{q} - p - q) M . \tag{A.26}$$

Using Eq.(A.24), we see that

$$
\begin{aligned}
\langle \overline{p}, \overline{q}, \overline{\lambda} | T | p, q, \lambda \rangle &= (2\pi)^4 \delta^4(\overline{p} + \overline{q} - p - q) M \\
&\overset{!}{=} \delta^4(\overline{p} + \overline{q} - p - q) 4 (2\pi)^6 \frac{\sqrt{s}}{\sqrt{p_{cm}\overline{p}_{cm}}} \langle \overline{\theta}, \overline{\phi}, \overline{\lambda} | T | \theta, \phi, \lambda \rangle ,
\end{aligned}
\tag{A.27}
$$

and thus

$$M = \langle \overline{\theta}, \overline{\phi}, \overline{\lambda} | T | \theta, \phi, \lambda \rangle \frac{16\pi^2 \sqrt{s}}{\sqrt{\overline{p}_{cm} p_{cm}}} . \tag{A.28}$$

The quantity, which we expand according to Eq.(5.5) and Eq.(5.7) in our calculation is the invariant matrix element. The definition of T expressed in helicity states thus reads

$$S^J_\lambda = \delta_{\overline{\lambda}\lambda} + iT^J_{\overline{\lambda}\lambda} = \delta_{\overline{\lambda}\lambda} + iM^J_{\overline{\lambda}\lambda} \frac{\sqrt{\overline{p}_{cm} p_{cm}}}{4\pi\sqrt{s}} , \tag{A.29}$$

where

$$T^J_{\bar{\lambda}\lambda} = \langle \bar{\lambda}|T^J|\lambda \rangle \,, \tag{A.30}$$

and $M_{\bar{\lambda}\lambda}$ denote the respective expansion coefficients of M. The additional factor of 4π arises due to the definition of the expansion coefficients in Eq.(5.7).

Polarisation vectors

Massive spin 1 particles are described by the Proca Lagrangian

$$\mathcal{L} = -\frac{1}{4}F_{\mu\nu}F^{\mu\nu} + \frac{m^2}{2}V_\mu V^\mu \,, \tag{A.31}$$

with V_μ being the vector field in the vector representation and $F_{\mu\nu} = \partial_\mu V_\nu - \partial_\nu V_\mu$. Applying the Euler-Lagrange equations, one finds the following equations of motion

$$(\Box + M_V^2)V_\mu = 0\,, \quad \partial_\mu V^\mu = 0\,. \tag{A.32}$$

The first equation tells us that every component of V_μ can be described by a wave and the second equation reduces the four degrees of freedom of the four-vector to three. In the rest frame the polarisation vectors should be the spin states, and therefore eigenstates of J_3. J_i are the three-dimensional representation matrices of SU(2), and we choose the explicit form

$$(J_i)_{jk} = -i\epsilon_{ijk}\,. \tag{A.33}$$

Thus, we can choose for the three-dimensional polarisation vectors in the rest frame

$$\vec{\epsilon}_{\pm 1} = \begin{pmatrix} \frac{\mp 1}{\sqrt{2}} \\ \frac{-i}{\sqrt{2}} \\ 0 \end{pmatrix}\,, \quad \vec{\epsilon}_0 = \begin{pmatrix} 0 \\ 0 \\ 1 \end{pmatrix}\,. \tag{A.34}$$

The extension to four dimensions is easily done by adding a zeroth component to the polarisation vectors $\epsilon^\mu(\lambda) = (0, \vec{\epsilon}_\lambda)$. In order to determine the polarisation vectors for a moving particle, we will first boost the vectors in z-direction and then rotate it. The boost in z-direction does not change the spin or helicity of the particle but after a rotation these states will not be spin eigenstates anymore. After a boost

$$\Lambda_{\mu\nu} = \frac{1}{M_V}\begin{pmatrix} E & 0 & 0 & p \\ 0 & 1 & 0 & 0 \\ 0 & 0 & 1 & 0 \\ p & 0 & 0 & E \end{pmatrix}\,, \tag{A.35}$$

the polarisation vectors are given by

$$\epsilon_\mu(p, \pm 1) = \begin{pmatrix} 0 \\ \frac{\mp 1}{\sqrt{2}} \\ \frac{-i}{\sqrt{2}} \\ 0 \end{pmatrix}\,, \quad \epsilon_\mu(p, 0) = \begin{pmatrix} \frac{p_{cm}}{M} \\ 0 \\ 0 \\ \frac{\omega}{M} \end{pmatrix}\,. \tag{A.36}$$

The rotation acts only on the three vectors and is given by

$$\vec{\epsilon}(\lambda, \theta, \phi) = \sum_{\lambda'} D^1_{\lambda\lambda'}\vec{\epsilon}(\lambda')\,, \tag{A.37}$$

111

with the Wigner rotation function $D^1_{\lambda\lambda'}$. In a frame, where the vector meson is flying with momentum p_{cm} and an angle θ to the z-axis the polarisation vectors become

$$\epsilon_\mu(\overline{p}, \pm 1) = \begin{pmatrix} 0 \\ \frac{\mp \cos\theta}{\sqrt{2}} \\ \frac{-i}{\sqrt{2}} \\ \frac{\pm \sin\theta}{\sqrt{2}} \end{pmatrix}, \quad \epsilon_\mu(\overline{p}, 0) = \begin{pmatrix} \frac{\overline{p}_{cm}}{M} \\ \frac{\overline{\omega}}{M} \sin\theta \\ 0 \\ \frac{\overline{\omega}}{M} \cos\theta \end{pmatrix}. \tag{A.38}$$

A.3. Wigner rotation matrices

The Wigner rotation matrices $D^J_{mm'}$ [Tun85] or Wigner functions represent the group elements of SO(3) in the various representation. They can be defined as

$$U(\alpha, \beta, \gamma)|j, m\rangle = |j, m'\rangle D^j(\alpha, \beta, \gamma)^{m'}_m, \tag{A.39}$$

where $U(\alpha, \beta, \gamma)$ is the operator representing the rotation by the Euler angles (α, β, γ). One also uses the simplified Wigner functions or d-functions

$$D_{\lambda\overline{\lambda}}(\alpha, \beta, \gamma) = e^{-i\alpha\lambda} d^J_{\lambda\overline{\lambda}}(\beta) e^{-i\gamma\overline{\lambda}} \tag{A.40}$$

with

$$d^J_{\lambda\overline{\lambda}}(\beta) = \langle jm'|e^{-i\beta J_2}|jm\rangle. \tag{A.41}$$

The d-functions can be expressed in closed form, for example, via the Jacobi polynomials

$$d^J(\beta)_{mm'} = \sqrt{\frac{(j+m')!(j-m')!}{(j+m)!(j-m)!}} \left(\cos\frac{\beta}{2}\right)^{m+m'} \left(\sin\frac{\beta}{2}\right)^{m-m'} P^{m'-m,m+m'}_{j-m'}(\cos\beta). \tag{A.42}$$

In particular, one sees

$$d_{mm'}(0) = \delta_{mm'} \tag{A.43}$$

The relation to the spherical harmonics is given by

$$Y_{lm}(\theta\phi) = \left(\frac{2l+1}{4\pi}\right)^{\frac{1}{2}} (D^l(\phi, \theta, 0)^l_{m0})^*. \tag{A.44}$$

The Wigner functions and the d-functions obey orthogonality relations

$$\int_0^\pi d^j_{\lambda\overline{\lambda}}(\theta) d^{j'}_{\lambda\overline{\lambda}}(\theta) \sin\theta d\theta = \frac{2\delta_{jj'}}{(2j+1)}, \tag{A.45}$$

$$\int d\Omega_l D^J_{M\lambda_2} D^{*J'}_{M'\lambda_2} = \int d\Omega_l e^{-i\phi_l(M-M')} d^J_{M\lambda_2} d^{J'}_{M'\lambda_2} = \frac{4\pi}{2J+1} \delta_{JJ'}\delta_{MM'}. \tag{A.46}$$

The Wigner functions are also needed in writing down the connection between angular momentum states and linear momentum states

$$|J, M, \lambda\rangle = \frac{2J+1}{4\pi} \int d\phi d\cos\theta |\theta, \phi, \lambda\rangle D^J(\phi, \theta, 0)_{M\lambda}. \tag{A.47}$$

The *d*-functions satisfy a number of symmetry relation, as for example

$$d^j(\beta)_{m'm} = d^j(\beta)_{-m'-m}(-1)^{m'-m}, \tag{A.48}$$

$$d^j(\beta)_{m'm} = d^j(-\beta)_{mm'}. \tag{A.49}$$

The explicit form of the *d*-functions for $j = 1$ is given by

$$d^1(\beta)_{00} = \cos\beta, \tag{A.50}$$

$$d^1(\beta)_{10} = -\frac{\sin\beta}{\sqrt{2}}, \tag{A.51}$$

$$d^1(\beta)_{11} = \frac{1+\cos\theta}{2}, \tag{A.52}$$

$$d^1(\beta)_{1-1} = \frac{1-\cos\theta}{2}. \tag{A.53}$$

Appendix B.

Orthogonality Relation of the Projectors

In this appendix we want to prove the orthogonality relation for the projectors. In order to do so we have to recall the meaning of the projectors. The task in the beginning was to expand a vertex with a tensor structure into partial waves. That was achieved by expanding the tensor in such a way that when we multiply with a polarisation vector, we get a definite angular momentum state. The relation we want to prove is

$$\int \frac{d^4l}{(2\pi)^4} Y^{JMP}_{\lambda_1\lambda_2\mu\alpha}(\overline{p},l,w) G^{\alpha\beta}(l,w) Y^{J'M'P'}_{\lambda_3\lambda_4\beta\nu}(l,p,w)$$
$$= \delta_{\lambda_2\lambda_3}\delta_{PP'}\delta_{JJ'}\delta_{MM'} Y^{JMP}_{\lambda_1\lambda_4\mu\nu}(\overline{p},p,w)(-I_{\phi V})\,, \tag{B.1}$$

with

$$G^{\mu\nu} = i\frac{g^{\mu\nu} - \frac{l^\mu l^\nu}{M_V^2}}{l^2 - M_V^2 + i\epsilon}\frac{1}{(w-l)^2 - M_\phi^2 + i\epsilon}\,. \tag{B.2}$$

When the particles are on shell, the polarisation vectors obey the following relation

$$-\left(g^{\mu\nu} - \frac{l^\mu l^\nu}{M^2}\right) = \sum_\lambda \epsilon(\lambda,l)^{\mu\dagger}\epsilon^\nu(\lambda,l)\,. \tag{B.3}$$

Since the particles in the loop are off shell, the relation is modified

$$-\left(g^{\mu\nu} - \frac{l^\mu l^\nu}{l^2}\right) = \sum_\lambda \epsilon(\lambda,l)^{\mu\dagger}\epsilon^\nu(\lambda,l)\,, \tag{B.4}$$

where also in the polarisation vectors, one has to substitute of course $M_V^2 \to l^2$. We further know that

$$-\left(g^{\mu\nu} - \frac{l^\mu l^\nu}{M^2}\right) = -\left(g^{\mu\nu} - \frac{l^\mu l^\nu}{l^2}\right) + \frac{l^\mu l^\nu}{l^2 M_V^2}(M_V^2 - l^2)\,. \tag{B.5}$$

Thus, we see that the longitudinal part of the propagator resists to the substitution of the numerator with a sum over the polarisation vectors. It is not surprising that the longitudinal part of the propagator, which can be identified with the unphysical spin zero part, makes trouble in a relation, which was constructed to hold for spin one particles. However, the additional contribution leads to tadpole terms, which we are used to drop, what we will also do in that case. Besides the usual argument, that the tadpole contributions are taken care of by the contact interactions, we have in that case the additional argument, that we do not want to propagate the unphysical spin zero part.

We multiply the projectors from the left with $\epsilon^\dagger_\mu(\overline{p},\lambda)$ and from the right with $\epsilon_\nu(p,\lambda)$. The projectors have the task that if they are multiplied with the respective polarisation vectors,

only the term with the appropriate quantum numbers will survive in the expansion Eq.(5.5). When one multiplies with the wrong polarisation vectors, one gets zero. This tells us immediately the polarisation of the vectors, which we multiply from the left and from the right. In general, after multiplying a projector with the polarisation vectors, we get

$$
\epsilon^{\mu\dagger}(\overline{p},\overline{\lambda})Y^{JMP}_{\lambda_1\lambda_2\mu\nu}(\overline{p},l,w)\epsilon^\nu(l,\lambda) = \delta_{|\overline{\lambda}|\lambda_1}\delta_{\lambda_2|\lambda|}(2J+1)D^{*J}_{M\overline{\lambda}}(\overline{\Omega})D^J_{M\lambda}(\Omega_l)
$$
$$
\cdot\left(\frac{1}{\sqrt{2}}\right)^{\lambda_1+\lambda_2}P^{(\overline{\lambda}-\lambda)/2}. \tag{B.6}
$$

The factors in the second line arise due to the definition of the parity states. In order to understand that factor, we look at an example, namely $Y^{1^+}_{11}$ and $Y^{1^-}_{11}$. When we want to expand the above projectors in helicity states, we know that $\langle 1_+|Y^{1^+}_{11}|1_+\rangle = 1$ and all other matrix elements are zero for $Y^{1^+}_{11}$. For $Y^{1^-}_{11}$ we have that $\langle 1_-|Y^{1^-}_{11}|1_-\rangle = 1$ and all others are zero. Further we know

$$
\langle 1_+|T^J|1_+\rangle = \langle 1|T^J|1\rangle + \langle 1|T^J|-1\rangle \tag{B.7}
$$

and

$$
\langle 1_-|T^J|1_-\rangle = \langle 1|T^J|1\rangle - \langle 1|T^J|-1\rangle . \tag{B.8}
$$

Thus, we get for $Y^{1^+}_{11}$

$$
\langle 1|Y^{1^+}_{11}|1\rangle = \frac{1}{2}, \qquad \langle 1|Y^{1^+}_{11}|-1\rangle = \frac{1}{2} \tag{B.9}
$$

and for $Y^{1^-}_{11}$

$$
\langle 1|Y^{1^-}_{11}|1\rangle = \frac{1}{2}, \qquad \langle 1|Y^{1^-}_{11}|-1\rangle = -\frac{1}{2}. \tag{B.10}
$$

which is reproduced by our definition. One can easily check that the form in Eq.(B.6) covers all possibilities in the correct way.

Now we plug in Eq.(B.6) on the left side of Eq.(B.1) after multiplying with the polarisation vectors, which leads to

$$
\int\frac{d^4l}{(2\pi)^4}\epsilon^{\dagger\mu}(\overline{p},\overline{\lambda})Y^{JMP}_{\lambda_1\lambda_2\mu\alpha}(\overline{p},l,w)G^{\alpha\beta}(l,w)Y^{J'M'P'}_{\lambda_3\lambda_4\beta\nu}(l,p,w)\epsilon^\nu(p,\lambda)
$$
$$
\rightarrow \sum_{\lambda_l}(-i)\int\frac{l^2dldl_0}{(2\pi)^4(l^2-M_V^2+i\epsilon)((w-l)^2-M_\phi^2+i\epsilon)}\int d\Omega_l
$$
$$
\left(\delta_{|\overline{\lambda}|\lambda_1}\delta_{\lambda_2|\lambda_l|}(2J+1)D^{*J}_{M\overline{\lambda}}(\overline{\Omega})D^J_{M\lambda_l}(\Omega_l)\left(\frac{1}{\sqrt{2}}\right)^{\lambda_1+\lambda_2}P^{(\overline{\lambda}-\lambda_l)/2}\right.
$$
$$
\left.\cdot\delta_{\lambda_3|\lambda_l|}\delta_{\lambda_4|\lambda|}(2J'+1)D^{*J'}_{M'\lambda_l}(\Omega_l)D^{J'}_{M'\lambda}(\Omega)\left(\frac{1}{\sqrt{2}}\right)^{\lambda_3+\lambda_4}P'^{(\lambda_l-\lambda)/2}\right)
$$
$$
= (-i)\delta_{|\overline{\lambda}|\lambda_1}\delta_{|\lambda|\lambda_4}\delta_{\lambda_2\lambda_3}(2J+1)(2J'+1)D^{*J}_{M\overline{\lambda}}(\overline{\Omega})D^{J'}_{M'\lambda}(\Omega)\int\frac{l^2dldl_0}{(2\pi)^4(...)(...)}\left(\frac{1}{\sqrt{2}}\right)^{\lambda_1+2\lambda_2+\lambda_4}
$$
$$
\cdot\left(\int d\Omega_l D^{*J}_{M'\lambda_2}(\Omega_l)D^{J'}_{M\lambda_2}(\Omega_l)P^{(\overline{\lambda}-\lambda_2)/2}P'^{(\lambda-\lambda_2)/2}\right.
$$
$$
\left.+\int d\Omega_l D^{*J'}_{M'-\lambda_2}(\Omega_l)D^J_{M-\lambda_2}(\Omega_l)P^{(\overline{\lambda}+\lambda_2)/2}P'^{(\lambda+\lambda_2)/2}\right)\left(\frac{1}{2}\right)^{1-\lambda_2}
$$
$$
= (-i)\delta_{|\overline{\lambda}|\lambda_1}\delta_{\lambda_4|\lambda|}\delta_{\lambda_2\lambda_3}(2J+1)D^{*J}_{M\overline{\lambda}}(\overline{\Omega})D^J_{M\lambda}(\Omega)\delta_{JJ'}\delta_{MM'}\left(\frac{1}{\sqrt{2}}\right)^{\lambda_1+\lambda_4}\frac{C_P}{2}\int\frac{4\pi l^2dldl_0}{(2\pi)^4(...)(...)},
$$

where abbreviated the factors arising from the parity terms with C_P, which is given by

$$C_P = P^{(\overline{\lambda}+\lambda_2)/2} P'^{(\lambda+\lambda_2)/2} + P^{(\overline{\lambda}-\lambda_2)/2} P'^{(\lambda-\lambda_2)/2}.$$

Next we will have a closer look at that factor and bring it into a simple form. In order to so, we look at the different possibilities for P and P' separately

- $P = P' = 1$

$$C_P = 2$$

- $P = P' = -1$
  In that case we know that $\lambda_2 = 1 = |\lambda| = |\overline{\lambda}|$ and we get the following possible values for C_P

$\overline{\lambda}$	λ	C_P
1	1	2
-1	-1	2
1	-1	-2
-1	1	-2

- $P = -P' = 1$
  In that case $\lambda_2 = 1 = |\lambda|$ and we see that $\overline{\lambda}$ has no influence on C_P and

$$C_P = 0$$

- $P = -P' = -1$
  In that case $\lambda_2 = 1 = |\overline{\lambda}|$ and λ has no influence and again

$$C_P = 0$$

Putting everything together, we have

$$C_P = 2\delta_{PP'} P^{(\lambda-\overline{\lambda})/2}. \tag{B.11}$$

Thus, we arrive at

$$\int \frac{d^4 l}{(2\pi)^4} \epsilon^{\dagger\mu}(\overline{p}, \overline{\lambda}) Y_{\lambda_1 \lambda_2 \mu\alpha}^{JMP}(\overline{p}, l, w) G^{\alpha\beta}(l, w) Y_{\lambda_2 \lambda_3 \beta\nu}^{J'M'P'}(l, p, w) \epsilon^{\nu}(p, \lambda)$$

$$= (-i)\delta_{|\overline{\lambda}|\lambda_1} \delta_{\lambda_4|\lambda|} \delta_{\lambda_2\lambda_3} (2J+1) D_{M\overline{\lambda}}^{*J}(\overline{\Omega}) D_{M'\lambda}^{J}(\Omega) \delta_{JJ'} \delta_{MM'} \left(\frac{1}{\sqrt{2}}\right)^{\lambda_1+\lambda_4} \delta_{PP'} P^{(\lambda-\overline{\lambda})/2}$$

$$\int \frac{4\pi l^2 dl dl_0}{(2\pi)^4 (...)(...)}$$

$$= \delta_{\lambda_2\lambda_3} \delta_{PP'} \delta_{JJ'} \delta_{MM'} \epsilon^{\dagger\mu}(\overline{p}, \overline{\lambda}) Y_{\lambda_1\lambda_4\mu\nu}^{JMP}(\overline{p}, p, s) \epsilon^{\nu}(p, \lambda)(-I_{\phi V}),$$

which proves Eq.(B.1).

B.1. Application to the a_1 loop integral

We will use the orthogonality relation in order to simplify the expression in Eq.(6.63), which was given by

$$
\begin{aligned}
W'^{\phi V}_\mu = &\Bigg[-c_{\phi V} \frac{gV_{ud}}{2\sqrt{2}F_0} \int \frac{d^4 l}{(2\pi)^4} \bigg(f_V(w \cdot l g^{\mu\alpha} - l^\mu w^\alpha) \\
&- 2g_V((w-l)\cdot l g^{\mu\alpha} - l^\mu(w-l)^\alpha - \frac{w^\mu w^\alpha}{s} l(w-l) + (w-l)^\alpha w^\mu \frac{lw}{s}) \bigg) G^{\phi V}_{\alpha\beta}(l) T^{\gamma\beta}_{\phi V}(l) \\
&- c_{\phi V} \frac{gV_{ud}}{2\sqrt{2}F_0} 2g_V \frac{m_\pi^2}{s-m_\pi^2} \frac{w^\mu}{s} \int \frac{d^4 l}{(2\pi)^4} (l(w-l)w^\alpha - lw(w-l)^\alpha) G^{\phi V}_{\alpha\beta}(l) T^{\gamma\beta}_{\phi V}(l) \Bigg] \\
&\cdot \frac{ig_V}{F_0^2} \frac{m_{12}^2}{m_{12}^2 - M_\rho^2 - \Pi} (q_1 - q_2)_\gamma \quad + \quad (q_1 \leftrightarrow q_3) \, .
\end{aligned}
$$

First, we have a look at the last integral. This corresponds to an integral between a scalar or spin 0 component and a vector component and should be zero by angular momentum conservation. In particular, we should not get a $J = 1$ component when we expand the term left to the propagator into projectors. That can indeed be easily seen

$$
l(w-l)w^\mu w^\alpha - lw(w-l)^\alpha w^\mu \longrightarrow \overline{pq}w^\mu w^\alpha - (w\overline{p})w^\mu \overline{q}^\alpha \longrightarrow \overline{pq}w^\mu w^\alpha - (w\overline{p})w^\mu \overline{w}^\alpha \, .
$$

Since we know that terms not proportional to x in F_2 do not contribute to the $J = 1$ part, we get no $J = 1$ contribution and due to the orthogonality relation that integral vanishes.

So we are left with

$$
\begin{aligned}
W'^{\phi V}_\mu = &-c_{\phi V} \frac{gV_{ud}}{2\sqrt{2}F_0} \int \frac{d^4 l}{(2\pi)^4} \bigg(f_V(w \cdot l g^{\mu\alpha} - l^\mu w^\alpha) \\
&- 2g_V \bigg((w-l)\cdot l g^{\mu\alpha} - l^\mu(w-l)^\alpha - \frac{w^\mu w^\alpha}{s} l(w-l) + (w-l)^\alpha w^\mu \frac{lw}{s} \bigg) \bigg) G^{\phi V}_{\alpha\beta}(l) T^{\gamma\beta}_{\phi V}(l) \\
&\cdot \frac{ig_V}{F_0^2} \frac{m_{12}^2}{m_{12}^2 - M_\rho^2 - \Pi} (q_1 - q_2)_\gamma \quad + \quad (q_1 \leftrightarrow q_3) \\
= &-c_{\phi V} \frac{igV_{ud}g_V}{2\sqrt{2}F_0^3} \int \frac{d^4 l}{(2\pi)^4} \bigg((f_V - 2g_V)(w \cdot l g^{\mu\alpha} - l^\mu w^\alpha) \\
&+ 2g_V \bigg(l^2 g^{\mu\alpha} - l^\mu l^\alpha - \frac{w^\mu w^\alpha}{s} l^2 + l^\alpha w^\mu \frac{lw}{s} \bigg) \bigg) G^{\phi V}_{\alpha\beta}(l) T^{\gamma\beta}_{\phi V}(l) \\
&\frac{m_{12}^2}{m_{12}^2 - M_\rho^2 - \Pi} (q_1 - q_2)_\gamma \quad + \quad (q_1 \leftrightarrow q_3) \, .
\end{aligned}
\tag{B.12}
$$

We note that due to our renormalisation scheme, terms proportional to $l^\alpha G_{\alpha\beta}$ vanish. The remaining terms are expanded into projectors

$$
l^2 g^{\mu\alpha} - \frac{w^\mu w^\alpha}{s} l^2 \longrightarrow -\frac{2}{3} M_V^2 Y_{11}^{\alpha\mu} - \frac{2}{3} M_V^2 \frac{\omega_{\phi V}}{\sqrt{2}M_V} Y_{01}^{\alpha\mu} - \frac{2}{3} M_V^2 \frac{\omega_a}{\sqrt{2}M_{Va}} Y_{10}^{\alpha\mu} - \frac{M_V^2 \omega_a \omega_{\phi V}}{3M_{Va}M_V} Y_{00}^{\alpha\mu} \, .
$$

M_V and M_ϕ are the masses of the particles in the loop corresponding to the outgoing channel in the expansion. The masses for the incoming channel (labeled with a) are artificially put

in to ease calculations, but the result should of course be independent of these masses. The second term, which we have to expand into projectors is

$$(w \cdot l g^{\mu\alpha} - l^{\mu}w^{\alpha}) = (w \cdot l g^{\mu\alpha} + (w - l)^{\mu}w^{\alpha}) - w^{\mu}w^{\alpha} = L_3^{\alpha\mu} + w \cdot l L_1^{\alpha\mu} + F_2 L_2^{\alpha\mu} \, .$$

Since there is no term proportional to x in F_2, it will not contribute to the spin 1 part. Thus, we can write

$$(w \cdot l g^{\mu\alpha} - l^{\mu}w^{\alpha}) = L_3^{\alpha\mu} + w \cdot l L_1^{\alpha\mu} + F_2 L_2^{\alpha\mu} \longrightarrow L_3^{\alpha\mu} + \sqrt{s}\omega_{\phi V} L_1^{\alpha\mu}$$

$$\longrightarrow -\frac{2}{3}\sqrt{s}\omega_{\phi V} Y_{11}^{\alpha\mu} - \frac{2}{3}\left(\frac{\omega_{\phi V}^2 \sqrt{s}}{\sqrt{2}M_V} - \frac{\sqrt{s}p_{\phi V}^2}{\sqrt{2}M_V}\right) Y_{01}^{\alpha\mu}$$

$$-\frac{2}{3}\sqrt{s}\omega_{\phi V}\frac{\omega_a}{\sqrt{2}M_{Va}} Y_{10}^{\alpha\mu} - \frac{2}{3}\frac{\omega_a}{\sqrt{2}M_{Va}}\left(\frac{\omega_{\phi V}^2 \sqrt{s}}{\sqrt{2}M_V} - \frac{\sqrt{s}p_{\phi V}^2}{\sqrt{2}M_V}\right) Y_{00}^{\alpha\mu}$$

$$\longrightarrow -\frac{2}{3}\sqrt{s}\omega_{\phi V} Y_{11}^{\alpha\mu} - \frac{2}{3}\frac{\sqrt{s}M_V}{\sqrt{2}} Y_{01}^{\alpha\mu} - \frac{2}{3}\sqrt{s}\omega_{\phi V}\frac{\omega_a}{\sqrt{2}M_{Va}} Y_{10}^{\alpha\mu} - \frac{2}{3}\frac{\omega_a}{\sqrt{2}M_{Va}}\frac{\sqrt{s}M_V}{\sqrt{2}} Y_{00}^{\alpha\mu} \, .$$

Using the first expansion and the orthogonality relation, we evaluate the part proportional to g_V. We will suppress the indices indicating the channel on the expansion coefficients, since it is always the same and write M_{ij} instead of $M_{1\phi Vij}$. Thus, we get

$$2g_V \int \frac{d^4l}{(2\pi)^4} T_{\phi V}^{\gamma\beta}(l) G_{\alpha\beta}^{\phi V}(l) l^2 \left(g^{\mu\alpha} - \frac{w^{\mu}w^{\alpha}}{s}\right)$$

$$= -2g_V \frac{1}{3}M_V^2 i I_{\phi V}\left(2M_{11}Y_{11}^{\gamma\mu} + 2M_{01}Y_{01}^{\gamma\mu} + \frac{\sqrt{2}\omega_{\phi V}}{M_V}M_{10}Y_{11}^{\gamma\mu} + \frac{\sqrt{2}\omega_{\phi V}}{M_V}M_{00}Y_{01}^{\gamma\mu}\right.$$

$$\left. + \frac{\sqrt{2}\omega_a}{M_{Va}}M_{11}Y_{10}^{\gamma\mu} + \frac{\sqrt{2}\omega_a}{M_{Va}}M_{01}Y_{00}^{\gamma\mu} + \frac{\omega_a\omega_{\phi V}}{M_{Va}M_V}M_{10}Y_{10}^{\gamma\mu} + \frac{\omega_a\omega_{\phi V}}{M_{Va}M_V}M_{00}Y_{00}^{\gamma\mu}\right)$$

$$= -\frac{2g_V M_V^2 i I_{\phi V}}{3}\left(Y_{11}^{\gamma\mu}\left(2M_{11} + \frac{\sqrt{2}\omega_{\phi V}}{M_V}M_{10}\right) + Y_{10}^{\gamma\mu}\frac{\omega_a}{\sqrt{2}M_{Va}}\left(2M_{11} + \frac{\sqrt{2}\omega_{\phi V}}{M_V}M_{10}\right)\right.$$

$$\left. + Y_{01}^{\gamma\mu}\left(2M_{01} + \frac{\sqrt{2}\omega_{\phi V}}{M_V}M_{00}\right) + Y_{00}^{\gamma\mu}\frac{\omega_a}{\sqrt{2}M_{Va}}\left(2M_{01} + \frac{\sqrt{2}\omega_{\phi V}}{M_V}M_{00}\right)\right)$$

$$= -\frac{2g_V i I_{\phi V}}{3}\left(\alpha_1^{\phi V} Y_{11}^{\gamma\mu} + \alpha_1^{\phi V}\frac{\omega_a}{\sqrt{2}M_{Va}}Y_{10}^{\gamma\mu} + \alpha_1'^{\phi V} Y_{01} + \alpha_1'^{\phi V}\frac{\omega_a}{\sqrt{2}M_{Va}}Y_{00}\right)$$

with

$$\alpha_1^{\phi V} = 2M_V^2 M_{11} + \sqrt{2}\omega_{\phi V} M_V M_{10} \quad \text{and} \quad \alpha_1'^{\phi V} = 2M_V^2 M_{01} + \sqrt{2}\omega_{\phi V} M_V M_{00} \qquad \text{(B.13)}$$

So far we did not use an explicit representation for the projectors, which means we have not chosen a coordinate system, and we still need to show that the dependence on the incoming masses cancel out. Since we sum over the polarisation of the W bosons, there is no preferred direction and we are free to put the fictitious and the outgoing particles on the z-axis to ease calculations. We can also choose to use the projectors, we already have and we should see that the result is the same (which is easily seen by putting $x = 0$ in the projectors). No matter

which choice we make, the result is

$$
= -\frac{2g_V i I_{\phi V}}{3}\left(\alpha_1^{\phi V}Y_{11}^{\gamma\mu} + \alpha_1^{\phi V}\frac{\omega_a}{\sqrt{2}M_{Va}}Y_{10}^{\gamma\mu} + \alpha_1'^{\phi V}Y_{01} + \alpha_1'^{\phi V}\frac{\omega_a}{\sqrt{2}M_{Va}}Y_{00}\right)
$$

$$
= g_V i I_{\phi V}\left(\alpha_1^{\phi V}L_1^{\gamma\mu} + L_2^{\gamma\mu}x\left(-\frac{\omega_a\omega_{\pi\rho}}{p_ap_{\pi\rho}s}\alpha_1^{\phi V} + \alpha_1^{\phi V}\frac{\omega_a M_{Va}\omega_{\pi\rho}}{p_ap_{\pi\rho}sM_{Va}}\right.\right.
$$

$$
\left.+ \alpha_1'^{\phi V}\frac{2M_\rho\omega_a}{\sqrt{2}p_ap_{\pi\rho}s} - \alpha_1'^{\phi V}\frac{2M_{Va}M_\rho\omega_a}{p_ap_{\pi\rho}s\sqrt{2}M_{Va}}\right)
$$

$$
\left.+ L_3^{\gamma\mu}\left(\alpha_1^{\phi V}\frac{\omega_{\pi\rho}}{p_{\pi\rho}^2\sqrt{s}} - \alpha_1'^{\phi V}\frac{2M_\rho}{\sqrt{2}\sqrt{s}p_{\pi\rho}^2}\right) + L_4^{\gamma\mu}\alpha_1^{\phi V}\left(\frac{\omega_a}{p_a^2\sqrt{s}} - \frac{2\omega_a}{\sqrt{2}M_{Va}}\frac{M_{Va}}{\sqrt{2}\sqrt{s}p_a^2}\right)\right)
$$

$$
= g_V i I_{\phi V}(\alpha_1^{\phi V}L_1^{\gamma\mu} + \alpha_3^{\phi V}L_3^{\gamma\mu})
$$

with

$$
\alpha_3^{\phi V} = \alpha_1^{\phi V}\frac{\omega_{\pi\rho}}{p_{\pi\rho}^2\sqrt{s}} - \alpha_1'^{\phi V}\frac{\sqrt{2}M_\rho}{p_{\pi\rho}^2\sqrt{s}}\,. \tag{B.14}
$$

As expected the result does not depend on the masses of the incoming channel.

Next we calculate the part in Eq.(B.12) proportional to $(f_V - 2g_V)$

$$
(f_V - 2g_V)\int\frac{d^4l}{(2\pi)^4}T_{\phi V}^{\gamma\beta}G_{\alpha\beta}^{\phi V}(l)(l)(w\cdot lg^{\mu\alpha} - l^\mu w^\alpha)
$$

$$
= -\frac{2}{3}(f_V - 2g_V)iI_{\phi V}\left(\omega_{\phi V}\sqrt{s}M_{11}Y_{11}^{\gamma\mu} + \omega_{\phi V}\sqrt{s}M_{01}Y_{01}^{\gamma\mu}\right.
$$

$$
+ \frac{M_V\sqrt{s}}{\sqrt{2}}M_{10}Y_{11}^{\gamma\mu} + \frac{M_V\sqrt{s}}{\sqrt{2}}M_{00}Y_{01}^{\gamma\mu} + \frac{\omega_a}{\sqrt{2}M_{Va}}\omega_{\phi V}\sqrt{s}M_{11}Y_{10}^{\gamma\mu} + \frac{\omega_a}{\sqrt{2}M_{Va}}\omega_{\phi V}\sqrt{s}M_{01}Y_{00}^{\gamma\mu}
$$

$$
\left.+ \frac{\omega_a}{\sqrt{2}M_{Va}}\frac{M_V\sqrt{s}}{\sqrt{2}}M_{10}Y_{10}^{\gamma\mu} + \frac{\omega_a}{\sqrt{2}M_{Va}}\frac{M_V\sqrt{s}}{\sqrt{2}}M_{00}Y_{00}^{\gamma\mu}\right)
$$

$$
= -\frac{1}{3}(f_V - 2g_V)iI_{\phi V}\left(\alpha_2^{\phi V}Y_{11}^{\gamma\mu} + \alpha_2^{\phi V}\frac{\omega_a}{\sqrt{2}M_{Va}}Y_{10}^{\gamma\mu} + \alpha_2'^{\phi V}Y_{01} + \alpha_2'^{\phi V}\frac{\omega_a}{\sqrt{2}M_{Va}}Y_{00}\right)
$$

$$
= \frac{1}{2}(f_V - 2g_V)iI_{\phi V}(\alpha_2^{\phi V}L_1^{\gamma\mu} + \alpha_4^{\phi V}L_3^{\gamma\mu})
$$

with

$$
\alpha_2^{\phi V} = 2\omega_{\phi V}\sqrt{s}M_{11} + \frac{2M_V\sqrt{s}}{\sqrt{2}}M_{10}\,, \quad \alpha_2'^{\phi V} = 2\omega_{\phi V}\sqrt{s}M_{01} + \frac{2M_V\sqrt{s}}{\sqrt{2}}M_{00} \tag{B.15}
$$

and

$$
\alpha_4^{\phi V} = \alpha_2^{\phi V}\frac{\omega_{\pi\rho}}{p_{\pi\rho}^2\sqrt{s}} - \alpha_2'^{\phi V}\frac{\sqrt{2}M_\rho}{p_{\pi\rho}^2\sqrt{s}}\,. \tag{B.16}
$$

Altogether we have

$$
W_{\phi V}'^\mu = \frac{c_{\phi V}gV_{ud}g_V}{2\sqrt{2}F_0^3}I_{\phi V}\left(g_V(\alpha_1^{\phi V}L_1^{\gamma\mu} + \alpha_3^{\phi V}L_3^{\gamma\mu})\frac{m_{12}^2}{m_{12}^2 - M_\rho^2 - \Pi}(q_1 - q_2)_\gamma\right.
$$

$$
\left.+ \frac{1}{2}(f_V - 2g_V)(\alpha_2^{\phi V}L_1^{\gamma\mu} + \alpha_4^{\phi V}L_3^{\gamma\mu})\frac{m_{12}^2}{m_{12}^2 - M_\rho^2 - \Pi}(q_1 - q_2)_\gamma\right) \quad + \quad (q_1 \leftrightarrow q_3)\,.
$$

The expression is again rendered finite by substituting $I_{\phi V} \to J_{\phi V}(\mu_2)$.

Appendix C.

Construction of the Higher Order Lagrangian

We want to construct all terms with two Goldstone boson momenta contributing to the scattering of a Goldstone boson off a vector meson. Since the derivatives on the vector mesons do not count as small, there could be an arbitrary number of them. But as one can imagine, if there are too many derivatives on the vector mesons, they just contract with themselves and lead to factors of M_V^2 by employing the equations of motion. In order to write down this statement more rigorously, we first note that we can only have an even number of derivatives, if we want to construct a Lorentz scalar and want to have only two derivatives on the pseudoscalar mesons. In case the derivatives of the vector mesons have the same index as one of the vector mesons, we can always partially integrate, to put that derivative on the respective vector meson and use $\partial_\mu V^\mu = 0$, e.g.,

$$\partial_\mu V^\nu \partial_\alpha V^\mu u_\nu u^\alpha \rightarrow -V^\nu \partial_\alpha \underbrace{\partial_\mu V^\mu}_{=0} u_\nu u^\alpha - V^\nu \partial_\alpha V^\mu \underbrace{\partial_\mu (u_\nu u^\alpha)}_{\mathcal{O}(q^3)} = \mathcal{O}(q^3) \,. \tag{C.1}$$

Thus, we can contract the derivatives on the vector mesons only with themselves or with the derivatives on the Goldstone bosons. When we contract the derivatives with themselves, we can use the equations of motion to replace $\partial^2 V_\mu = M_V^2 V_\mu$, which leads to a term which has the same structure as a term without the two additional derivatives. Altogether this means, we can have at most two derivatives on the vector mesons, since there are only two derivatives on the Goldstone bosons.

The building blocks of interest and the corresponding transformations under parity and charge conjugation are given in Tab. C.1. We introduced two new quantities which are potentially interesting for the Lagrangian we want to construct

$$u_{\mu\nu} = i u^\dagger D_\mu D_\nu U u^\dagger \tag{C.2}$$

and

$$\chi_+ = u^\dagger \chi u^\dagger + u \chi^\dagger u \,. \tag{C.3}$$

	P	C
V_μ	V^μ	$-V_\mu^T$
u_μ	$-u^\mu$	u_μ^T
$u_{\mu\nu}$	$-u^{\mu\nu\dagger}$	$u_{\mu\nu}^T$
χ_+	χ_+	χ_+^T

Table C.1.: Transformation properties of the building blocks.

The remaining expressions have been defined already in Chapter 2 and Chapter 3. (See also [EGPdR89] for a detailed discussion.) Instead of $u_{\mu\nu}$ one could also use $\nabla_\mu u_\nu$, which are related by

$$\nabla_\mu u_\nu = u_{\mu\nu} + \frac{i}{2}(u_\mu u_\nu + u_\nu u_\mu).\qquad\text{(C.4)}$$

First of all, we recognise that it is not possible to build a parity invariant term contributing to our process by using $\nabla_\mu u_\nu$ or $u_{\mu\nu}$ with only two derivatives. Secondly, we omit terms containing χ_+, because the pion masses compared to the momenta are negligible from a practical point of view and the strangeness terms do not play an important role at all. Thus, we are left with finding all possibilities to build terms out of two u_μ and either two vector fields or two field strength tensors of the vector fields. There are two ways to contract two vector fields with two u_μ and the following possibilities to order them and to take the trace

1. $V_\mu V^\mu u_\nu u^\nu$

   - $\text{Tr}[V_\mu V^\mu u_\nu u^\nu]$
   - $\text{Tr}[V_\mu u_\nu V^\mu u^\nu]$
   - $\text{Tr}[V_\mu V^\mu]\,\text{Tr}[u_\nu u^\nu]$
   - $\text{Tr}[V_\mu u_\nu]\,\text{Tr}[V^\mu u^\nu]$

2. $V_\mu V_\nu u^\mu u^\nu$

   - $\text{Tr}[V_\mu V_\nu u^\mu u^\nu]$
   - $\text{Tr}[V_\mu V_\nu u^\nu u^\mu]$
   - $\text{Tr}[V_\mu u^\mu V_\nu u^\nu]$
   - $\text{Tr}[V_\mu u^\nu V_\nu u^\mu]$
   - $\text{Tr}[V_\mu V_\nu]\,\text{Tr}[u^\mu u^\nu]$
   - $\text{Tr}[V_\mu u_\nu]\,\text{Tr}[V^\nu u^\mu]$
   - $\text{Tr}[V_\mu u^\mu]\,\text{Tr}[V^\nu u_\nu].$

All terms are invariant under parity, but the following terms are not invariant under charge conjugation

$$\text{Tr}[V_\mu u^\mu V_\nu u^\nu]\xrightarrow{C}\text{Tr}[V_\mu^T u^{\mu T}V_\nu^T u^{\nu T}]=\text{Tr}[u^\nu V_\nu u^\mu V_\mu]=\text{Tr}[V_\mu u^\nu V_\nu u^\mu]\qquad\text{(C.5)}$$

and

$$\text{Tr}[V_\mu u^\nu V_\nu u^\mu]\xrightarrow{C}\text{Tr}[V_\mu^T u^{\nu T}V_\nu^T u^{\mu T}]=\text{Tr}[u^\mu V_\nu u^\nu V_\mu]=\text{Tr}[V_\mu u^\mu V_\nu u^\nu].\qquad\text{(C.6)}$$

Thus, we see that only the sum of both terms is invariant under charge conjugation, which eliminates one independent structure. Using the trace relations Eq.(A.20) and Eq.(A.21), we can eliminate two more terms. The terms containing the field strength tensors are treated completely analogously, and we end up with the following Lagrangian

$$\begin{aligned}
\mathcal{L}_{ho} =\ & \lambda_1'\,\text{Tr}[V_\mu V^\mu u_\nu u^\nu] + \lambda_2'\,\text{Tr}[V_\mu u_\nu V^\mu u^\nu]\\
& + \lambda_3'\,\text{Tr}[V_\mu V_\nu u^\mu u^\nu] + \lambda_4'\,\text{Tr}[V_\mu V^\nu u_\nu u^\mu] + \lambda_5'\,\text{Tr}[V_\mu u^\mu V_\nu u^\nu + V_\mu u^\nu V_\nu u^\mu]\\
& + \lambda_6'\,\text{Tr}[V_{\mu\nu} V^{\nu\alpha} u_\alpha u^\mu] + \lambda_7'\,\text{Tr}[V_{\mu\nu} V^{\nu\alpha} u^\mu u_\alpha] + \lambda_8'\,\text{Tr}[V_{\mu\nu} u_\alpha V^{\nu\alpha} u^\mu + V_{\mu\nu} u^\mu V^{\nu\alpha} u_\alpha]\\
& + \lambda_9'\,\text{Tr}[V_\mu u^\nu]\,\text{Tr}[V^\mu u_\nu] + \lambda_{10}'\,\text{Tr}[V_\mu u^\mu]\,\text{Tr}[V_\nu u^\nu] + \lambda_{11}'\,\text{Tr}[V_\mu u_\nu]\,\text{Tr}[V^\nu u^\mu]\\
& + \lambda_{12}'\,\text{Tr}[V_{\mu\alpha} u^\mu]\,\text{Tr}[V_\nu^\alpha u^\nu] + \lambda_{13}'\,\text{Tr}[V_{\mu\alpha} u_\nu]\,\text{Tr}[V^{\nu\alpha} u^\mu].
\end{aligned}$$

This Lagrangian might still be over complete, but at least no term is missing. (Concerning completeness see also [EFS02] and [FMMS00].)
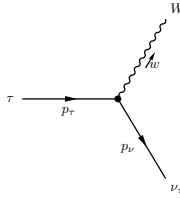
Appendix D.

Vertices

Here, we gather all vertices, which have been used in the calculations, together with the Feynman rules and the Lagrangian from which they result.
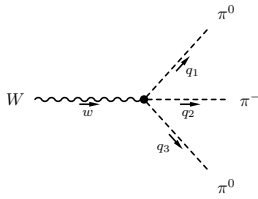
- $\tau^- \to \nu_\tau W^-$

$$\mathcal{L}_W = \frac{g}{\sqrt{2}}(W_\mu^+ \bar{\nu}_L \gamma^\mu \tau_L) \text{ with } g = \sqrt{\frac{8M_W^2 G_F}{\sqrt{2}}}$$

$$= i\sqrt{\frac{G_F M_W^2}{\sqrt{2}}}\gamma^\mu(1 - \gamma_5)$$

- $W^- \to \pi^-\pi^0\pi^0$

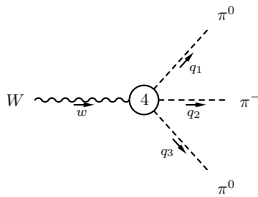$$\mathcal{L} = \frac{F_0^2}{4}\operatorname{Tr}[D_\mu U (D^\mu U)^\dagger]$$

$$= \frac{gV_{ud}}{3F_0}(q_1 + q_3 - 2q_2)^\mu$$

and the higher order contribution

$$\mathcal{L} = -\frac{if_V g_V}{4}\operatorname{Tr}[f_+^{\mu\nu}[u_\mu, u_\nu]] + \frac{g_V^2}{8}\operatorname{Tr}[[u^\mu, u^\nu][u_\mu, u_\nu]]$$
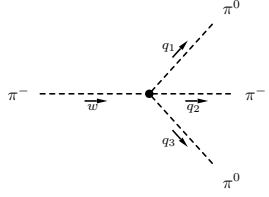

$$= -\frac{f_V g_V g V_{ud}}{F_0^3}(q_2^\mu(w \cdot q_1) + q_2^\mu(w \cdot q_3) - (q_1 + q_3)^\mu(w \cdot q_2))$$

$$+ \frac{2g_V^2 g V_{ud}}{F_0^3}(2q_2^\mu(q_3 \cdot q_1) - q_1^\mu(q_2 \cdot q_3) - q_3^\mu(q_1 \cdot q_2))$$
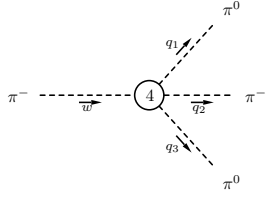
- $\pi^- \rightarrow \pi^- \pi^0 \pi^0$

$$\mathcal{L} = \frac{F_0^2}{4} \, \text{Tr}[D_\mu U (D^\mu U)^\dagger] + \frac{F_0^2}{4} \, \text{Tr}[\chi U^\dagger + U \chi^\dagger]$$

$$= \frac{i}{6 F_0^2} \left(4w(q_1 + q_3 - 2q_2) + 2m_\pi^2 \right)$$

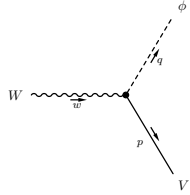and the higher order contribution

$$\mathcal{L} = \frac{i g_V^2}{8} \, \text{Tr}[[u^\mu, u^\nu][u_\mu, u_\nu]]$$

$$= \frac{4 i g_V^2}{F_0^4} \left(2(w \cdot q_2)(q_3 \cdot q_1) - (w \cdot q_1)(q_2 \cdot q_3) - (w \cdot q_3)(q_1 \cdot q_2) \right)$$

- $W_\mu^- \rightarrow (V_\nu^- \phi^0 - V_\nu^0 \phi^-)$

$$\mathcal{L} = -\frac{f_V}{4} \, \text{Tr}[V_{\mu\nu} f_+^{\mu\nu}] - \frac{i g_V}{4} \, \text{Tr}[V^{\mu\nu}[u_\mu, u_\nu]]$$
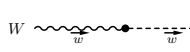
$$= \frac{g V_{ud} c_{\phi V}}{2 \sqrt{2} F_0} \left(f_V (w \cdot p g_{\mu\nu} - p^\mu w^\nu) - g_V (2 q \cdot p g_{\mu\nu} - 2 p^\mu q^\nu) \right)$$

with $c_{\pi\rho} = \sqrt{2}$ and $c_{KK^*} = -1$

- $W^- \rightarrow \pi^-$

$$\mathcal{L} = \frac{F_0^2}{4} \, \text{Tr}[D_\mu U (D^\mu U)^\dagger]$$

$$= \frac{F_0 g V_{ud}}{2} w^\mu$$

- $\rho^- \rightarrow \pi^- \pi^0$

$$\mathcal{L} = -\frac{i g_V}{4} \, \text{Tr}[V^{\mu\nu}[u_\mu, u_\nu]]$$

$$= -\frac{i g_V}{F_0^2} p^2 (q_1 - q_2)^\mu$$

124

- $\pi^- \to (V_\nu^- \phi^0 - V_\nu^0 \phi^-)$

$$\mathcal{L} = -\tfrac{ig_V}{4}\,\mathrm{Tr}[V^{\mu\nu}[u_\mu, u_\nu]]$$

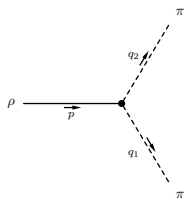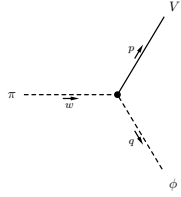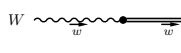$$= -\frac{i\sqrt{2}g_V c_{\phi V}}{F_0^2}\big((q\cdot p)w^\mu - (w\cdot p)q^\mu\big)$$

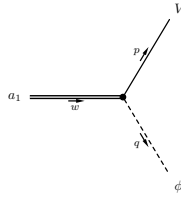with $c_{\pi\rho} = \sqrt{2}$ and $c_{KK^*} = -1$

- $W^- \to a_1^-$

$$\mathcal{L} = -\tfrac{f_A}{4}\,\mathrm{Tr}[A_{\mu\nu} f_-^{\mu\nu}]$$

 $\quad = \frac{if_A g V_{ud}}{2} w^2 \left(g^{\mu\nu} - \frac{w^\mu w^\nu}{w^2}\right)$

- $a_{1\mu}^- \to (V_\nu^- \phi^0 - V_\nu^0 \phi^-)$

$$\mathcal{L} = ic_1\,\mathrm{Tr}[V_{\mu\nu}[A^\mu, u^\nu]] + ic_2\,\mathrm{Tr}[A^{\mu\nu}[V_\mu, u_\nu]]$$

$$= -\frac{2\sqrt{2}c_{\phi V}}{F_0}c_1(q^\nu p^\mu - p\cdot q g^{\mu\nu}) - \frac{2\sqrt{2}c_{\phi V}}{F_0}c_2(w^\nu q^\mu - w\cdot q g^{\mu\nu})$$

with $c_{\pi\rho} = \sqrt{2}$ and $c_{KK^*} = -1$

The corresponding vertex for the decay of a positively charged a_1 one gets by multiplying the above vertex with -1, i.e.

$$a_{1\mu}^+ \to (V_\nu^+ \phi^0 - V_\nu^0 \phi^+)\ :\ \frac{2\sqrt{2}c_{\phi V}}{F_0}c_1(q^\nu p^\mu - p\cdot q g^{\mu\nu}) + \frac{2\sqrt{2}c_{\phi V}}{F_0}c_2(w^\nu q^\mu - w\cdot q g^{\mu\nu})$$

D.1. Weinberg-Tomozawa term

The general form of the amplitude for the scattering of a pion off a target with isospin has been written down in [Wei66, Tom66] by just invoking chiral symmetry without applying Lagrangian field theory. Thus, that term cannot be a relict of a certain representation and it should be present in any field theoretical formulation.

In the vector field Lagrangian the Weinberg-Tomozawa term can be found in the kinetic term

of the Lagrangian

$$-\frac{1}{8}\text{Tr}[V_{\mu\nu}V^{\mu\nu}] = -\frac{1}{8}\text{Tr}[(\nabla_\mu V_\nu - \nabla_\nu V_\mu)(\nabla^\mu V^\nu - \nabla^\nu V^\mu)]$$

$$\rightarrow -\frac{1}{4}\text{Tr}[\partial_\mu V_\nu[\Gamma^\mu, V^\nu] + [\Gamma_\mu, V_\nu]\partial^\mu V^\nu - \partial_\mu V_\nu[\Gamma^\nu, V^\mu] - [\Gamma_\mu, V_\nu]\partial^\nu V^\mu] \quad \text{(D.1)}$$

$$= -\frac{1}{2}\text{Tr}[[V^\nu, \partial_\mu V_\nu]\Gamma^\mu - [V^\mu, \partial_\mu V_\nu]\Gamma^\nu].$$

The second term is higher order because one can partially integrate the Lagrangian density, which leads to a term containing $\partial_\mu V^\mu = 0$ and to a term with two derivatives on the pions, which is higher order.

Keeping only the terms relevant in our case, Γ_ν can be written as

$$\Gamma_\mu \rightarrow \frac{1}{2}(u^\dagger\partial_\mu u + u\partial_\mu u^\dagger) \rightarrow \frac{1}{8F_0^2}[\phi, \partial_\mu\phi], \quad \text{(D.2)}$$

and thus the Lagrangian for the scattering of a Goldstone boson off a vector meson to lowest order is

$$\mathcal{L}_{V\phi\rightarrow V\phi} = -\frac{1}{16F_0^2}\text{Tr}[[V^\nu, \partial_\mu V_\nu][\phi, \partial_\mu\phi]], \quad \text{(D.3)}$$

which is the Weinberg-Tomozawa term (WT term).

Isospin decomposition

In our calculation, we are interested in the $I^G = 1^-$ channel, since these are the quantum numbers of the a_1 and in the following we will project Eq.(D.3) on that channel. ϕ and V_μ can be written as [LK02]

$$\phi = \tau \cdot \pi + \alpha^\dagger \cdot K + K^\dagger \cdot \alpha + \eta\lambda_8 \quad \text{(D.4)}$$

$$V_\mu = \tau \cdot \rho_\mu + \alpha^\dagger \cdot K_\mu + K_\mu^\dagger \cdot \alpha + \left(\frac{2}{3} + \frac{1}{\sqrt{3}}\lambda_8\right)w_\mu + \left(\frac{\sqrt{2}}{3} - \sqrt{\frac{2}{3}}\lambda_8\right)\phi_\mu \quad \text{(D.5)}$$

with $\tau = (\lambda_1, \lambda_2, \lambda_3)$ and $\alpha^\dagger = \frac{1}{\sqrt{2}}(\lambda_4 + i\lambda_5, \lambda_6 + i\lambda_7)$, with the λ_i are the Gell-Mann matrices given in Appendix A. Since ω_μ, ϕ_μ and η do not contribute to the channel we consider in the present work, we can immediately drop these terms.

We will need the following identities

$$\alpha_i^\dagger\tau_j = 0, \quad \tau_i\alpha_j^\dagger = (\alpha^\dagger \cdot \sigma^i)_j \quad \Longrightarrow \quad [\tau_i, \alpha_j^\dagger] = (\alpha^\dagger \cdot \sigma_i)_j, \quad \text{(D.6)}$$

$$\tau_i\alpha_j = 0, \quad \alpha_i\tau_j = (\sigma^j \cdot \alpha)_i \quad \Longrightarrow \quad [\tau_i, \alpha_j] = -(\sigma_i\alpha)_j, \quad \text{(D.7)}$$

$$\alpha_i\alpha_j = 0, \quad \alpha_i^\dagger\alpha_j^\dagger = 0, \quad \alpha_i\alpha_j^\dagger = \left(\frac{2}{3}\mathbb{1} - \frac{2}{\sqrt{3}}\lambda_8\right)\delta_{ij}, \quad \text{(D.8)}$$

$$[\alpha_i, \alpha_j^\dagger] = -(\tau \cdot \sigma - \sqrt{3}\lambda_8 I_2)_{ij}, \quad \tau_i\tau_j = \left(\frac{2}{3}\mathbb{1} + \frac{1}{\sqrt{3}}\lambda_8\right)\delta_{ij} + i\epsilon_{ijk}\tau_k, \quad \text{(D.9)}$$

and traces

$$\text{Tr}[\alpha_i\alpha_j^\dagger] = 2\delta_{ij}, \quad \text{Tr}[\tau_i\tau_j] = 2\delta_{ij}, \quad \text{(D.10)}$$

where

$$\left(\frac{2}{3}\mathbb{1} + \frac{1}{\sqrt{3}}\lambda_8\right) = \begin{pmatrix} 1 & 0 & 0 \\ 0 & 1 & 0 \\ 0 & 0 & 0 \end{pmatrix}, \quad \left(\frac{2}{3}\mathbb{1} - \frac{2}{\sqrt{3}}\lambda_8\right) = \begin{pmatrix} 0 & 0 & 0 \\ 0 & 0 & 0 \\ 0 & 0 & 2 \end{pmatrix}. \quad \text{(D.11)}$$

Keeping only the relevant terms, Eq.(D.3) becomes

$$\text{Tr}([V^\mu, \partial^\nu V_\mu][\phi, \partial_\nu \phi]) \to \text{Tr}([\tau \cdot \rho^\mu, \tau \cdot \partial^\nu \rho_\mu][\tau \cdot \pi, \tau \cdot \partial_\nu \pi])$$
$$+ \text{Tr}([\tau \cdot \rho^\mu, \alpha^\dagger \partial^\nu K_\mu][\tau \cdot \pi, \partial_\nu K^\dagger \cdot \alpha]) + \text{Tr}([\tau \cdot \rho^\mu, \alpha^\dagger \partial^\nu K_\mu][K^\dagger \cdot \alpha, \tau \cdot \partial^\nu \pi])$$
$$+ \text{Tr}([\tau \cdot \rho^\mu, \partial^\nu K_\mu^\dagger \cdot \alpha][\tau \cdot \pi, \alpha^\dagger \cdot \partial_\nu K]) + \text{Tr}([\tau \cdot \rho^\mu, \partial^\nu K_\mu^\dagger \cdot \alpha][\alpha^\dagger \cdot K, \tau \cdot \partial^\nu \pi])$$
$$+ \text{Tr}([\alpha^\dagger K^\mu, \tau \cdot \partial^\nu \rho_\mu][\tau \cdot \pi, \partial_\nu K^\dagger \cdot \alpha]) + \text{Tr}([\alpha^\dagger K^\mu, \tau \cdot \partial^\nu \rho_\mu][K^\dagger \cdot \alpha, \tau \cdot \partial_\nu \pi]) \quad \text{(D.12)}$$
$$+ \text{Tr}([\alpha^\dagger K^\mu, \partial^\nu K_\mu^\dagger \alpha][\alpha^\dagger K, \partial_\nu K^\dagger \alpha]) + \text{Tr}([\alpha^\dagger K^\mu, \partial^\nu K_\mu^\dagger \alpha][K^\dagger \alpha, \alpha^\dagger \partial_\nu K])$$
$$+ \text{Tr}([K^{\mu\dagger}\alpha, \tau \cdot \partial^\nu \rho_\mu][\tau \cdot \pi, \alpha^\dagger \partial_\nu K]) + \text{Tr}([K^{\mu\dagger}\alpha, \tau \cdot \partial^\nu \rho_\mu][\alpha^\dagger K, \tau \cdot \partial_\nu \pi])$$
$$+ \text{Tr}([K^{\mu\dagger}\alpha, \alpha^\dagger \partial^\nu K_\mu][\alpha^\dagger K, \partial_\nu K^\dagger \alpha]) + \text{Tr}([K^{\mu\dagger}\alpha, \alpha^\dagger \partial^\nu K_\mu][K^\dagger \alpha, \alpha^\dagger \partial_\nu K]).$$

We recognise that there are only 3 different traces left, which we evaluate by using the properties Eq.(D.6-D.10)

$$\text{Tr}[[\tau_i, \tau_j][\tau_k, \tau_l]] = -4\epsilon_{ijs}\epsilon_{klt}\text{Tr}[\tau_s\tau_t] = -8(\delta_{ik}, \delta_{jl} - \delta_{il}, \delta_{jk}), \quad \text{(D.13)}$$

$$\text{Tr}[[\tau_i, \alpha_j^\dagger][\tau_k, \alpha_l]] = \text{Tr}[(\alpha^\dagger \sigma^i)_j(-\sigma^k \alpha)_l] = -\sigma_{sj}^i \sigma_{lt}^k \text{Tr}[\alpha_s^\dagger \alpha_t] = -2(\sigma^k \cdot \sigma^i)_{lj}, \quad \text{(D.14)}$$

$$\text{Tr}[\alpha_i^\dagger, \alpha_j][\alpha_k^\dagger, \alpha_l] = \text{Tr}[(\tau \cdot \sigma + \sqrt{3}\lambda_8)_{ij}(\tau \cdot \sigma + \sqrt{3}\lambda_8)_{kl}]$$
$$= \sigma_{ij}^s \sigma_{kl}^t \text{Tr}[\tau_s\tau_t] + \sqrt{3}\sigma_{ij}^s \delta_{kl}\text{Tr}[\tau_s\lambda_8] + \sqrt{3}\sigma_{kl}^s \delta_{ij}\text{Tr}[\lambda_8\tau_s] + 3\delta_{ij}\delta_{kl}\text{Tr}[\lambda_8^2] \quad \text{(D.15)}$$
$$= 2\sigma_{ij} \cdot \sigma_{kl} + 6\delta_{ij}\delta_{kl}.$$

We sort the remaining terms according to the three traces, we just evaluated. The terms, which correspond to one trace, only differ in the exchange of the derivatives, and every such exchange comes with a minus. That structure can already be seen in the WT term at the very beginning.

$$\mathcal{L}_{WT} \to -\frac{1}{16F_0^2}(-8\rho_i^\mu \partial^\nu \rho_{\mu j}\pi_k \partial_\nu \pi_l(\delta_{ik}\delta_{jl} - \delta_{il}\delta_{jk})$$
$$- 2(\sigma^k \cdot \sigma^i)_{lj}(\rho_i^\mu \partial^\nu K_{\mu j}\pi_k \partial_\nu K_l^\dagger - \rho_i^\mu \partial^\nu K_{\mu j}K_l^\dagger \partial_\nu \pi_k - \partial^\nu \rho_i^\mu K_{\mu j}\pi_k \partial_\nu K_l^\dagger$$
$$+ \partial^\nu \rho_i^\mu K_{\mu j}\partial_\nu \pi_k K_l^\dagger + \rho_k^\mu \partial^\nu K_{\mu l}^\dagger \pi_i \partial_\nu K_j - \rho_k^\mu \partial^\nu K_{\mu l}^\dagger K_j \partial_\nu \pi_i - \partial^\nu \rho_k^\mu K_{\mu l}^\dagger \pi_i \partial_\nu K_j$$
$$+ \partial^\nu \rho_k^\mu K_{\mu l}^\dagger \partial_\nu \pi_i K_j) \quad \text{(D.16)}$$
$$+ (2\sigma_{ij} \cdot \sigma_{kl} + 6\delta_{ij}\delta_{kl})(\partial^\nu K_{\mu i}^\dagger K_j^\mu K_l \partial_\nu K_k^\dagger - \partial^\nu K_{\mu i}^\dagger K_j^\mu K_k^\dagger \partial_\nu K_l$$
$$+ K_{\mu i}^\dagger \partial^\nu K_j^\mu \partial_\nu K_l K_k^\dagger - K_{\mu i}^\dagger \partial^\nu K_j^\mu K_l \partial_\nu K_k^\dagger).$$

Using

$$\sigma^i \sigma^j = \delta_{ij} + i\epsilon_{ijk}\sigma^k,$$

the interaction term turns into

$$\mathcal{L}_{WT} \to -\frac{1}{16F_0^2}\Big(-8(\rho^\mu \cdot \pi)(\partial^\nu \rho_\mu \cdot \partial_\nu \pi) + 8(\rho^\mu \cdot \partial_\nu \pi)(\partial^\nu \rho_\mu \cdot \pi)$$
$$- 2(\pi \cdot \rho^\mu)(\partial^\nu K^\dagger \partial_\nu K_\mu + \partial^\nu K_\mu^\dagger \partial_\nu K) \pm \text{derivatives exchanged}$$
$$- 2i(\pi \times \rho^\mu)(\partial^\nu K^\dagger \sigma \partial_\nu K_\mu - \partial^\nu K_\mu^\dagger \sigma \partial_\nu K) \pm \text{derivatives exchanged}$$
$$+ 2\partial^\nu K_\mu^\dagger \sigma K^\mu K\sigma \partial_\nu K^\dagger + 6\partial^\nu K_\mu^\dagger K^\mu K\partial_\nu K^\dagger \pm \text{derivatives exchanged}\Big),$$
$$\text{(D.17)}$$

where we only wrote down one term explicitly and the others one can get by exchanging derivatives, as mentioned above.

Isospin projection for $\pi\rho$ channel

Eq.(D.17) still carries contributions from different isospin channels, which will be projected out in the following. The projectors on the different isospins are given by

$$
\begin{aligned}
P_{I=0} &= \frac{1}{3}((\vec{t}_\pi \vec{t}_\rho)^2 - 1) \\
P_{I=1} &= \frac{1}{2}(2 - \vec{t}_\pi \vec{t}_\rho - (\vec{t}_\pi \vec{t}_\rho)^2) \\
P_{I=2} &= \frac{1}{6}(2 + 3\vec{t}_\pi \vec{t}_\rho + (\vec{t}_\pi \vec{t}_\rho)^2)\,,
\end{aligned}
\tag{D.18}
$$

which can be verified by noting that

$$
\vec{t}_\pi \vec{t}_\rho |\pi\rho\rangle = \begin{cases} -2|\pi\rho\rangle & I = 0 \\ -1|\pi\rho\rangle & I = 1 \\ 1|\pi\rho\rangle & I = 2 \end{cases}.
\tag{D.19}
$$

The Lagrangian is written in cartesian coordinates. Therefore, we use the projectors in that basis, which means that we use the representation Eq.(A.33). Applying the $I = 1$ projector on the possible combinations of π_i and ρ_j, we get

$$
P_{I=1}\pi_i\rho_i = 0\,,
\tag{D.20}
$$

$$
P_{I=1}\pi_i\rho_j = \frac{1}{2}(\pi_i\rho_j - \pi_j\rho_i) \quad \text{for} \quad i \neq j\,,
\tag{D.21}
$$

where the first equation does not imply a summation over the index i. Applying to the first term in Eq.(D.17), we get

$$
\begin{aligned}
&P_{I=1}(-\rho_i^\mu \pi_i \partial^\nu \rho_{\mu j} \partial_\nu \pi_j + \rho_i^\mu \partial_\nu \pi_i \partial^\nu \rho_{\mu j} \pi_j) \\
&= -\frac{1}{2}(\rho_i^\mu \partial_\nu \pi_j - \rho_j^\mu \partial_\nu \pi_i)(\pi_i \partial^\nu \rho_{\mu j}) + \ldots \quad (i \neq j) \\
&= -\frac{1}{2}\epsilon_{ijk}(\rho_i^\mu \partial_\nu \pi_j)\epsilon_{lmk}(\pi_l \partial^\nu \rho_{\mu m}) + \ldots \\
&= -\frac{1}{2}(\rho^\mu \times \partial_\nu \pi)(\pi \times \partial^\nu \rho_\mu) + \frac{1}{2}(\rho^\mu \times \pi)(\partial_\nu \pi \times \partial^\nu \rho_\mu)\,.
\end{aligned}
\tag{D.22}
$$

The second line in Eq.(D.17) can easily be seen to be isospin zero and the third line is already isospin 1.

Isospin projection for $K\overline{K}$

For two isospin $\frac{1}{2}$ particles it is much more obvious how to project on an isospin=1 channel and we can read off the relevant terms directly. Explicitly evaluating the last term of Eq.(D.17) and keeping only the relevant terms, we get

$$
2(\partial^\nu K_\mu^\dagger \sigma K^\mu)(\partial_\nu K^\dagger \sigma K) + 6\partial^\nu K_\mu^\dagger K^\mu K \partial_\nu K^\dagger \rightarrow 4K_\mu^+ \partial^\nu \overline{K}^0 \partial_\nu K^{\mu-} K^0 + 4K_\mu^0 \partial^\nu K^- \partial_\nu \overline{K}^{\mu 0} K^+\,.
\tag{D.23}
$$

Looking closely at that term and remembering that there are also the terms with the derivatives exchanged, we arrive at

$$
\begin{aligned}
&4K_\mu^+ \partial^\nu \overline{K}^0 \partial_\nu K^{\mu-} K^0 + 4K^+ \partial^\nu \overline{K}^{\mu 0} \partial_\nu K^- K_\mu^0 \pm \text{derivatives exchanged} \\
&= 2(K^{+\mu}\partial^\nu \overline{K}^0 - \overline{K}^{0\mu}\partial^\nu K^+)(\partial_\nu K_\mu^- K^0 - \partial_\nu K_\mu^0 K^-) \pm \text{derivatives exchanged} \\
&+ 2(K^{+\mu}\partial^\nu \overline{K}^0 + \overline{K}^{0\mu}\partial^\nu K^+)(\partial_\nu K_\mu^- K^0 + \partial_\nu K_\mu^0 K^-) \pm \text{derivatives exchanged}\,,
\end{aligned}
\tag{D.24}
$$

The second term has positive G-parity, and therefore we drop it.

Physical states

The $I^G = 1^+$ Lagrangian is

$$
\begin{aligned}
\mathcal{L}_{1^-} \to -\frac{1}{16F_0^2}\Big(& 4(\partial^\nu\pi \times \rho^\mu)(\pi \times \partial_\nu\rho_\mu) - 4(\partial^\nu\pi \times \partial_\nu\rho^\mu)(\pi \times \rho_\mu) \\
& + 2i(\pi \times \partial^\nu\rho^\mu)(\partial_\nu K^\dagger \sigma K_\mu - K_\mu^\dagger \sigma \partial_\nu K) \pm \text{derivatives exchanged} \\
& + 2(K_\mu^+\partial\overline{K}^0 - \overline{K}^{0\mu}\partial K^+)(\partial K_\mu^- K^0 - \partial K^{0\mu}K^-) \pm \text{derivatives exchanged}\Big).
\end{aligned}
\tag{D.25}
$$

In order to be able to read off the physical states, we rewrite the states in the charge basis

$$
\rho_\mu \times \partial_\nu\pi = \begin{pmatrix}
\frac{1}{\sqrt{2}i}((\rho_\mu^-\partial_\nu\pi^0 - \partial_\nu\pi^-\rho_\mu^0) - (\rho_\mu^+\partial_\nu\pi^0 - \rho_\mu^0\partial_\nu\pi^+)) \\
\frac{1}{\sqrt{2}}(-(\rho_\mu^-\partial_\nu\pi^0 - \partial_\nu\pi^-\rho_\mu^0) - (\rho_\mu^+\partial_\nu\pi^0 - \rho_\mu^0\partial_\nu\pi^+)) \\
i(\rho_\mu^-\partial_\nu\pi^+ - \rho_\mu^+\partial_\nu\pi^-)
\end{pmatrix},
\tag{D.26}
$$

where we used

$$
\pi_1 = \frac{1}{\sqrt{2}}(\pi^- + \pi^+), \quad \pi_2 = \frac{1}{\sqrt{2}i}(\pi^- - \pi^+).
\tag{D.27}
$$

This relation follows from the parametrisation we chose in Eq.(2.26) (see also [Sch03]). The kaon term can be written as

$$
K_\mu^\dagger\sigma\partial_\nu K - \partial_\nu K^\dagger\sigma K_\mu = \begin{pmatrix}
(K_\mu^-\partial_\nu K^0 - K_\mu^0\partial_\nu K^-) - (K_\mu^+\partial_\nu\overline{K}^0 - \overline{K}_\mu^0\partial_\nu^+) \\
-i(K_\mu^-\partial_\nu K^0 - K_\mu^0\partial_\nu K^-) - i(K_\mu^+\partial_\nu\overline{K}^0 - \overline{K}_\mu^0\partial_\nu^+) \\
(K_\mu^-\partial_\nu K^+ - K_\mu^+\partial_\nu K^-) + (K_\mu^0\partial_\nu\overline{K}^0 - \overline{K}_\mu^0\partial_\nu^0).
\end{pmatrix}
\tag{D.28}
$$

Using these expression, we can read off the Feynman rules for the different transitions

$$
(\pi^0\rho_\mu^- - \pi^-\rho_\mu^0) \to (\pi^0\rho_\nu^- - \pi^-\rho_\nu^0) \quad : \quad -\frac{2}{8F_0^2}(\overline{p}q + pq + \overline{p}q + p\overline{q})g_{\mu\nu}
$$

$$
(\pi^0\rho_\mu^- - \pi^-\rho_\mu^0) \leftrightarrow (K_\nu^- K^0 - K_\nu^0 K^-) \quad : \quad \frac{\sqrt{2}}{8F_0^2}(\overline{p}q + pq + \overline{p}q + p\overline{q})g_{\mu\nu}
\tag{D.29}
$$

$$
(K_\mu^- K^0 - K_\mu^0 K^-) \leftrightarrow (K_\nu^- K^0 - K_\nu^0 K^-) \quad : \quad -\frac{1}{8F_0^2}(\overline{p}q + pq + \overline{p}q + p\overline{q})g_{\mu\nu}.
$$

Using $(\rho^-\pi^0 - \rho^0\pi^+)$ as channel 1 and $(K_\mu^- K^0 - K_\mu^0 K^-)$ as channel 2, the kernel for the process $a \to b$ can be written as

$$
K_{ab}^{\mu\nu} = -\frac{1}{8F_0^2}(\overline{p}q + pq + \overline{p}q + p\overline{q})g^{\mu\nu}C_{ab}^{WT},
\tag{D.30}
$$

with

$$
C_{WT} = \begin{pmatrix} 2 & -\sqrt{2} \\ -\sqrt{2} & 1 \end{pmatrix}
\tag{D.31}
$$

Normalisation of the states

First we note that the sign in the upper right corner of the WT-matrix depends on the definition of states. Secondly, we comment on the normalisation of the states, which means

we explain, why we have to put the factor of $1/\sqrt{2}$ in front of the states. Of course the result will not depend on it, but only if one puts the right factors of $\sqrt{2}$ everywhere.

One way to look at the situation is to regard the final state as a superposition of the two differently charged states. These states should be normalised, and therefore, we have to put a factor of $\sqrt{2}$ in front of the states. This means, we would also catch a factor of $\sqrt{2}$ in the W decay vertex. The final state dissolves the superposition and the remaining factor of $\sqrt{2}$ cancels the one at the W decay vertex. Thus, the states we use are

$$\frac{1}{\sqrt{2}}(\rho^- \pi^0 - \rho^0 \pi^+)\,, \tag{D.32}$$

$$\frac{1}{\sqrt{2}}(K_\mu^- K^0 - K_\mu^0 K^-)\,. \tag{D.33}$$

Another illuminating way to see the right position for the factors is to look at the reaction without superimposing the states. Then we would not have two channels, but four channels with a coupled channel matrix with the following schematic structure

$$\begin{pmatrix} a & -a & b & -b \\ -a & a & -b & b \\ b & -b & c & -c \\ -b & b & -c & c \end{pmatrix}\,, \tag{D.34}$$

where the four rows and columns correspond to $\pi^0 \rho^+, \pi^+ \rho^0, K_\mu^+ \overline{K}^0, \overline{K}_\mu^0 K^+$. For simplicity we leave out the helicity structure for the moment, which does not affect the following arguments. From Eq.(4.74), we can see that the Bethe-Salpeter equation in that case leads to the following formula

$$M_{ij} = V_{ij} + \sum_{c=1}^{4} V_{ic} M_{cj} (-I_c)\,.$$

We notice that

$$V_{1j} = -V_{2j}\,, \quad V_{3j} = -V_{4j}\,, \quad V_{i1} = -V_{i2}\,, \quad V_{i3} = -V_{i4}\,, \tag{D.35}$$

and therefore

$$M_{i1} = -M_{i2}\,, \quad M_{i3} = -M_{i4}\,, \quad M_{1j} = -M_{2j}\,, \quad M_{3j} = -M_{4j}\,. \tag{D.36}$$

Thus, two channels are redundant, and we can more efficiently sum over only two channels, but catching a factor of 2

$$M_{ij} = V_{ij} + 2 \sum_{c=1}^{2} V_{ic} M_{cj} (-I_c)\,.$$

We also have to consider what consequences we get at the other vertices. First there is the W decay vertex, where we have to sum over two more channels, which are the same as the other two channels except that we catch a minus sign. That minus sign is compensated by the respective minus sign from the solution of the Bethe-Salpeter equation. Thus we get a factor of 2, which we can hide in the Bethe-Salpeter equation. From here on the final state tells us, which state we use further. We only have to remember that the Bethe-Salpeter equation gives us an additional minus sign, when we choose the other charge state. Everything else is compensated by multiplying the kernel by 2.

D.2. Higher order terms

We want to evaluate the contribution to the kernel from the Lagrangian in Eq.(6.94). We see that the terms have common structures and that we only have to evaluate

$$\text{Tr}[V^\mu V^\nu u^\alpha u^\beta] \to \frac{1}{F_0^2} \text{Tr}[V^\mu V^\nu \partial^\alpha \phi \partial^\beta \phi] \,, \tag{D.37}$$

$$\text{Tr}[V^\mu u^\nu V^\alpha u^\beta] \to \frac{1}{F_0^2} \text{Tr}[V^\mu \partial^\nu \phi V^\alpha \partial^\beta \phi] \,, \tag{D.38}$$

$$\text{Tr}[V^\mu u^\nu] \text{Tr}[V^\alpha u^\beta] \to \frac{1}{F_0^2} \text{Tr}[V^\mu \partial^\nu \phi] \text{Tr}[V^\alpha \partial^\beta \phi] \,, \tag{D.39}$$

from which we can deduce the result for all terms by contracting with the corresponding metric tensors.

We start with the first term and use again the isospin decomposition in Eq.(D.4) and Eq.(D.5). Keeping only terms, which contribute to the channel we are investigating, we get

$$
\begin{aligned}
\text{Tr}[V^\mu V^\nu \partial^\alpha \phi \partial^\beta \phi] \to{} & \rho_i^\mu \rho_j^\nu \partial^\alpha \pi_k \partial^\beta \pi_l \text{Tr}[\tau_i \tau_j \tau_k \tau_l] + \rho_i^\mu K_j^\nu \partial^\alpha K_k^\dagger \partial^\beta \pi_l \text{Tr}[\tau_i \alpha_j^\dagger \alpha_k \tau_l] \\
& + K_i^\mu K_j^{\dagger\nu} \partial^\alpha K_k \partial^\beta K_l^\dagger \text{Tr}[\alpha_i^\dagger \alpha_j \alpha_k^\dagger \alpha_l] + K_i^{\dagger\mu} \rho_j^\nu \partial^\alpha \pi_k \partial^\beta K_l \text{Tr}[\alpha_i \tau_j \tau_k \alpha_l^\dagger] \\
& + K_i^{\dagger\mu} K_j^\nu \partial^\alpha K_k^\dagger \partial^\beta K_l \text{Tr}[\alpha_i \alpha_j^\dagger \alpha_k \alpha_l^\dagger] \,.
\end{aligned}
\tag{D.40}
$$

The three different traces which appear are given by

$$
\begin{aligned}
\text{Tr}[\tau_i \tau_j \tau_k \tau_l] &= \text{Tr}[((2/3\mathbb{1} + \lambda_8/\sqrt{3})\delta_{ij} + i\epsilon_{ijm}\tau_m)((2/3\mathbb{1} + \lambda_8/\sqrt{3})\delta_{kl} + i\epsilon_{klm}\tau_m)] \\
&= 2\delta_{ij}\delta_{kl} - 2\epsilon_{ijm}\epsilon_{klm} = 2(\delta_{ij}\delta_{kl} - \delta_{ik}\delta_{jl} + \delta_{il}\delta_{jk}) \,,
\end{aligned}
\tag{D.41}
$$

$$\text{Tr}[\tau_i \alpha_j^\dagger \alpha_k \tau_l] = \sigma_{nj}^i \sigma_{km}^l \text{Tr}[\alpha_n^\dagger \alpha_m] = 2(\sigma^l \cdot \sigma^i)_{kj} \,, \tag{D.42}$$

$$\text{Tr}[\alpha_i^\dagger \alpha_j \alpha_k^\dagger \alpha_l] = 4\delta_{il}\delta_{jk} \,. \tag{D.43}$$

Thus, we get

$$
\begin{aligned}
\text{Tr}[V^\mu V^\nu \partial^\alpha \phi \partial^\beta \phi] \to{} & 2((\rho^\mu \cdot \rho^\nu)(\partial^\alpha \pi \cdot \partial^\beta \pi) - (\rho^\mu \cdot \partial^\alpha \pi)(\rho^\nu \cdot \partial^\beta \pi) + (\rho^\mu \cdot \partial^\beta \pi)(\rho^\nu \cdot \partial^\alpha \pi)) \\
& + 2i(\partial^\beta \pi \times \rho^\mu)(\partial^\alpha K^\dagger \sigma K^\nu) + 2i(\rho^\nu \times \partial^\alpha \pi)(K^{\dagger\mu} \sigma \partial^\beta K) \\
& + 4(\partial^\beta K^\dagger K^\mu)(K^{\dagger\nu} \partial^\alpha K) + 4(K^{\dagger\mu} K^\nu)(\partial^\alpha K^\dagger \partial^\beta K) \,.
\end{aligned}
\tag{D.44}
$$

Projecting the first line on isospin 1 and keeping only the relevant terms in the last line yields

$$
\begin{aligned}
\text{Tr}[V^\mu V^\nu \partial^\alpha \phi \partial^\beta \phi] \to{} & 2(\rho^\mu \times \partial^\beta \pi)(\rho^\nu \times \partial^\alpha \pi) \\
& + 2i(\partial^\beta \pi \times \rho^\mu)(\partial^\alpha K^\dagger \sigma K^\nu) + 2i(\rho^\nu \times \partial^\alpha \pi)(K^{\dagger\mu} \sigma \partial^\beta K) \\
& + 4(K^{\nu+} \partial^\alpha \overline{K}^0 K^{-\mu} \partial^\beta K^0 + \partial^\beta K^+ \overline{K}^{0\mu} \partial^\alpha K^- K^{0\nu}) \,.
\end{aligned}
\tag{D.45}
$$

Contracting with the respective metric tensors, we get

$$
\begin{aligned}
\lambda_1' \text{Tr}[V_\mu V^\mu u_\nu u^\nu] \to{} & \frac{\lambda_1'}{F_0^2} [2(\rho^\mu \times \partial^\nu \pi)(\rho_\mu \times \partial_\nu \pi) \\
& + 2i(\partial^\nu \pi \times \rho^\mu)(\partial_\nu K^\dagger \sigma K_\mu - K_\mu^\dagger \sigma \partial_\nu K) \\
& + 4(K^{+\mu} \partial^\nu \overline{K}^0 K_\mu^- \partial_\nu K^0 + \partial^\nu K^+ \overline{K}^{0\mu} \partial_\nu K^- K_\mu^0)] \,,
\end{aligned}
\tag{D.46}
$$

$$\lambda_3' \operatorname{Tr}[V^\mu V^\nu u_\mu u_\nu] \rightarrow \frac{\lambda_3'}{F_0^2}[2(\rho^\mu \times \partial^\nu \pi)(\rho_\nu \times \partial_\mu \pi)$$
$$+ 2i(\partial^\nu \pi \times \rho^\mu)(\partial_\mu K^\dagger \sigma K_\nu - K_\nu^\dagger \sigma \partial_\mu K) \tag{D.47}$$
$$+ 4(K^{+\nu} \partial^\mu \overline{K}^0 K_\mu^- \partial_\nu K^0 + \partial^\nu K^+ \overline{K}^{0\mu} \partial_\mu K^- K_\nu^0)].$$

The expression for $\lambda_4' \operatorname{Tr}[V_\mu V^\nu u_\nu u^\mu]$ one gets by simply exchanging $\partial_\mu \leftrightarrow \partial_\nu$ and of course $\lambda_3' \leftrightarrow \lambda_4'$ in the above equation. We simplify the terms including the field strength of the vector mesons by using $\partial_\mu V^\mu = 0$ and dropping higher orders

$$\lambda_6' \operatorname{Tr}[V_{\mu\nu} V^{\nu\alpha} u^\mu u_\alpha] \rightarrow \lambda_6' \operatorname{Tr}[-\partial_\mu V_\nu \partial^\alpha V^\nu u^\mu u_\alpha - \partial_\nu V_\mu \partial^\nu V^\alpha u^\mu u_\alpha]. \tag{D.48}$$

Since $\partial^2 V_\mu = M_V^2 V_\mu$, the second term has the same structure as the λ_2' term, and therefore we drop it, because we can effectively include it in λ_3'. Thus, we end up with

$$-\lambda_6' \operatorname{Tr}[\partial_\mu V_\nu \partial^\alpha V^\nu u^\mu u_\alpha] \rightarrow -\frac{\lambda_6'}{F_0^2}[2(\partial^\mu \rho^\nu \times \partial^\alpha \pi)(\partial_\alpha \rho_\nu \times \partial_\mu \pi)$$
$$+ 2i(\partial^\alpha \pi \times \partial^\mu \rho^\nu)(\partial_\mu K^\dagger \sigma \partial_\alpha K_\nu - \partial_\mu K_\nu^\dagger \sigma \partial_\alpha K) \tag{D.49}$$
$$+ 4(\partial^\alpha K^{+\nu} \partial^\mu \overline{K}^0 \partial_\mu K_\nu^- \partial_\alpha K^0 + \partial^\alpha K^+ \partial^\mu \overline{K}^{0\nu} \partial_\mu K^- \partial_\alpha K_\nu^0)].$$

The expression for the λ_7' term one gets again by exchanging the derivatives on the mesons. The last line still contains a contribution with positive G-parity, which we can be seen by looking at Eq.(D.24). Using Eq.(D.26), Eq.(D.28) and the definition of the states in Eq.(D.32) and Eq.(D.33), we can read off the contribution to the kernel from the above expressions, which yields

$$K_1^{\mu\nu} = \frac{4C_{WT}}{F_0^2}((\bar{q} \cdot q)g^{\mu\nu}\lambda_1' + \bar{q}^\nu q^\mu \lambda_3' + \bar{q}^\mu q^\nu \lambda_4' - (w \cdot q)(w \cdot \bar{q})g^{\mu\nu}(\lambda_6' + \lambda_7')). \tag{D.50}$$

Next we evaluate the second term. We start again by evaluating the trace for arbitrary indices and afterwards contract with the respective metric tensors to get the results, we are interested in:

$$\operatorname{Tr}[V^\mu \partial^\nu \phi V^\alpha \partial^\beta \phi] \rightarrow \rho_i^\mu \partial^\nu \pi_j \rho_k^\alpha \partial^\beta \pi_l \operatorname{Tr}[\tau_i \tau_j \tau_k \tau_l]$$
$$+ \rho_i^\mu \partial^\nu K_j K_k^{\dagger\alpha} \partial^\beta \pi_l \operatorname{Tr}[\tau_i \alpha_j^\dagger \alpha_k \tau_l] + \rho_i^\mu \partial^\nu \pi_j K_k^\alpha \partial^\beta K_l^\dagger \operatorname{Tr}[\tau_i \tau_j \alpha_k^\dagger \alpha_l]$$
$$+ K_i^\mu \partial^\nu K_j^\dagger \rho_k^\alpha \partial^\beta \pi_l \operatorname{Tr}[\alpha_i^\dagger \alpha_j \tau_k \tau_l] + K_i^{\dagger\mu} \partial^\nu \pi_j \rho_k^\alpha \partial^\beta K_l \operatorname{Tr}[\alpha_i \tau_j \tau_k \alpha_l^\dagger] \tag{D.51}$$
$$+ K_i^\mu \partial^\nu K_j^\dagger K_k^\alpha \partial^\beta K_l^\dagger \operatorname{Tr}[\alpha_i^\dagger \alpha_j \alpha_k^\dagger \alpha_l] + K_i^{\dagger\mu} \partial^\nu K_j K_k^{\dagger\alpha} \partial^\beta K_l \operatorname{Tr}[\alpha_i \alpha_j^\dagger \alpha_k \alpha_l^\dagger].$$

Using the relations Eq.(D.41-D.43) for the traces, we get

$$\operatorname{Tr}[V^\mu \partial^\nu \phi V^\alpha \partial^\beta \phi] \rightarrow 2((\rho^\mu \cdot \partial^\nu \pi)(\rho^\alpha \cdot \partial^\beta \pi) - (\rho^\mu \cdot \rho^\alpha)(\partial^\nu \pi \cdot \partial^\beta \pi) + (\rho^\mu \cdot \partial^\beta \pi)(\partial^\nu \pi \cdot \rho^\alpha))$$
$$+ 2i(\partial^\beta \pi \times \rho^\mu)K^{\dagger\alpha}\sigma \partial^\nu K + 2(\rho^\mu \times \partial^\nu \pi)\partial^\beta K^\dagger \sigma K_k^\alpha$$
$$+ 2i(\rho^\alpha \times \partial^\beta \pi)\partial^\nu K^\dagger \sigma K^\mu + 2(\partial^\nu \pi \times \rho^\alpha)K^{\dagger\mu}\sigma \partial^\beta K \tag{D.52}$$
$$+ 4(\partial^\beta K^\dagger K^\mu)(\partial^\nu K^\dagger K^\alpha) + 4(K^{\dagger\mu}\partial^\nu K)(K^{\dagger\alpha}\partial^\beta K).$$

Projecting the first line on isospin 1 and keeping only the relevant terms in the last line, we

end up with

$$
\begin{aligned}
\mathrm{Tr}[V^\mu \partial^\nu \phi V^\alpha \partial^\beta \phi] \to{} & -2(\rho^\mu \times \partial^\beta \pi)(\rho^\alpha \times \partial^\nu \pi) - 2(\rho^\mu \times \partial^\nu \pi)(\rho^\alpha \times \partial^\beta \pi) \\
& + 2i(\partial^\beta \pi \times \rho^\mu)K^{\dagger\alpha}\sigma\partial^\nu K + 2(\rho^\mu \times \partial^\nu \pi)\partial^\beta K^\dagger \sigma K_k^\alpha \\
& + 2i(\rho^\alpha \times \partial^\beta \pi)\partial^\nu K^\dagger \sigma K^\mu + 2(\partial^\nu \pi \times \rho^\alpha)K^{\dagger\mu}\sigma\partial^\beta K \\
& + 4(\partial^\beta K^- K^{0\alpha}K^{+\mu}\partial^\nu \overline{K}^0 + \partial^\nu K^- K^{0\mu}K^{+\alpha}\partial^\beta \overline{K}^0 \\
& + K^{-\mu}\partial^\beta K^0 \partial^\nu K^+ \overline{K}^{0\alpha} + K^{-\alpha}\partial^\nu K^0 \partial^\beta K^+ \overline{K}^{0\mu}) \,.
\end{aligned}
\tag{D.53}
$$

Thus, we get the following expressions

$$
\begin{aligned}
\lambda_2' \, \mathrm{Tr}[V^\mu u^\nu V_\mu u_\nu] \to{} & \frac{\lambda_2'}{F_0^2}[-4(\rho^\mu \times \partial^\nu \pi)(\rho_\mu \times \partial_\nu \pi) \\
& + 4i(\rho^\mu \times \partial^\nu \pi)(\partial_\nu K^\dagger \sigma K_\mu - K_\mu^\dagger \sigma \partial_\nu K) \\
& + 8(\partial^\nu K^- K^{0\mu}K_\mu^+ \partial_\nu \overline{K}^0 + K^{-\mu}\partial^\nu K^0 \partial_\nu K^+ \overline{K}_\mu^0)] \,,
\end{aligned}
\tag{D.54}
$$

$$
\begin{aligned}
\lambda_5' \, \mathrm{Tr}[V_\mu u^\mu V_\nu u^\nu + V_\mu u^\nu V_\nu u^\mu] \to{} & \frac{\lambda_5'}{F_0^2}[-4(\rho^\mu \times \partial^\nu \pi)(\rho_\nu \times \partial_\mu \pi) - 4(\rho^\mu \times \partial_\mu \pi)(\rho_\nu \times \partial^\nu \pi) \\
& + 4i(\rho^\mu \times \partial^\nu \pi)(\partial_\mu K^\dagger \sigma K_\nu - K_\nu^\dagger \sigma \partial_\mu K) + 4i(\rho^\mu \times \partial_\mu \pi)(\partial^\nu K^\dagger \sigma K_\nu - K^{\dagger\nu}\sigma\partial_\nu K) \\
& + 8(\partial^\nu K^- K_\nu^0 K^{+\mu}\partial_\mu \overline{K}^0 + K^{-\mu}\partial^\nu K^0 \partial_\mu K^+ \overline{K}_\nu^0) \\
& + \partial^\mu K^- K^{0\nu}K_\mu^+ \partial_\nu \overline{K}^0 + K^{-\mu}\partial_\mu K^0 \partial^\nu K^+ \overline{K}_\nu^0)] \,.
\end{aligned}
\tag{D.55}
$$

The expression containing the field strength will again be simplified first

$$
\begin{aligned}
\lambda_8' \, \mathrm{Tr}[V_{\mu\nu}u_\alpha V^{\nu\alpha}u^\mu + V_{\mu\nu}u^\mu V^{\nu\alpha}u_\alpha] \to{} & -\mathrm{Tr}[\partial_\mu V_\nu u_\alpha \partial^\alpha V^\nu u^\mu + \partial_\mu V_\nu u^\mu \partial^\alpha V^\nu u_\alpha] \\
\to{} & -2\,\mathrm{Tr}[\partial_\mu V_\nu u_\alpha \partial^\alpha V^\nu u^\mu] \,,
\end{aligned}
\tag{D.56}
$$

where we omitted terms with the same structure as the term with λ_5' and terms of order $\mathcal{O}(q^3)$. Thus, we get

$$
\begin{aligned}
& \lambda_8' \, \mathrm{Tr}[V_{\mu\nu}u_\alpha V^{\nu\alpha}u^\mu + V_{\mu\nu}u^\mu V^{\nu\alpha}u_\alpha] \\
& \to -\frac{2\lambda_8'}{F_0^2}[-2(\partial^\mu \rho^\nu \times \partial^\alpha \pi)(\partial_\alpha \rho_\nu \times \partial_\mu \pi) - 2(\partial^\mu \rho^\nu \times \partial_\mu \pi)(\partial^\alpha \rho_\nu \times \partial_\alpha \pi) \\
& + 4i(\partial^\mu \rho^\nu \times \partial^\alpha \pi)(\partial_\mu K^\dagger \sigma \partial_\alpha K_\nu - \partial_\alpha K_\nu^\dagger \sigma \partial_\mu K) \\
& + 8(\partial^\alpha K^- \partial_\alpha K_\nu^0 \partial^\mu K^{+\nu}\partial_\mu \overline{K}^0 + \partial^\mu K^{-\nu}\partial_\alpha K^0 \partial_\mu K^+ \partial^\alpha \overline{K}_\nu^0)] \,.
\end{aligned}
\tag{D.57}
$$

Similar to before, we read off the contribution to the kernel from these expressions, which yields

$$
K_2^{\mu\nu} = \frac{-8C_{WT}}{F_0^2}((\overline{q} \cdot q)g^{\mu\nu}\lambda_2' + (\overline{q}^\nu q^\mu + \overline{q}^\mu q^\nu)\lambda_5' - 2(w \cdot q)(w \cdot \overline{q})g^{\mu\nu}\lambda_8') \,.
\tag{D.58}
$$

Next we evaluate the terms with two traces

$$
\begin{aligned}
\mathrm{Tr}[V^\mu \partial^\nu \phi]\,\mathrm{Tr}[V^\alpha \partial^\beta \phi] \to{} & 4(\rho^\mu \cdot \partial^\nu \pi)(\rho^\alpha \cdot \partial^\beta \pi) \\
& + 4(K^{\mu\dagger} \cdot \partial^\nu K + \partial^\nu K^\dagger \cdot K^\mu)(K^{\alpha\dagger} \cdot \partial^\beta K + \partial^\beta K^\dagger \cdot K^\alpha) \,,
\end{aligned}
\tag{D.59}
$$

where we only kept terms relevant for the channel we are interested in. Thus, we get

$$\lambda_9' \, \mathrm{Tr}[V_\mu u^\nu] \, \mathrm{Tr}[V^\mu u_\nu] \to \frac{\lambda_9'}{F_0^2} (2(\rho^\mu \times \partial_\nu \pi)(\partial^\nu \pi \times \rho_\mu)$$
$$+ 4(K^{\mu\dagger} \cdot \partial^\nu K + \partial^\nu K^\dagger \cdot K^\mu)(K_\mu^\dagger \cdot \partial_\nu K + \partial_\nu K^\dagger \cdot K_\mu)),$$

(D.60)

$$\lambda_{10}' \, \mathrm{Tr}[V_\mu u^\mu] \, \mathrm{Tr}[V_\nu u^\nu] \to \frac{\lambda_{10}'}{F_0^2} (2(\rho^\mu \times \partial^\nu \pi)(\partial_\mu \pi \times \rho_\nu) + 4(K^{\mu\dagger} \cdot \partial_\mu K + \partial^\mu K^\dagger \cdot K_\mu)^2, \quad \text{(D.61)}$$

$$\lambda_{11}' \, \mathrm{Tr}[V_\mu u_\nu] \, \mathrm{Tr}[V^\nu u^\mu] \to \frac{\lambda_{11}'}{F_0^2} (2(\rho^\mu \times \partial_\mu \pi)(\partial^\nu \pi \times \rho_\nu)$$
$$+ 4(K^{\mu\dagger} \cdot \partial^\nu K + \partial^\nu K^\dagger \cdot K^\mu)(K_\nu^\dagger \cdot \partial_\mu K + \partial_\mu K^\dagger \cdot K_\nu).$$

(D.62)

The terms containing the field strength are again simplified by using the equations of motion and dropping structures we already have, which yields

$$\lambda_{12}' \, \mathrm{Tr}[V_{\mu\alpha} u^\mu] \, \mathrm{Tr}[V_\nu^\alpha u^\nu] \to \frac{\lambda_{12}'}{F_0^2} \, \mathrm{Tr}[\partial_\mu V_\alpha u^\mu] \, \mathrm{Tr}[\partial_\nu V^\alpha u^\nu], \quad \text{(D.63)}$$

$$\lambda_{13}' \, \mathrm{Tr}[V_{\mu\alpha} u_\nu] \, \mathrm{Tr}[V^{\nu\alpha} u^\mu] \to \frac{\lambda_{13}'}{F_0^2} \, \mathrm{Tr}[\partial_\mu V_\alpha u_\nu] \, \mathrm{Tr}[\partial^\nu V^\alpha u^\mu]. \quad \text{(D.64)}$$

Apart from higher orders, the second term is the same as the first one.
One can read off the contribution to the kernel from the above terms to be

$$K_3^{\mu\nu} = -\frac{8 \mathbb{1}_2}{F_0^2}((\lambda_9'(q \cdot \bar{q}) + (\lambda_{12}' + \lambda_{13}')(w \cdot q)(w \cdot \bar{q}))g^{\mu\nu} + \lambda_{10}' q^\mu \bar{q}^\nu + \lambda_{11}' \bar{q}^\mu q^\nu). \quad \text{(D.65)}$$

Therefore, altogether we get

$$K_{ho}^{\mu\nu} = K_1^{\mu\nu} + K_2^{\mu\nu} + K_3^{\mu\nu} = \frac{4C_{WT}}{F_0^2} \big((\bar{q} \cdot q)g^{\mu\nu}(\lambda_1' - 2\lambda_2') + \bar{q}^\nu q^\mu(\lambda_3' - 2\lambda_5')$$
$$+ \bar{q}^\mu q^\nu(\lambda_4' - 2\lambda_5') - (w \cdot q)(w \cdot \bar{q})g^{\mu\nu}(\lambda_6' + \lambda_7' - 2\lambda_8'))$$
$$- \frac{8\mathbb{1}_2}{F_0^2}((\lambda_9'(q \cdot \bar{q}) + (\lambda_{12}' + \lambda_{13}')(w \cdot q)(w \cdot \bar{q}))g^{\mu\nu} + \lambda_{10}' q^\mu \bar{q}^\nu + \lambda_{11}' \bar{q}^\mu q^\nu).$$

(D.66)

Appendix E.

Miscellaneous

E.1. Parameters

F_0	$0.09\,\mathrm{GeV}$
m_π	$0.137\,\mathrm{GeV}$
M_ρ	$0.77\,\mathrm{GeV}$
m_K	$0.496\,\mathrm{GeV}$
M_{K^*}	$0.894\,\mathrm{GeV}$
M_τ	$1.777\,\mathrm{GeV}$
Γ_τ	$2.3 \cdot 10^{-12}\,\mathrm{GeV}$
M_W	$80.2\,\mathrm{GeV}$
G_F	$1.166 \cdot 10^{-5}\,\mathrm{GeV}^{-2}$
V_{ud}	0.9735
f_V	$\frac{0.154\mathrm{GeV}}{M_\rho}$
g_V	$\frac{0.069\mathrm{GeV}}{M_\rho}$

Table E.1.: Parameters, which are used in the calculation.

E.2. Regularisation

The divergent loop integral we encounter in our calculation is

$$I_{\phi V} = i \int \frac{d^4 l}{(2\pi)^4} \frac{1}{(w-l)^2 - M_\phi^2 + i\epsilon} \frac{1}{l^2 - M_V^2 + i\epsilon}. \tag{E.1}$$

There are different ways to regularise the integral, and we want to give the formulas for the most prominent ways.

Dimensional regularisation

Using Feynman parameters [PS95]

$$\frac{1}{AB} = \int_0^1 dx \frac{1}{(xA + (1-x)B)^2} \,, \tag{E.2}$$

we get

$$I_{\phi V} = \frac{i}{(2\pi)^4} \int dx \int d^4l \frac{1}{(l^2 - \Delta)^2} \tag{E.3}$$

with $\Delta = (x^2 - x)w^2 + xM_\phi^2 + (1-x)M_V^2$. Using dimensional regularisation (see e.g. [PS95]), this becomes

$$I_{\phi V} = -\int dx \frac{1}{4\pi^{d/2}} \frac{\Gamma(2-d/2)}{\Gamma(2)} \Delta^{d/2-2} \,. \tag{E.4}$$

We rewrite the expression using the notation from [BL99]

$$\alpha = \frac{M_\phi}{M_V}, \quad \Omega = \frac{w^2 - M_\phi^2 - M_V^2}{2M_\phi M_V} \,, \tag{E.5}$$

$$\begin{aligned}
\Delta^{d/2-2} &= M_V^{d-4} \left((x^2 - x)\frac{w^2}{M_V^2} + x\alpha^2 + (1-x) \right)^{d/2-2} \\
&= M_V^{d-4} \left((x^2 - x)(1 + 2\alpha\Omega + \alpha^2) + (1-x)\alpha^2 + x \right)^{d/2-2} \equiv M_V^{d-4} C^{d/2-2} \,.
\end{aligned} \tag{E.6}$$

Introducing $\epsilon = 2 - d/2$ and applying the limit $d \to 4$ or $\epsilon \to 0$ we get

$$I_{\phi V} = -\frac{1}{(4\pi)^2} \left(\frac{1}{\epsilon} - 2\ln(M_V) - \gamma + \ln(4\pi) - \int_0^1 dx \ln C \right) \,. \tag{E.7}$$

The integral on the right hand side is

$$\int_0^1 \ln C \, dz = -2 + \frac{M_\phi^2 - M_V + w^2}{2w^2} \ln\left(\frac{M_\phi^2}{M_V^2}\right) + \frac{2M_\phi M_V}{w^2} F(\Omega) \tag{E.8}$$

with

$$F(\Omega) = \begin{cases} \sqrt{\Omega^2 - 1} \ln\left(-\Omega - \sqrt{\Omega^2 - 1}\right), & \Omega < -1 \\ \sqrt{1 - \Omega^2} \arccos(-\Omega), & -1 < \Omega < 1 \\ \sqrt{\Omega^2 - 1} \ln\left(\Omega + \sqrt{\Omega^2 - 1}\right) - i\pi\sqrt{\Omega^2 - 1}, & \Omega > 1 \end{cases} \,. \tag{E.9}$$

Thus, the loop integral is

$$\begin{aligned}
I_{\phi V} = -\frac{1}{(4\pi)^2} \bigg(&\frac{1}{\epsilon} - 2\ln(M_V) - \gamma + \ln(4\pi) + 2 \\
&- \frac{M_\phi^2 - M_V^2 + w^2}{2w^2} \ln\frac{M_\phi^2}{M_V^2} - \frac{2M_\phi M_V}{w^2} F(\Omega) \bigg) \,,
\end{aligned} \tag{E.10}$$

which is the same result as in [FGJS03], besides an arbitrary subtraction.

Dispersive evaluation

The integral can also be evaluated with a dispersion relation, because the imaginary part is well known to be

$$\Im I_{\phi V} = -\frac{p_{cm}}{8\pi\sqrt{s}} \,. \tag{E.11}$$

Thus, we have (see [BD67] for a discussion of dispersion relations.)

$$I_{\phi V} = \sum_{k=0}^{n-1} s^k \frac{a_k}{k!} + \frac{s^n}{\pi} \int_{s_0}^{\infty} \frac{\Im(I_{\phi V}(\zeta))}{\zeta^n(\zeta - s - i\epsilon)} d\zeta \,, \tag{E.12}$$

with $s_0 = (M_V + M_\phi)^2$. In principle n is the number such that

$$\left| \frac{I_{\phi V}(z)}{z^n} \right| \overset{|z| \to \infty}{\longrightarrow} \infty \,. \tag{E.13}$$

Since we do not know the right n from first principles, we choose the easiest one, namely $n = 1$. This way we get the same number of unknown parameters (one subtraction constant a_0) as in the previous scheme. We expect $n = 1$ to be a good choice since the real part of the loop integral should not be proportional to arbitrarily high powers of s.

Euclidian Cutoff

We transform (Wick-rotate) the integral into euclidian coordinates and afterwards use a cutoff in four dimensions. The integral in euclidian coordinates is given by

$$\begin{aligned} I_{\phi V} &= \frac{i}{(2\pi)^4} \int dx \int d^4l \frac{1}{(l^2 - \Delta)^2} = \frac{-1}{(2\pi)^4} \int dx \int d^4l_E \frac{1}{(l_E^2 + \Delta)^2} \\ &= -\frac{1}{16\pi^2} \int dx \left(\frac{\Delta}{(\Delta + \Lambda^2)} - 1 + \ln(\Delta + \Lambda^2) - \ln \Delta \right) \,. \end{aligned} \tag{E.14}$$

with Δ defined above and Λ being the cutoff.

Three-momentum cutoff

Here we will first perform the integral over the time component and then cut off the three-momentum (which breaks Lorentz invariance). The integral over the first pole is given by

$$\begin{aligned} I_{\phi V} &= \frac{1}{2\pi^2} \left(\int l^2 \frac{1}{2E_{lV}} \frac{1}{(E_{lV} + \sqrt{s})^2 - E_{l\pi}^2} dl + \int \frac{1}{2E_{l\pi}} \frac{1}{(\sqrt{s} - E_{l\pi})^2 - E_{lV}^2 + i\epsilon} l^2 dl \right) \\ &= \frac{1}{4\pi^2} \left(\int_{M_V}^{\sqrt{M_V^2 + p_{max}^2}} \frac{\sqrt{E_{lV}^2 - M_V^2}}{s + 2\sqrt{s} E_{lV} + M_V^2 - M_\phi^2} dE_{lV} \right. \\ &\quad \left. + \int_{M_\phi}^{\sqrt{M_\phi^2 + p_{max}^2}} \frac{\sqrt{E_{l\phi}^2 - M_\phi^2}}{s - 2\sqrt{s} E_{l\phi} + M_\phi^2 - M_V^2} dE_{l\phi} \right), \end{aligned} \tag{E.15}$$

where p_{max} denotes the cutoff in the three-momentum.

Comparison

In Fig. E.1, we see the real part of the loop function $I_{\pi\rho}$ calculated with the different schemes which we just discussed. In order to better distuingish the curves and not to overload the figures, we show two plots. In the left plot of Fig. E.1 we used dimensional regularisation with two different subtraction points ($\mu_1 = M_\rho^2$ and $\mu_1 = 9M_\rho^2$), which of course just results in a shift of the curve. For the curve labelled 'w. spec.fun' we use in addition a spectral distribution for the ρ (cf. Eq.(6.39)), which basically smoothes the kink. The right plot of
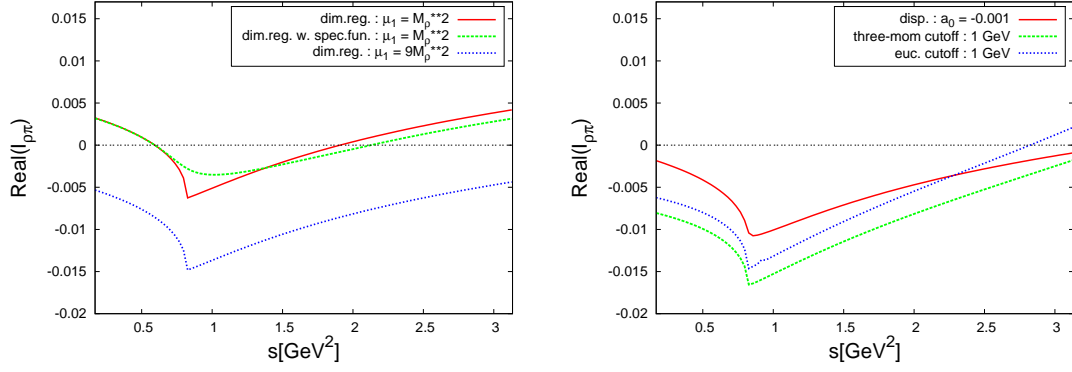
Figure E.1.: Real part of the loop function $I_{\pi\rho}$ for different renormalisation prescriptions. The curves labelled '$\mu_1 = M_\rho^2$' and $\mu_1 = 9M_\rho^2$ in the left plot are calculated with dimensional regularisation with the subtraction point at μ_1. 'w.spec.fun.' is also calculated using dimensional regularisation and $\mu_1 = M_\rho^2$, but in addition a spectral distribution for the vector mesons in the loop is used (cf. Eq.(6.39)). The curve label 'disp. : a_0 = -0.001' in the right plot is calculated with a dispersion relation with the subtraction constant $a_0 = -0.001$. The curves labelled 'three-mom cutoff : 1 GeV' and 'euc. cutoff : 1 GeV' are calculated with a cutoff at $1\,\text{GeV}$ in three-momentuma and in euclidian space, respectively.

Fig. E.1 shows the real part calculated with a dispersion relation and a subtraction constant $a_0 = -0.001$, with a three-momentum cutoff at $1\,\text{GeV}$ and with a euclidian cutoff at $1\,\text{GeV}$. All curves essentially have the same structure, and we see that a subtraction point of about $9M_\rho^2$ gives approximately the same real part as the cutoff schemes with a cutoff at $1\,\text{GeV}$.

In Fig. E.2 we see the imaginary part of the loop function $I_{\pi\rho}$. The imaginary part is of course the same for all prescriptions, except when we include the spectral distribution for the ρ. In that case the threshold smears out a little.
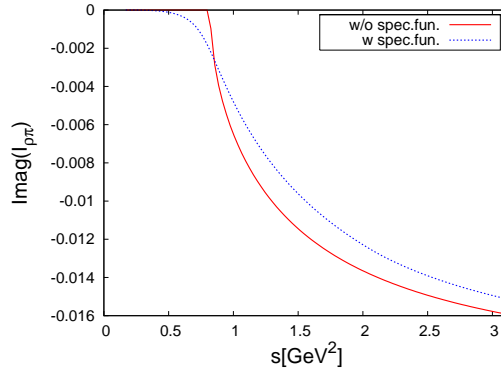

Figure E.2.: Imaginary part of the loop function $I_{\pi\rho}$ with ('w. spec.fun') and without ('w/o spec.fun.') using a spectral distribution for the ρ (cf. Eq.(6.39)).

138

E.3. Adding the singular diagrams

We want to add the two singular diagrams, which we encountered in Chapter 6. We recall that these diagrams were singular at $s = M_a^2$ due the bare propagator. Adding the two diagrams, we properly create the width of the a_1, which takes care of the singularity. The two diagrams are given by

$$
\begin{aligned}
W_{a1\phi V}^{\mu} = \frac{c_{\phi V} f_A g V_{ud} g_V}{\sqrt{2} F_0^3} \frac{s}{s - M_a^2} J_{\phi V}(\mu_1) \left(g_\alpha^\mu - \frac{w^\mu w_\alpha}{w^2} \right) \\
\left((c_1 \beta_1^{\phi V} + c_2 \beta_2^{V\phi}) L_1^{\delta\alpha} + (c_1 \beta_3^{V\phi} + c_2 \beta_4^{V\phi}) L_3^{\delta\alpha} \right) \frac{m_{12}^2}{m_{12}^2 - M_\rho^2 - \Pi} (q_1 - q_2)_\delta \\
+ \quad (q_1 \leftrightarrow q_3) .
\end{aligned}
\tag{E.16}
$$

and

$$
\begin{aligned}
W_{tree}^{\mu} = \frac{2 f_A g V_{ud} g_V}{F_0^3} \frac{s}{s - M_a^2} \left(g^{\mu\alpha} - \frac{w^\mu w^\alpha}{w^2} \right) \frac{m_{12}^2}{m_{12}^2 - M_\rho^2 - \Pi} (q_1 - q_2)^\beta \\
\left(c_1 (q_{3\beta} m_{12\alpha} - q_3 m_{12} g_{\alpha\beta}) + c_2 (w_\beta q_{3\alpha} - w q_3 g_{\alpha\beta}) \right) \quad + \quad (q_1 \leftrightarrow q_3) .
\end{aligned}
$$

Adding the diagrams, we get

$$
\begin{aligned}
& W_{a1\pi\rho}^{\mu} + W_{a1KK^*}^{\mu} + W_{tree}^{\mu} \\
& = \frac{f_A g V_{ud} g_V}{\sqrt{2} F_0^3} \frac{s}{s - M_a^2} \left(g^{\mu\alpha} - \frac{w^\mu w^\alpha}{w^2} \right) \frac{m_{12}^2}{m_{12}^2 - M_\rho^2 - \Pi} (q_1 - q_2)^\beta A_{\alpha\beta} + \quad (q_1 \leftrightarrow q_3) .
\end{aligned}
\tag{E.17}
$$

We see that they have most factors in common and we only have to focus on $A^{\alpha\beta}$, which is given by

$$
\begin{aligned}
A^{\alpha\beta} = & \sqrt{2} 2 \left(c_1 (q_3^\beta m_{12}^\alpha - q_3 m_{12} g^{\alpha\beta}) + c_2 (w^\beta q_3^\alpha - w q_3 g^{\alpha\beta}) \right) \\
& + \sum_{\phi V} c_{\phi V} J_{\phi V}(\mu_1) \left(c_1 (\beta_1 L_1^{\beta\alpha} + c_1 \beta_3 L_3^{\beta\alpha}) + c_2 (\beta_2 L_1^{\beta\alpha} + \beta_4 L_3^{\beta\alpha}) \right) \\
& \rightarrow \sqrt{2} 2 \left(c_1 (-L_3^{\beta\alpha} - \frac{1}{2}(s - m_\pi^2 - M_\rho^2) L_1^{\beta\alpha}) + c_2 (L_3^{\beta\alpha} - \frac{1}{2}(s + m_\pi^2 - M_\rho^2) L_1^{\beta\alpha}) \right) \\
& + \sum_{\phi V} c_{\phi V} J_{\phi V}(\mu_1) \left(c_1 (\beta_1 L_1^{\beta\alpha} + c_1 \beta_3 L_3^{\beta\alpha}) + c_2 (\beta_2 L_1^{\beta\alpha} + \beta_4 L_3^{\beta\alpha}) \right) \\
& \equiv a_{11} c_1 L_1^{\alpha\beta} + a_{13} c_1 L_3^{\alpha\beta} + a_{21} c_2 L_1^{\alpha\beta} + a_{23} c_2 L_3^{\alpha\beta} .
\end{aligned}
\tag{E.18}
$$

We used the fact that terms proportional to w^α or m_{12}^β in $A^{\alpha\beta}$ are irrelevant, since they vanish in W_{a1}^{μ}. In addition, we substituted

$$
q_3 \cdot m_{12} \rightarrow \frac{1}{2}(s - m_\pi^2 - M_\rho^2) ,
\tag{E.19}
$$

which is only true onshell. However, we will need this substitution in order to arrive at the desired result, and we expect that this difference does not effect the result seriously. The first term we look at is a_{11}

$$
a_{11} = -\sqrt{2}(s - m_\pi^2 - M_\rho^2) + \sum c_{\phi V} J_{\phi V}(\mu_1) \left((s - M_\phi^2 - M_V^2) M_{11}^{V\phi} + \frac{M_V}{\sqrt{2}\sqrt{s}}(s + M_\phi^2 - M_V^2) M_{10}^{V\phi} \right) .
\tag{E.20}
$$

We notice that

$$-\sqrt{2}(s - m_\pi^2 - M_\rho^2) = - \left[(1 - VJ)^{-1}(1 - VJ) \begin{pmatrix} \sqrt{2}(s - m_\pi^2 - M_\rho^2) \\ -(s - M_K^2 - M_{K^*}^2) \\ \frac{M_\rho}{\sqrt{s}}(s + m_\pi^2 - M_\rho^2) \\ -\frac{M_{K^*}}{\sqrt{2}\sqrt{s}}(s + M_K^2 - M_{K^*}^2) \end{pmatrix} \right]_1 \qquad \text{(E.21)}$$

with VJ defined in Eq.(5.47), and

$$M_{1b1j} = \left[(1 - VJ)^{-1} \begin{pmatrix} V_{1b1j} \\ V_{2b1j} \\ V_{1b0j} \\ V_{2b0j} \end{pmatrix} \right]_1 . \qquad \text{(E.22)}$$

Thus, we can write

$$\sum c_{V\phi} J_{\phi V}(\mu_1) \left((s - M_\phi^2 - M_V^2) M_{11}^{V\phi} + \frac{M_V}{\sqrt{2}\sqrt{s}}(s + M_\phi^2 - M_V^2) M_{10}^{V\phi} \right)$$
$$= - \left[(1 - VJ)^{-1} VJ \begin{pmatrix} \sqrt{2}(s - m_\pi^2 - M_\rho^2) \\ -(s - M_K^2 - M_{K^*}^2) \\ \frac{M_\rho}{\sqrt{s}}(s + m_\pi^2 - M_\rho^2) \\ -\frac{M_{K^*}}{\sqrt{2}\sqrt{s}}(s + M_K^2 - M_{K^*}^2) \end{pmatrix} \right]_1 , \qquad \text{(E.23)}$$

from which we see that a_{11} is given by

$$a_{11} = - \left[(1 - VJ)^{-1} \begin{pmatrix} \sqrt{2}(s - m_\pi^2 - M_\rho^2) \\ -(s - M_K^2 - M_{K^*}^2) \\ \frac{M_\rho}{\sqrt{s}}(s + m_\pi^2 - M_\rho^2) \\ -\frac{M_{K^*}}{\sqrt{2}\sqrt{s}}(s + M_K^2 - M_{K^*}^2) \end{pmatrix} \right]_1 . \qquad \text{(E.24)}$$

In the above simplifications, we used that the subtraction point of the entry loop and the one in the scattering amplitude are the same. Otherwise a_{11} would be modified by a factor $(1 - VJ(\mu_1) + VJ(\mu_3))$. This seems to be similar to the relation between μ_1 and μ_2, but differs in the fact that the entry vertex, which gets modified is the same as the one appearing in the loop. Neglecting the WT term, it would be clear that both subtraction points are the same, since the first loop diagram would be the same as all others. With this in mind it is obviously the best solution to choose both subtraction points the same.

a_{21} can be calculated similar and one gets

$$a_{21} = - \left[(1 - VJ)^{-1} \begin{pmatrix} \sqrt{2}(s + m_\pi^2 - M_\rho^2) \\ -(s + M_K^2 - M_{K^*}^2) \\ \frac{\sqrt{s}}{M_\rho}(s - m_\pi^2 - M_\rho^2) \\ -\frac{\sqrt{s}}{\sqrt{2}M_{K^*}}(s - M_K^2 - M_{K^*}^2) \end{pmatrix} \right]_1 . \qquad \text{(E.25)}$$

Now we do the same for the prefactors in front of L_3. We start with

$$a_{13} = -2\sqrt{2} + \sum c_{V\phi} J_{\phi V}(\mu_1) g_1 = -2\sqrt{2} + \sum c_{V\phi} J_{\phi V}(\mu_1) \frac{1}{p_{cm\pi\rho}^2 \sqrt{s}} (\omega_{\rho\pi} f_1 - \sqrt{2} M_\rho f_2)$$

$$= -2\sqrt{2} + \sum c_{V\phi} J_{\phi V}(\mu_1) \frac{1}{p_{cm\pi\rho}^2 \sqrt{s}} \Big(\omega_{\rho\pi} ((s - m_\phi^2 - M_V^2) M_{11} + \frac{M_V}{\sqrt{2}\sqrt{s}} (s + m_\phi^2 - M_V^2) M_{10})$$

$$- \sqrt{2} M_\rho ((s - m_\phi^2 - M_V^2) M_{01} + \frac{M_V}{\sqrt{2}\sqrt{s}} (s + m_\phi^2 - M_V^2) M_{00}) \Big)$$

$$(E.26)$$

and notice that

$$M_{1b2j} = \left[(1 - VJ)^{-1} \begin{pmatrix} V_{1b1j} \\ V_{2b1j} \\ V_{1b0j} \\ V_{2b0j} \end{pmatrix} \right]_3 . \tag{E.27}$$

Therefore, we can write

$$\sum c_{V\phi} J_{\phi V}(\mu_1) \frac{1}{p_{cm\pi\rho}^2 \sqrt{s}} \Big(\omega_{\rho\pi} \big((s - m_\phi^2 - M_V^2) M_{11}^{\phi V} + \frac{M_V}{\sqrt{2}\sqrt{s}} (s + m_\phi^2 - M_V^2) M_{10}^{\phi V} \big)$$

$$- \sqrt{2} M_\rho \big((s - m_\phi^2 - M_V^2) M_{01}^{\phi V} + \frac{M_V}{\sqrt{2}\sqrt{s}} (s + m_\phi^2 - M_V^2) M_{00}^{\phi V} \big) \Big)$$

$$= -\frac{\omega_{\pi\rho}}{\sqrt{s} p_{cm\pi\rho}^2} \left[(1 - VJ)^{-1} VJ \begin{pmatrix} \sqrt{2}(s - m_\pi^2 - M_\rho^2) \\ -(s - M_K^2 - M_{K^*}^2) \\ \frac{M_\rho}{\sqrt{s}} (s + m_\pi^2 - M_\rho^2) \\ -\frac{M_{K^*}}{\sqrt{2}\sqrt{s}} (s + M_K^2 - M_{K^*}^2) \end{pmatrix} \right]_1$$

$$+ \frac{\sqrt{2} M_\rho}{\sqrt{s} p_{cm\pi\rho}^2} \left[(1 - VJ)^{-1} VJ \begin{pmatrix} \sqrt{2}(s - m_\pi^2 - M_\rho^2) \\ -(s - M_K^2 - M_{K^*}^2) \\ \frac{M_\rho}{\sqrt{s}} (s + m_\pi^2 - M_\rho^2) \\ -\frac{M_{K^*}}{\sqrt{2}\sqrt{s}} (s + M_K^2 - M_{K^*}^2) \end{pmatrix} \right]_3 .$$

Next we artificially rewrite the simple factor $-2\sqrt{2}$ in a more complicated way in order to be able to add it easily to the term above

$$-2\sqrt{2} = -\frac{\omega_{\pi\rho}}{\sqrt{s} p_{cm\pi\rho}^2} \sqrt{2}(s - m_\pi^2 - M_\rho^2) + \sqrt{2} \frac{M_\rho^2}{s p_{cm\pi\rho}^2} (s + m_\pi^2 - M_\rho^2)$$

$$= -\frac{\omega_{\pi\rho}}{\sqrt{s} p_{cm\pi\rho}^2} \left[(1 - VJ)^{-1} (1 - VJ) \begin{pmatrix} \sqrt{2}(s - m_\pi^2 - M_\rho^2) \\ -(s - M_K^2 - M_{K^*}^2) \\ \frac{M_\rho}{\sqrt{s}} (s + m_\pi^2 - M_\rho^2) \\ -\frac{M_{K^*}}{\sqrt{2}\sqrt{s}} (s + M_K^2 - M_{K^*}^2) \end{pmatrix} \right]_1$$

$$+ \frac{\sqrt{2} M_\rho}{\sqrt{s} p_{cm\pi\rho}^2} \left[(1 - VJ)^{-1} (1 - VJ) \begin{pmatrix} \sqrt{2}(s - m_\pi^2 - M_\rho^2) \\ -(s - M_K^2 - M_{K^*}^2) \\ \frac{M_\rho}{\sqrt{s}} (s + m_\pi^2 - M_\rho^2) \\ -\frac{M_{K^*}}{\sqrt{2}\sqrt{s}} (s + M_K^2 - M_{K^*}^2) \end{pmatrix} \right]_3 .$$

Thus, we get

$$
a_{13} = -\frac{\omega_{\pi\rho}}{\sqrt{s}p_{cm\pi\rho}^2} \left[(1-VJ)^{-1} \begin{pmatrix} \sqrt{2}(s - m_\pi^2 - M_\rho^2) \\ -(s - M_K^2 - M_{K^*}^2) \\ \frac{M_\rho}{\sqrt{s}}(s + m_\pi^2 - M_\rho^2) \\ -\frac{M_{K^*}}{\sqrt{2}\sqrt{s}}(s + M_K^2 - M_{K^*}^2) \end{pmatrix} \right]_1
$$
$$
+ \frac{\sqrt{2}M_\rho}{\sqrt{s}p_{cm\pi\rho}^2} \left[(1-VJ)^{-1}(1-VJ) \begin{pmatrix} \sqrt{2}(s - m_\pi^2 - M_\rho^2) \\ -(s - M_K^2 - M_{K^*}^2) \\ \frac{M_\rho}{\sqrt{s}}(s + m_\pi^2 - M_\rho^2) \\ -\frac{M_{K^*}}{\sqrt{2}\sqrt{s}}(s + M_K^2 - M_{K^*}^2) \end{pmatrix} \right]_3 .
$$

(E.28)

a_{23} can be calculated in a similar way and one ends up with

$$
a_{23} = -\frac{\omega_{\pi\rho}}{\sqrt{s}p_{cm\pi\rho}^2} \left[(1-VJ)^{-1} \begin{pmatrix} \sqrt{2}(s + m_\pi^2 - M_\rho^2) \\ -(s + M_K^2 - M_{K^*}^2) \\ \frac{\sqrt{s}}{M_\rho}(s - m_\pi^2 - M_\rho^2) \\ -\frac{\sqrt{s}}{\sqrt{2}M_{K^*}}(s - M_K^2 - M_{K^*}^2) \end{pmatrix} \right]_1
$$
$$
+ \frac{\sqrt{2}M_\rho}{\sqrt{s}p_{cm\pi\rho}^2} \left[(1-VJ)^{-1} \begin{pmatrix} \sqrt{2}(s + m_\pi^2 - M_\rho^2) \\ -(s + M_K^2 - M_{K^*}^2) \\ \frac{\sqrt{s}}{M_\rho}(s - m_\pi^2 - M_\rho^2) \\ -\frac{\sqrt{s}}{\sqrt{2}M_{K^*}}(s - M_K^2 - M_{K^*}^2) \end{pmatrix} \right]_3 .
$$

Introducing some abbreviations

$$
(M_1^{a1})_1 = \frac{1}{s - M_a^2} \left[(1-VJ)^{-1} \begin{pmatrix} \sqrt{2}(s - m_\pi^2 - M_\rho^2) \\ -(s - M_K^2 - M_{K^*}^2) \\ \frac{M_\rho}{\sqrt{s}}(s + m_\pi^2 - M_\rho^2) \\ -\frac{M_{K^*}}{\sqrt{2}\sqrt{s}}(s + M_K^2 - M_{K^*}^2) \end{pmatrix} \right]_1 ,
$$

(E.29)

$$
(M_2^{a1})_1 = \frac{1}{s - M_a^2} \left[(1-VJ)^{-1} \begin{pmatrix} \sqrt{2}(s + m_\pi^2 - M_\rho^2) \\ -(s + M_K^2 - M_{K^*}^2) \\ \frac{\sqrt{s}}{M_\rho}(s - m_\pi^2 - M_\rho^2) \\ -\frac{\sqrt{s}}{\sqrt{2}M_{K^*}}(s - M_K^2 - M_{K^*}^2) \end{pmatrix} \right]_1 ,
$$

(E.30)

$$
(M_1^{a1})_3 = \frac{1}{s - M_a^2} \left[(1-VJ)^{-1} \begin{pmatrix} \sqrt{2}(s - m_\pi^2 - M_\rho^2) \\ -(s - M_K^2 - M_{K^*}^2) \\ \frac{M_\rho}{\sqrt{s}}(s + m_\pi^2 - M_\rho^2) \\ -\frac{M_{K^*}}{\sqrt{2}\sqrt{s}}(s + M_K^2 - M_{K^*}^2) \end{pmatrix} \right]_3 ,
$$

(E.31)

$$
(M_2^{a1})_3 = \frac{1}{s - M_a^2} \left[(1-VJ)^{-1} \begin{pmatrix} \sqrt{2}(s + m_\pi^2 - M_\rho^2) \\ -(s + M_K^2 - M_{K^*}^2) \\ \frac{\sqrt{s}}{M_\rho}(s - m_\pi^2 - M_\rho^2) \\ -\frac{\sqrt{s}}{\sqrt{2}M_{K^*}}(s - M_K^2 - M_{K^*}^2) \end{pmatrix} \right]_3 ,
$$

(E.32)

we can write the result in a more compact way as

$$W_{new}^\mu \equiv W_{tree}^\mu + W_{a1}^\mu = \frac{f_A g V_{ud} g_V s}{\sqrt{2} F_0^3} \left(g_\alpha^\mu - \frac{w^\mu w_\alpha}{w^2} \right) \frac{m_{12}^2}{m_{12}^2 - M_\rho^2 - \Pi} (q_1 - q_2)_\beta$$

$$\left(c_1 \left(-(M_1^{a1})_1 L_1^{\alpha\beta} + \left(-\frac{\omega_{\pi\rho}}{\sqrt{s} p_{cm\pi\rho}^2} (M_1^{a1})_1 + \frac{\sqrt{2} M_\rho}{\sqrt{s} p_{cm\pi\rho}^2} (M_1^{a1})_3 \right) L_3^{\beta\alpha} \right) \right.$$

$$\left. + c_2 \left(-(M_2^{a1})_1 L_1^{\alpha\beta} + \left(-\frac{\omega_{\pi\rho}}{\sqrt{s} p_{cm\pi\rho}^2} (M_2^{a1})_1 + \frac{\sqrt{2} M_\rho}{\sqrt{s} p_{cm\pi\rho}^2} (M_2^{a1})_3 \right) L_3^{\beta\alpha} \right) \right)$$

$$+ \quad (q_1 \leftrightarrow q_3) \,. \tag{E.33}$$

This expression has no singularity at $s = M_a^2$ anymore, which, however, is not so easy to see directly from the above formula.

Bibliography

[A+00]   D. M. Asner et al. *Hadronic structure in the decay $\tau^- \to \nu_\tau \pi^- \pi^0 \pi^0$ and the sign of the tau neutrino helicity.* Phys. Rev. **D61** (2000), 012002.

[AH03]   I. J. R. Aitchison and A. J. G. Hey. *Gauge Theories in Particle Physics, Volume II.* Institute of Physics Publishing, 3. edition (2003).

[AT04]   C. Amsler and N. A. Toernqvist. *Mesons beyond the naive quark model.* Phys. Rept. **389** (2004), 61–117.

[BD67]   J. Bjorken and S. Drell. *Relativistische Quantenfeldtheorie.* B.I. Wissenschaftsverlag (1967).

[BKY88]   M. Bando, T. Kugo, and K. Yamawaki. *Nonlinear realization and hidden local symmetries.* Phys. Rept. **164** (1988), 217–314.

[BL99]   T. Becher and H. Leutwyler. *Baryon chiral perturbation theory in manifestly Lorentz invariant form.* Eur. Phys. J. **C9** (1999), 643–671.

[BM00]   T. Barnes and H.-P. Morsch. *Baryon Excitations.* Forschungszentrum Jülich (2000).

[BM05]   P. C. Bruns and U.-G. Meissner. *Infrared regularization for spin-1 fields.* Eur. Phys. J. **C40** (2005), 97–119.

[BP96]   J. Bijnens and E. Pallante. *On the tensor formulation of effective vector Lagrangians and duality transformations.* Mod. Phys. Lett. **A11** (1996), 1069–1080.

[CCWZ69]   C. G. Callan(Jr.), S. R. Coleman, J. Wess, and B. Zumino. *Structure of Phenomenological Lagrangians. II.* Phys. Rev. **177** (1969), 2247–2250.

[CDD56]   L. Castillejo, R. H. Dalitz, and F. J. Dyson. *Low's Scattering Equation for the Charged and Neutral Scalar Theories.* Phys. Rev. **101** (1956), 453–458.

[CFU96]   G. Colangelo, M. Finkemeier, and R. Urech. *τ decays and chiral perturbation theory.* Phys. Rev. **D54** (1996), 4403–4418.

[CI86]   S. Capstick and N. Isgur. *Baryons in a relativized quark model with chromodynamics.* Phys. Rev. **D34** (1986), 2809–2835.

[CP76]   D. G. Caldi and H. Pagels. *A solution to the $\rho - \pi$ puzzle: Spontaneously broken symmetries of the quark model.* Phys. Rev. **D14** (1976), 809–826.

[CR00]   S. Capstick and W. Roberts. *Quark models of baryon masses and decays.* Prog. Part. Nucl. Phys. **45** (2000), S241–S331.

[CWZ69]   S. R. Coleman, J. Wess, and B. Zumino. *Structure of Phenomenological Lagrangians. I.* Phys. Rev. **177** (1969), 2239–2247.

[EFS02]   T. Ebertshaeuser, H. W. Fearing, and S. Scherer. *The anomalous chiral perturbation theory meson Lagrangian to order p^6 revisited.* Phys. Rev. **D65** (2002), 054033.

[EGL⁺89]   G. Ecker, J. Gasser, H. Leutwyler, A. Pich, and E. de Rafael. *Chiral lagrangians for massive spin-1 fields.* Phys. Lett. **B223** (1989), 425–432.

[EGPdR89]   G. Ecker, J. Gasser, A. Pich, and E. de Rafael. *The role of resonances in chiral perturbation theory.* Nucl. Phys. **B321** (1989), 311–342.

[FGJS03]   T. Fuchs, J. Gegelia, G. Japaridze, and S. Scherer. *Renormalization of relativistic baryon chiral perturbation theory and power counting.* Phys. Rev. **D68** (2003), 056005.

[FMMS00]   N. Fettes, U.-G. Meissner, M. Mojzis, and S. Steininger. *The Chiral Effective Pion-Nucleon Lagrangian of Order p^4.* Ann. Phys. **283** (2000), 273–302.

[FS00]   H. W. Fearing and S. Scherer. *Field transformations and simple models illustrating the impossibility of measuring off-shell effects.* Phys. Rev. **C62** (2000), 034003.

[Gas75]   S. Gasiorowicz. *Elementarteilchen-Physik.* B.I. Wissenschaftsverlag (1975).

[GDPP04]   D. Gomez Dumm, A. Pich, and J. Portoles. $\tau \rightarrow \nu\pi\pi\pi$ *decays in the resonance effective theory.* Phys. Rev. **D69** (2004), 073002.

[Geo84]   H. Georgi. *Weak Interactions and Modern Particle Theory.* Addison-Wesley (1984).

[GI85]   S. Godfrey and N. Isgur. *Mesons in a relativized quark model with chromodynamics.* Phys. Rev. **D32** (1985), 189–231.

[GK91]   C. Gale and J. I. Kapusta. *Vector dominance model at finite temperature.* Nucl. Phys. **B357** (1991), 65–89.

[GL84]   J. Gasser and H. Leutwyler. *Chiral perturbation theory to one loop.* Ann. Phys. **158** (1984), 142–210.

[GL85]   J. Gasser and H. Leutwyler. *Chiral perturbation theory: Expansions in the mass of the strange quark.* Nucl. Phys. **B250** (1985), 465–516.

[GMN00]   M. Gell-Mann and Y. Ne'eman. *The Eightfold Way.* Perseus Books (2000).

[GNP02]   A. Gomez Nicola and J. R. Pelaez. *Meson-meson scattering within one-loop chiral perturbation theory and its unitarization.* Phys. Rev. **D65** (2002), 054009.

[GRLN04]   C. Garcia-Recio, M. F. M. Lutz, and J. Nieves. *Quark mass dependence of s-wave baryon resonances.* Phys. Lett. **B582** (2004), 49–54.

[Gro99]   D. J. Gross. *Twenty five years of asymptotic freedom.* Nucl. Phys. Proc. Suppl. **74** (1999), 426–446.

[GSS88]   J. Gasser, M. E. Sainio, and A. Svarc. *Nucleons with chiral Loops.* Nucl. Phys. **B307** (1988), 779–853.

[GW73a]   D. J. Gross and F. Wilczek. *Asymptotically Free Gauge Theories. 1.* Phys. Rev. **D8** (1973), 3633–3652.

[GW73b]   D. J. Gross and F. Wilczek. *Ultraviolet Behavior of Non-Abelian Gauge Theories.* Phys. Rev. Lett. **30** (1973), 1343–1346.

[JMW95]   E. E. Jenkins, A. V. Manohar, and M. B. Wise. *Chiral Perturbation Theory for Vector Mesons.* Phys. Rev. Lett. **75** (1995), 2272–2275.

[JOO$^+$03]   D. Jido, J. A. Oller, E. Oset, A. Ramos, and U. G. Meissner. *Chiral dynamics of the two $\Lambda(1405)$ states.* Nucl. Phys. **A725** (2003), 181–200.

[JW59]   M. Jacob and G. Wick. *On the general theory of collisions for particles with spin.* Ann. Phys. **7** (1959), 404. Reprinted in Ann. Phys. **281** (2000), 774.

[KKW97]   F. Klingl, N. Kaiser, and W. Weise. *Current correlation functions, QCD sum rules and vector mesons in baryonic matter.* Nucl. Phys. **A624** (1997), 527–563.

[KL04]   E. E. Kolomeitsev and M. F. M. Lutz. *On baryon resonances and chiral symmetry.* Phys. Lett. **B585** (2004), 243–252.

[KLF01]   S. Kondratyuk, A. D. Lahiff, and H. W. Fearing. *The equivalence theorem and the Bethe-Salpeter equation.* Phys. Lett. **B521** (2001), 204–210.

[KM90]   N. Kaiser and U. G. Meissner. *Generalized hidden symmetry for low-energy hadron physics.* Nucl. Phys. **A519** (1990), 671–696.

[KNT07]   K. Kampf, J. Novotny, and J. Trnka. *On different Lagrangian formalisms for vector resonances within chiral perturbation theory.* Eur. Phys. J. **C50** (2007), 385–403.

[Kog83]   J. B. Kogut. *The lattice gauge theory approach to quantum chromodynamics.* Rev. Mod. Phys. **55** (1983), 775–836.

[Kra90]   A. Krause. *Baryon matrix elements of the vector current in chiral perturbation theory.* Helv. Phys. Acta **63** (1990), 3–70.

[KSW95a]   N. Kaiser, P. B. Siegel, and W. Weise. *Chiral dynamics and the low-energy kaon-nucleon interaction.* Nucl. Phys. **A594** (1995), 325–345.

[KSW95b]   N. Kaiser, P. B. Siegel, and W. Weise. *Chiral dynamics and the $S_{11}(1535)$ nucleon resonance.* Phys. Lett. **B362** (1995), 23–28.

[Leu94]   H. Leutwyler. *On the Foundations of Chiral Perturbation Theory.* Ann. Phys. **235** (1994), 165–203.

[Leu06]   S. Leupold. *Properties of the vector meson nonet at large N_c beyond the chiral limit.* Phys. Rev. **D73** (2006), 085013.

[Leu07]   S. Leupold. *Selfconsistent approximations, symmetries and choice of representation.* Phys. Lett. **B646** (2007), 155–164.

[LK02]   M. F. M. Lutz and E. E. Kolomeitsev. *Relativistic chiral $SU(3)$ symmetry, large-N_c sum rules and meson-baryon scattering.* Nucl. Phys. **A700** (2002), 193–308.

[LK04]   M. F. M. Lutz and E. E. Kolomeitsev. *On meson resonances and chiral symmetry.* Nucl. Phys. **A730** (2004), 392–416.

[LWF02]   M. F. M. Lutz, G. Wolf, and B. Friman. *Scattering of vector mesons off nucleons.* Nucl. Phys. **A706** (2002), 431–496.

[Mos89]   U. Mosel. *Fields, Symmetries and Quarks.* McGraw-Hill Book Company GmbH (1989).

[MSL$^+$06]   P. Muehlich, V. Shklyar, S. Leupold, U. Mosel, and M. Post. *The spectral function of the omega meson in nuclear matter from a coupled-channel resonance model.* Nucl. Phys. **A780** (2006), 187–205.

[OM01]   J. A. Oller and U. G. Meissner. *Chiral dynamics in the presence of bound states: Kaon nucleon interactions revisited.* Phys. Lett. **B500** (2001), 263–272.

[OO97]   J. A. Oller and E. Oset. *Chiral symmetry amplitudes in the S-wave isoscalar and isovector channels and the σ, $f_0(980)$, $a_0(980)$ scalar mesons.* Nucl. Phys. **A620** (1997), 438–456.

[OO99]   J. A. Oller and E. Oset. *N/D description of two meson amplitudes and chiral symmetry.* Phys. Rev. **D60** (1999), 074023.

[OOP99]   J. A. Oller, E. Oset, and J. R. Pelaez. *Meson-meson interactions in a nonperturbative chiral approach.* Phys. Rev. **D59** (1999), 074001.

[OR98]   E. Oset and A. Ramos. *Non-perturbative chiral approach to s-wave $\overline{K}N$ interactions.* Nucl. Phys. **A635** (1998), 99–120.

[PDG06]   W. -M. Yao et al. *Review of particle physics.* J. Phys. **G33** (2006), 1–1232.

[Pen06]   M. R. Pennington. *Scalars in the hadron world: The Higgs sector of the strong interaction.* Int. J. Mod. Phys. **A21** (2006), 747–756.

[Pol73]   H. D. Politzer. *Reliable Perturbative Results for Strong Interactions?* Phys. Rev. Lett. **30** (1973), 1346–1349.

[PS95]   M. E. Peskin and D. V. Schroeder. *An Introduction to Quantum Field Theory.* Perseus Books (1995).

[ROS05]   L. Roca, E. Oset, and J. Singh. *Low lying axial-vector mesons as dynamically generated resonances.* Phys. Rev. **D72** (2005), 014002.

[RPO04]   L. Roca, J. E. Palomar, and E. Oset. *Decay of axial-vector mesons into VP and $P\gamma$.* Phys. Rev. **D70** (2004), 094006.

[RW00]   R. Rapp and J. Wambach. *Chiral Symmetry Restoration and Dileptons in Relativistic Heavy-Ion Collisions.* Adv. Nucl. Phys. **25** (2000), 1–205.

[S$^+$05]   S. Schael et al. *Branching ratios and spectral functions of τ decays: Final ALEPH measurements and physics implications.* Phys. Rept. **421** (2005), 191–284.

[Sak69]   J. J. Sakurai. *Currents and Mesons.* University of Chicago Press (1969).

[SB51]   E. E. Salpeter and H. A. Bethe. *A Relativistic Equation for Bound-state Problems.* Phys. Rev. **84** (1951), 1232–1242.

[Sch03]   S. Scherer. *Introduction to chiral perturbation theory.* Adv. Nucl. Phys. **27** (2003), 277.

[SOVV05]   S. Sarkar, E. Oset, and M. J. Vicente Vacas. *Baryonic resonances from baryon decuplet-meson octet interaction.* Nucl. Phys. **A750** (2005), 294–323.

[Swa06]   E. S. Swanson. *The new heavy mesons: A status report.* Phys. Rept. **429** (2006), 243–305.

[Tom66]   Y. Tomozawa. *Axial-vector coupling renormalization and the meson-baryon scattering lengths.* Nuovo Cim. **46A** (1966), 707–717.

[Tun85]   W.-K. Tung. *Group Theory in Physics.* World Scientific (1985).

[UBW02]   M. Urban, M. Buballa, and J. Wambach. *Vector and axial-vector correlators in a chirally symmetric model.* Nucl. Phys. **A697** (2002), 338–371.

[Wei66]   S. Weinberg. *Pion Scattering Lengths.* Phys. Rev. Lett. **17** (1966), 616–621.

[Wei67]   S. Weinberg. *Precise Relations between the Spectra of Vector and Axial-Vector Mesons.* Phys. Rev. Lett. **18** (1967), 507–509.

[Wei68]   S. Weinberg. *Nonlinear Realizations of Chiral Symmetry.* Phys. Rev. **166** (1968), 1568–1577.

[Wei73]   S. Weinberg. *Non-Abelian Gauge Theories of the Strong Interactions.* Phys. Rev. Lett. **31** (1973), 494–497.

[Wei79]   S. Weinberg. *Phenomenological Lagrangians.* Physica **A96** (1979), 327–340.

Deutsche Zusammenfassung

Eines der Ziele der Hadronenphysik ist die Beantwortung der Frage nach der Natur hadronischer Resonanzen. Das Quark Modell ist sehr erfolgreich in der Beschreibung von Teilen des beobachteten Spektrums. Insbesondere für Systeme, die aus schweren Quarks bestehen, liefert das Quark Modell verlässliche Ergebnisse. Andererseits existieren noch eine Reihe ungeklärter Fragen bezüglich des Spektrums der Hadronen, die aus leichten Quarks aufgebaut sein könnten. Ein Beispiel hierfür, das schon lange diskutiert wurde und auch immer noch aktuell diskutiert wird, ist der Bereich der leichten skalaren Mesonen. Diese Zustände können nicht mit dem naiven Quark Modell erklärt werden. Es existieren eine Reihe möglicher Modelle, um die Phänomenologie dieser Zustände zu beschreiben. Die Vorschläge für die Natur dieser Resonanzen variert zwischen $q\bar{q}$ states, $K\overline{K}$ Molekülen oder Superpositionen der beiden. Eine andere Möglichkeit besteht darin, diese Zustände als dynamisch generierte Resonanzen zu beschreiben, die durch die Wechselwirkung zwischen den pseudoskalaren Mesonen dynamisch erzeugt werden. Rechnungen dieser Art wurden furchgeführt, und sie liefern Pole in den Streuamplituden, die man den skalaren Resonanzen zuordnen kann.

Ein weiterer Bereich, in dem man eine ähnliche Diskussion antrifft, ist der Bereich der baryonischen Resonanzen. In diesem Sektor hat das Quark Modell ebenfalls Schwierigkeiten, einige der Resonanzen zu beschreiben. Auch hier ist ein alternativer Weg, diese Zustände durch die Wechselwirkung zwischen Baryonen und pseudoskalaren Mesonen dynamisch zu erzeugen. In der Streuung des Baryonenoktets mit den pseudoskalaren Mesonen findet man wiederum Strukturen in den Streuamplituden, die man den baryonischen $J^P = \frac{1}{2}^-$ Resonanzen zuordnen kann. Prominente Beispiele hierfür sind das $\Lambda(1405)$ und das $N^*(1535)$. Die Streuung des Dekuplets der Baryonen mit den pseudoskalaren Mesonen führt ebenfalls zur Erzeugung einiger $J^P = \frac{3}{2}^-$ Resonanzen, wie zum Beispiel dem $\Lambda(1520)$.

Aktuellere Arbeiten dehnen diese Diskussion auch auf die Axial-Vektor Mesonen aus. Hier wird die Streuamplitude für die Streung von Goldstone Bosonen an Vektor Mesonen berechnet. In führender Ordnung, in einer chiralen Entwicklung, ist die Streuung durch den sogenannten Weinberg-Tomozawa (WT) Term bestimmt, der parameterfrei durch die chirale Symmetrie bestimmt ist. Um die Korrelationen der stark wechselwirkenden Teilchen zu berücksichtigen, wird dieser Term mittels der Bethe-Salpeter Gleichung iteriert. Wiederum findet man resonante Strukturen, die man den Axial-Vektor Mesonen zuschreiben kann.

Die Identifikation der Resonanzen über die Streuamplitude allein ist notwendigerweise indirekt und modellabhängig, da die Streuamplitude selbst nicht die Größe ist, die gemessen wird. Wir wollen die eben erwähnte Methode nutzen, um sie auf einen physikalischen, direkt gemessenen Prozess anzuwenden, den τ Zerfall. Der τ Zerfall bietet ein ideales Umfeld, um verlässliche Informationen zu extrahieren, da man die starke Wechselwirkung sauber von der gut bekannten schwachen Wechselwirkung trennen kann. Der Kanal, der uns interessiert ist, ist der Zerfall in drei Pionen. Dieser Kanal wird dominiert durch eine resonante Struktur, die man üblicherweise dem a_1 zuschreibt. Die meisten der Rechnungen, die zu diesem Zerfall durchgeführt wurden, beruhen auf Parametrisierungen von Breit-Wigner Funktionen mit vielen Parametern. Es existiert jedoch auch eine Rechnung im Rahmen einer effektiven chiralen Feldtheorie, in der die Daten mittels eines expliziten a_1 gut beschrieben werden. In dieser

Rechnung wird die Breite des a_1 parametrisiert. In einer weiteren Rechnung im Rahmen des linearen Sigma Modells werden die Daten ebenfalls zufriedenstellend reproduziert. Die Breite des a_1 wird durch den elementaren Zerfall in Vektor und pseudoskalares Meson beschrieben. In dieser Arbeit jedoch wird der WT Term nicht berücksichtigt. Wir berechnen den Zerfall im Wesentlichen unter zwei verschiedenen Annahmen. In einer Rechnung berücksichtigen wir das a_1 nicht explizit, sondern nehmen an, dass die auftretende Struktur durch die Endzustandswechselwirkung zwischen dem Vektor Meson und dem Goldstone Boson hervorgerufen wird. In einer zweiten Version führen wir das a_1 als elementares Feld explizit ein. Anders jedoch als in den oben erwähnten Modellen, erzeugen wir die Breite des a_1 durch den elementaren Zerfall in Vektor Meson und Goldstone Boson *und* beziehen zusätzlich den WT Term mit ein. Da der WT Term in einem chiralen Zählschema sogar eine Ordnung unter der a_1 Wechselwirkung liegt, gibt es keinen Grund, diesen Term nicht mit einzubeziehen.

Nachdem in den ersten Kapiteln die Grundlagen für die Rechnung geschaffen werden, teilen wir die eigentliche Rechnung in drei Teile:

1. Im ersten Szenario beschreiben wir die Korrelationen des Endzustands einzig durch die Iteration des WT Terms. Das heißt, der Prozess wird in diesem Rahmen wie folgt beschrieben: Aus dem schwachen Zerfall entsteht ein Vektor Meson und ein pseudoskalares Meson, durch deren starke Wechselwirkung die resonante Struktur erzeugt wird. Der schwache Zerfall, der den τ Zerfall einleitet, wird im Rahmen des Standard Modells erklärt. Der WT Term ist parameterfrei von der chiralen Symmetrie vorrausgesagt. Die restlichen Kopplungskonstanten sind durch die gut bekannten Eigenschaften des ρ Meson bestimmt. Die einzigen unbekannten Größen in dieser Rechnung treten in der Renormierung der divergenten Loopintegrale auf. Wir führen zwei Subtraktionspunkte ein, um die auftretenden Divergenzen zu eliminieren. Einer dieser Punkte renormiert das Loopintegral aus der Bethe-Salpeter Gleichung, und der andere Punkt renormiert den Loop, der den W Zerfallsvertex beinhaltet. Legt man den Subtraktionpunkt wie in [LK04] durch crossing Symmetrie Argumente fest, beinhaltet diese Rechnung nur einen freien Parameter. Durch Anpassung dieses Parameters sind wir in der Lage, die Daten erfolgreich zu beschreiben.

2. In der zweiten Rechnung führen wir das a_1 als elementares Feld explizit ein. Dies führt notwendigerweise zu zusätzlichen Parametern, nämlich die Masse des a_1, seine Kopplung an das W Boson und die Kopplung an Vektor Meson und Goldstone Boson. Die auffallendste Eigenschaft in dieser Rechnung ist die starke Präsenz des WT Terms. Diese starke Präsenz macht sich im Auftreten einer zweiten Erhöhung in der Spektralfunktion bemerkbar, die für fast jede Wahl der Parameter auftritt. Nur durch eine sehr genau abgestimmte Wahl der Parameter kann man erreichen, dass die beiden Erhöhungen zu einer verschmelzen. Dies ist eine äußerst künstliche Methode, um die richtige Struktur zu erklären. Vergleicht man dieses künstliche Vorgehen mit dem Erfolg des Szenarios ohne explizites a_1, kann man von einem Hinweis auf eine dynamisch erzeugte Struktur reden.

3. Anschließend führen wir eine dritte Rechnung durch, in der wir das a_1 wiederum nicht explizit einbeziehen. Anders als in der ersten Rechnug addieren wir zusätzlich Korrekturen höherer Ordnung zum Kern der Bethe-Salpeter Gleichung. Mit diesen zusätzlichen Termen ist es möglich, die Ergebnisse aus dem ersten Szenario noch systematisch zu verbessern. Die Möglichkeit, das Modell systematisch zu verbessern, stellt einen wesentlichen, erfolgreich bestandenen Test für das Modell da. Die Korrekturen höherer Ordnung führen zu sechs neuen Parameters, deren Stärke nicht von der chiralen Symmetrie vorrausgesagt wird. Wir weisen an dieser Stelle darauf hin, dass der Erfolg dieser Rechnung nicht darin besteht, die Daten mit weiteren sechs zusätzlichen Parametern zu beschreiben, sondern dass es möglich ist, das Modell systematisch zu verbessern. Man findet viele Werte für die Parameter, so dass die Spektralfunktion erfolgreich beschrieben werden kann. Die Dalitz Projektionsdaten, die eine de-

taillierter Analyse zulassen, zeigen außerdem, dass man diese Parametersätze weiter diskriminieren kann. Es stellt sich heraus, dass die qualitative Beschreibung der Daten eng verknüpft ist mit der Präsenz von d-Wellen Komponenten. Genauer gesagt ist Qualität korreliert mit der Stärke der Übergänge von s- nach d-Welle.

Zusammenfassend kann man sagen, dass man ohne die explizite Berücksichtigung des a_1 ein vielversprechendes Modell hat, das die Daten sehr erfolgreich beschreibt. Die meisten Parameter, im einfachsten Fall alle bis auf einen, sind bestimmt durch chirale Symmetrie und die Eigenschaften des ρ Meson. Führt man ein explizites a_1 ein, weisen die Ergebnisse seltsame Eigenschaften auf, wenn man zusätzlich auch den WT Term berücksichtigt. Dieser Term ist jedoch durch die chirale Symmetrie parameterfrei vorgegeben und sollte in jedem Fall mit einbezogen werden. Dies alles weist auf eine dynamisch erzeugte Struktur des a_1 hin.

Danksagung

Zu guter Letzt möchte ich noch allen danken, die mehr oder weniger direkt zum Gelingen dieser Arbeit beigetragen haben.

An erster Stelle möchte PD Dr. Stefan Leupold für die interessante Themenstellung und die erstklassige Betreuung danken. Meine Fragen fanden stets ein offenes Ohr und in zahlreichen Diskussionen konnte ich viel lernen.

Danken möchte ich auch Prof. Dr. Ulrich Mosel für die Aufnahmen an sein Institut. Weiterhin ermöglichte er mir die Teilnahme an zahlreichen Konferenzen und Workshops. Sein fortlaufendes Interesse an meiner Arbeit wirkte stets sehr ermutigend.

Ein herzlicher Dank geht auch an Elke Jung, die für einen reibungslosen Ablauf der Bürokratie sorgte.

Weiterhin danke ich Matthias F.M. Lutz, der sich die Zeit nahm, meine Fragen bezüglich seiner Arbeiten erfolgreich zu beantworten und wertvolle Anregungen für meine Arbeit gab. Danke auch an Hasko Stenzel für die Aufklärung meiner Fragen bezüglich der ALEPH Daten.

Auch meinen Eltern möchte ich danken, die ebenfalls stets ein offenes Ohr für mich hatten in sämtlichen Fragen nicht physikalischer Natur.

Für die nötige Abwechslung und den geistigen Ausgleich wurde von meinen Freunden gesorgt; auch dafür ein Danke.

Nicht fehlen darf natürlich auch ein Dankeschön an meine Freundin Luci, die sich ebenfalls immer große Mühe gab, für Ablenkung zu sorgen und dennoch viel Rücksicht auf meine Arbeit nahm.